

Distribution Agreement

In presenting this thesis or dissertation as a partial fulfillment of the requirements for an advanced degree from Emory University, I hereby grant to Emory University and its agents the non-exclusive license to archive, make accessible, and display my thesis or dissertation in whole or in part in all forms of media, now or hereafter known, including display on the world wide web. I understand that I may select some access restrictions as part of the online submission of this thesis or dissertation. I retain all ownership rights to the copyright of the thesis or dissertation. I also retain the right to use in future works (such as articles or books) all or part of this thesis or dissertation.

Signature:

Erica Modeste

Date

**Proteomic profiling of the cerebrospinal fluid of African Americans and Caucasians
reveals common and unique biomarkers of Alzheimer's disease**

By
Erica Modeste
Doctor of Philosophy

Graduate Division of Biological and Biomedical Sciences
Molecular and Systems Pharmacology

Nicholas Seyfried
Advisor

David Weinshenker
Committee Member

Ellen Hess
Committee Member

John Hepler
Committee Member

Accepted:

Kimberley Jacob Arriola, PhD
Dean of the James T. Laney School of Graduate School

Date

**Proteomic profiling of the cerebrospinal fluid of African Americans and Caucasians
reveals common and unique biomarkers of Alzheimer's disease**

By

Erica Modeste
B.S. University of Richmond, 2015

Advisor: Nicholas Seyfried, Ph.D.

An abstract of
a dissertation submitted to the faculty of the
James T. Laney School of Graduate Studies of Emory University
in partial fulfillment of the requirements for the degree of Doctor of Philosophy
in the Graduate Division of Biological and Biomedical Sciences
Molecular and Systems Pharmacology

2024

ABSTRACT

Proteomic profiling of the cerebrospinal fluid of African Americans and Caucasians reveals common and unique biomarkers of Alzheimer's disease

By Erica Modeste

Despite being twice as likely to get Alzheimer's disease (AD), African Americans have been grossly underrepresented in AD research. While emerging evidence indicates that African Americans with AD have lower cerebrospinal fluid (CSF) levels of Tau compared to Caucasians, other differences in AD CSF biomarkers have not been fully elucidated. In this thesis, we performed unbiased proteomic profiling of CSF from African Americans and Caucasians with and without AD to identify both common and divergent AD CSF biomarkers. Multiplex tandem mass tag-based mass spectrometry (TMT-MS) quantified 1,840 proteins from 105 control and 98 AD patients of which 100 identified as Caucasian and 103 identified as African American. Differential protein expression and co-expression approaches were then utilized to assess how changes in the CSF proteome were related to race and AD. Co-expression network analysis organized the CSF proteome into 14 modules associated with brain cell-types and biological pathways. Consistent with previous findings, the increase of Tau levels in AD was greater in Caucasians than in African Americans by both immunoassay and TMT-MS measurements. Similarly, modules enriched with proteins involved with glycolysis and neuronal/cytoskeletal proteins were more increased in Caucasians than in African Americans with AD. In contrast, a module enriched with synaptic proteins including VGF, SCG2, and NPTX2 was significantly lower in African Americans than Caucasians with AD. CSF modules which included 14-3-3 proteins (YWHAZ and YWHAG) demonstrated equivalent disease-related elevations in both African Americans and Caucasians with AD. A targeted mass spectrometry method, selected reaction monitoring (SRM), with heavy labeled internal standards was then used to measure a subset of CSF module proteins and a receiver operating characteristic (ROC) curve analysis assessed the performance of each protein biomarker in differentiating controls and AD by race. Following SRM and ROC analysis, VGF, SCG2, and NPTX2 were significantly better at classifying African Americans than Caucasians with AD. In total, these findings provide insight into additional protein biomarkers and pathways reflecting underlying brain pathology that are shared or differ by race.

**Proteomic profiling of the cerebrospinal fluid of African Americans and Caucasians
reveals common and unique biomarkers of Alzheimer's disease**

By

Erica Modeste
B.S. University of Richmond, 2015

Advisor: Nicholas Seyfried, Ph.D.

A dissertation submitted to the faculty of the
James T. Laney School of Graduate Studies of Emory University
in partial fulfillment of the requirements for the degree of Doctor of Philosophy
in the Graduate Division of Biological and Biomedical Sciences
Molecular and Systems Pharmacology

2024

TABLE OF CONTENTS

LIST OF FIGURES.....	9
LIST OF TABLES.....	10
LIST OF ABBREVIATIONS.....	11
LIST OF PROTEINS.....	13
CHAPTER 1: INTRODUCTION.....	18
1.1 The increasing burden of Alzheimer’s disease (AD).....	19
1.2 Monitoring memory loss in those with AD.....	22
1.3 The initial discovery of AD.....	27
1.4 Neuropathological hallmarks of AD.....	28
1.4.1 <i>Amyloid cascade.....</i>	<i>28</i>
1.4.2 <i>Pathologic Tau.....</i>	<i>31</i>
1.5 The ATN network for staging AD progression.....	35
1.6 Early-onset AD versus late-onset AD.....	36
1.6.1 <i>Early-onset AD.....</i>	<i>36</i>
1.6.2 <i>Late-onset AD.....</i>	<i>36</i>
1.7. Risk factors for AD.....	37
1.7.1. <i>Age.....</i>	<i>37</i>
1.7.2 <i>Sex.....</i>	<i>38</i>
1.8 Modifiable risk factors for AD.....	38
1.8.1 <i>Role of modifiable risk factors in AD.....</i>	<i>38</i>
1.8.2 <i>Cardiovascular health.....</i>	<i>39</i>
1.8.3 <i>Smoking / physical activity / diet.....</i>	<i>40</i>
1.9 Social determinants of health.....	40
1.9.1 <i>Education.....</i>	<i>40</i>
1.9.2 <i>Employment.....</i>	<i>41</i>
1.9.3 <i>Environment.....</i>	<i>42</i>
1.9.4 <i>Stress.....</i>	<i>43</i>
1.9.5 <i>Discrimination and social exclusion.....</i>	<i>44</i>
1.9.6 <i>Final conclusions.....</i>	<i>44</i>
1.10 Therapeutic attempts to slow the progression of AD.....	45
1.11 Cerebrospinal fluid (CSF) as a gateway to neuropathological changes in AD..	46
1.12 African Americans: the most at risk racial group for AD.....	51
1.13 The utility of mass spectrometry (MS)-based proteomics in identifying novel	

protein signatures in AD	52
1.13.1 <i>Strategies for MS-based quantification of proteomes</i>	52
1.13.2 <i>Fundamentals of network construction and module identification</i>	53
1.13.3 <i>Why prioritize the study of the proteome over the genome?</i>	54
1.13.4 <i>Core modules of the AD brain network proteome</i>	55
1.13.5 <i>The CSF proteome as a reflection of AD brain changes</i>	56
1.14 Summary	56
CHAPTER 2: MATERIALS AND METHODS	58
2.1 CSF samples	59
2.2 Protein digestion of CSF	60
2.3 Tandem mass tag labeling of CSF peptides	60
2.4 High-pH fractionation	61
2.5 Mass spectrometry analysis and data acquisition	62
2.6 Database search and protein quantification	62
2.7 Adjustment for batch and other sources of variance	63
2.8 Differential expression analysis	66
2.9 Weighted Gene Co-expression Network Analysis	66
2.10 Gene ontology and cell type enrichment analysis	66
2.11 Selected Reaction Monitoring	67
CHAPTER 3: RESULTS	69
3.1 CSF Cohort characteristics	70
3.2 Discovery tandem mass spectrometry analysis of CSF from African Americans and Caucasians reveals unique and shared changes in Alzheimer’s disease	72
3.2.1 <i>Correlation analysis uncovers a strong relationship between mass spectrometry and immunoassay measurements of Tau</i>	72
3.2.2 <i>Differential expression analysis of African American and Caucasian CSF proteome reveals unique and shared changes in AD</i>	72
3.2.3 <i>Network analysis of the CSF proteome reveals modules related to pathways and brain cell-types</i>	75
3.2.4 <i>CSF protein modules correlate to race and clinicopathological phenotypes of AD</i>	81

3.3 Selected reaction monitoring validates protein alterations across Alzheimer's disease and race.....	89
CHAPTER 4: DISCUSSION.....	98
4.1 Protein co-expression between the brain and CSF reflects the crucial role of CSF in brain function and health.....	99
4.2 CSF network analysis indicated differences in endothelial markers across race, irrespective of disease, yet there is insufficient evidence to indicate that these differences stem from variations in endothelial damage.....	101
4.3 Unveiling the interplay between neuronal alterations in AD and the role of the CSF in mirroring cognitive decline.....	103
4.4 Future directions.....	107
CHAPTER 5: REFERENCES.....	110
CHAPTER 6: APPENDIX.....	126

LIST OF FIGURES

Figure 1.1: Projected number of people in the United States with Alzheimer’s disease (AD) in millions from 2010 to 2050.....	20
Figure 1.2: Healthy brain compared to a brain affected by Alzheimer’s disease.....	23
Figure 1.3: A comparison of the scoring patterns of the Mini-Mental State Examination (MMSE) with the Montreal Cognitive Assessment (MoCA).....	25
Figure 1.4: The amyloidogenic and non-amyloidogenic pathways of amyloid precursor protein (APP) processing.....	29
Figure 1.5: Hypothesized time course of neuropathological and clinical changes in Alzheimer’s disease based on biomarker alterations.....	32
Figure 1.6: Cerebrospinal fluid (CSF) creation and flow alongside sample immunoassay measurements of Amyloid-beta ₁₋₄₂ (A β ₄₂) and Tau from 105 controls and 98 Alzheimer’s disease (AD) samples.....	47
Figure 1.7: Methods by which pathological Tau can be secreted or released into extracellular space.....	49
Figure 2.1: Batch correction, outlier removal and bootstrap regression.....	65
Figure 3.1: Schematic of experimental workflow and correlation between proteomic Tau and total Tau immunoassay measurements.....	73
Figure 3.2: Differential expression of Caucasian and African American CSF proteomes in AD...	76
Figure 3.3: Network analysis classifies the CSF proteome into modules associated with specific brain cell-types and gene ontologies.....	79
Figure 3.4: Protein overlap between modules in CSF network and modules in a human AD brain network.....	82
Figure 3.5: CSF protein modules correlate to race and clinicopathological phenotypes of AD...	84
Figure 3.6: Additional CSF network protein modules.....	87
Figure 3.7: Validation of shared and divergent CSF protein levels across AD and race.....	90
Figure 3.8: Stratification of SRM CSF protein measurements in by APOE genotype and comorbidity.....	93
Figure 3.9: ROC analysis to evaluate CSF protein classification of AD by race.....	96
Figure 4.1: Hypothesized time course differences in neuropathological and clinical changes based on biomarker alterations between Caucasians and African Americans with AD.....	104

LIST OF TABLES

Table 3.1: Cohort characteristics.....	71
---	----

LIST OF ABBREVIATIONS

A β : Amyloid beta peptides

A β ₄₂: Amyloid beta peptide₁₋₄₂

ACh: Acetylcholine

ACN: Acetonitrile

AD: Alzheimer's disease

ADRC: Alzheimer's Disease Research Center

BBB: Blood brain barrier

BICOR: Biweight midcorrelation coefficient

CBF: cerebral blood flow

CDR: Clinical Dementia Rating

CSF: Cerebrospinal fluid

CV: Coefficient of variation

ϵ : epsilon

EOAD: Early-onset Alzheimer's disease

FAIMS: High-field asymmetric waveform ion mobility spectrometry

FDR: False discovery rate

GIS: Global internal standards

GO: Gene ontology

GWAS: Genome Wide Association Studies

LC: Liquid chromatography

LC-MS/MS: Liquid chromatography tandem mass spectrometry

LOAD: Late-onset Alzheimer's disease

LFQ: Label-free quantification

LysC: Lysyl endopeptidase

MCI: Mild cognitive impairment

MDS: Multidimensional scaling plots

MoCA: Montreal Cognitive Assessment

MMSE: Mini-Mental Status Examination

MS: Mass spectrometry

NFT: Neurofibrillary tangles

NIA-AA: National Institute on Aging and Alzheimer's Association

PC: Principal component

PET: Positron emission tomography

PHF: Paired helical filaments

pTau₁₈₁: Phosphorylated Tau₁₈₁

QC: Quality controls

ROC: Receiver operating characteristic

SRM: Selected reaction monitoring

TMT: Tandem Mass Tag

tTau: Total Tau

WGCNA: Weighted Gene Co-expression Network Analysis

LIST OF PROTEINS

ADAM10: ADAM Metallopeptidase Domain 10

ADAM17: ADAM Metallopeptidase Domain 17

ADM: Adrenomedullin

AICD: Amyloid Precursor Protein Intracellular Domain

ALB: Albumin

ALDOA: Aldolase

ANG: Angiogenin

ANG1: Angiopoietin-1

ANP: Atrial Natriuretic Peptide

ANXA5: Annexin A5

APLP1: Amyloid Beta Precursor Like Protein 1

APOE: Apolipoprotein E

APP: Amyloid Precursor Protein

BASP1: Brain Abundant Membrane Attached Signal Protein 1

BGN: Biglycan

BIN1: Bridging Integrator 1

BNP: B-Type Natriuretic

CACNA2D: Calcium Voltage-Gated Channel Auxiliary Subunit Alpha 2/Delta

CADM3: Cell Adhesion Molecule 3

CAMK2A: Calcium / Calmodulin Dependent Protein Kinase II alpha

CD33: CD33 Molecule

CTF83: C-terminal Fragment 83

CTF99: C-terminal Fragment 99

CTSB: Cathepsin B

CTSH: Cathepsin H

CTSZ: Cathepsin Z

C1QA: Complement C1q A Chain

C1QB: Complement C1q B Chain

C1QC: Complement C1q C Chain

C1RL: Complement C1r Subcomponent Like

C2: Complement C2

C3: Complement C3

ECM2: Extracellular Matrix Protein 2

ENO2: Enolase 2

F5: Coagulation Factor V

FGB: Fibrinogen

FLNA: Filamin A

GAPDH: Glyceraldehyde-3-Phosphate Dehydrogenase

GAP43: Growth Associated Protein 43

GDA: Guanine Deaminase

GOT1: Glutamic-Oxaloacetic Transaminase 1

HEXA: Hexosaminidase Subunit Alpha

HEXB: Hexosaminidase Subunit Beta

ICAM1: Intracellular adhesion molecule 1

IDUA: Alpha-L-iduronidase

IGFBP7: Insulin Like Growth Factor Binding Protein 7

IGSF8: Immunoglobulin Superfamily Member 8

LAMA5: Laminin Subunit Alpha 5

LAMC1: Laminin Subunit Gamma 1

LCP1: Lymphocyte Cytosolic Protein 1

LDHB: Lactate Dehydrogenase B

LINGO2: Leucine Rich Repeat and Ig Domain Containing 2

LTBP4: Latent Transforming Growth Factor Beta Binding Protein 4

L1CAM: L1 Cell Adhesion Molecule

MAPT: Microtubule Associated Protein Tau

MYL6: Myosin Light Chain 6

NBL1: Neuroblastoma Suppressor Of Tumorigenicity 1

NID2: Nidogen 2

NPTXR: Neuronal Pentraxin Receptor

NPTX1: Neuronal Pentraxin 1

NPTX2: Neuronal Pentraxin 2

NEFL: Neurofilament Light Chain

NEFM: Neurofilament Medium Chain

NEGR: Neuronal Growth Regulator 1

NEO1: Neogenin 1

NRGN: Neurogranin

NRN1: Neuritin 1

OLFM1: Olfactomedin 1

OPN: Osteopontin

PAI1: plasminogen activator inhibitor-1

PAM: Peptidylglycine Alpha-Amidating Monooxygenase

PARK7: Parkinsonism Associated Deglycase

PCSK1: Proprotein Convertase Subtilisin/Kexin Type 1

PICALM: Phosphatidylinositol Binding Clathrin Assembly Protein

PKM: Pyruvate Kinase M1

PLXNA2: Plexin A2

PPIA: Peptidylprolyl Isomerase A

PSEN1: Presenilin 1

PSEN2: Presenilin 2

PTPRN: Protein Tyrosine Phosphatase Receptor Type N

RTN4R1: Reticulon 4 Receptor

S100A11: S100 Calcium Binding Protein A11

SCG2: Secretogranin II

SDCBP: Syndecan Binding Protein

SHARPIN: Shank Associated RH Domain Interactor

SLIT1: Slit Guidance Ligand 1

SMOC1: Secreted Modular Calcium-binding Protein I

SNCB: Synuclein Beta

SNX1: Sorting Nexin 1

SORL1: Sortilin Related Receptor 1

SORT1: Sortilin 1

SPDGFRB: Soluble Platelet-Derived Growth Factor Receptor-Beta

SYN1: Synapsin 1

SYT1: Synaptotagmin 1

TMEM106B: Transmembrane Protein 106B

TPI1: Triosephosphate Isomerase 1

TREM2: Triggering Receptor Expressed on Myeloid Cells 2

TSPAN14: Tetraspanin 14

VCAM1: vascular cell adhesion molecule 1

VCAN: Versican

VEGFA: Vascular Endothelial Growth Factor A

VGEF: Vascular Endothelial Cadherin

VGF: VGF Nerve Growth Factor Inducible

VSTM2A: V-set and Transmembrane Domain Containing 2a

WDR81: WD Repeat Domain 81

YWAHB: Tyrosine 3-Monooxygenase/Tryptophan 5-Monooxygenase Activation Protein Beta

YWHAE: Tyrosine 3-Monooxygenase/Tryptophan 5-Monooxygenase Activation Protein Epsilon

YWHAG: Tyrosine 3-Monooxygenase/Tryptophan 5-Monooxygenase Activation Protein Gamma

YWHAZ: Tyrosine 3-Monooxygenase/Tryptophan 5-Monooxygenase Activation Protein Zeta

**CHAPTER 1:
INTRODUCTION**

1.1 The increasing burden of Alzheimer's disease (AD)

Alzheimer's disease (AD) is a progressive and irreversible disorder of the brain that affects memory, thinking, and behavior (1). It is the most common form of dementia, accounting for approximately 60 to 80 % of all dementia cases (2). AD primarily affects older adults, typically starting in individuals over the age of 65 years old (2-6). Notably, the elderly population in the United States has been undergoing rapid expansion since 2011 as the first wave of baby boomers transitioned into the age of 65 (7). The baby boom era, which spanned from 1946 to 1964, marked a distinctive phase in American history characterized by a surge in birth rates following World War II (7). Consequently, with the progression of the baby boomer population from middle to older ages, there has also been a substantial increase in the incidence of AD (7; 8). Up from approximately 4.7 million people in 2010, an estimated 6.7 million people in the United States are currently affected by this disease, and this number is only expected to double by the year 2050 (2; 7; 8) (**Figure 1.1**). Alongside this rise, there also comes the substantial burden the disease places on caregivers and society (2; 8). In 2022 alone, over 11 million Americans selflessly provided 18 billion hours of unpaid care to older adults afflicted with dementia; a collective contribution valued at nearly \$340 billion (2). Furthermore, total annual payments for healthcare and long-term care for people with AD and other dementias are expected to increase from \$345 billion in 2023 to just under \$1 trillion by 2050, exceeding the costs of treatments for cancer and cardiovascular disease (2; 9). This projection includes three-fold increases in government spending in Medicare and Medicaid, as well as out-of-pocket expenditures (2). Taking into account all of these factors, if there is no progress made in preventing or delaying the onset of AD, coupled with the substantial rise in the number of individuals affected by AD, the proportion of the population impacted by the disease will also increase. This, in turn, will escalate the overall societal burden of AD.

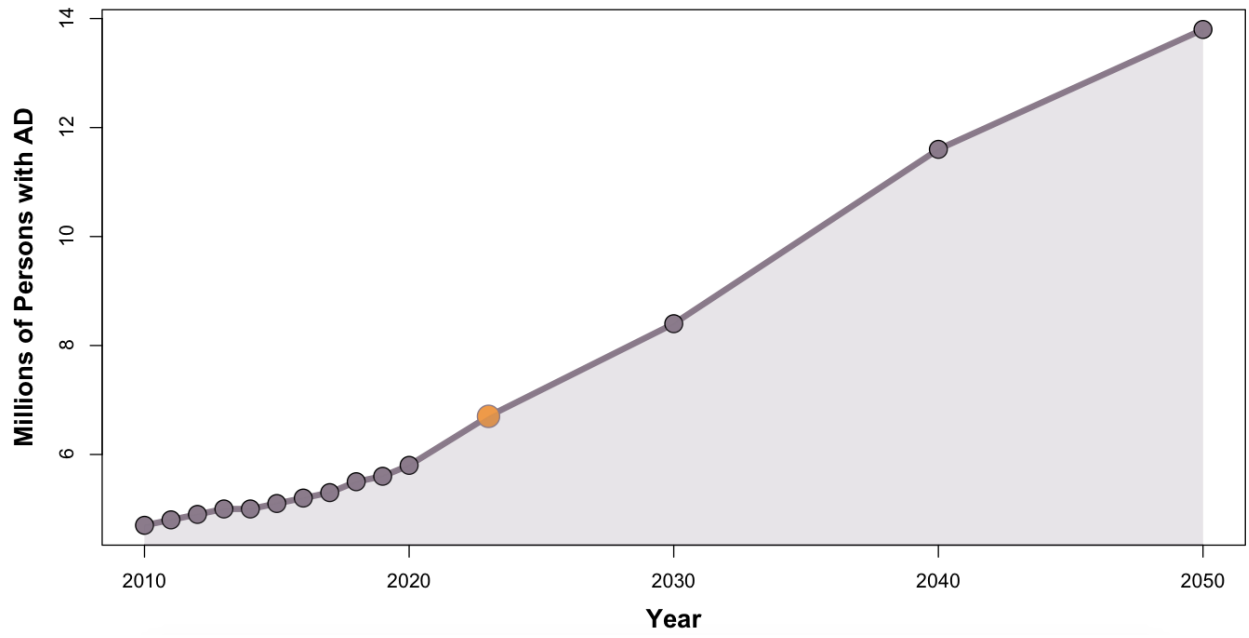
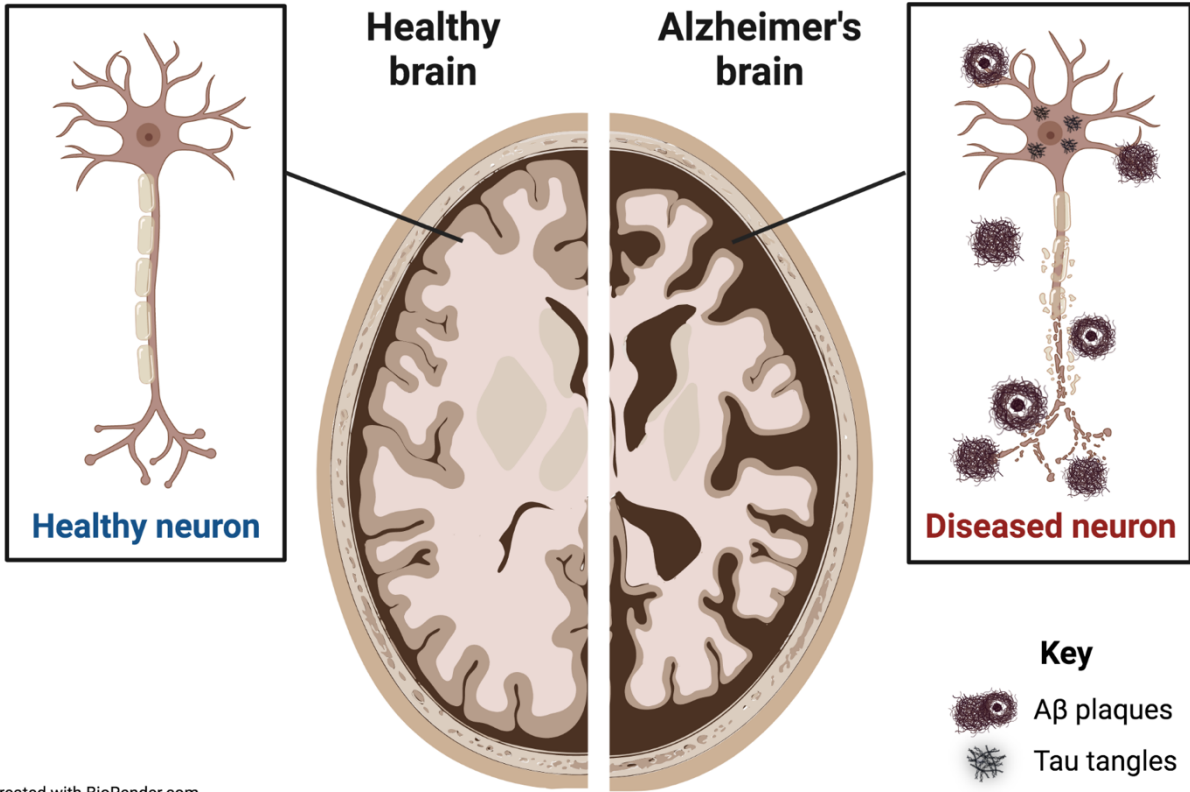


Figure 1.1: Projected number of people in the United States with Alzheimer’s disease (AD) in millions from 2010 to 2050. The estimated number of people with AD in the United States in 2023 (orange circle) is predicted to nearly double by 2050.

1.2 Monitoring memory loss in those with AD

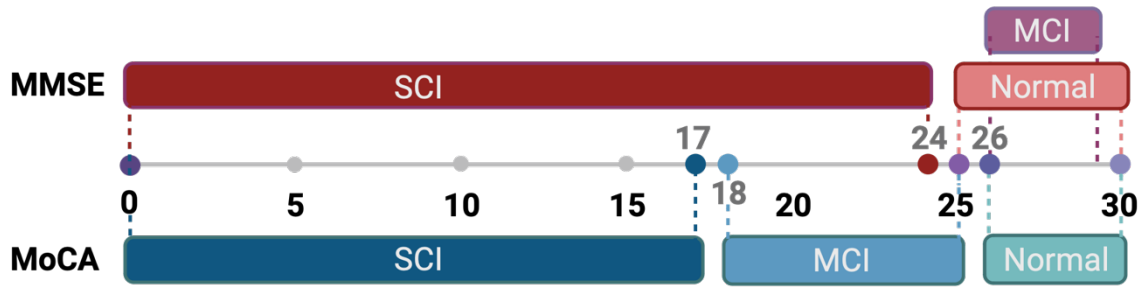
AD can be most notably recognized by its incapacitating and progressive memory loss. This gradual decline in memory with disease progression is a consequence of spreading neuronal damage across the brain (**Figure 1.2**) (1; 2). Common early signs of memory loss in AD include forgetfulness, difficulty in finding words, misplacing items, and struggling with familiar tasks like tying a shoe (1; 2). As the disease progresses, individuals may begin to experience confusion, mood swings, disorientation, and difficulties in communication and decision-making (1; 2). Ultimately, in the later stages, individuals often require full time care, as they lose the ability to recognize love ones, communicate, and perform basic activities of daily living (1; 2). In the clinic, patients undergo cognitive exams such as the Mini-Mental Status Examination (MMSE) and the Montreal Cognitive Assessment (MoCA). These assessments serve as crucial clinical diagnostic tools for evaluating and monitoring cognitive impairment. (10-12). While the MoCA test is the preferred test for the early detection of dementia such as in cases of mild cognitive impairment (MCI), MMSE is often used for monitoring cognitive decline over time (11; 13).

MCI is an intermediate stage between typical cognitive aging and dementia (11). In the beginning, physicians heavily depended on the MMSE to gauge cognitive impairment in individuals (12). The MMSE was found to be effective in distinguishing cognitively normal individuals from those with cognitive impairment with significant specificity, where a score below 25 on the MMSE was indicative of impairment (12) (**Figure 1.3**). Its efficacy declined, however, when attempting to identify those with MCI, as individuals with MCI could score between 26 and 29, falling within the range for cognitively normal individuals (14-16) (**Figure 1.3**). This highlighted a significant limitation of the test: its difficulty in detecting early dementia-related changes (17). Consequently, the MoCA test was developed with a heightened emphasis on MCI, while maintaining the scoring ranges of the MMSE (11). Aligned with this, the generally accepted optimal threshold for discerning between individuals with typical cognitive function and those with



Created with BioRender.com

Figure 1.2: Healthy brain compared to a brain affected by Alzheimer's disease. In comparison to a healthy brain, brain changes observed in Alzheimer's disease include injured neuronal cells that are accompanied by abnormal accumulations of amyloid beta ($A\beta$) plaques and tangles of hyperphosphorylated Tau.



Created with BioRender.com

Figure 1.3: A comparison of the scoring patterns of the Mini-Mental State Examination (MMSE) with the Montreal Cognitive Assessment (MoCA).

MCI in the MoCA test was determined to be 26 (11) (**Figure 1.3**). Though, more recent meta-analysis has suggested that a cutoff score of 23 may be better (18). Moreover, individuals with MCI may score between 18 and 25, while those with dementia typically scored below 18 with significant specificity (**Figure 1.3**). Overall, the MoCA test has demonstrated superior effectiveness compared to the MMSE in monitoring the progression from MCI to severe dementia in clinical settings involving living patients (19-22).

There are various factors to consider when utilizing the specified scores mentioned above. Firstly, studies have indicated that education can significantly impact overall MoCA score (11; 23). It was found that persons with 12 years of education or less tended to have worse performance on the MoCA (11). To mitigate this, it has become common practice to add 1 point to the final score for individuals with 12 years or less of education (11). There is debate, however, as to whether this adjustment adequately addresses education-related disparities (24). In some cases, it has been observed that this adjustment may in fact reduce the test's sensitivity (25). Besides education, age can also impact the score (23; 26; 27). This places older individuals with lower levels of education as the group most vulnerable to obtaining false positive results (24). Finally, studies have revealed that MoCA performance can also be influenced by racial background (26; 28; 29). Including minority participants in a study led to lower cutoffs for distinguishing between normal cognition and MCI (26; 28; 29). In addition, when directly comparing optimal MoCA score cutoffs across multiple races, it was found that the optimal cutoff for both African Americans and Hispanics was lower than that of Caucasians (30). This implies that lower MoCA cutoffs may be more appropriate when assessing the MoCA score of minority individuals (26; 28-30). In conclusion, considering factors such as education, age, and racial background is essential for accurately interpreting and applying MoCA scores in clinical settings.

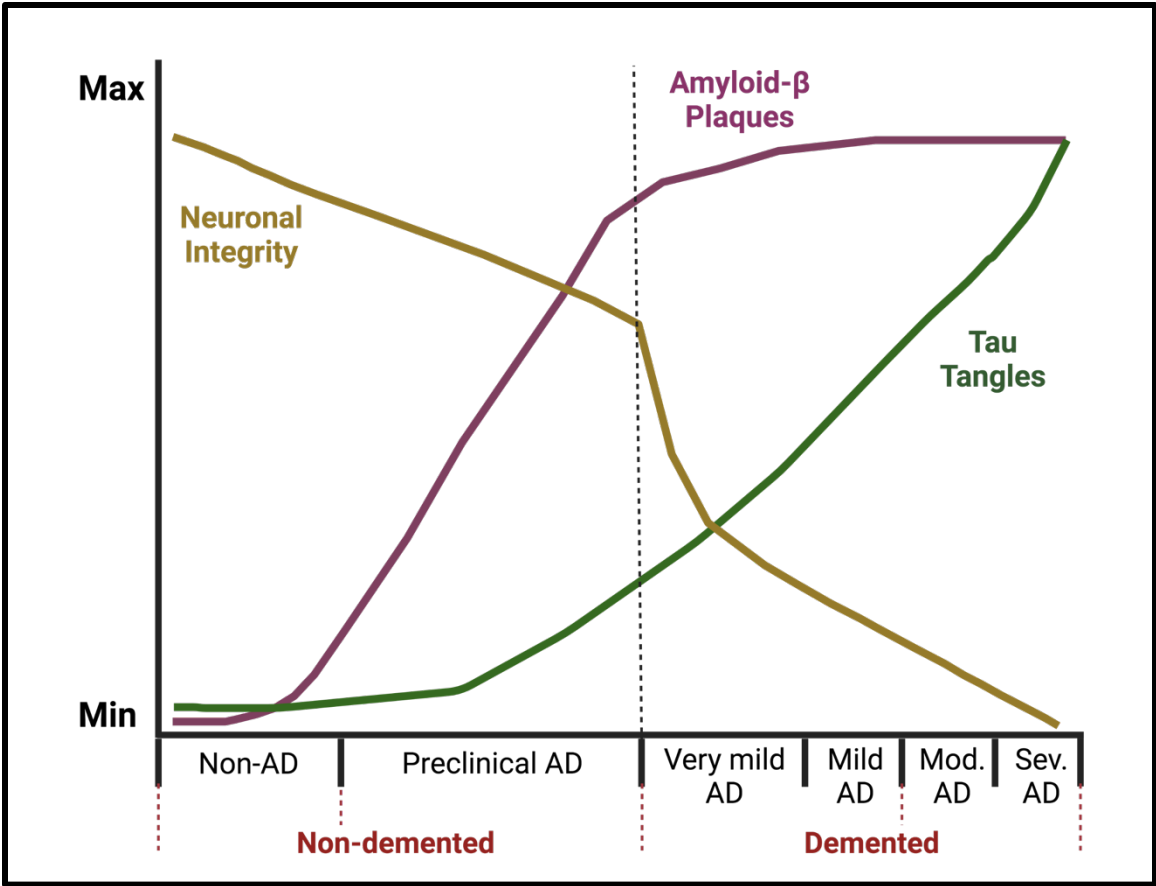
1.3 The initial discovery of AD

Alois Alzheimer was a German psychiatrist and neuropathologist who discovered AD through his work with a patient named Auguste Deter. In 1901, Deter, who was in her early 50s,

was admitted to the mental asylum where Alzheimer worked for exhibiting symptoms of memory loss, confusion, and hallucinations (31). Intrigued by her condition, Alzheimer meticulously documented the continued progression of her disease up until her death on April 6, 1906. Following her death, Alzheimer was able to investigate the brain of Auguste both morphologically and histologically. During the autopsy, Alzheimer noted significant abnormalities in her brain, including unusual protein deposits (now identified as amyloid plaques) and tangled nerve fibers (now known as neurofibrillary tangles) (31; 32). These observations led him to hypothesize that Deter's symptoms stemmed from physical changes in her brain (31). Shortly thereafter, Alzheimer published his findings, presenting the case as a distinct form of dementia that differed from the typical symptoms associated with aging (31). His work laid the groundwork for understanding Alzheimer's disease as a progressive neurodegenerative disorder characterized by cognitive decline and distinct brain pathology. Today, the disease bears Alois Alzheimer's name in recognition of his pioneering research.

1.4 Neuropathological hallmarks of AD

1.4.1 Amyloid Cascade: The amyloid cascade hypothesis is a central theory in AD research that proposes that the deposition of amyloid-beta ($A\beta$) peptides in the brain occurs prior to and initiates a series of events that culminate in neurodegeneration and the distinctive symptoms of AD (**Figure 1.4**). More specifically, according to this hypothesis, the abnormal accumulation of $A\beta$ peptides leads to the formation of amyloid plaques, which disrupt neuronal function and activate inflammatory responses (33). As a consequence, a cascade of subsequent events is initiated, including the hyperphosphorylation of Tau protein, the formation of neurofibrillary tangles, synaptic dysfunction, and ultimately neuronal death (32). Given its crucial role, the formation and inhibition of $A\beta$ has profoundly shaped investigations into the underlying mechanisms of AD and the creation of potential therapeutic approaches, which primarily focused on $A\beta$ pathways (32; 33). The abnormal accumulation of insoluble $A\beta$ plaques in the extracellular space surrounding neurons has become a hallmark pathology of AD (34; 35) (**Figure 1.2**). $A\beta$ is

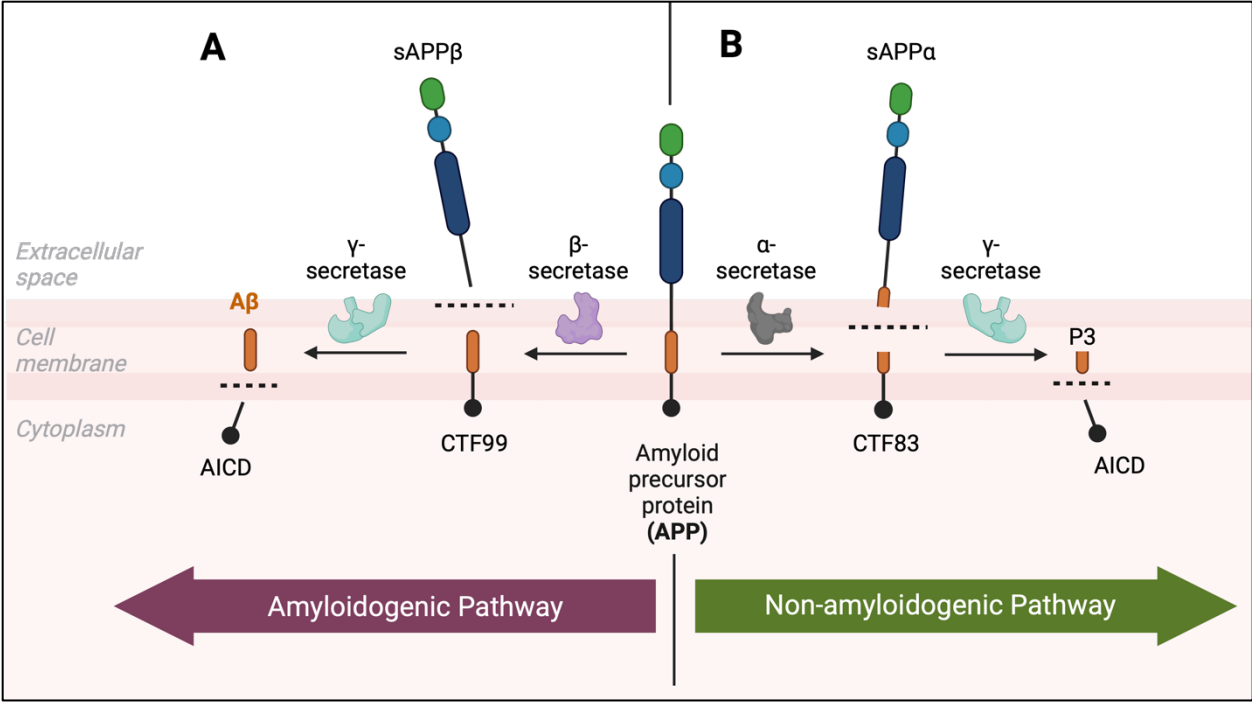


Created with BioRender.com

Figure 1.4: Hypothesized time course of neuropathological and clinical changes in Alzheimer's disease based on biomarker alterations. In Alzheimer's disease (AD), the conversion from a non-demented to demented state is associated with a buildup of amyloid beta (A β) plaques (purple line), a more gradual accumulation of neurofibrillary Tau tangles (green line), and neuronal and synaptic loss (yellow line). Modified from Craig-Schapiro, R., Fagan, A. M., and Holtzman, D. M. (2009) Biomarkers of Alzheimer's disease. *Neurobiol Dis* 35, 128-140.

a peptide ranging from 38-43 amino acids long and is the result of sequential cleavages on amyloid precursor protein (APP) by β -secretase and γ -secretase (36) (**Figure 1.5A**). Initially, APP is cleaved by β -secretase producing a long soluble secreted form of APP (sAPP β) and a C-terminal fragment 99 (CTF99) (37) (**Figure 1.5A**). Subsequently, CTF99 is cleaved by γ -secretase complex to form A β and an intracellular amyloid precursor protein intracellular domain (AICD) (38) (**Figure 1.5A**). This cleavage can produce peptides of 43, 45, 46, 48, 49, or 51 amino acids, which are subsequently processed to generate two forms of A β , A β_{40} or A β_{42} (39). While A β_{40} is the most prevalent form, A β_{42} has been noted to be more prominently present in amyloid plaques (40). Because this pathway leads to the formation of the A β peptides that make up the plaques found in AD, its considered amyloidogenic and is associated with the pathological changes observed in AD. The accumulation of A β peptides in the brain is central to the amyloid cascade hypothesis, even though A β can be extensively present in the human brain without AD symptoms (36; 41-43) (**Figure 1.4, purple line**). The production of A β peptides is not the sole outcome of APP processing. Alternatively, APP can also undergo cleavages that diverts the protein toward a non-amyloidogenic pathway (**Figure 1.5B**). Here, α -secretase cleaves APP to release soluble APP α (sAPP α) and CTF83 (**Figure 1.5B**). Importantly, this pathway prevents the generation of A β as the cleavage site for α -secretase is within the A β domain (37). γ -secretase then cleaves CTF83 to form AICD and p3. This neuroprotective pathway promotes neuronal survival, neurite outgrowth and neural stem cell proliferation, providing an avenue for mitigating AD (44-47). Under typical circumstances, these two pathways operate in equilibrium, permitting neurons to remove unnecessary A β as required. Nevertheless, in AD, the balance shifts towards heightened A β formation, triggering the cascading events described earlier.

1.4.2 Pathologic Tau: The next hallmark of AD is the formation of neurofibrillary tangles (NFT) that consist of hyperphosphorylated microtubule-associated protein Tau (MAPT). Tau is primarily located intracellularly within neurons, but it can also be found in other cell types of the



Created with BioRender.com

Figure 1.5: The amyloidogenic and non-amyloidogenic pathways for processing the amyloid precursor protein (APP). **(A)** The amyloidogenic pathway involves cleavages by β -secretase and γ -secretase resulting in the generation of a long-secreted form of APP (sAPP β), and C-terminal fragments, CTF99, amyloid precursor protein intracellular domain (AICD), and A β . **(B)** The nonamyloidogenic pathway involves cleavages by α -secretase and γ -secretase resulting the generation of a long-secreted form of APP, sAPP α , and C-terminal fragments, CTF83, AICD, and P3.

brain, such as microglia (34; 35). In the brain, normal Tau protein plays a crucial role in promoting tubulin assembly and microtubule stabilization. Microtubules are essential structures for maintaining the structural integrity of neurons and facilitating intracellular transport, acting like highways within neurons, allowing molecules and organelles to move to different parts of the cell. Tau protein binds to and stabilizes these microtubules, helping to maintain their structure and function. In addition to this, Tau is also involved in regulating synaptic function, which is essential for communication between neurons. It interacts with various proteins involved in synaptic transmission, contributing to the proper functioning of synapses. Overall, normal Tau protein in the brain is involved in maintaining the structural integrity of neurons by stabilizing microtubules and regulating synaptic function; both of which are critical for normal brain function.

The distinction between normal Tau and pathologic Tau primarily lies in several structural and functional characteristics: conformation, phosphorylation, and aggregation (1). Normal Tau protein is typically structured in a way that allows it to bind and stabilize microtubules within neurons. In contrast, pathological Tau undergoes conformational changes, leading to the formation of abnormal Tau aggregates, such as NFTs (48). In addition to conformational changes, phosphorylation, which is the addition of phosphate groups to proteins, plays a crucial role in deciphering Tau's normal function from that of pathologic Tau. Under normal conditions, Tau is moderately phosphorylated, allowing it to bind and unbind to microtubules effectively. However, in AD, Tau becomes hyperphosphorylated, leading to its detachment from microtubules and the formation of insoluble aggregates (3). Under normal conditions, Tau remains soluble and distributed throughout the neuron, and primarily associated with microtubules. Pathological tau, on the other hand, aggregates into insoluble structures, such as paired helical filaments (PHFs) and NFTs which disrupt neuronal function. These insoluble structures then obstruct transport of essential nutrients and molecules vital for the regular function and survival of neurons (1), making it a more immediate precursor to neurodegeneration (**Figure 1.4, green and yellow lines**) (49-51).

1.5 The ATN framework for staging AD progression

As defining features of AD, A β deposition (A), Tau tangle formation (T), and neurodegeneration (N) make up the basis of the ATN framework (52). Essentially, this framework proposes different sets of biomarkers to represent hallmark pathological features (A β and Tau) and cognitive aspects (neurodegeneration) of AD, utilizing them to categorize patients along the AD continuum (52). In this framework, amyloid biomarkers represent the earliest indicators of AD neuropathological changes in living persons (53-57). Given this, A β biomarkers help determine whether an individual falls within the AD continuum (52). Examples of biomarkers indicative of A β plaques include amyloid positron emission tomography (PET) imaging of radiolabeled ligands binding to A β plaques in the brain and reduced levels of A β_{42} in cerebrospinal fluid (CSF) (58-62). The quantification of both A β and Tau are required for the diagnosis of AD. Therefore, the presence of pathologic Tau biomarkers is what ultimately determines whether an individual within the AD continuum truly has AD (52). Examples of Tau biomarkers include monitoring elevations in the phosphorylation of Tau at residues Thr181, Thr217, and among other sites (59) within the CSF and PET scans of cortical Tau using radiolabeled ligands that bind to Tau tangles (59; 63-65). Finally, biomarkers of neurodegeneration gauge the severity of neuronal injury. However, these markers do not strictly contribute to the understanding of where a person lies along the AD continuum (52). This is because these markers are not specific to neurodegeneration induced by AD, making it difficult to determine whether neuronal injury is directly attributed to disease or some other comorbid condition (52). Despite this, indicators of neurodegeneration still provide vital staging information when combined with measures of pathologic biomarkers for A β and Tau (52). Biomarkers of neurodegeneration include total Tau levels in the CSF, cortical PET scans measuring diminished glucose metabolism, and indicators of brain atrophy detected through magnetic resonance imaging (66-73).

1.6 Early-onset AD versus late-onset AD

The majority of people who develop AD are 65 and older. The presentation of AD at older ages is referred to as late-onset AD (LOAD). It is believed that LOAD, like other chronic diseases, is brought on as result of multiple factors, i.e. environmental and genetics, rather than a single genetic cause. The exception to these would-be cases of AD related to uncommon genetic changes that greatly affect risk. In those cases, the person typically develops AD before the age of 65. This presentation of AD at younger ages is referred to as early-onset AD (EOAD). While the greatest risk factors for LOAD are older age, environmental exposures (i.e lifestyle, education, financial attainment), and genetics, EOAD is primarily caused by genetics alone (74-80).

1.6.1 Early-onset AD: EOAD accounts for only ~2 percent of all cases. Individuals who experience familial AD experience rapid decline and die within several years of symptom onset (81). EOAD has been most notably tied to gene mutations that affect the processing or production of A β , whose abnormal accumulation contributes to disease. For this reason, despite being on different chromosomes, mutations in *APP*, *PSEN1*, or *PSEN2* are known to cause AD (5; 82-85). Remarkably, both *PSEN1* and *PSEN2* make up the catalytic components of γ -secretase which assists in the cleavage of APP into A β . In addition to these three genetic variants that are known to cause AD, individuals with Down syndrome are often at high risk for developing EOAD (2). This is because they possess an extra chromosome 21, which carries the *APP* gene. Estimates suggests that nearly 50% or more of individuals living with Down syndrome will develop symptoms of AD by their 50s or 60s (86; 87).

1.6.2. Late-onset AD: Contrary to EOAD, LOAD is the most common form of AD, mainly occurring in individuals over 65 (3-6). Also known as sporadic AD, LOAD accounts for the remaining 98% of cases (2; 81). Multiple gene loci have been implicated in LOAD. As a result, LOAD is often considered a polygenic disorder (2). One of the most impactful genetic susceptibilities to LOAD involves the Apolipoprotein E gene (5; 88; 89). Apolipoprotein E (APOE) epsilon (ϵ) protein has three different variants that differ at residues 112 and 158: APOE ϵ 2

contains a cysteine at both residues 112 and 158 while APOE ϵ 3 contains a cysteine at residue 112 but an arginine at residue 158. Lastly, APOE ϵ 4 has two arginine residues that occupy position 112 and 158 in the full-length protein. Those who inherit a copy of the APOE ϵ 4 allele have three times the risk of developing AD while those who inherit two copies have an eight- to 12-fold risk (90-92). Contrastingly, the inheritance of the APOE ϵ 3 allele has no risk of developing AD while the APOE ϵ 2 offers some protection. Although genetic studies support that APOE is the largest modifier of an individual's risk of developing LOAD, half of the individuals with LOAD do not possess an APOE ϵ 4 allele indicating that other loci influence LOAD development. Innovations in genomic sequencing technology have allowed for the identification of other genetic polymorphisms linked to AD through genome wide association studies (GWAS). Such genes include genes that encode for proteins involved in the dysregulation of microglia (CD33, SHARPIN, TREM2), α -secretase (ADAM10, ADAM17, TSPAN14), endocytosis (BIN1, PICALM, WDR81), the lysosome (CTSB, CTSH, IDUA, TMEM106B), and sorting receptors (SORL1, SORT1, SNX1) (93; 94). More genes are expected to be revealed as genomic studies continue to expand and grow in sample size and ethnic background.

1.7 Risk factors for AD

1.7.1 Age: The most significant contributor to AD risk is age (2; 74). This is evident by the steep increases in the percentage of people with AD with advancing age. For example, five percent of individuals between 65 and 74 years old have AD which then increases to 13.1 % for those aged from 75 to 84 (95). By the time one reaches 85, this number doubles, affecting 33.3% of this population range (95). It is worth highlighting again that these prevalence statistics are projected to steadily increase as the baby-boom generation continues to move throughout these age ranges (8; 95). Although age plays a major role in risk, AD is not a natural outcome of the aging process; in other words, simply reaching an older age is not adequate enough to trigger the onset of AD (96).

1.7.2 Sex: Approximately two-thirds of AD patients are women (97). While men have only a 1 in 10 chance of developing AD, women's likelihood is twice as high, 1 in 5 (95). Although it has been speculated that women's heightened risk of developing AD could be due to their longer lifespan, studies indicate that differences in several biological factors such as sex hormones, immune response, and metabolic regulation can modulate risk (98). One significant factor affecting risk is the sex hormone, estrogen. Estrogen receptors are distributed throughout the brain, regulating various physiological processes, some of which exert protection against AD pathology. Studies show that estrogen achieves this protective effect by stimulating the generation of vesicles containing APP from the Golgi network (99; 100). This mechanism then facilitates the transport of APP to the cell surface where, it either undergoes cleavage by α -secretase, yielding the soluble and neuroprotective molecule, sAPP α , or is re-internalized through an endosomal/lysosomal degradation pathway (101-103). Both of which precludes the production of insoluble A β peptide (99-104). Additionally, estrogen has been shown to decrease the presence of hyperphosphorylated Tau and increase the presence of dephosphorylated of Tau (105). In the perimenopausal phase, however, which occurs 1-4 years prior to menopause, estrogen levels fluctuate significantly. This variability contributes to dysfunction in metabolic, inflammatory, and sensory-processing pathways associated with estrogen (106; 107). Consequently, the eventual loss of estrogen during menopause contributes to females' susceptibility to AD (108; 109). In contrast, men do not undergo an equivalent of perimenopause. Instead, they experience a gradual decline in testosterone (110). This gradual transition elucidates the age-related dysfunction in male hormonal pathways compared to those in females (110).

1.8 Modifiable risk factors for AD

1.8.1 *Role of modifiable risk factors in AD:* Although age and sex cannot be changed, some risk factors can be modified to reduce the risk of cognitive decline and dementia without relying on a cure or medicine (111). In fact, studies suggest that addressing modifiable risk factors may prevent or delay up to 40% of all dementia cases (112). Notably, nearly a third of cases of

AD and other dementias in the United States are associated with at least one of eight modifiable risk factors: physical activity, smoking, depression, low education, diabetes, midlife obesity, midlife hypertension, and hearing loss (113). Of these, the greatest factors to AD risk have been shown to be midlife obesity, physical inactivity, and low educational attainment (113).

Timing also holds significant importance in relation to modifiable risk factors in that the age in which these risk factors develop affects the impact on AD risk. For example, developing obesity, hypertension, and high cholesterol during midlife can elevate one's risk of dementia in later stages of life (114-120). For example, those between 40 and 79 years old lacking a number of modifiable risk factors (low education, hypertension, hearing loss, traumatic brain injury, alcohol or substance abuse, diabetes, smoking and depression) have been shown to exhibit cognitive performance akin to individuals 10-20 years younger with multiple modifiable risk factors (121). Conversely, the onset of obesity and hypertension in late life, after the age of 80, is associated with a reduced risk in dementia (122; 123). Moreover, addressing modifiable risk factors during midlife was connected to decreased dementia risk, even among individuals with a heightened genetic predisposition to dementia (124). In essence, while genetic inheritance is unalterable, exerting an influence on cognitive function becomes feasible by avoiding modifiable risk factors.

1.8.2 Cardiovascular health: The interdependence between brain health and cardiovascular health has been recognized for a considerable time. This connection is likely rooted in the fact that, despite accounting for just 2% of the body's weight, the brain utilizes approximately 20% of the body's oxygen and energy resources. In this context, a healthy heart is crucial for facilitating adequate blood supply to the brain, while healthy blood vessels ensure the delivery of oxygen and nutrient-rich blood to this vital organ. As a result of this intricate relationship between brain and cardiovascular health, many factors that increase the risk of cardiovascular disease are also associated with a higher risk of dementia (125). Notably, these factors encompass conditions such as hypertension and diabetes (114; 116; 118; 119).

1.8.3 Smoking / physical activity / diet: Due to the close relationship between cardiovascular health and brain function, behaviors that impact the heart's well-being can also influence the brain, thereby affecting the risk of developing dementia. Not surprisingly, smoking has been associated with an elevated risk of dementia (126), whereas engaging in physical activity has been shown to decrease risk (127-136). Now despite extensive exploration into various forms of physical activity, determining the specific types, frequencies, and durations that yield the most significant reduction in risk remains an ongoing challenge. In addition to physical activity, emerging evidence suggest that adhering to a heart-healthy diet could decrease one's risk of dementia (137-142). A heart-healthy diet places emphasis on fruits, vegetables, whole grains, fish, poultry, nuts, legumes, and beneficial fats such as olive oil while simultaneously limiting the intake of saturated fats, red meat, and sugar (2).

1.9 Social determinants of health

Historically, the healthcare sector bore the primary responsibility for addressing health and disease concerns, as it was widely recognized for its role in delivering care to those most in need (143). However, it's increasingly evident that medical care alone is not sufficient to improve health outcome or mitigate health disparities (144). In fact, research suggests that differences in life expectancy and disease prevalence among various demographics are largely shaped by the conditions in which individuals are raised, live, work, and age (143). These nonmedical factors, encompassing socioeconomic status, educational attainment, job opportunities, social support networks, healthcare accessibility, and the quality of the physical environment, profoundly influence health outcomes and overall well-being, and are collectively referred to, today, as social determinants of health (143). Some of these factors that most notably affect disease risk include education, employment, income, environment, discrimination and exposure to stress.

1.9.1. Education: Education can improve health by increasing health knowledge and healthy behaviors (144). In support of this, higher educational attainment has been linked to engaging in health-promoting behaviors and adopting health-related recommendations earlier

(145; 146). This could partially be attributed to literacy (147; 148). It is believed that literacy enables individuals with higher education levels to make more informed health-related decisions for themselves and their families (147; 148). Education also holds significance in health by influencing employment opportunities (144). Higher levels of education are associated with reduced unemployment rates, a factor strongly correlated with poorer health and increased mortality (149). Similarly, individuals with higher educational attainment are more inclined to hold positions offering healthier physical working environments, superior health-related benefits, and higher compensation (150; 151). Lastly, education may also affect health by influencing social and psychological factors where higher education levels have been correlated with heightened perceived personal control, a factor frequently associated with improved health outcomes and health-related behaviors (145; 147). In summary, higher levels of education are associated with improved health outcomes because education equips individuals with the knowledge and ability to make healthier choices, to obtain secure employment conducive to better access to healthcare, and to exercise greater personal control over their health.

1.9.2. Employment: The physical aspects of work can have clear impacts on health (144). For instance, occupations involving repetitive movements and/or high physical demands increase the likelihood of workers experiencing muscular or skeletal injuries and disorders (152). Similarly, individuals with sedentary jobs who are physically inactive face elevated risks of obesity and chronic diseases such as diabetes and heart disease (153). Besides physical factors, the psychosocial aspects of work also have an impact on health (144). Psychosocial factors refer to the circumstances wherein a person's social environment, cultural norms, interpersonal relationships, and overall well-being shapes their mindset and behavior. For instance, employees in roles marked by high demands coupled with low control or perceived imbalance of efforts and rewards face an increased risk of experiencing poor health (154; 155). Those who are socially disadvantaged frequently contend with lower wages or income and are typically the ones most likely to confront these health-harming physical and psychosocial conditions in their workplaces

(156). In conclusion, both the physical and psychosocial aspects of work play crucial roles in determining individuals' health outcomes, with socially disadvantaged groups often bearing a disproportionate burden of these adverse conditions, further exacerbating health disparities.

Work can also affect health through the opportunities and resources it provides (144). In general, for most Americans, earnings from employment constitute their primary economic resource. Consequently, health can be influenced by employment-related benefits such as medical insurance, paid leave, flexible scheduling, workplace wellness initiatives, resources for child and elder care, and retirement benefits (144). Positions with higher salaries are likelier to provide benefits, increased financial security, and the means to afford healthier living environments (144). On the flip side, those categorized as the working poor generally earn inadequate income to meet basic needs and are less likely to have access to health-related benefits (157; 158). In summary, the opportunities and resources available through employment significantly impact health outcomes. While higher salaries often come with benefits and financial security conducive to healthier living, those who are poor often face challenges accessing basic necessities and health-related benefits. This underscores how the socioeconomic impacts of employment can contribute to disparities in health.

1.9.3 Environment: There are many characteristics of one's environment and neighborhood that can influence health (144). Regarding physical characteristics, the quality of air and water, along with the accessibility of nutritious foods and safe exercise spaces, can collectively influence an individual's health (159-165). For example, exposure to pollutants, unsafe living conditions, and limited access to green spaces can contribute to respiratory problems, injuries, and chronic diseases such as cardiovascular diseases. In addition to the physical characteristics, the availability and quality of the services a neighborhood offers could also influence health. Services such as schools, transportation, medical care and employment resources can influence health by shaping individuals' opportunities to earn a living (166-168). Interestingly, neighborhood features can be linked to health even when considering individuals

within the same neighborhood (169). Remarkably, some researchers have found poorer health among disadvantaged individuals living in relatively advantaged neighborhoods (170-172). This could be largely due to the adverse psychological effects of feeling worse off than one's neighbors, the perception of having weaker social ties to other residents in the neighborhood, or even having increased exposure to discrimination (173). In conclusion, the environment, or neighborhood, in which one lives plays a significant role in shaping an individual's health outcomes. Beyond the physical aspects such as air and water quality and access to nutritious foods and safe exercise spaces, the availability and quality of neighborhood services also exert considerable influence. Surprisingly, even within the same neighborhood, disparities in health outcomes can persist, highlighting the complex interplay of social and psychological factors. As we continue to explore these dynamics, it becomes increasingly clear that addressing health disparities requires a multifaceted approach that considers not only physical environments but also social and economic factors.

1.9.4 Stress: Coping with daily challenges can be particularly taxing, especially when an individual's financial and social resources are restricted (144). Recent evidence suggests that, in fact, chronic stress connects many social determinants of health and likely plays a causal role in their effects on health (174; 175). Stressful experiences, such as those associated with social disadvantage, like economic hardship and racial discrimination, triggers the release of cortisol, cytokines, and other substances that can damage immune defenses, vital organs, and physiologic systems (174; 176-179). Subsequently, this harm contributes to the accelerated onset or advancement of chronic conditions, such as cardiovascular disease, and the physical toll from chronic stress may hasten the aging process (175; 180-182). In fact, evidence suggest that the accumulated strain from repeatedly attempting to cope with daily challenges, especially with limited resources, may actually cause more physiological damage than a single significantly stressful event would (180). In conclusion, the intricate relationship between chronic stress and health emphasizes the urgent need for comprehensive interventions that address the systemic

inequities contributing to daily challenges. This highlights the increased significance of allocating resources and establishing support systems to address health disparities.

1.9.5 Discrimination and social exclusion: In the United States and many other societies, race or ethnic group is another important social factor that influences health, primarily because of racism (144). It's important to note that the associations between discrimination and health are not uniquely observed in the United States and has been also observed in other countries (178). Racism encompasses not only explicit, intentional acts and beliefs of discrimination, but also entrenched societal systems that, even without explicit discriminatory intent, systematically limit the opportunities and resources available to certain individuals based on their race or ethnic background (144). Racial segregation in residential areas is a critical mechanism by which racism generates and sustains social disadvantage (168; 183). African American and Hispanic individuals are more prone to living in underprivileged neighborhoods characterized by poorly equipped schools, leading to lower educational achievement and quality, which can result in health consequences through the pathways outlined earlier (184). Racism can also have a more direct impact on health by triggering chronic stress. Persistent stress resulting from encounters with racial or ethnic bias, including subtle instances lacking overt prejudicial intent, can potentially contribute to health inequalities based on race or ethnicity, regardless of one's neighborhood, income, or educational attainment (178; 185). In fact, research suggests that African Americans and Hispanic Americans with more education or income are exposed to more discrimination than those who are disadvantaged (144). Acknowledging the widespread impact of racial or ethnic bias on health outcomes underscores the imperative of addressing systemic inequities to achieve genuine health equity.

1.9.6 Final conclusions: Ultimately, insufficient and unequal living conditions arise from flawed social policies, unfair economic structures, and ineffective governance (143). As a result, tackling the social determinants of health necessitates a holistic approach involving government at various levels, civil society, local communities, businesses, international organizations, and

global initiatives (143). Consequently, policies and programs designed to enhance health outcomes must encompass all sectors of society, rather than solely concentrating on healthcare (143). Collaboration among these sectors is crucial for implementing policies and programs that address the root causes of health disparities, especially across racial and ethnic background.

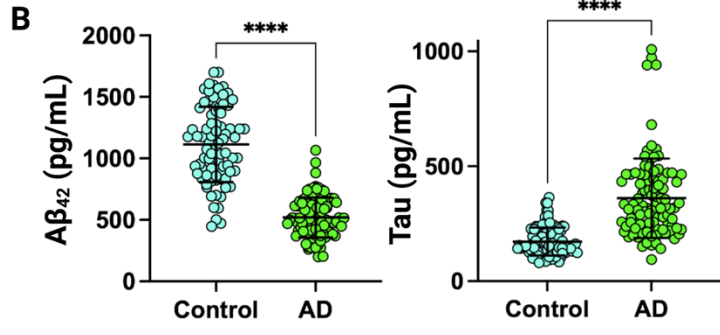
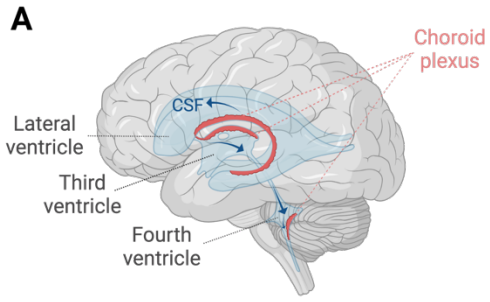
1.10 Therapeutic attempts to slow the progression of AD

Despite decades of research, we still have no disease modifying treatment and no cure. Although the clinical symptoms of AD are frequently diagnosed in older age, the degenerative process of AD can begin many years prior to disease onset where individuals can remain cognitively normal for 10-20 years despite accumulating pathology (**Figure 1.4**) (186-188). Given this, AD has remained an elusive disease to treat and cure. Current treatments available mainly alleviate the cognitive deficits associated with AD. Cholinesterase inhibitors, such as galantamine, rivastigmine, donepezil, and memantine, have remained routine treatment options for the symptomatic relief of mild to moderate AD. Drugs such as these were first implemented to combat the theory that the loss of acetylcholine (ACh) neurons is to blame for the cognitive deficits observed in AD (189). Similarly, declines in nicotinic ACh receptors and M2 muscarinic ACh receptors have been shown to be responsible for AD progression (190; 191). Overall, these treatments have remained ineffective in removing the root of AD pathogenesis, merely targeting symptoms so as to only temporarily improve a patient's cognitive outcome. Consequently, it has become a critical goal of AD research to develop drugs that target the underlying mechanisms and processes involved in the progression of AD. Such therapies would aim to modify the course of the disease by reducing the build-up of A β plaques and Tau tangles, which are hallmarks of AD pathology. For this reason, immunotherapeutic strategies such as A β -directed immunotherapy dominated the AD research for its potential to directly target the plaques associated with disease. Passive immunotherapies, such as bapineuzumab and ALZ 801, relied on the direct injection of monoclonal antibodies into the patient's body, utilizing the immune system to increase clearance of pathologic A β fragments (192). Remarkably, recent amyloid immunotherapy treatments

lacanemab and donanemab were found to not only reduce amyloid burden in the brain but also moderately slow cognitive decline (193; 194). Despite this, however, they were unable to reverse the neuronal loss and cognitive impairments observed in advanced stages of AD (193-196). This failure has been attributed to the initial treatment being administered at too advanced stage of AD in which neuronal damage is severe (195; 197; 198). Thus, it has become a prioritization of AD research to shift towards the early detection and or prevention of AD (52).

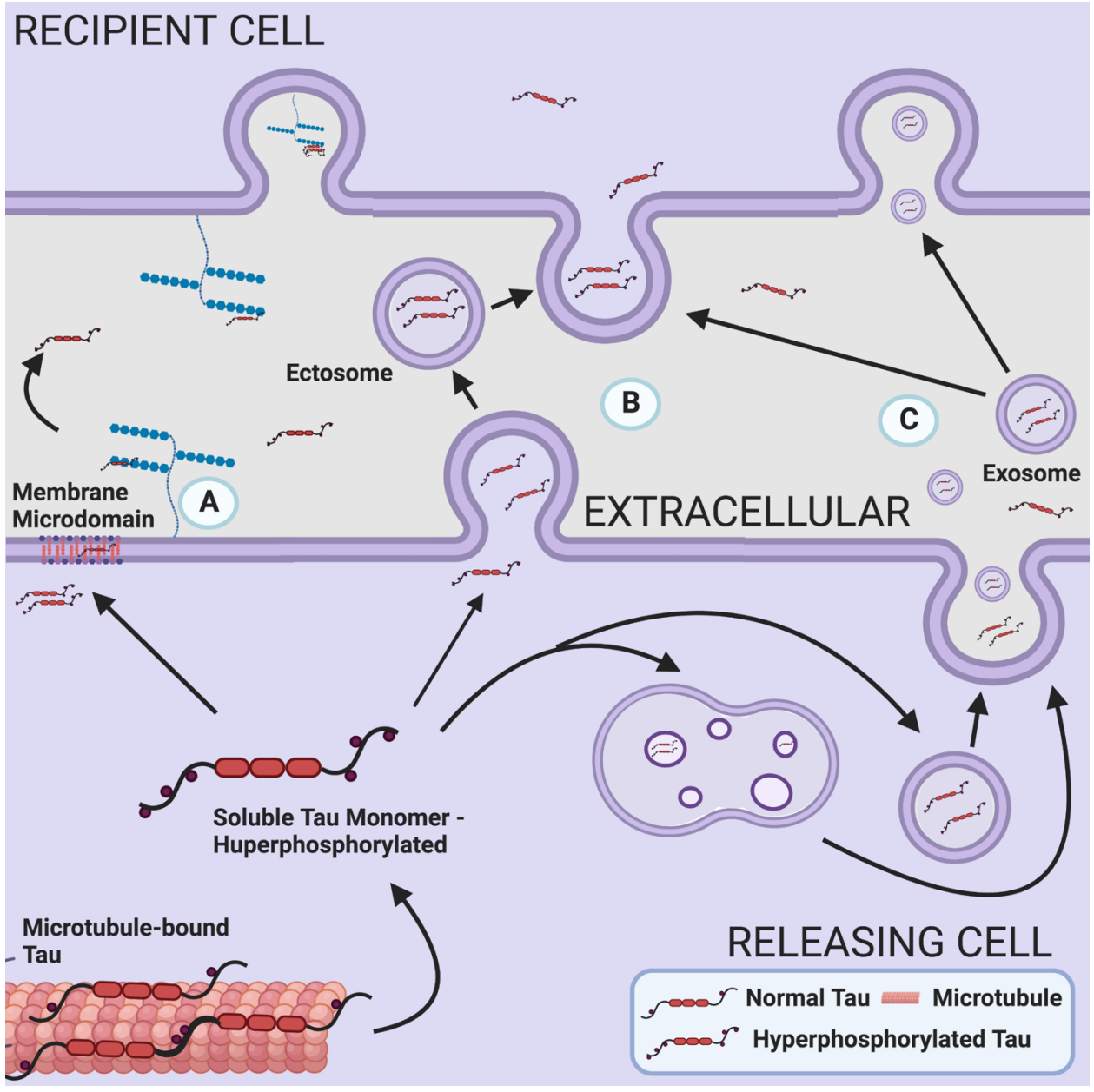
1.11 Cerebrospinal fluid (CSF) as a gateway to neuropathological changes in AD

CSF has become a promising source of biomarkers for the early detection and monitoring of AD in living patients. CSF is made by highly vascularized tissue within the ventricles of the brain called choroid plexus (199). Once created, CSF flows from the lateral ventricles to the third and fourth ventricles, and then into the subarachnoid space and spinal cord (**Figure 1.6A**). This direct contact with the brain gives CSF, removed via lumbar puncture from the spinal cord, the ability to reflect neuropathological changes in the brain of living patients (200). More specifically, decreases in A β and elevations in Tau in the CSF have been shown to distinguish healthy controls from AD (201) (**Figure 1.6B**). Decreases in A β in the CSF is thought to be the result of increases in accumulations of A β into plaques in the brain which have been largely found to be the result of the impaired clearance of A β out of neurons during disease (202). Interestingly, only a fraction of Tau found in the CSF is due to the passive release of Tau from dying cells (203). Markedly, increasing levels of Tau in the CSF are predominantly the result of the enhanced secretion or release of Tau from the intracellular regions of neurons into the extracellular space. In fact, studies have shown that Tau hyperphosphorylation may be critical for its secretion (**Figure 1.7**). For example, studies have shown that Tau can be secreted at the synaptic terminal during normal synaptic activity (204; 205). Tau hyperphosphorylation, however, can enhance its secretion at the synaptic terminal as hyperphosphorylated Tau has been shown to be preferentially secreted during both ectosome shedding and exosome fusion (**Figure 1.7B & C**) (204; 206). Moreover, unlike normal physiological Tau, hyperphosphorylated Tau can also be secreted directly across



Part A of this figure was created with BioRender.com

Figure 1.6. Cerebrospinal fluid (CSF) creation and flow alongside sample immunoassay measurements of Amyloid beta₁₋₄₂ (A β ₄₂) and Tau from 105 controls and 98 AD cases. (A) CSF is created by and secreted from highly vascularized tissue called the choroid plexus located within each ventricle of the brain. The CSF flows from the lateral ventricles to the the third and fourth ventricles and then into the subarachnoid space and spinal cord. **(B)** A β ₄₂ and total Tau levels as measured by Roche Elecsys Platform between 105 control and 98 AD cases. T-test determined significance and A β ₄₂ values that reached saturation (1700 pg/mL) were excluded.



Created with BioRender.com

Figure 1.7. Methods by which pathological Tau can be secreted or released into extracellular space. (A) Tau can be actively secreted through the plasma membrane. (B) Tau can be released by ectosome shedding from the plasma membrane. (C) Tau can be packed into exosomes by inward budding and become secreted by of multivesicular bodies along the plasma membrane. Modified from Brunello, C. A, Merezko, M., Uronen, R., and Huttunen, H. J. (2019) Mechanisms of secretion and spreading of pathological tau protein. *Cellular and Molecular Life Sciences*. <https://doi.org/10.1007/s00018-019-03349-1>

the plasma membrane (**Figure 1.7A**) (207; 208). While the exact mechanism by which Tau is secreted into the CSF is unclear, it remains evident that the CSF of AD patients displays changes in Tau composition and that these changes, particularly that of phosphorylated Tau species, significantly correlate with neocortical NFT pathology in the brain (209). Together, these changes observed in CSF biomarkers, A β and Tau, give physicians the ability to determine individuals at risk of developing AD and researchers the ability to use CSF as a tool for assessing biological processes reflective of early disease stages (210).

1.12 African Americans: the most at-risk racial group for AD

African Americans are almost twice as likely to have AD compared to Caucasians (211-213). Current evidence suggests that this difference in risk could be explained by a multitude of factors including genetic ancestry and disparities in health, socioeconomic and environmental conditions (214-217). For example, GWAS show that the *ABCA7* gene has stronger associations with AD risk in individuals with African ancestry than in individuals with European ancestry (216; 217). *ABCA7* also has a stronger effect size in African Americans than even the strongest genetic risk factor gene for AD, the *APOE* ϵ 4 allele (216). Yet, despite the *APOE* ϵ 4 allele being more prevalent amongst African Americans, *APOE* ϵ 4 confers a lower risk for AD compared to Caucasians (76). Beyond genetic ancestry, chronic health conditions associated with higher risk for dementia, such as cardiovascular disease and diabetes, also disproportionately affect African Americans (214; 215). Furthermore, societal and environmental disparities that disproportionately affect African Americans, including lower levels and quality of education, higher rates of poverty, and greater exposure to adversity and discrimination, increase risk for both chronic diseases and dementia (214; 215). This highlights how racial differences in AD risk cannot be explained by genetics alone (214). Currently there is a gap in knowledge of the racial differences in underlying pathophysiology related to AD. Therefore, a better understanding of these mechanisms can help move towards a more precise definition of AD across diverse racial, ethnic, and genetic

backgrounds. An unbiased analysis into the CSF proteome of African Americans could provide insight into additional biomarkers reflecting underlying brain pathology that differ by race in AD.

1.13 The utility of mass spectrometry (MS)-based proteomics in identifying novel protein signatures in AD

1.13.1 Strategies for MS-based quantification of proteomes: Proteomic analyses of AD brain have predominantly utilized "bottom-up" mass spectrometry (MS) for protein identification and quantification. This workflow generally involved enzymatic digestion of proteins with trypsin, followed by protein separation via liquid chromatography (LC), and subsequent measurement of protein peptides using tandem mass spectrometry (MS/MS) (218). The first stage of measurement (MS1) involves the selection of several precursor peptides for fragmentation. The fragmented peptides are then identified through spectral matching and quantified using well-established statistical and informatic methods during the second stage of tandem MS (219-224). In summary, the "bottom up" approach to MS has become a cornerstone in the comprehensive analysis of proteomic profiles in AD research. Since then, significant advancements have been made to enhance protein identification and quantification, resulting in more detailed proteomic profiles.

Over the years technological strategies have further improved this workflow by enhancing the quantification and depth of proteomic datasets. Initially, label-free quantification (LFQ) was the preferred technique. Using this technique, each sample is individually prepared and analyzed using LC-MS/MS. Since each sample is analyzed individually, a limitation of this technique is that the peptides selected and analyzed can vary significantly between samples. This is due to the inherent nature of MS1 where peptide selection is biased toward the most intense signals (225). When trying to quantify proteins that are lost in a disease, this means that a protein quantified in a healthy state may be completely absent in the disease state and therefore not quantified. This results in a well-documented "missing value" problem, ultimately reducing the number of proteins retained in an LFQ dataset (225-228). Multiplex isobaric peptide labeling with tandem mass tags (TMTs) helps address the issue of missing values by allowing the simultaneous analysis of

multiple samples within a single LC-MS/MS run, currently accommodating up to 16 samples per run (229; 230). When combined with off-line fractionation, this strategy can quantify thousands of additional proteins compared to LFQ, which has enabled remarkably deep proteomic analysis of AD brain tissue (227; 228; 231; 232). A study that came out of the Seyfried Lab, Johnson et al., demonstrated this advantage in one of the first TMT-MS network proteome studies of the AD brain. This study quantified 6,533 proteins across 47 brain tissues compared to just 2,736 proteins quantified by LFQ-MS using the same samples (227). Despite these advancements in quantification, TMT-MS may still produce missing values across multiple batches which occurs when analyzing large numbers of samples (233). Targeted approaches such as selected reaction monitoring (SRM) can serve as a mitigation for the limitation of “missing values” by utilizing its ability to identify nearly all detectable peptides within a selected mass range. This allows for comprehensive and accurate quantification of the identified proteins in the sample with minimal to no missing values. This method is often used in research settings for more robust quantification of pre-specified individual peptides (234). Utilizing a targeted approach like this can be useful in validating discovery-driven data that results from tandem MS, as it requires specifying a target beforehand. In conclusion, the evolution of technological strategies, from LFQ to multiplex isobaric peptide labeling and targeted approaches like SRM, has significantly enhanced proteomic workflows, enabling comprehensive and accurate quantification of proteins.

1.13.2 Fundamentals of network construction and module identification: Unbiased proteomics of human brain coupled with network analysis has emerged as a valuable approach for organizing complex proteomic data into groups or “modules” of co-expressed proteins that reflect various biological functions (227; 235-237). Co-expression network analysis operates on the premise that proteins react to biological stimuli as a “system,” altering expression collectively within groups or “modules” of a network. Effectively organizing proteomic datasets into the described co-expression protein modules requires a thoroughly validated statistical algorithm. One such extensively validated algorithm, commonly employed in transcriptomic studies, is

Weighted Gene Co-expression Network Analysis (WGCNA) (235; 238-241). This algorithm applies graph theory principles to detect modules of proteins exhibiting highly correlated abundance levels across samples. Through evaluating the connectivity of each protein within a module, researchers can identify module-specific hubs or proteins that play central roles in module function. Typically, the most centrally connected proteins in a module serve as key drivers (238; 240; 242). Module-level abundance profiles can then be correlated with various phenotypic traits of the disease, such as amyloid burden, tangle deposition, and cognitive decline (243). These module-trait correlations reveal protein groups with strong positive or inverse relationships to the disease. In addition to module-trait correlations, module enrichment profiles can also provide important insights into proteomic composition. This analysis seeks to identify the over-representation of module proteins linked to specific cell types, biological functions, or genetic risk factors. It accomplishes this by cross-referencing the proteins within a module with well-validated databases. For instance, cell type enrichment is usually conducted by comparing module proteins with marker lists from established reference proteomes or transcriptomes of purified murine brain cells (218; 227; 228). In addition to cell enrichment lists, numerous resources are available for pathway and ontology analysis. Go Elite is a versatile analytical tool that enables users to incorporate both reference and custom databases to investigate ontological over-representation at biological, molecular, and organellar levels (244). Altogether, network analysis offers the ability to resolve the complex nature of disease by utilizing mathematical and computational tenets of system biology which results in the formation of communities (modules) of proteins, which can be representative of phenotypes that arise out of the molecular pathophysiology of disease.

1.13.3 Why prioritize the study of the proteome over the genome: Proteins are the ideal markers for understanding diseases such as AD because they are most proximal to the phenotypic changes seen in AD. Protein-level analysis offers the advantage of revealing disease-related changes that are not easily detectable in transcriptomic networks. Notably, only 30-40% of the modules in the AD brain network proteome overlap with those in the network transcriptome.

(235; 245). Furthermore, despite the fact that differential protein expression within these overlapping modules has been found to exhibit a reasonable degree of concordance, with a correlation coefficient of approximately 0.5, it has been repeatedly observed that the targets within the most concordant modules across transcriptomics and proteomics exhibit highly discordant changes at the protein and RNA levels (235; 245; 246). These discrepancies highlight the complexity and non-linear relationship between the transcriptome and proteome, stressing the importance of the numerous events that occur from the initial transcription of DNA to the point when a protein performs its function. This also aligns with the observation that only half of the disease-related variance in the AD network proteome is mirrored in transcriptome-level gene expression, while the remaining 50% results from transcriptional and post-translational effects (246). These findings align with previous comparisons of protein and mRNA data (237), and strongly supports the value of protein profiling in AD research, highlighting the unique aspects of proteomic changes that can only be achieved through protein analysis.

1.13.4 Core modules of the AD brain network proteome: Nearly a dozen comprehensive network-based analyses of the AD proteome in the human brain have led to the identification of six highly conserved modules, each with reproducible associations to specific cell types, organelles, and biological functions (217; 221; 225; 226; 235-241). Several modules, such as inflammatory, myelination, and RNA binding/splicing, consistently showed increases in the AD brain network proteome, while others, like synaptic, mitochondrial, and cytoskeleton, displayed consistent decreases. Notably, some of these modules (inflammatory, myelination, synaptic, and mitochondrial) appear to be driven by cell-type-specific perturbations (226), while those lacking such enrichment (RNA binding/splicing and cytoskeleton) represented underlying biochemical changes associated with the disease. The complexity of the modules preserved in AD confirms the multifactorial nature of the condition, which has led to inherent challenges in understanding AD and, consequently, in developing effective interventions.

1.13.5 The CSF proteome as a reflection of AD brain changes: The close proximity of CSF to the brain, along with its ability to reflect changes in amyloid burden and neurodegeneration through markers like A β and Tau, provides a compelling rationale for integrating the CSF proteome with the brain proteome. Furthermore, the reflection of other AD pathophysiologies in the CSF would provide additional avenues for detecting and monitoring treatment responses, especially at earlier stages of disease. Our first attempt to validate this interaction via proteomics was based on findings by Johnson et al., which identified that approximately 20 proteins from the highly conserved microglial module showed significant elevations in AD CSF (237). This provided the initial evidence necessary to explore this interaction more deeply. In another large-scale study by the Seyfried lab, Higginbotham et al. used a similar integrative proteomic approach to examine the statistical overlap between the entire AD brain network proteome and differentially expressed proteins in the AD CSF proteome (245). Notably, fifteen of the 44 brain modules identified in this study showed a strong overlap with the markers differentially expressed in AD CSF. Collectively, those 15 modules from the brain were being represented by 300 proteins that were significantly altered in AD CSF compared to controls. Based on their corresponding brain modules, these approximately 300 CSF AD targets were then segregated into five biomarker panels that represented a wide range of brain pathophysiology. These panels included synaptic transmission, vascular biology, myelination, glial-mediated inflammation, and energy metabolism. The panels highlighting brain changes in AD that could potentially be monitored through CSF. This comprehensive approach highlights the potential of CSF proteomics to uncover diverse aspects of AD pathology and to enhance the precision of biomarker-based diagnosis and therapeutic monitoring.

1.14 Summary

Evidence of differences in AD biomarkers between African Americans and Caucasians exists yet the underrepresentation of African Americans in research means data to support such alterations is lacking. This demonstrates a greater need for broad investigations into the

underlying biological differences of AD in African Americans as a means to identify AD biomarkers that are representative of and generalizable across diverse racial, ethnic, and genetic backgrounds. Including participants from diverse racial backgrounds ensures that research findings are more representative of the entire population and can be generalized to different racial and ethnic groups. Without this, there lies a risk of bias and limited applicability of research outcomes to specific populations. The following research will demonstrate how an integrated proteomic and network approach can be utilized to comprehensively define the proteomic profiles of AD within individuals of African American or Caucasian background. We hypothesize that the biological pathways most relevant or impacted by changes in Tau burden will demonstrate varying expression levels in the CSF of African Americans and Caucasians with AD. Through a combination of unbiased system level and target approaches, I have been able to (i) directly characterize CSF within a large cohort of individuals (ii) gain insight into race-specific molecular signatures of AD and (iii) validate novel race-dependent signatures for AD pathogenesis using an independent mass spectrometry technique. In total, there is a significant gap in our knowledge of the racial differences underlying molecular mechanisms of AD biology. A better understanding of these mechanisms is critical to move the field towards clearer biological methodologies for the early detection of AD across a diverse population of people.

CHAPTER 2: MATERIALS AND METHODS

This Materials and Methods was originally published in *Molecular Neurodegeneration*:

Modeste, E.S., Ping, L., Watson, C.M. *et al.* Quantitative proteomics of cerebrospinal fluid from African Americans and Caucasians reveals shared and divergent changes in Alzheimer's disease. *Mol Neurodegeneration* **18**, 48 (2023). <https://doi.org/10.1186/s13024-023-00638-z>

A full list of tables can be accessed at the following link:

<https://molecularneurodegeneration.biomedcentral.com/articles/10.1186/s13024-023-00638-z>

2.1 CSF samples

All cerebrospinal fluid (CSF) samples were collected as part of ongoing studies at Emory's Goizueta Alzheimer's Disease Research Center (ADRC) including participants in the ADRC Clinical Core, the Emory Healthy Brain Study, and the ADRC-affiliated Emory Cognitive Neurology Clinic. All participants provided informed consent under protocols approved by Emory University's Institutional Review Board. Clinical diagnosis of AD as well as classification as cognitively normal controls was based on review of clinical history, neurological examination, detailed cognitive testing, and diagnostic studies including Magnetic Resonance Imaging and CSF AD biomarker testing. Diagnosis of AD was made by subspecialty certified Cognitive and Behavioral Neurologists with additional input from Neuropsychologists based on current NIA-AA criteria (247; 248). A consensus clinical diagnosis of controls was made without consideration of CSF biomarkers by a panel of experts at the Emory Goizueta ADRC. Criteria for assigning diagnosis are provided in the National Alzheimer Coordination Center coding guidelines, form D1, based on clinician judgment. The basis for this judgment includes many metrics, with controls considered to have normal cognition and normal behavior after reviewing all testing including Montreal Cognitive Assessment (MoCA), Clinical Dementia Rating (CDR) score, and detailed neuropsychological testing. Hence, control participants may have MoCA scores that are lower than traditional cut points for impairment on this screening test. CSF was collected by lumbar puncture and banked according to best practice guidelines outlined by the National Institute on Aging for Alzheimer's Disease Centers (<https://alz.washington.edu/BiospecimenTaskForce.html>), and identical pre-analytic steps were followed in all groups. Measurements of Amyloid-beta₁₋₄₂ (A β ₄₂), total Tau (tTau), and phosphorylated Tau₁₈₁ (pTau₁₈₁) was performed on the Roche Diagnostics Elecsys platform (249-251) using recommended protocols. In total, the cohort was comprised of 105 healthy controls and 98 AD. The racial background of each case was based upon self-identification. Of the 203 cases, 100 identified as Caucasian or White while 103 identified as African American or Black. Case metadata can be found in **Appendix Table 6.1**.

2.2 Protein digestion of CSF

In order to sample the CSF proteome in an unbiased manner and given that we have previously shown that immunodepletion resulted in only a marginal improvement in proteomic coverage, the CSF samples were not immunodepleted prior to digestion (252; 253). First, 70 μL of CSF was transferred to 1 mL deep well plates for digestion with lysyl endopeptidase (LysC) and trypsin. The samples were then reduced and alkylated with 1.4 μL of 0.5 M tris-2(-carboxyethyl)-phosphine (ThermoFisher) and 7 μL of 0.4 M chloroacetamide in a 90°C water bath for 10 min. The water bath was then turned off and allowed to cool to room temperature along with samples for 5 minutes. Following this, water bath sonication was performed for 5 min. The samples were then allowed to cool again to room temperature for 5 mins prior to adding urea. Then 78 μL of 8M urea buffer (8M urea, 10mM Tris, 100mM NaH_2PO_4 , pH 8.5) and 3.5 μg of LysC (Wako), was added to each sample, resulting in a final urea concentration of 4M. The samples were then mixed well, gently spun down, and incubated overnight at 25°C for digestion with LysC. The following day, samples were diluted to 1M urea with a blend of 468 μL of 50 mM ammonium bicarbonate (254) and 7 μg of trypsin (ThermoFisher). The samples were subsequently incubated overnight at 25°C for digestion with trypsin. The next day, the digested peptides were acidified to a final concentration of 1% formic acid and 0.1% trifluoroacetic acid. This was immediately followed by desalting on 30 mg HLB columns (Waters) and then eluted with 1 mL of 50% acetonitrile (ACN) as previously described (228). To normalize protein quantification across batches, 100 μl was taken from all CSF samples and then combined to generate a pooled sample. This pooled sample was then divided into global internal standards (GIS) (255). All individual samples and the pooled standards were then dried using a speed vacuum (Labconco).

2.3 Tandem mass tag labeling of CSF peptides

All CSF samples were balanced for diagnosis, race, age, and sex (in that order) across 16 batches using ARTS (automated randomization of multiple traits for study design) (256). Using

a 16-plex Tandem Mass Tag (TMT) pro kit (Thermo Fisher Scientific, A44520, Lot number: VH3111511), 13 channels of each batch were allocated to a CSF sample (127N, 127C, 128N, 128C, 129N, 129C, 130N, 130C, 131N, 131C, 132N, 132C, 133N). The remaining 3 channels were occupied with a GIS pool (126), a standard biomarker negative pool (133C), and a standard biomarker positive pool sample (134N). Information regarding the origination of these pooled samples were reported previously (257). **Appendix Table 6.2** provides the sample to batch arrangement. In preparation for labeling, each CSF peptide digest was resuspended in 75 μ l of 100 mM triethylammonium bicarbonate buffer meanwhile 5 mg of TMT reagent was dissolved into 200 μ l of ACN. Once both were in suspension, 15 μ l of TMT reagent solution was subsequently added to the resuspended CSF peptide digest. After 1 hour, the reaction was quenched with 4 μ l of 5% hydroxylamine (Thermo Fisher Scientific, 90115) for 15 min. Then, the peptide solutions were combined according to the batch arrangement. Finally, each TMT batch was desalted with 60 mg HLB columns (Waters) and dried via speed vacuum (Labconco).

2.4 High-pH peptide fractionation

Dried samples were re-suspended in high pH loading buffer (0.07% vol/vol NH_4OH , 0.045% vol/vol FA, 2% vol/vol ACN) and loaded onto a Water's BEH column (2.1 mm x 150 mm with 1.7 μ m particles). A Vanquish UPLC system (ThermoFisher Scientific) was used to carry out the fractionation. Solvent A consisted of 0.0175% (vol/vol) NH_4OH , 0.01125% (vol/vol) FA, and 2% (vol/vol) ACN; solvent B consisted of 0.0175% (vol/vol) NH_4OH , 0.01125% (vol/vol) FA, and 90% (vol/vol) ACN. The sample elution was performed over a 25 min gradient with a flow rate of 0.6 mL/min with a gradient from 0 to 50% solvent B. A total of 96 individual equal volume fractions were collected across the gradient. Fractions were concatenated to 48 fractions and dried to completeness using vacuum centrifugation.

2.5 Mass spectrometry analysis and data acquisition

All samples (~1µg for each fraction) were loaded and eluted by an Easy-nLC 1200 (ThermoFisher Scientific) with an in-house packed 15 cm, 150 µm i.d. capillary column with 1.7 µm CSH (Water's) over a 35 min gradient. Mass spectrometry (MS) was performed with a high-field asymmetric waveform ion mobility spectrometry (FAIMS) Pro front-end equipped Orbitrap Lumos (Thermo) in positive ion mode using data-dependent acquisition with 1 second top speed cycles for each FAIMS compensative voltage. Each cycle consisted of one full MS scan followed by as many MS/MS events that could fit within the given 1 second cycle time limit. MS scans were collected at a resolution of 120,000 (410-1600 m/z range, 4×10^5 AGC, 50 ms maximum ion injection time, FAIMS compensative voltage of -45 and -65). Only precursors with charge states between 2+ and 5+ were selected for MS/MS. All higher energy collision-induced dissociation MS/MS spectra were acquired at a resolution of 50,000 (0.7 m/z isolation width, 35% collision energy, 1×10^5 AGC target, 86 ms maximum ion time). Dynamic exclusion was set to exclude previously sequenced peaks for 30 seconds within a 10-ppm isolation window.

2.6 Database search and protein quantification

All raw files were analyzed using the Proteome Discoverer Suite (v.2.4.1.15, Thermo Fisher Scientific). MS/MS spectra were searched against the UniProtKB human proteome database (downloaded in 2019 with 20338 total sequences). The Sequest HT search engine was used to search the RAW files, with search parameters specified as follows: fully tryptic specificity, maximum of two missed cleavages, minimum peptide length of six, fixed modifications for TMTPro tags on lysine residues and peptide N-termini (+304. 304.2071 Da) and carbamidomethylation of cysteine residues (+57.02146 Da), variable modifications for oxidation of methionine residues (+15.99492 Da), serine, threonine and tyrosine phosphorylation (+79.966 Da) and deamidation of asparagine and glutamine (+0.984 Da), precursor mass tolerance of 10 ppm and a fragment mass tolerance of 0.05 Da. Percolator was used to filter peptide spectral matches and peptides to a false discovery rate (FDR) <1%. Following spectral assignment, peptides were assembled into proteins and were further filtered based on the combined probabilities of their constituent peptides

to a final FDR of 1%. Peptides were grouped into proteins following strict parsimony principles. A complete TMT reporter ion abundance-based table output of assembled protein abundances without adjustments can be found at <https://www.synapse.org/EmoryDiversityCSF>.

2.7 Adjustment for batch and other sources of variance

Only proteins quantified in $\geq 50\%$ of samples were included in subsequent analysis ($n = 1,840$ proteins). Of the 1,840 proteins, 1,327 proteins were quantified across all samples. As previously reported (236; 237; 252; 258), batch correction was performed using a Tunable Approach for Median Polish of Ratio, (<https://github.com/edammer/TAMPOR>), an iterative median polish algorithm for removing technical variance across batch. Multidimensional scaling plots (MDS) were used to visualize batch contributions to variation before and after batch correction. Noticeably, prior to batch correction, cases within the same batch clustered together and batches ran consecutively tended to cluster more closely together (**Figure 2.1A**). Following batch correction using a median polish algorithm, the cases were no longer clustering by batch (**Figure 2.1B**). The data was then subjected to outlier removal using a robust principal component analysis method, *PcaGrid* (259). A scree plot graphing the eigenvalue against the principal component (PC) number was utilized to determine the number of PCs to include in the parameters (**Figure 2.1C**). Briefly, the parameters used for outlier detection were as follows: the desired number of principal components = 7, method = mean absolute deviation, and criterion for computing cutoff values = 0.99 (**Figure 2.1D**). This resulted in the detection and removal of 15 outliers, resulting in a final $n=189$ samples. Bootstrap regression was then performed to remove for covariates such as age at collection and sex. Variance partition analysis was performed to confirm appropriate regression of these traits (**Figure 2.1E & F**). Since the *variancePartition* package does not allow missing values, proteins with missing quantifications were temporarily imputed using the *impute.knn* function of the *impute* R package. The final cleaned dataset after regression and log2 transformation can be found at <https://moleculareurodegeneration.biomedcentral.com/articles/10.1186/s13024-023-00638-z>.

Figure 2.1: Batch correction, outlier removal and bootstrap regression. Multidimensional scaling plots (MDS) were used to illustrate batch contributions to variance before and after batch correction. In MDS plots, the distance a case is from one another is reflective of how similar or dissimilar a case is from the other. **(A)** Prior to batch correction, the samples clustered by batch **(B)** After batch correction, the samples no longer cluster by batch. **(C)** After batch correction, a principal component (PC)-based outlier removal method was utilized to detect outliers. By graphing the eigenvalue of each component against the PC number, the elbow or bend in the graph, which in this case was 7, was indicative of the ideal number of components to include within the parameters. **(D)** With a criterion for computing cutoff values set to 0.99, the cutoffs for the detection of outliers for the orthogonal distance and score were 16.79257 and 4.654674 respectively. This resulted in the detection of 15 outliers (b1.128N, b11.130C, b13.130N, b14.127N, b14.133N, b15.128C, b15.131N, b2.127C, b2.128C, b2.133N, b5.131C, b7.127C, b7.130N, b8.129N, b9.127C). B14.133N was such an extreme outlier because it was an empty channel. **(E)** After outlier removal, the matrix underwent bootstrap regression to remove variations in the dataset that were due to age and sex. Variance partition plots were employed to illustrate the percent contribution of diagnosis, race, age, and sex to the variance of each protein. **(F)** Following bootstrap regression, variations explained by age and sex were removed.

2.8 Differential expression analysis

One-way ANOVA followed by Tukey's post hoc adjustment for multiple comparisons was performed on four groups (Control-Caucasian, Control-African American, AD-Caucasian, and AD-African American) to identify differentially expressed proteins across diagnosis and within each race. Differentially expressed proteins for comparisons of interest (i.e., Control-Caucasian vs AD-Caucasian and Control-African American vs AD-African American) were then presented as volcano plots using the *ggplot2* package in R v4.1.2. A list of all comparisons computed with corresponding adjusted p-values is provided in **Appendix Table 6.3**.

2.9 Weighted Gene Co-expression Network Analysis

As previously published (235-237; 252), the *blockwiseModules* function from the WGCNA package in R was utilized to derive the weighted protein co-expression network. Briefly, the following parameters were used: soft threshold power $\beta = 3$, *deepSplit* = 4, minimum module size = 5, merge cut height = 0.07, and a signed network with partitioning about medoids. Using the *pairwise.wilcox.test* R function with Bonferroni correction, a pairwise Wilcoxon test was performed to calculate pairwise comparisons between each group with corrections for multiple testing.

2.10 Gene ontology and cell type enrichment analysis

To characterize co-expressed protein module biology, gene ontology (GO) annotations were retrieved from the Bader Lab's monthly updated .GMT formatted ontology lists downloaded July 5, 2022 (260). A Fisher's exact test for enrichment was performed into each module's protein membership using an in-house script (<https://github.com/edammer/GOparallel>). For cell type enrichment analysis, an in-house marker list was used as previously described (236). A Fisher's exact test was performed for each module member list using the merged human cell type marker list to determine cell type enrichment. For brain-CSF module overlap a one-sided Fisher's exact test to compare significance of module membership.

2.11 Selected reaction monitoring

Selected reaction monitoring (SRM) assays were performed on 195 of the 203 cases to determine whether a separate targeted proteomic approach could replicate proteomic changes seen in TMT discovery proteomics. An attempt was made to include all 203 samples from discovery TMT for SRM analysis however, samples 52524, 51520, 52055, 48617, 48615, 48769, 49537, 45707 had low remaining sample volume and had to be removed. Sample 62762 was later removed due to irregularities in retention time shifts. Peptide selection, sample preparation, peptide quantification, and data acquisition for the SRM assay was performed as previously described (257). Briefly, peptides were selected based on their robust detection and significant differential expression in previous CSF discovery proteomic projects for synthesis as heavy standards (237; 252). More specifically, the peptide had to i) have one or more spectral matches, ii) be significantly differentially abundant when evaluating AD versus Control cases, iii) and map to proteins that appeared in brain-based biological panels outlined in Higginbotham et al 2020 (252) that differed in AD. Ultimately, this led to approximately 200 peptides being nominated for synthesis by Thermo Fisher Scientific (Thermo PEPotec SRM Peptide Libraries; Grade 2; crude as synthesized). In addition to the 195 clinical samples from before, two pools of CSF were utilized as AD biomarker positive and AD-biomarker negative quality controls (QC) standards (257). After the CSF samples were blinded and randomized, each sample (50 μ L) was reduced, alkylated, denatured and then subjected to digestion as described (257). After digestion, the heavy labeled standards, 15 μ L per 50 μ L of CSF, were added to each digested sample. Each digested sample then underwent acidified, desalted and dried under vacuum. Following this, the peptide targets were quantified using TSQ Altis Triple Quadrupole mass spectrometer as previously described (257). The resulting raw files were uploaded to Skyline-daily software (version 21.2.1.455) for peak integration and quantification by peptide ratios. Peptides were filtered by first assessing retention time reproducibility, then by matching light and heavy transitions, and finally by determining the peptide ratio precision using the coefficient of variation (CV) as described by

Watson et al 2023 (257). The technical CV of each peptide was calculated based on the peptide area ratio for the AD-positive and AD-negative QC pools (**Appendix Table 6.4**). CSF peptide targets with CVs $\leq 20\%$ in at least one pooled standard were determined as peptides with high precision and were kept for subsequent analysis, leaving a total of 85 peptides that mapped to 58 proteins. The total area ratio for each targeted peptide in each sample made up the final data matrix. Due to the nature of SRM in that each peptide is explicitly targeted, a value for each peptide is always assigned in each sample (down to and including the limit of detection) as previously published by our group (257). As a result, the total area ratio for each targeted peptide in each sample made up the final data matrix, leaving a matrix with no blank cells or missing values. In preparation for analysis, this matrix of peptide ratios was \log_2 transformed and true zero values were replaced after \log_2 -transformation with the minimum value for that peptide minus 1. Bootstrap regression was then used to regress for age and sex (**Appendix Table 6.5**). Bicolor was then utilized to calculate the correlation between SRM peptides and TMT-MS protein measurements (**Appendix Table 6.6**). In cases where multiple peptides mapped to one protein, the most correlated peptide was kept for further analysis (**Appendix Table 6.7**). One-way ANOVA analysis with Tukey adjustment was then utilized once again to examine pairwise interactions (**Appendix Table 6.8**) and receiver operating characteristic (ROC) curve analysis was performed as previously described (257) (**Appendix Table 6.9**).

CHAPTER 3: RESULTS

These Results were originally published in *Molecular Neurodegeneration*:

Modeste, E.S., Ping, L., Watson, C.M. *et al.* Quantitative proteomics of cerebrospinal fluid from African Americans and Caucasians reveals shared and divergent changes in Alzheimer's disease. *Mol Neurodegeneration* **18**, 48 (2023). <https://doi.org/10.1186/s13024-023-00638-z>

A full list of tables can be accessed at the following link:

<https://molecularneurodegeneration.biomedcentral.com/articles/10.1186/s13024-023-00638-z>

3.1 CSF cohort characteristics

This study was comprised of two balanced groups of cerebrospinal fluid (CSF) samples from African American and Caucasian individuals, matched for age and sex with roughly equal numbers of control and Alzheimer disease (AD) cases (**Table 3.1**). This included 53 Caucasian controls, 52 African American controls, 47 AD Caucasians, and 51 AD African Americans. The majority were female and on average the controls (64.5 years) were slightly younger than AD (68 years). Notably, there were no statistical differences between the ages of the African Americans and the Caucasians within diagnosis (control: $p=0.8848$, AD: $p=0.9998$). As expected, AD cases had lower Montreal Cognitive Assessment (MoCA) scores than controls, but there were no statistically significant differences between MoCA scores across race within controls and AD (control: $p=0.7559$, AD: $p=0.2055$). The AD cases also had lower Amyloid-beta ($A\beta_{42}$) levels and elevated total Tau (tTau) and phosphorylated Tau₁₈₁ (pTau₁₈₁) levels. Notably, $A\beta_{42}$ levels were significantly lower in African American Controls compared to Caucasian controls ($p = 0.0021$) but not different between African American AD and Caucasian AD. This may indicate potentially early changes in brain amyloid deposition or processing of APP in African American controls versus Caucasian controls. Notably, the distribution of APOE4 carriers did not differ significantly by race in the control population and so does not account for the pattern observed (**Appendix Table 6.1**). Conversely, tTau and pTau₁₈₁ levels were significantly lower in African Americans with AD (tTau: $p<0.0001$, pTau₁₈₁: $p<0.0001$) but not different between African American and Caucasian controls. Data on comorbid conditions, including whether or not the person had hypertension, diabetes, dyslipidemia, or cerebrovascular disease, is presented for all cases in **Appendix Table 6.1**. Notably, none of the comorbid conditions was statistically overrepresented in either racial group.

Sample Size	CT Cau 53	CT AA 52	p – value ^a	AD Cau 47	AD AA 51	p – value ^a
Characteristics						
Sex	33 F, 20 M	33 F, 19 M	-	29 F, 18 M	32 F, 19 M	-
Age ^b	65 ± 8	64 ± 8	0.8848	68 ± 9	68 ± 9	0.9998
MoCA ^c	26 ± 2	25 ± 3	0.7559	16 ± 6	14 ± 6	0.2055
*Aβ ₄₂ ^d	1195.2 ± 262.0	1021.4 ± 301.1	0.0021	558.2 ± 169.9	483.4 ± 151.8	0.4026
tTau ^d	186.2 ± 61.6	158.5 ± 56.5	0.6573	423.7 ± 189.2	301.5 ± 134.8	< 0.0001
pTau ₁₈₁ ^d	16.6 ± 5.6	14.1 ± 4.9	0.7787	43.3 ± 20.8	30.1 ± 14.1	< 0.0001
tTau/Aβ ₄₂ ^d	0.14 ± 0.03	0.14 ± 0.03	0.9994	0.78 ± 0.31	0.66 ± 0.30	0.0850

^a p-values were calculated using one-way ANOVA with Tukey correction, bold indicates p < 0.05.

^b Age in years. Values given as average ± standard deviation

^c Most recent Montreal Cognitive Assessment (MoCA) score. Values given as average ± standard deviation

^d Aβ₄₂, tTau, pTau₁₈₁, and tTau/Aβ₄₂ in pg/mL. Values given as average ± standard deviation

*Aβ₄₂ levels that reached saturation (1700 pg / mL) were excluded from calculations and analysis

Abbreviations: CT, Control; AD, Alzheimer's disease; Cau, Caucasian / White; AA, African American / Black

Table 3.1. Cohort Characteristics

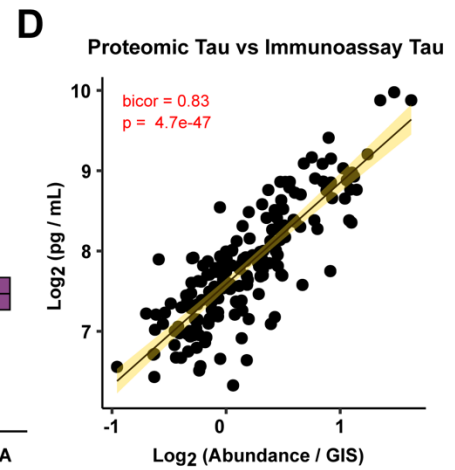
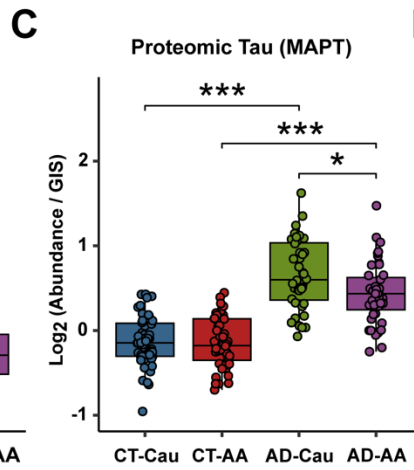
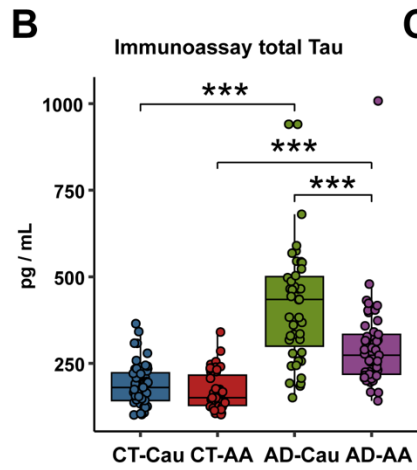
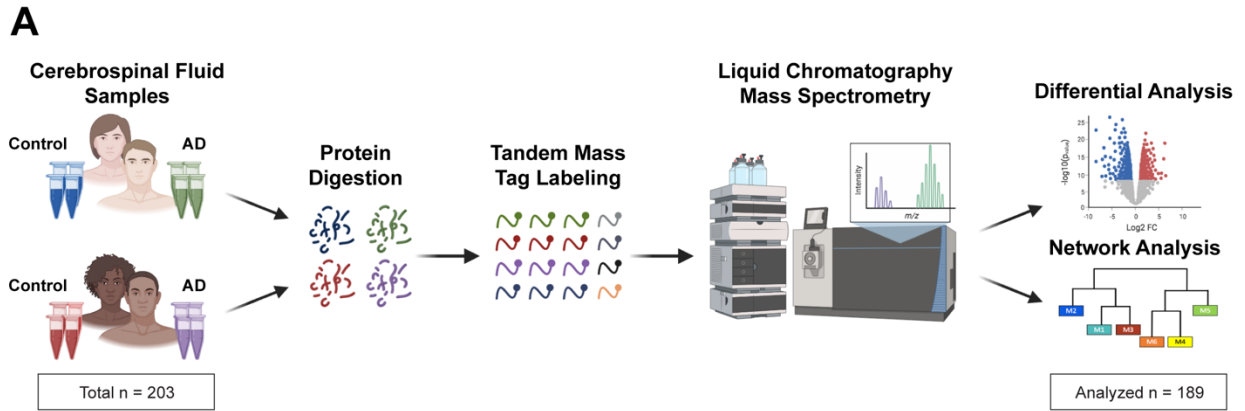
3.2: Discovery tandem mass spectrometry analysis of cerebrospinal fluid from African Americans and Caucasians reveals unique and shared changes in Alzheimer's disease

3.2.1 Correlation analysis uncovers a strong relationship between mass spectrometry and immunoassay measurements of Tau

Following enzymatic digestion, tandem mass tag (TMT) labeling, and off-line fractionation, all samples were subjected to liquid chromatography mass spectrometry (MS) (**Figure 3.1A**). In total, TMT-MS proteomic analysis identified 34,330 peptides mapping to 2,941 protein groups across the 203 samples (16 total batches). To account for missing protein measurements across batches, we included only those proteins quantified in at least 50% of samples following outlier removal as previously described (227; 235-237; 252), resulting in the final quantification of 1,840 proteins. Protein abundance was adjusted for batch and age and sex were regressed. As expected, Tau levels were significantly elevated in both African Americans and Caucasians with AD across both platforms compared to controls (**Figure 3.1B and C**). Consistent with the immunoassay measurements, TMT-MS Tau levels also showed significantly lower levels in African Americans with AD compared to Caucasians with AD (**Figure 3.1C**). Notably, protein levels of Tau (MAPT) by TMT-MS correlated strongly to independently measured tTau levels via immunoassay ($r=0.83$, $p = 4.7e-47$) (**Figure 3.1D**). Thus, in this study, both platform measures of CSF Tau support a reduction of total Tau levels in African Americans with AD, consistent with previous findings (261; 262).

3.2.2 Differential expression analysis of African American and Caucasian CSF proteome reveals unique and shared changes in AD

Differential expression analysis was performed to identify changes in the CSF proteome by race in AD (**Appendix Table 6.3**). Consistent with previous proteomic analyses of AD CSF (237; 252; 263-265), there was a significant increase in Tau (MAPT), 14-3-3 proteins, (YWHAZ, YWHAG, and YWHAE), SMOC1, neurofilaments (NEFM and NEFL) and proteins involved in



Part A of this figure was created with BioRender.com

Figure 3.1: Schematic of experimental workflow and correlation between proteomic Tau and total Tau immunoassay measurements. (A) Schematic of experimental workflow for quantification of cerebrospinal fluid proteome. (B) Total Tau levels as measured by Roche Elecsys Platform between control (CT) and AD cases and stratified by self-identified race: Caucasian (Cau) or African American (AA) (C) Tau levels measured by mass spectrometry. One-way ANOVA with Tukey post-hoc correction determined pairwise relationships (D) Correlation of Tau levels by TMT-MS (x-axis) to paired immunoassay total Tau levels (y-axis). Biweight midcorrelation coefficient (bicor) with associated p-value is shown. Only 179 cases were included in the linear regression analysis because of sample outlier removal and missing values in the TMT-MS.

glucose metabolism in both African Americans and Caucasians with AD compared with race matched controls (**Figure 3.2A & B**). However, Caucasians with AD exhibited a bias towards proteins that were increased in AD, where the number of differentially expressed proteins (DEPs) was nearly double (n=183 proteins) the number of decreased DEPs in AD (n=74 proteins) (**Figure 3.2A**). In contrast, in African Americans, the number of increased and decreased DEPs was more balanced (151 increased proteins vs. 162 decreased proteins) (**Figure 3.2B**). A Venn diagram illustrates the overlap of DEPs from African Americans and Caucasians with AD (**Figure 3.2C**), with the majority of proteins (n=168 proteins) differentially expressed in both races. Furthermore, a correlation analysis of both shared and unique DEPs showed overall high agreement in direction of change (bicor=0.887, p=2.47e-136, **Figure 3.2D**). However, there were some exceptions including SLIT1 and VSTM2A, which were significantly increased in Caucasians, but decreased in African Americans with AD. Both proteins are predominantly enriched in neuronal-cell types (266; 267). Thus, despite the differences in the number of significant DEPs in African Americans compared to Caucasians with AD, the direction of change with disease remains largely similar across both races.

3.2.3 Network analysis of the CSF proteome reveals modules related to pathways and brain cell-types

Co-expression network analysis of the AD brain proteome organizes proteins into modules related to molecular pathways, organelles, and cell types impacted by AD pathology (227; 235-237). Moreover, integration of the human AD brain and CSF proteome revealed that approximately 70% of the CSF proteome overlapped with the brain proteome (252). While proteomic networks in AD brain have been examined, network changes in the AD CSF proteome, including those associated with race and AD biomarkers are less well understood. Thus, we applied Weighted Gene Co-expression Network Analysis (WGCNA) to define trends in protein co-expression across 1840 CSF proteins in all individuals. These parameters identified 14 modules

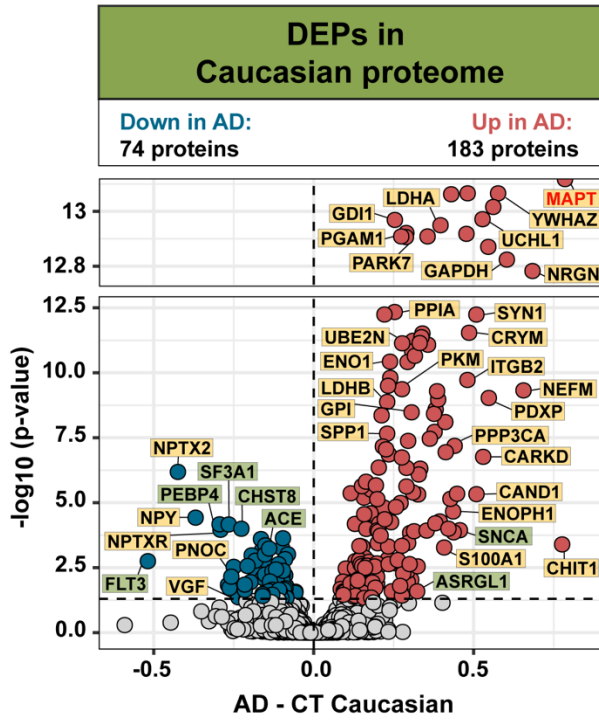
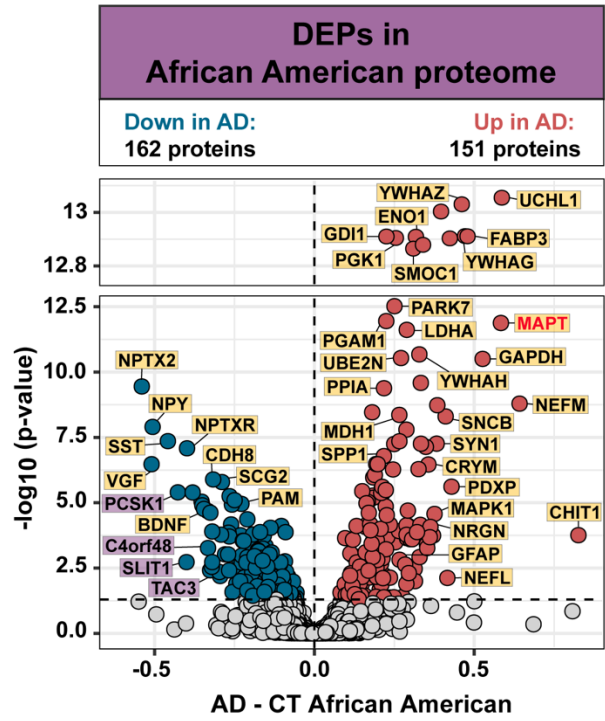
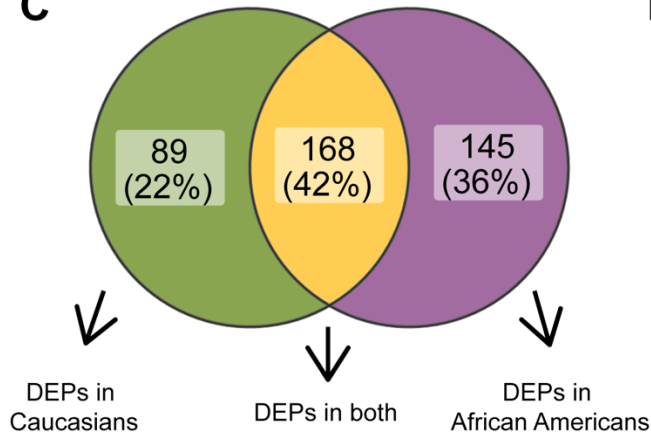
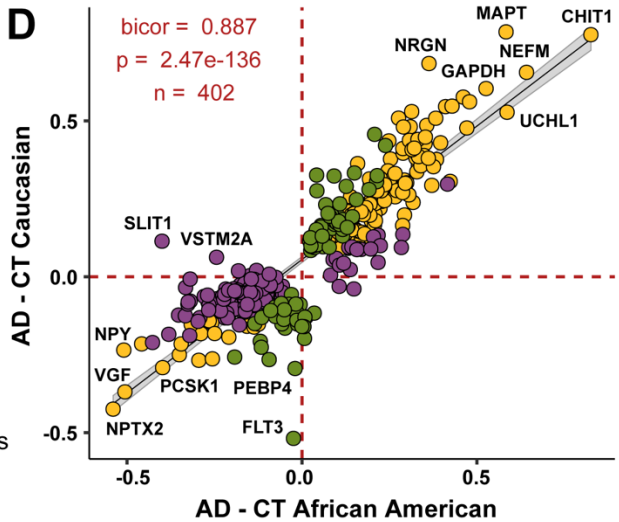
A**B****C****D**

Figure 3.2. Differential expression of Caucasian and African American CSF proteomes in AD. Volcano plot displaying the \log_2 fold change (FC) (x-axis) against one-way ANOVA with Tukey correction derived $-\log_{10}$ p-value (y-axis) for all proteins (n=1840) comparing AD versus Controls for Caucasians (**A**) and African Americans (**B**). Cutoffs were determined by significant differential expression ($p < 0.05$) between control (CT) and AD cases. Proteins with significantly decreased levels in AD are shown in blue while proteins with significantly increased levels in disease were indicated in red. Select proteins were denoted and labeled by whether they were differentially expressed in both proteomes (yellow), in only the Caucasian proteome (green), or in only the African American proteome (purple). (**C**) Venn diagram illustrating the number of differentially expressed proteins (DEPs) that were uniquely changed in one proteome (green or purple) or changed in both proteomes (yellow) (**D**) The correlation between the fold change of all DEPs (n=402) across the African American proteome (x-axis) and the Caucasian proteome (y-axis) were strongly correlated (bicor=0.887, $p=2.47e-136$), regardless of whether the DEP was significant in one (green or purple) or both proteomes (yellow).

(M), ranked by size, ranging from the largest M1, with 370 proteins to the smallest, M14, with 16 proteins (**Figure 3.3A**). Many of these modules were significantly enriched for brain-specific cell types (**Figure 3.3B**) as well as established brain gene ontologies (GO), cellular functions and/or organelles (**Figure 3.3C**). The three largest modules were associated with categories of “Postsynaptic Membrane” (M1), “Complement Activation” (M2), and “Extracellular Matrix” (M3) whereas M5 represented “Lysosome / Catabolism” and M6 “Gluconeogenesis”. Other modules included those with GO terms linked to “Cell Morphogenesis” (M4), “Cell Redox / Proteasome” (M7), “Protein Polyubiquitination” (M8), “Angiogenesis / Cell Migration” (M9), “Synapse Assembly” (M10), Myofibril Assembly (M11), “Actin Cytoskeleton” (M12), “Kinase Signaling / Activity” (M13), and “Carbohydrate Metabolism” (M14).

Protein-based network analysis in AD brain tissue has shown that the cellular composition represents a major source of biological variance and that many of the network modules are enriched in proteins that are expressed by specific brain cell types (236; 237). To determine if a similar relationship exists with protein-based networks in CSF, we evaluated the overlap of proteins in each module with brain cell-type specific makers (**Figure 3.3B**), generated previously from cultured or acute isolated neurons, oligodendrocytes, astrocytes, endothelial, and microglia from brain (266; 267). The largest module, M1, was enriched with neuron/synaptic proteins (i.e., NPTX1, NPTXR, SCG2, VGF, NRN1, and L1CAM) and to a lesser degree oligodendrocyte proteins (i.e., IGSF8, VCAN, APLP1). Neuronal loss or the active secretion of neuronal proteins into the extracellular space could account for the presence of neuronal proteins in the CSF. The M4 module was also enriched for neuronal protein markers including RTN4R1, LINGO2, OLFM1, and PLXNA2, associated with “Nervous Systems and Cell Morphogenesis”. Modules most enriched with microglia markers were M2 (i.e., C2, C3, C1RL, C1QA, C1QB, C1QC, LCP1, etc.) and M5 (i.e., HEXB, CTSZ, HEXA, CTSA, CTSB) consistent with a role in complement activation and lysosome function, respectively. Finally, endothelial markers were mainly overrepresented in

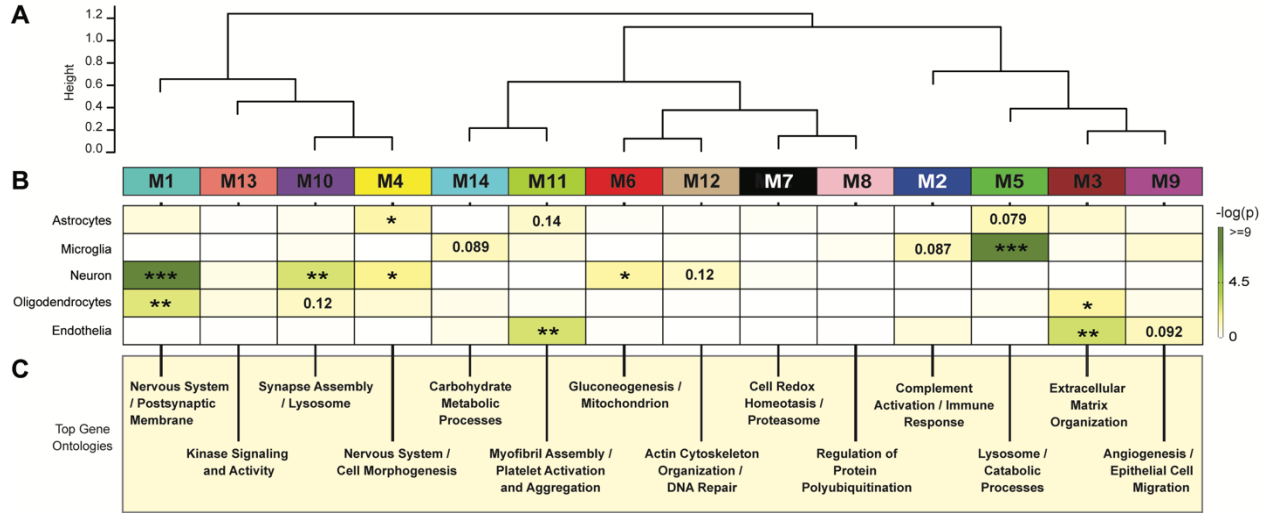


Figure 3.3: Network analysis classifies the CSF proteome into modules associated with specific brain cell-types and gene ontologies. (A) Weighted Gene Co-expression Network Analysis cluster dendrogram groups proteins (n=1840) into 14 distinct protein modules (M1-M14). (B) Cell-type enrichment was assessed by cross referencing module proteins by matching gene symbols using a one-tailed Fisher's exact test against a list of proteins determined to be enriched in neurons, oligodendrocytes, astrocytes, microglia and endothelia. The degree of cell-type enrichment increases from yellow to dark green with asterisks denoting the following statistical significance (* $p \leq 0.05$; ** $p \leq 0.01$; *** $p \leq 0.001$). Top gene ontology (GO) terms were selected from significant GO annotations.

modules M3 (i.e., NID2, ECM2, NID1, LTBP4, LAMA5, LAMC1), M9 (IGFBP7, F5, SDCBP, BGN) and M11 (FLNA, ANXA5, S100A11, MYL6) consistent with roles in extracellular matrix, angiogenesis and myofibril assembly, respectively. Thus, as seen in the network analysis of bulk proteome from human brain (236; 237), certain modules of co-expressed proteins in CSF were enriched with markers of specific brain cell-types. To further support this observation, we assessed the protein overlap between modules in CSF and modules from a recent large-scale consensus TMT-MS proteomic network of bulk human AD brain tissue (236). (**Figure 3.4**). Except for M9, M10 and M14, which had minimal overlap with the brain, all other modules (79% total) in the CSF network significantly overlapped with at least one of the 44 brain modules (B-M1 to B-M44). For example, there is overlap with CSF proteins in M1 “Postsynaptic Membrane” with several neuronal modules in the consensus brain network (B-M1, B-M4, B-M5, B-M10, and B-M15). In addition, M2 “Complement Activation” in CSF overlaps with modules in human brain associated with complement and immune response (B-M26 and B-M40), whereas M3 “Extracellular Matrix” strongly overlap with B-M27 in brain enriched with endothelial cell markers (**Figure 3.4**). Collectively, this supports that the co-expression in protein levels is, in part, shared between CSF and brain tissue, which could reflect changes in activation or phenotypes of specific brain cell types.

3.2.4 CSF protein modules correlate to race and clinicopathological phenotypes of AD

We assessed module correlation to race, cognitive scores (MoCA), and the hallmark AD biomarkers A β ₄₂, tTau, and pTau₁₈₁. The protein network resulted in three main groups/clusters based on module relatedness (**Figure 3.5A**). The first cluster (Group 1) was comprised of four modules (M2 “Complement Activation”, M5 “Lysosome / Catabolism”, M3 “Extracellular Matrix”, and M9 “Angiogenesis / Cell Migration”. Of these modules, M3 and M9 exhibited baseline racial differences in abundance levels (**Figure 3.5B**). Notably, the eigenprotein, which corresponds to

Figure 3.4: Protein overlap between modules in CSF network and modules in a human AD brain network. (A) Protein module enrichment across the CSF and brain was assessed by matching gene symbols of proteins in each module from the CSF network against gene symbols for protein in each module from a human AD consensus brain network using a one-tailed Fisher's exact test. The degree of enrichment increases from pink to light purple to dark purple with asterisks denoting the following statistical significance (** $p \leq 0.01$ and *** $p \leq 0.001$). (B) Similar to CSF, cell-type enrichment was assessed by cross referencing brain module proteins against a list of proteins determined to be enriched in neurons, oligodendrocytes, astrocytes, and microglia using a one-tailed Fisher's exact test. The degree of cell-type enrichment increases from yellow to green-yellow to dark green with asterisks denoting the following statistical significance (** $p \leq 0.01$ and *** $p \leq 0.001$).

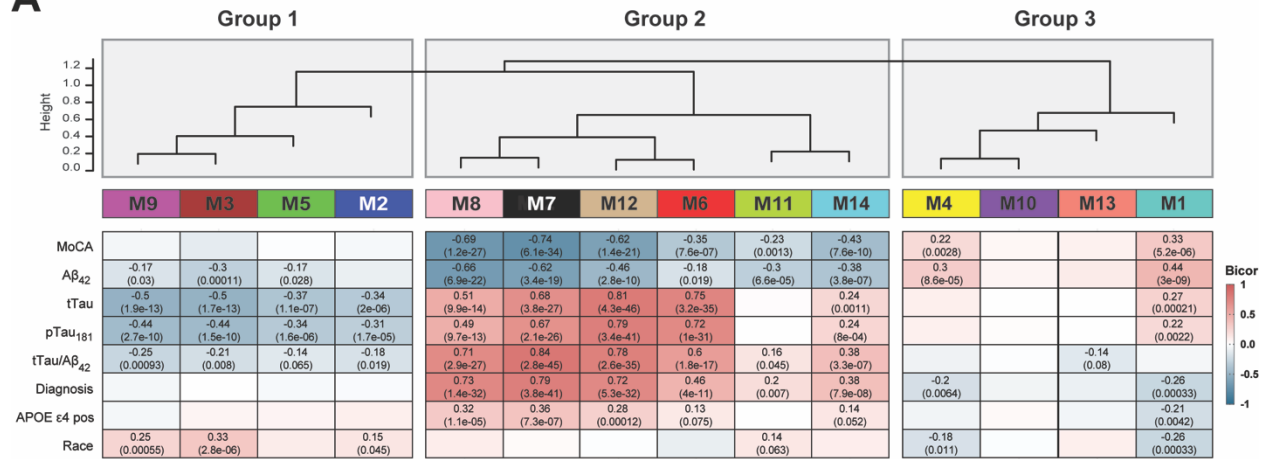
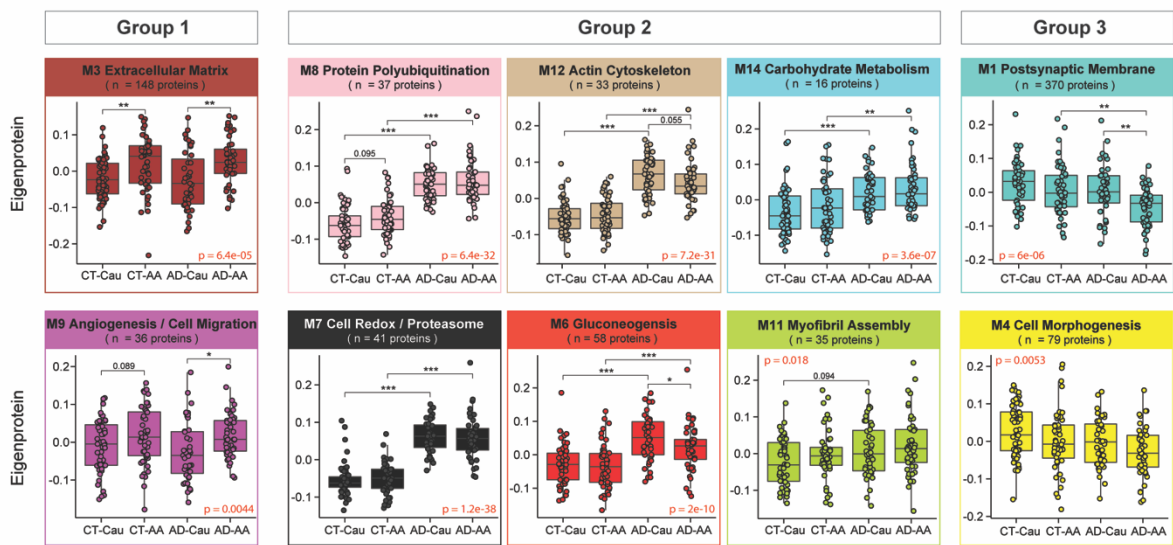
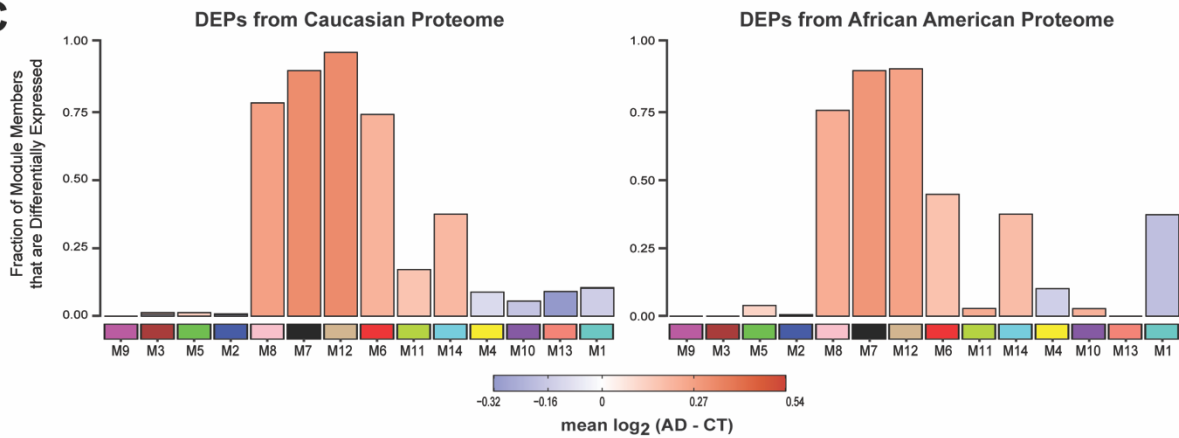
A**B****C**

Figure 3.5: CSF protein modules correlate to race and clinicopathological phenotypes of AD. (A) Modules were clustered based on relatedness defined by correlation of protein co-expression eigenproteins (indicated by position in color bar). There were three main clusters in the network: Groups 1, 2 and 3. Biweight midcorrelation (bicor) analysis of module eigenprotein levels with diagnostic measures of AD, including MoCA score, immunoassay Amyloid-beta₁₋₄₂ (A β ₄₂), total Tau (tTau), phosphorylated Tau₁₈₁ (pTau₁₈₁), ratio measures of tTau/A β ₄₂, diagnosis, whether the sample has *APOE* ϵ 4 allele or not, and race. The strength of positive (red) and negative correlations are shown by a heatmap with annotated bicor correlations and associated p-values. (B) Eigenprotein values distributed by race and diagnosis of representative modules for each cluster. (C) Differential protein abundance AD samples compared to controls, by module with Caucasian proteome on the left and African Americans on the right. The height of the bars represents the fraction of module member proteins that DEPs compared to controls. The bars are color coded by heatmap for average log₂ difference in abundance, where red represents an increase in abundance in AD, and blue represents a decrease in abundance in AD.

the first principal component of a given module and serves as a summary expression profile for all proteins within a module, were increased for these two modules in African Americans compared to Caucasians. Of note, these modules were enriched with endothelial cell markers (**Figure 3.3B**) which suggests that genetic ancestry and/or environmental differences influence expression or secretion of these cell-type markers. Similarly, M2 and M5, both of demonstrated enrichment for microglial markers, trended towards higher levels in both African American controls and AD (**Figure 3.3B and 3.6**), suggesting an accompanying immune response to the vascular alterations seen in modules M3 and M9.

The second cluster of modules (Group 2) was comprised of six modules (M8, M7, M12, M6, M11, and M14) that were all increased in AD (**Figure 3.5A**). These AD modules also demonstrated significant negative correlations to MoCA scores and, conversely, significant positive correlations to tTau/A β_{42} ratio. With the exception of M11, these modules also exhibited positive correlations to APOE $\epsilon 4$ risk (**Figure 3.5A**). Interestingly, a hub protein of the M12 “Actin Cytoskeleton” module was Tau (MAPT). Consistent with CSF levels observed for Tau by immunoassay and TMT-MS (**Figure 3.1B and C**), the M12 eigenprotein had lower levels in African Americans, compared to Caucasians with AD, albeit not significant ($p=0.055$) (**Figure 3.5B**). Notably, M6 “Gluconeogenesis” was significantly lower in African Americans compared to Caucasians with AD, highlighting another module of CSF proteins that differed by race in AD (**Figure 3.5A and B**). This also indicated that the increased glycolytic signature of AD previously reported in CSF (237; 252) is higher in Caucasians with AD. Consistently, a greater proportion of increased DEPs in Caucasians with AD mapped to M6 compared to African Americans with AD (**Figure 3.5C**). In contrast, M7 “Cell Redox / Proteasome” and M8 “Protein Polyubiquitination”, had the strongest correlations to tTau/A β_{42} ratio and cognition (**Figure 3.5B**), and both demonstrated strong, equivalent elevations in African Americans and Caucasians with AD (**Figure 3.5B**). This is consistent with an equivalent fraction of increased DEPs mapping to these modules in African American and Caucasians with AD (**Figure 3.5C**). Therefore, proteins in these

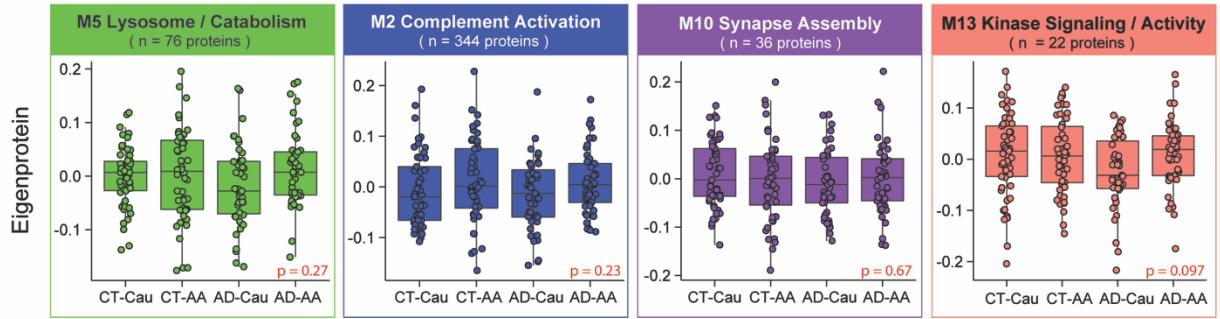
A

Figure 3.6: Additional CSF network protein modules. (A) Eigenprotein levels were distributed by race and diagnosis for remaining modules not shown in main Figure 4. This includes M5, M2, M10, and M13.

modules including 14-3-3 family members (YWHAZ, YWAHB, YWHAG, YWHAE) likely represent the best class of CSF AD biomarkers that are not influenced by race. M14 “Carbohydrate Metabolism” and M11 “Myofibril Assembly” were both elevated in both African Americans and Caucasians with AD (**Figure 3.5A and B**), yet to a lesser degree than M7 and M8.

The final group of modules (Group 3) contained two modules, M1 “Postsynaptic Membrane” and M4 “Cell Morphogenesis”, that showed strong correlations to both race and AD diagnosis (**Figure 3.5A**). Both modules were i) decreased in AD compared to controls and ii) and were lower in African Americans compared to Caucasians. In addition, both M1 and M4 were enriched with neuronal markers and positively associated with cognitive MoCA scores (**Figure 3.5A**). Markedly, pairwise statistical analysis of eigenprotein levels for M1 across diagnosis and race revealed significantly lower levels in African Americans with AD (**Figure 3.5B**). To this end, most of the decreased DEPs in African Americans with AD mapped to M1 and to a lesser degree M4, whereas decreased DEPs in Caucasians with AD were equally distributed to M1, M4, M13 and M10 (**Figure 3.5C**). Notably, M10 and M13 within Group 3 did not show any differences with AD or race and did not significantly correlate with traits explored in this study (**Figure 3.5 and Figure 3.6**). Overall, network analysis effectively organizes the CSF proteome into protein modules that are strongly linked to hallmark AD biomarkers ($A\beta_{42}$, tTau and pTau₁₈₁) and cognition, which in some cases were also influenced by race.

3.3 Selected reaction monitoring validates protein alterations across Alzheimer's disease and race

To further validate these network findings, we used a targeted mass spectrometry method, selected reaction monitoring (SRM), with heavy labeled internal standards to measure CSF proteins across 195 of the 203 cases included in the discovery TMT-MS assays (**Figure 3.7A**). The proteins and corresponding targeted peptides were previously selected based on their robust

Figure 3.7 Validation of shared and divergent CSF protein levels across AD and race. (A) Schematic of experimental workflow for SRM analysis of cerebrospinal fluid proteome **(B)** Heatmap of peptides that were significantly differentially expressed between Control and AD Caucasians or African Americans. Stars are indicative of the level of significant difference (* $p \leq 0.05$; ** $p \leq 0.01$; *** $p \leq 0.001$) seen for each peptide between AD and Control within each race. Meanwhile the colors are indicative of the \log_2 fold change (FC) of each peptide from Control and AD for each race where blue is indicative of the degree of decrease and shade of red is indicative of the degree of increase. **(C)** \log_2 abundance of peptides that mapped to modules of interest distributed by race and diagnosis. Pairwise significance was calculated using one-way ANOVA with Tukey adjustment.

(252; 268). We used pooled CSF samples of control, and AD cases as quality controls replicates (n=29 samples total) to assess technical reproducibility. Of the peptides targeted, 85 (mapping to 58 proteins) had a coefficient of variation of <20% in both the control and AD pools with no missing values (**Appendix Tables 6.4**). Following adjustments of co-variates (i.e., age and sex), peptide levels were highly correlated with protein levels measured by TMT-MS from the same samples (**Appendix Table 6.6**). If a protein was measured by more than one peptide the most correlated peptide to the TMT-MS protein level was selected for further analysis. The final peptide list can be found in **Appendix Table 6.7**. ANOVA analyses determined pairwise significance between the four groups (i.e., Control-Caucasians vs Control-African Americans vs AD-Caucasians vs AD-African Americans, **Appendix Table 6.8**). **Figure 3.7B** highlights peptides (n=24) that reached significance and that mapped to proteins in CSF modules associated with race and/or AD. Consistent with the TMT-MS protein measurements, proteins measured by SRM within M7 (GAPDH and YWHAG) and M8 (YWAHB and PPIA) had strong elevations ($p < 0.001$) in abundance in AD in both races, whereas proteins in M12 (SMOC1, PARK7, and LDHB) had a greater magnitude of change in Caucasians than African Americans with AD (for a list of all M12 members, see Supplemental Table 6) . Similarly, a majority of the proteins measured by SRM in M6 (PKM, GDA, TPI1, GOT1, ALDOA and ENO2) were more increased in Caucasians than African Americans with AD (**Figure 3.7B and C**). Proteins in the synaptic M1 module (VGF, SCG2, NPTX2, and NPTXR) were significantly decreased in African Americans with AD compared to Caucasians (**Figure 3.7B and C**), again consistent with TMT-MS protein level abundance. Notably, African Americans with or without APOE $\epsilon 4$ allele in the AD group had reduced levels of these CSF peptide biomarkers compared to Caucasians indicating that race and not APOE status was driving the difference in abundance (**Figure 3.8A**). Furthermore, these differences across race remained consistent even after removing patients with one or more comorbid condition (i.e., hypertension, diabetes, dyslipidemia, or cerebrovascular disease; **Figure 3.8B**).

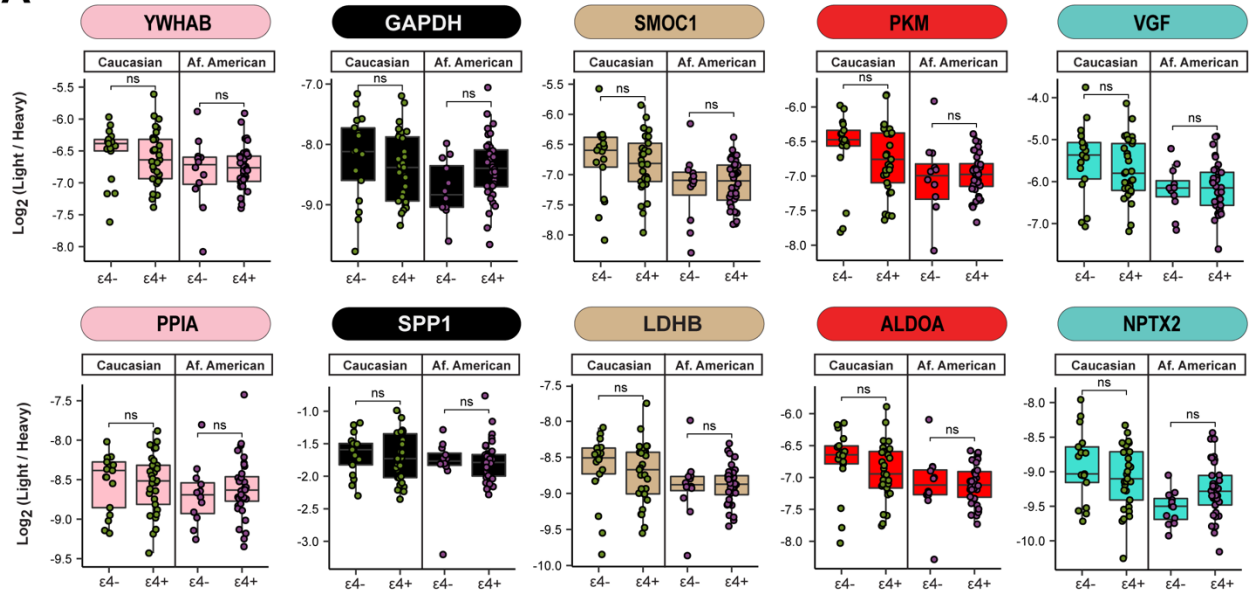
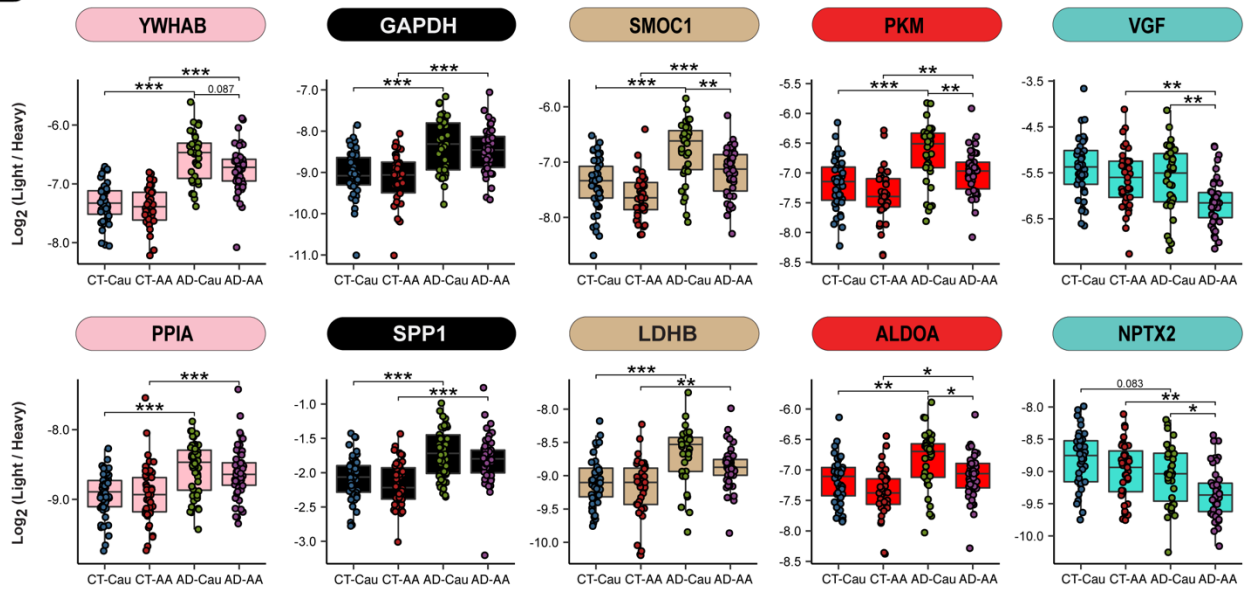
A**B**

Figure 3.8. Stratification of SRM CSF protein measurements by APOE genotype and comorbidity. (A) Within each race, protein levels for were not affected by APOE ϵ 4 genotype for YWHAB, GAPDH, SMOC1, PKM, VGF, PPIA, SPP1, LDHB, ALDOA, and NPTX2. (B) Within each race, protein levels were not affected by patient co-morbidities (hypertension, diabetes, dyslipidemia, or cerebrovascular disease) for YWHAB, GAPDH, SMOC1, PKM, VGF, PPIA, SPP1, LDHB, ALDOA, and NPTX2.

Finally, a receiver operating characteristic (ROC) curve analysis was performed to assess the performance of each peptide biomarker in differentiating controls and AD by race (**Figure 3.9 and Appendix Table 6.9**). We generated an area under the curve (AUC) for AD in African American and Caucasian individuals for each protein biomarker (considered separately in each race). As expected, proteins mapping to M8 and M7 including 14-3-3 proteins (YWHAB, YWHAG and YWHAZ) were equally able to discriminate AD from control irrespective of racial background. Notably, despite having lower levels in African Americans with AD compared to Caucasians with AD, only a modest improvement in the AUC for SMOC1 was observed for classifying AD in Caucasians AUC=0.8255 ($p=1.71e-08$, CI=0.7421-0.9090) compared to African Americans AUC=0.7618 ($p=4.12e-06$, CI=0.6660-0.8576). Similar findings were observed for another M12 protein, LDHB, as well as M6 proteins PKM and ALDOA. However, the M1 protein VGF was only nominally significant at classifying AD in Caucasian AUC=0.6030 ($p=0.0406$, CI=0.4887-0.7173), yet highly significant in African Americans AUC=0.7593 ($p=5.03e-06$, CI=0.6634-0.8552). Similar results were observed for other synaptic M1 proteins, NPTX2 and SCG2, whereas NPTXR showed only a modest improvement in the AUC between African Americans compared to Caucasians with AD (**Figure 4.9 and Appendix Table 7.15**). Collectively this supports a hypothesis that African Americans with AD have lower levels of a subset of neuronal biomarkers compared to Caucasians with AD.

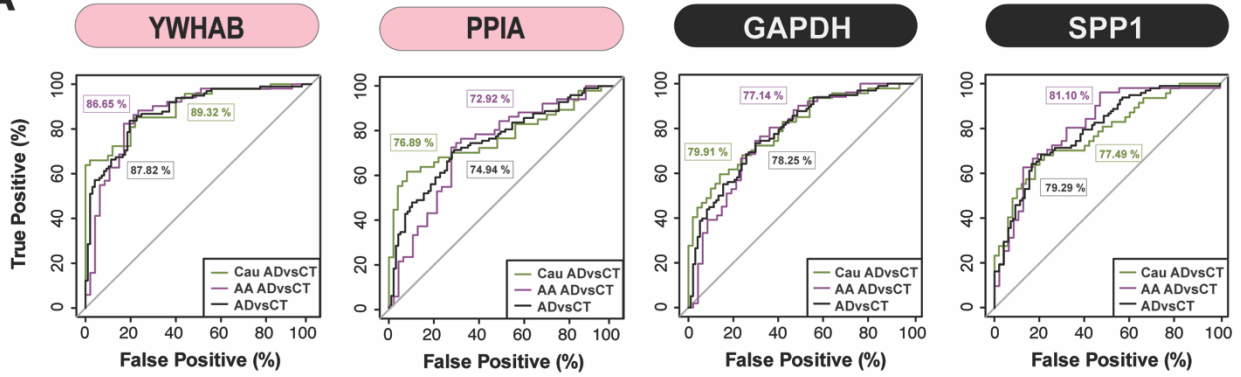
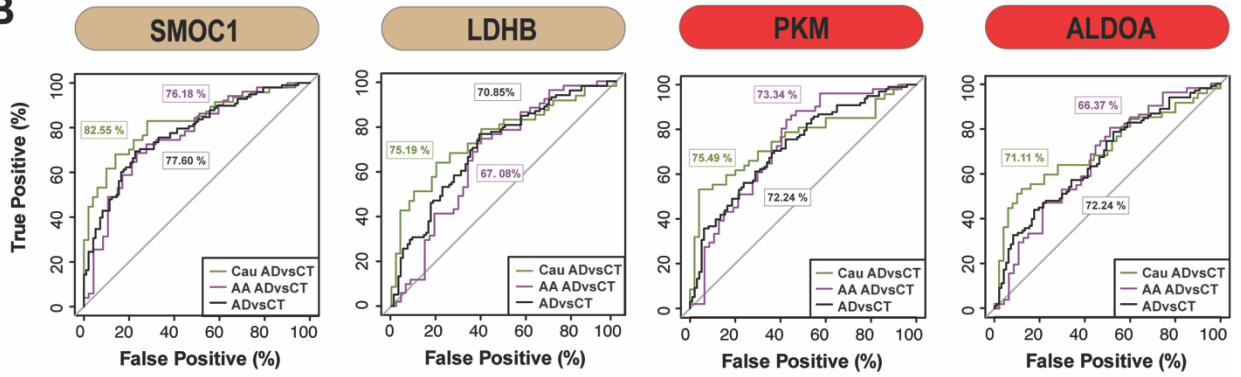
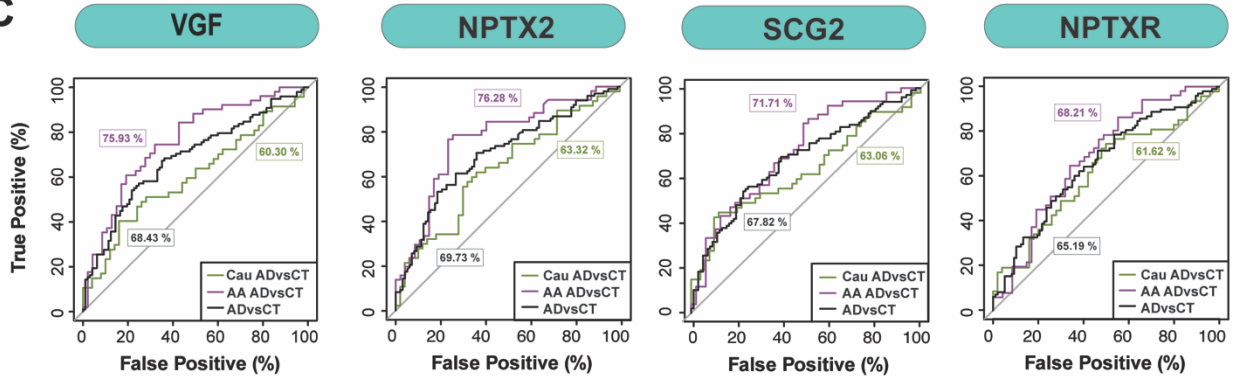
A**B****C**

Figure 3.9: ROC analysis evaluated CSF protein classification of AD by race. (A) YWHAB, PPIA, GAPDH, and SPP1 had similar performance in classifying Caucasians and African Americans with AD (B) SMOC1, PKM, LDHB and ALDOA showed modest improvement in the AUC for Caucasians with AD compared to African Americans with AD (C) VGF, SCG2, and NPTX2 were better classifiers for AD in African Americans compared to Caucasians, whereas NPTXR showed modest improvement in classification of AD in African Americans. All protein AUCs with p-values and confidence intervals (CI) are provided in **Supplemental Table 15**.

CHAPTER 4: DISCUSSION

Segments of this discussion were originally published in *Molecular Neurodegeneration*:

Modeste, E.S., Ping, L., Watson, C.M. *et al.* Quantitative proteomics of cerebrospinal fluid from African Americans and Caucasians reveals shared and divergent changes in Alzheimer's disease. *Mol Neurodegeneration* **18**, 48 (2023). <https://doi.org/10.1186/s13024-023-00638-z>

Here we performed an unbiased quantitative analysis of the CSF proteome to identify protein biomarkers reflective of underlying AD brain physiology that are shared or unique across race. Using network analysis, we organized the CSF proteome into 14 modules of proteins with highly correlated levels in CSF. Notably, these modules were associated with cell-types and biological pathways in brain and largely overlapped with modules from a consensus human AD brain proteomic network (236). Consistent with previous findings (261; 262), we also show that Tau levels were lower in African Americans with AD compared to Caucasians in CSF. Notably, Tau mapped to a CSF module enriched with other related neuronal/cytoskeletal proteins with a magnitude of increase greater in Caucasians than in African Americans with AD. This indicated that an entire network of proteins, rather than a single protein, is changing differently with disease between these two racial groups. In contrast, CSF modules which included 14-3-3 proteins, were elevated equivalently in both African Americans and Caucasians with AD, suggesting similar changes in pathophysiology. Lastly, a module enriched with neuronal/synaptic proteins including VGF, SCG2, and NPTX2 was significantly lower in African Americans than Caucasians with AD. These findings were consistent when VGF, SCG2, and NPTX2 levels in CSF were measured using SRM analysis, which also showed significantly better classification of African Americans with AD compared to Caucasians. Together, our findings suggest that there are likely distinct mechanisms underlying the abundance and/or secretion of neuronal markers including Tau and VGF that differ by race. Collectively, these data underscore the need for further investigations into how AD biomarkers and underlying physiology vary across different racial backgrounds.

4.1 Protein co-expression between the brain and CSF reflects the intricate role of CSF in brain function and health.

In a previous study we performed unbiased TMT-MS on a small discovery cohort of control and AD CSF samples (n=40) and mapped these proteins onto a human AD brain co-expression network, revealing that approximately 70% (n=1936) of the CSF proteome (N=2,875) overlapped

with the brain network (N=8817) (252). Additionally, it was found that 271 of the proteins that were significantly altered in the CSF were also differentially expressed in the brain (245). The increased sample size in this study afforded the opportunity to extend beyond this analysis by constructing an independent co-expression network on the CSF proteome and assessing its overlap with modules in a consensus brain network. This analysis revealed a strong overlap between CSF and brain modules, with 11 of the 14 CSF modules significantly overlapping with one or more brain modules, further supporting that protein co-expression in the brain is conserved in the CSF. These findings are not surprising considering the close relationship between CSF and brain. It is already known that substrates needed by the brain can be transported from the blood through the choroid plexus into the CSF, and then from the CSF into the extracellular space within the brain (269). Inversely, CSF aids in the removal of brain metabolism waste products, such as glycosylated proteins, excess neurotransmitters, and other unnecessary molecules, from the cerebral region (269). As a result of these exchanges, changes in brain chemistry can ultimately influence CSF composition, allowing the CSF to mirror neuropathological changes in the brain. Our studies suggests that the observed changes in CSF are mainly driven by cell-type alterations, as most CSF modules were enriched with either neuronal (M1, M4, M6, M10 and M12), glial (M2, M5, and M14), astrocyte (M4 and M5), oligodendrocyte (M1 and M3), and endothelial-specific markers (M3, M9, and M11). The remaining modules that did not exhibit enrichment with cell type markers represented processes related to cellular signaling (M13) and degradation pathways (M7 and M8), including kinase signaling and activity, protein polyubiquitination, and cell redox/proteasome processes. This reflects another crucial function of the CSF, which is aiding in the clearance of waste products from the brain (269). In conclusion, network analysis of the CSF underscores the intricate relationship between CSF and brain biology in AD, revealing shared protein alterations and cell-type enrichments across both compartments. These findings support our understanding of CSF as a conduit for biomarkers of neuropathological changes in AD and provide insights into the underlying mechanisms driving early disease progression.

4.2 CSF network analysis indicated differences in endothelial markers across race, irrespective of disease, yet there is insufficient evidence to indicate that these differences stem from variations in endothelial damage.

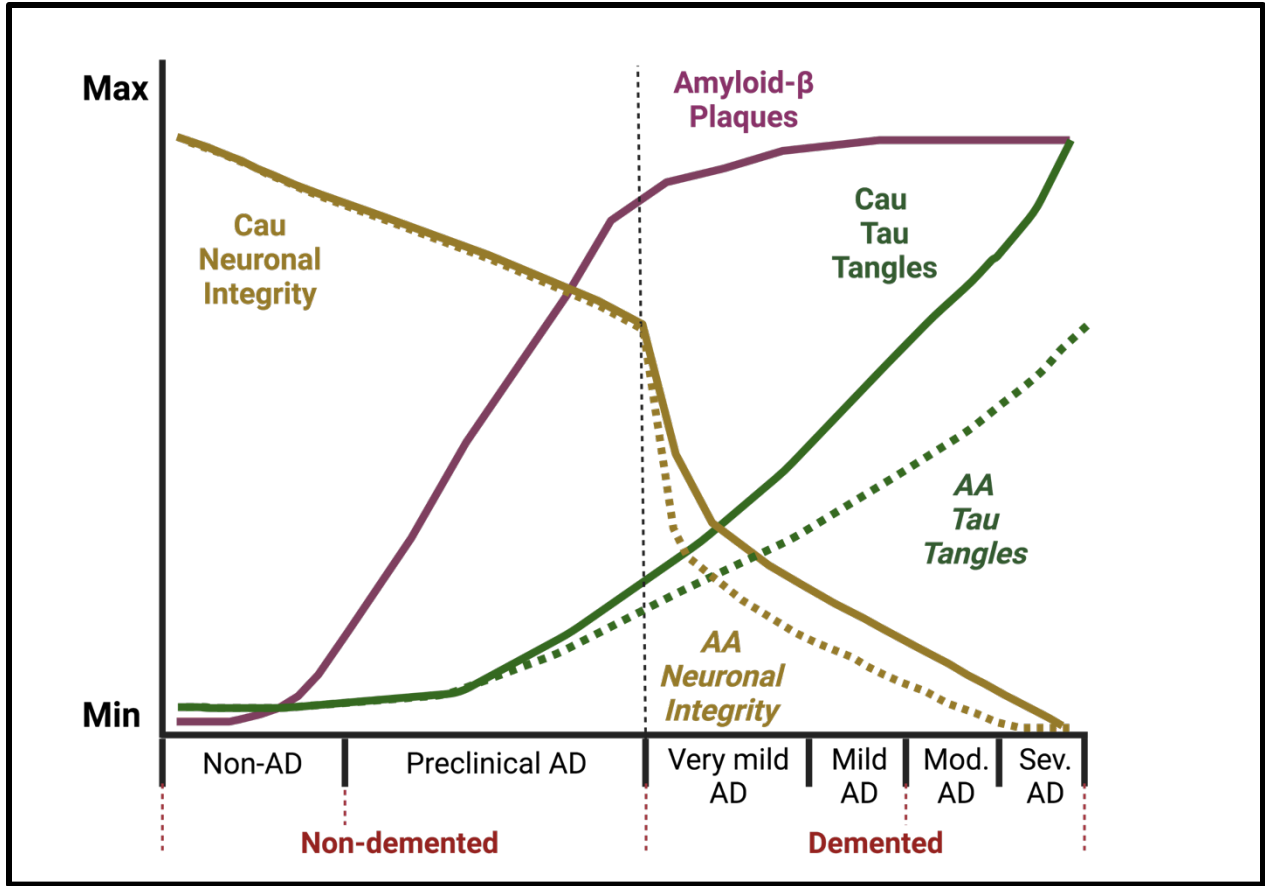
In regards to the CSF network biology that differed by race, it's noteworthy that modules significantly enriched in endothelial proteins (M3 and M9) were elevated in African Americans across both control and AD individuals. M3 is primarily comprised of extracellular matrix (ECM) proteins, and ECM proteins make up the dynamic network of macromolecules providing structural support for cells and tissues. In the brain, ECM proteins are vital for maintaining the integrity of the blood-brain barrier (BBB) and neurovascular units (262-265). ECM proteins in the BBB are crucial for preserving brain tissue homeostasis by preventing the entry of unwanted cells and molecules and by removing metabolic waste. Additionally, ECM proteins within the neurovascular unit play a crucial role in regulating cerebral blood flow (CBF), ensuring sufficient blood supply to meet the demands of neurons (266; 267). Consequently, malfunctioning ECM proteins in the brain can result in compromised function of both the BBB and neurovascular units. Notably, two critical vascular changes associated with AD are the breakdown of the BBB (270; 271) and compromised CBF (272). Moreover, these dysfunctions can subsequently trigger increases in proteins associated with angiogenesis, the process of forming new blood vessels. Pathological angiogenesis has been significantly implicated in perpetuating AD by fostering further A β generation, which, in turn, can exacerbate BBB dysfunction and impaired CBF (273). It is noteworthy that the M9 module is enriched with proteins involved in angiogenesis and is also elevated in African Americans compared to Caucasians, irrespective of disease status. In conclusion, the increased presence of endothelial proteins among African Americans implies that vascular differences may play a role in the heightened susceptibility to AD within this demographic. This highlights the necessity for additional investigation into how differences in vascular health between racial groups may impact the susceptibility and advancement of AD.

Currently, growing evidence suggests that endothelial dysfunction plays a significant role in the cognitive decline associated with AD (268), raising the question of whether the elevated levels observed in African Americans could indicate such injury. Furthermore, endothelial impairment is common among individuals with atherosclerosis, hypertension, diabetes, and chronic kidney disease (266), conditions that are more prevalent in the African American population. Several studies have already highlighted plausible biomarkers for endothelial dysfunction (268). Osteopontin (OPN) (269; 270) and cell adhesion molecules like VCAM1 and ICAM1 (271-273) are indicators of vascular inflammation, while albumin (ALB) (274-277), soluble platelet-derived growth factor receptor-beta (sPDGFR β) (278), vasoactive molecules such as atrial natriuretic peptide (ANP), adrenomedullin (ADM), and B-type natriuretic (BNP) (279; 280), metalloproteinases (MMPs) (281-286), and blood coagulation proteins like fibrinogen (FGB) (287) and plasminogen activator inhibitor-1 (PAI1) (288) reflect vascular damage. Additionally, growth factors such as vascular endothelial cadherin (VGEF) (289-297), angiogenin (ANG) (292; 298), and angiopoietin-1 (ANG1) (299) have been shown to be altered during endothelial injury. When overlaying these indicators over proteins assigned to module memberships in the CSF proteome, it was found that only one of these markers, ANG, mapped to M9 or M3. Most of the other proteins identified within this CSF proteome (ICAM1, CDH5, ALB, MMP2, FGB) mapped to the blue module, which remained largely unchanged across both control and AD groups as well as between races. One exception was sPDGFR β , which mapped to the M1 module. Increased CSF levels of sPDGFR β have been linked to BBB breakdown in individuals with mild cognitive impairment (274). It has also been demonstrated that heightened levels of sPDGFR β correlate with cognitive decline in the early stages of AD (275). Nevertheless, the module members of M1 decrease with disease progression, and even exhibit even greater declines in African Americans. Remarkably, alongside being identified as elevated in AD, sPDGFR β levels have been noted to be lower in African Americans compared to Caucasians (276). Together, the data is insufficient to support that the elevated levels of endothelial markers observed in African Americans in this

study are indicative of endothelial impairment or injury. However, this study still indicates fundamental differences in the levels and/or activation states of cells residing in the vasculature between African Americans and Caucasians. Whether this biological difference is observed in brain tissues or relates to a higher incidence of vascular health disparities between African Americans and Caucasians (300) requires further investigation. Genomic analysis could prove invaluable in this endeavor, shedding light on whether these elevations are attributable to genetic variations. Furthermore, it is crucial to consider the influence of social determinants of health, such as education, socioeconomic status, and exposure to adversity and discrimination, on overall health, and thus AD risk and progression. Future studies should aim to integrate CSF protein levels with vascular risk factors, environmental metrics, and sociodemographic data to better elucidate the underlying racial differences in the CSF proteome. This holistic approach will help uncover the complex interplay between genetic, environmental, and social factors that contribute to AD pathogenesis and inform on the development of targeted interventions for diverse populations.

4.3 Unveiling the interplay between neuronal alterations in AD and the role of the CSF in mirroring cognitive decline

The current biological framework for the pre-symptomatic stages of AD is based on the presence of A β deposition (A), tauopathy (T), and neurodegeneration (N) also termed the A/T/N framework (277). CSF remains the gold standard for A/T/N biomarkers of neurodegenerative disease as it maintains direct contact with the brain and reflects biochemical changes in amyloid (**Figure 4.1, purple line**), Tau (**green line**) and neurodegeneration (**yellow line**). A strength of our study was the balanced nature of African American samples, which offered the ability to examine racial differences in both cognitively normal controls with individuals diagnosed with AD. Our mass spectrometry measurements of Tau strongly correlated with immunoassay levels



Created with BioRender.com

Figure 4.1: Hypothesized time course differences in neuropathological and clinical changes based on biomarker alterations between Caucasians and African Americans with Alzheimer's disease. In Alzheimer's disease (AD), the conversion from a non-demented to demented state is associated with a buildup of amyloid-beta ($A\beta$) plaques (purple line), the accumulation of neurofibrillary Tau tangles (green line), and neuronal and synaptic loss (yellow line). Based on biomarker studies, the trajectory of change for the accumulation of Tau and the subsequent neuronal loss differs in African Americans with AD (dashed lines).

measured on the Roche Elecsys platform reinforcing measurements made by TMT-MS. Increased Tau in CSF is considered to result from neurodegeneration, however, it has also been shown to be increased in early pre-symptomatic disease stages when neurodegeneration is limited (277; 278) (**Figure 4.1, preclinical AD**). Recently, Tau CSF levels have been linked to enhanced synaptic plasticity where high levels of CSF Tau levels can be reflective of increased neuronal plasticity (279). Network analysis revealed a cluster of proteins, M12, along with another module, M6, exhibiting similar fluctuations in levels as Tau across racial groups, suggesting the involvement of other proteins that may function similarly to Tau in early disease synaptic plasticity. Other proteins that have been associated with synaptic plasticity include Calcium/calmodulin-dependent protein kinase II (CaMKII), cAMP-response element binding protein (CREB), Protein Kinases A and B (PRKAC1A and PRKAC1B), and growth-associated protein (GAP43) (269-273). Interestingly, all these proteins, including CAMK2A, CAMK2B, PRKAC1A, PRKAC1B, and GAP43, were categorized within the M6 module, indicating the potential association of other proteins within this module in synaptic plasticity. Further exploration of these proteins and their implications in racial disparities could provide valuable insights into AD pathogenesis and aid in developing targeted interventions.

Significantly, a considerable portion of synaptic proteins identified in this study aligned with M1 and M4. These modules demonstrated an overall decrease in levels with cognitive decline. We, also, observed that African Americans in this study had on average lower levels of neuronal markers mapping to M1 and M4 in the network, which are reduced in AD. Paradoxically, African Americans also have lower levels of neuronal proteins in M6 and M12, which all increase in AD. Consistent with this observation, in a recent CSF proteomic study in an asymptomatic Caucasian European population stratified by Tau CSF levels, individuals deemed to have high Tau levels maintained levels of M1 post-synaptic proteins (CADM3, NEO1, NPTX1, CHGB, PCSK1, NEGR, L1CAM, PTPRN, CACNA2D, PAM, VEGFA, NBL1 etc.) compared to individuals with lower Tau levels (279). This observation is analogous to differences we see between African

Americans and Caucasians with AD. M1 members VGF and NPTX2, strongly correlate to antemortem cognitive measures (280-282) and VGF and NPTX2 have been nominated as biomarkers of neurodegeneration (N) as their CSF levels enhance prediction of MCI to AD (282-284). Collectively, this would suggest that a specific sub-group of individuals with AD, including African Americans, have a higher burden of neurodegeneration (N) despite low CSF Tau levels (**Figure 4.1, dashed lines**). Longitudinal studies examining changes in CSF levels of neuronal proteins and other module constituents over time, with a specific focus on diverse racial populations, will be essential. By tracking the temporal patterns of protein biomarkers, researchers can gain a better understanding of critical timeframes for potentially delaying cognitive decline associated with the disease and addressing racial disparities in disease progression. Moreover, longitudinal studies can offer insights into the efficacy of therapeutic interventions and assist in devising personalized treatment approaches.

Collectively, these data suggest that there are likely distinct mechanisms responsible for the dysregulation of neuronal proteins, resulting in two separate pools of neuronal proteins that either go up or down with disease in CSF. Further investigations should be conducted to explore the distinct mechanisms that contribute to the differences in abundance and/or secretion of neuronal markers such as Tau and other proteins increased in AD CSF like CAMK2A, SNCB, and SYN1, In conjunction, the interplay between the neuronal markers that increase and neuronal markers that decrease with disease like VGF, NPTX2, and SCG2, which have also been found to differ by race, should be further explored.

4.4 Future directions

Although a strength of our study was the large number of African Americans included, there are several limitations that should be noted. First, we acknowledge that many of the protein changes we observe in the CSF across race could be due to ancestral or genetic differences (285; 286). There were no genetics *a priori* performed on these study participants to confirm

enrichment of African *vis a vis* European ancestry (287) as we stratified race solely by self-identification. Future studies, which include the integration of genetics and protein abundance to define protein quantitative trait loci (pQTL) will be necessary to resolve which proteins are under genetic control across race (288-290). It is noteworthy that the expression level of most modules which differed between racial groups were decreased in African Americans relative to Caucasians. Upon integration with whole genome profiling of larger cohorts, these patterns may help in the future to identify pQTLs or other mechanisms influencing synthesis and turnover of proteins that differ by race. Additionally, only a few studies to date have investigated proteomic difference by race in AD (291; 292), which have predominately focused on brain tissues and not on the scale of this current study. However, a major initiative of the Accelerating Medicine Partnership (AMP)-AD partnership (293) is to increase the number of diverse tissues included in multi-omic analyses, which will complement data generated from these previous studies. To support this effort, 81 brain tissue samples, obtained from Emory's Alzheimer's Disease Research Center, were prepared for future analysis. These samples have since been integrated with brain tissues from other AMP-AD partners, broadening the scope of the large-scale brain analyses (294; 295). Furthermore, despite the well documented differences in the quality of education, higher rates of poverty, and greater exposure to adversity and discrimination that increase risk for dementia (214; 215), these metrics were not captured on the participants in this study. Integrating CSF protein levels with vascular risk factors, and other environmental metrics in larger cohorts may help better resolve some of the underlying racial differences in the CSF proteome. Finally, in this study we adjusted for co-factors such as age and sex to pinpoint changes that are most likely to be associated with race and AD. Sex and age have an impact on the abundance of CSF Tau and other protein levels (296). Therefore, future studies that assess the interactions between, age, sex and race will be informative. Nevertheless, this study reveals an impressive view of protein co-expression in AD CSF across race, which provides new insights into the pathways underlying cell-type changes and further evidence that race may mediate these in AD. Future

directions in AD research should aim to unravel the distinct mechanisms underlying racial differences in AD biomarkers and underlying physiology. Integrating genetic, proteomic, and sociodemographic data, along with longitudinal investigations, will contribute to a more comprehensive understanding of AD pathogenesis and facilitate the development of targeted interventions for diverse populations affected by AD.

CHAPTER 5: REFERENCES

1. 2022. 2022 Alzheimer's disease facts and figures. *Alzheimers Dement* 18:700-89
2. 2023. 2023 Alzheimer's disease facts and figures. *Alzheimers Dement* 19:1598-695
3. Corder EH, Saunders AM, Risch NJ, Strittmatter WJ, Schmechel DE, et al. 1994. Protective effect of apolipoprotein E type 2 allele for late onset Alzheimer disease. *Nat Genet* 7:180-4
4. Corder EH, Saunders AM, Strittmatter WJ, Schmechel DE, Gaskell PC, et al. 1993. Gene dose of apolipoprotein E type 4 allele and the risk of Alzheimer's disease in late onset families. *Science* 261:921-3
5. Masters CL, Bateman R, Blennow K, Rowe CC, Sperling RA, Cummings JL. 2015. Alzheimer's disease. *Nat Rev Dis Primers* 1:15056
6. Stoccoro A, Coppede F. 2018. Role of epigenetics in Alzheimer's disease pathogenesis. *Neurodegener Dis Manag* 8:181-93
7. Hebert LE, Beckett LA, Scherr PA, Evans DA. 2001. Annual incidence of Alzheimer disease in the United States projected to the years 2000 through 2050. *Alzheimer Dis Assoc Disord* 15:169-73
8. Hebert LE, Weuve J, Scherr PA, Evans DA. 2013. Alzheimer disease in the United States (2010-2050) estimated using the 2010 census. *Neurology* 80:1778-83
9. Baker DJ, Petersen RC. 2018. Cellular senescence in brain aging and neurodegenerative diseases: evidence and perspectives. *J Clin Invest* 128:1208-16
10. Fasnacht JS, Wueest AS, Berres M, Thomann AE, Krumm S, et al. 2023. Conversion between the Montreal Cognitive Assessment and the Mini-Mental Status Examination. *J Am Geriatr Soc* 71:869-79
11. Nasreddine ZS, Phillips NA, Bedirian V, Charbonneau S, Whitehead V, et al. 2005. The Montreal Cognitive Assessment, MoCA: a brief screening tool for mild cognitive impairment. *J Am Geriatr Soc* 53:695-9
12. Folstein MF, Folstein SE, McHugh PR. 1975. "Mini-mental state". A practical method for grading the cognitive state of patients for the clinician. *J Psychiatr Res* 12:189-98
13. Hlavka JP, Kinoshita AT, Fang S, Hunt A. 2021. Clinical Outcome Measure Crosswalks in Alzheimer's Disease: A Systematic Review. *J Alzheimers Dis* 83:591-608
14. Ihl R, Frolich L, Dierks T, Martin EM, Maurer K. 1992. Differential validity of psychometric tests in dementia of the Alzheimer type. *Psychiatry Res* 44:93-106
15. Tombaugh TN, McIntyre NJ. 1992. The mini-mental state examination: a comprehensive review. *J Am Geriatr Soc* 40:922-35
16. Wind AW, Schellevis FG, Van Staveren G, Scholten RP, Jonker C, Van Eijk JT. 1997. Limitations of the Mini-Mental State Examination in diagnosing dementia in general practice. *Int J Geriatr Psychiatry* 12:101-8
17. Salis F, Costagiu D, Mandas A. 2023. Mini-Mental State Examination: Optimal Cut-Off Levels for Mild and Severe Cognitive Impairment. *Geriatrics (Basel)* 8
18. Carson N, Leach L, Murphy KJ. 2018. A re-examination of Montreal Cognitive Assessment (MoCA) cutoff scores. *Int J Geriatr Psychiatry* 33:379-88
19. Damian AM, Jacobson SA, Hentz JG, Belden CM, Shill HA, et al. 2011. The Montreal Cognitive Assessment and the mini-mental state examination as screening instruments for cognitive impairment: item analyses and threshold scores. *Dement Geriatr Cogn Disord* 31:126-31
20. Dalrymple-Alford JC, MacAskill MR, Nakas CT, Livingston L, Graham C, et al. 2010. The MoCA: well-suited screen for cognitive impairment in Parkinson disease. *Neurology* 75:1717-25

21. Freitas S, Simoes MR, Alves L, Santana I. 2013. Montreal cognitive assessment: validation study for mild cognitive impairment and Alzheimer disease. *Alzheimer Dis Assoc Disord* 27:37-43
22. Dong Y, Lee WY, Basri NA, Collinson SL, Merchant RA, et al. 2012. The Montreal Cognitive Assessment is superior to the Mini-Mental State Examination in detecting patients at higher risk of dementia. *Int Psychogeriatr* 24:1749-55
23. Freitas S, Simoes MR, Alves L, Santana I. 2012. Montreal Cognitive Assessment: influence of sociodemographic and health variables. *Arch Clin Neuropsychol* 27:165-75
24. Malek-Ahmadi M, Powell JJ, Belden CM, O'Connor K, Evans L, et al. 2015. Age- and education-adjusted normative data for the Montreal Cognitive Assessment (MoCA) in older adults age 70-99. *Neuropsychol Dev Cogn B Aging Neuropsychol Cogn* 22:755-61
25. Gagnon G, Hansen KT, Woolmore-Goodwin S, Gutmanis I, Wells J, et al. 2013. Correcting the MoCA for education: effect on sensitivity. *Can J Neurol Sci* 40:678-83
26. Rossetti HC, Lacritz LH, Cullum CM, Weiner MF. 2011. Normative data for the Montreal Cognitive Assessment (MoCA) in a population-based sample. *Neurology* 77:1272-5
27. Larouche E, Tremblay MP, Potvin O, Laforest S, Bergeron D, et al. 2016. Normative Data for the Montreal Cognitive Assessment in Middle-Aged and Elderly Quebec-French People. *Arch Clin Neuropsychol* 31:819-26
28. Goldstein FC, Ashley AV, Miller E, Alexeeva O, Zanders L, King V. 2014. Validity of the montreal cognitive assessment as a screen for mild cognitive impairment and dementia in African Americans. *J Geriatr Psychiatry Neurol* 27:199-203
29. Sink KM, Craft S, Smith SC, Maldjian JA, Bowden DW, et al. 2015. Montreal Cognitive Assessment and Modified Mini Mental State Examination in African Americans. *J Aging Res* 2015:872018
30. Milani SA, Marsiske M, Cottler LB, Chen X, Striley CW. 2018. Optimal cutoffs for the Montreal Cognitive Assessment vary by race and ethnicity. *Alzheimers Dement (Amst)* 10:773-81
31. Stelzma RA, Schnitzlein HN, Murlagh FR. 1995. An English l'ranslation of Alzheimer's 1907 Paper, "ijber eine eigenartige Erlranliung der Hirnrinde. *Clinical anatomy* 8:429-31
32. Karran E, Mercken M, De Strooper B. 2011. The amyloid cascade hypothesis for Alzheimer's disease: an appraisal for the development of therapeutics. *Nat Rev Drug Discov* 10:698-712
33. McGeer PL, McGeer EG. 2013. The amyloid cascade-inflammatory hypothesis of Alzheimer disease: implications for therapy. *Acta Neuropathol* 126:479-97
34. Ballatore C, Lee VM, Trojanowski JQ. 2007. Tau-mediated neurodegeneration in Alzheimer's disease and related disorders. *Nat Rev Neurosci* 8:663-72
35. Selkoe DJ. 1989. Amyloid beta protein precursor and the pathogenesis of Alzheimer's disease. *Cell* 58:611-2
36. Selkoe DJ. 1998. The cell biology of beta-amyloid precursor protein and presenilin in Alzheimer's disease. *Trends Cell Biol* 8:447-53
37. Zhang YW, Thompson R, Zhang H, Xu H. 2011. APP processing in Alzheimer's disease. *Mol Brain* 4:3
38. Kasim JK, Kavianinia I, Harris PWR, Brimble MA. 2019. Three Decades of Amyloid Beta Synthesis: Challenges and Advances. *Front Chem* 7:472
39. Chen GF, Xu TH, Yan Y, Zhou YR, Jiang Y, et al. 2017. Amyloid beta: structure, biology and structure-based therapeutic development. *Acta Pharmacol Sin* 38:1205-35
40. Roche J, Shen Y, Lee JH, Ying J, Bax A. 2016. Monomeric Aβ(1-40) and Aβ(1-42) Peptides in Solution Adopt Very Similar Ramachandran Map Distributions That Closely Resemble Random Coil. *Biochemistry* 55:762-75
41. Alvarez G, Munoz-Montano JR, Satrustegui J, Avila J, Bogonez E, Diaz-Nido J. 2002. Regulation of tau phosphorylation and protection against beta-amyloid-induced

- neurodegeneration by lithium. Possible implications for Alzheimer's disease. *Bipolar Disord* 4:153-65
42. Selkoe DJ. 1999. Translating cell biology into therapeutic advances in Alzheimer's disease. *Nature* 399:A23-31
 43. Selkoe DJ. 2000. Toward a comprehensive theory for Alzheimer's disease. Hypothesis: Alzheimer's disease is caused by the cerebral accumulation and cytotoxicity of amyloid beta-protein. *Ann N Y Acad Sci* 924:17-25
 44. Gakhar-Koppole N, Hundeshagen P, Mandl C, Weyer SW, Allinquant B, et al. 2008. Activity requires soluble amyloid precursor protein alpha to promote neurite outgrowth in neural stem cell-derived neurons via activation of the MAPK pathway. *Eur J Neurosci* 28:871-82
 45. Mattson MP. 1997. Cellular actions of beta-amyloid precursor protein and its soluble and fibrillogenic derivatives. *Physiol Rev* 77:1081-132
 46. Caille I, Allinquant B, Dupont E, Bouillot C, Langer A, et al. 2004. Soluble form of amyloid precursor protein regulates proliferation of progenitors in the adult subventricular zone. *Development* 131:2173-81
 47. Ohsawa I, Takamura C, Morimoto T, Ishiguro M, Kohsaka S. 1999. Amino-terminal region of secreted form of amyloid precursor protein stimulates proliferation of neural stem cells. *Eur J Neurosci* 11:1907-13
 48. Arakhamia T, Lee CE, Carlomagno Y, Duong DM, Kunding SR, et al. 2020. Posttranslational Modifications Mediate the Structural Diversity of Tauopathy Strains. *Cell* 180:633-44 e12
 49. Jack CR, Jr., Knopman DS, Jagust WJ, Shaw LM, Aisen PS, et al. 2010. Hypothetical model of dynamic biomarkers of the Alzheimer's pathological cascade. *Lancet Neurol* 9:119-28
 50. Jack CR, Jr., Knopman DS, Jagust WJ, Petersen RC, Weiner MW, et al. 2013. Tracking pathophysiological processes in Alzheimer's disease: an updated hypothetical model of dynamic biomarkers. *Lancet Neurol* 12:207-16
 51. Jack CR, Jr., Holtzman DM. 2013. Biomarker modeling of Alzheimer's disease. *Neuron* 80:1347-58
 52. Jack CR, Jr., Bennett DA, Blennow K, Carrillo MC, Dunn B, et al. 2018. NIA-AA Research Framework: Toward a biological definition of Alzheimer's disease. *Alzheimers Dement* 14:535-62
 53. Bateman RJ, Xiong C, Benzinger TL, Fagan AM, Goate A, et al. 2012. Clinical and biomarker changes in dominantly inherited Alzheimer's disease. *N Engl J Med* 367:795-804
 54. Fleisher AS, Chen K, Quiroz YT, Jakimovich LJ, Gutierrez Gomez M, et al. 2015. Associations between biomarkers and age in the presenilin 1 E280A autosomal dominant Alzheimer disease kindred: a cross-sectional study. *JAMA Neurol* 72:316-24
 55. Donohue MC, Jacqmin-Gadda H, Le Goff M, Thomas RG, Raman R, et al. 2014. Estimating long-term multivariate progression from short-term data. *Alzheimers Dement* 10:S400-10
 56. Young AL, Oxtoby NP, Daga P, Cash DM, Fox NC, et al. 2014. A data-driven model of biomarker changes in sporadic Alzheimer's disease. *Brain* 137:2564-77
 57. Xiong C, Jasielec MS, Weng H, Fagan AM, Benzinger TL, et al. 2016. Longitudinal relationships among biomarkers for Alzheimer disease in the Adult Children Study. *Neurology* 86:1499-506
 58. Fagan AM, Roe CM, Xiong C, Mintun MA, Morris JC, Holtzman DM. 2007. Cerebrospinal fluid tau/beta-amyloid(42) ratio as a prediction of cognitive decline in nondemented older adults. *Arch Neurol* 64:343-9

59. Mattsson N, Zetterberg H, Hansson O, Andreasen N, Parnetti L, et al. 2009. CSF biomarkers and incipient Alzheimer disease in patients with mild cognitive impairment. *JAMA* 302:385-93
60. Visser PJ, Verhey F, Knol DL, Scheltens P, Wahlund LO, et al. 2009. Prevalence and prognostic value of CSF markers of Alzheimer's disease pathology in patients with subjective cognitive impairment or mild cognitive impairment in the DESCRIPA study: a prospective cohort study. *Lancet Neurol* 8:619-27
61. Klunk WE, Engler H, Nordberg A, Wang Y, Blomqvist G, et al. 2004. Imaging brain amyloid in Alzheimer's disease with Pittsburgh Compound-B. *Ann Neurol* 55:306-19
62. Villain N, Chetelat G, Grassiot B, Bourgeat P, Jones G, et al. 2012. Regional dynamics of amyloid-beta deposition in healthy elderly, mild cognitive impairment and Alzheimer's disease: a voxelwise PiB-PET longitudinal study. *Brain* 135:2126-39
63. Buerger K, Ewers M, Pirttila T, Zinkowski R, Alafuzoff I, et al. 2006. CSF phosphorylated tau protein correlates with neocortical neurofibrillary pathology in Alzheimer's disease. *Brain* 129:3035-41
64. Brier MR, Gordon B, Friedrichsen K, McCarthy J, Stern A, et al. 2016. Tau and Abeta imaging, CSF measures, and cognition in Alzheimer's disease. *Sci Transl Med* 8:338ra66
65. Chhatwal JP, Schultz AP, Marshall GA, Boot B, Gomez-Isla T, et al. 2016. Temporal T807 binding correlates with CSF tau and phospho-tau in normal elderly. *Neurology* 87:920-6
66. Blennow K, Hampel H, Weiner M, Zetterberg H. 2010. Cerebrospinal fluid and plasma biomarkers in Alzheimer disease. *Nat Rev Neurol* 6:131-44
67. Seab JP, Jagust WJ, Wong ST, Roos MS, Reed BR, Budinger TF. 1988. Quantitative NMR measurements of hippocampal atrophy in Alzheimer's disease. *Magn Reson Med* 8:200-8
68. Fox NC, Crum WR, Scahill RI, Stevens JM, Janssen JC, Rossor MN. 2001. Imaging of onset and progression of Alzheimer's disease with voxel-compression mapping of serial magnetic resonance images. *Lancet* 358:201-5
69. Minoshima S, Giordani B, Berent S, Frey KA, Foster NL, Kuhl DE. 1997. Metabolic reduction in the posterior cingulate cortex in very early Alzheimer's disease. *Ann Neurol* 42:85-94
70. Besson FL, La Joie R, Dœuvre L, Gaubert M, Mezenge F, et al. 2015. Cognitive and Brain Profiles Associated with Current Neuroimaging Biomarkers of Preclinical Alzheimer's Disease. *J Neurosci* 35:10402-11
71. Dickerson BC, Bakkour A, Salat DH, Feczko E, Pacheco J, et al. 2009. The cortical signature of Alzheimer's disease: regionally specific cortical thinning relates to symptom severity in very mild to mild AD dementia and is detectable in asymptomatic amyloid-positive individuals. *Cereb Cortex* 19:497-510
72. Knopman DS, Jack CR, Jr., Wiste HJ, Weigand SD, Vemuri P, et al. 2013. Selective worsening of brain injury biomarker abnormalities in cognitively normal elderly persons with beta-amyloidosis. *JAMA Neurol* 70:1030-8
73. Landau SM, Harvey D, Madison CM, Koeppe RA, Reiman EM, et al. 2011. Associations between cognitive, functional, and FDG-PET measures of decline in AD and MCI. *Neurobiol Aging* 32:1207-18
74. Hebert LE, Bienias JL, Aggarwal NT, Wilson RS, Bennett DA, et al. 2010. Change in risk of Alzheimer disease over time. *Neurology* 75:786-91
75. Saunders AM, Strittmatter WJ, Schmechel D, George-Hyslop PH, Pericak-Vance MA, et al. 1993. Association of apolipoprotein E allele epsilon 4 with late-onset familial and sporadic Alzheimer's disease. *Neurology* 43:1467-72

76. Farrer LA, Cupples LA, Haines JL, Hyman B, Kukull WA, et al. 1997. Effects of age, sex, and ethnicity on the association between apolipoprotein E genotype and Alzheimer disease. A meta-analysis. APOE and Alzheimer Disease Meta Analysis Consortium. *JAMA* 278:1349-56
77. Green RC, Cupples LA, Go R, Benke KS, Edeki T, et al. 2002. Risk of dementia among white and African American relatives of patients with Alzheimer disease. *JAMA* 287:329-36
78. Fratiglioni L, Ahlbom A, Viitanen M, Winblad B. 1993. Risk factors for late-onset Alzheimer's disease: a population-based, case-control study. *Ann Neurol* 33:258-66
79. Mayeux R, Sano M, Chen J, Tatemichi T, Stern Y. 1991. Risk of dementia in first-degree relatives of patients with Alzheimer's disease and related disorders. *Arch Neurol* 48:269-73
80. Lautenschlager NT, Cupples LA, Rao VS, Auerbach SA, Becker R, et al. 1996. Risk of dementia among relatives of Alzheimer's disease patients in the MIRAGE study: What is in store for the oldest old? *Neurology* 46:641-50
81. Duyckaerts C, Delatour B, Potier MC. 2009. Classification and basic pathology of Alzheimer disease. *Acta Neuropathol* 118:5-36
82. Hardy JA, Higgins GA. 1992. Alzheimer's disease: the amyloid cascade hypothesis. *Science* 256:184-5
83. Tcw J, Goate AM. 2017. Genetics of beta-Amyloid Precursor Protein in Alzheimer's Disease. *Cold Spring Harb Perspect Med* 7
84. Scheuner D, Eckman C, Jensen M, Song X, Citron M, et al. 1996. Secreted amyloid beta-protein similar to that in the senile plaques of Alzheimer's disease is increased in vivo by the presenilin 1 and 2 and APP mutations linked to familial Alzheimer's disease. *Nat Med* 2:864-70
85. Goate A, Chartier-Harlin MC, Mullan M, Brown J, Crawford F, et al. 1991. Segregation of a missense mutation in the amyloid precursor protein gene with familial Alzheimer's disease. *Nature* 349:704-6
86. Fortea J, Vilaplana E, Carmona-Iragui M, Benejam B, Videla L, et al. 2020. Clinical and biomarker changes of Alzheimer's disease in adults with Down syndrome: a cross-sectional study. *Lancet* 395:1988-97
87. Fortea J, Zaman SH, Hartley S, Rafii MS, Head E, Carmona-Iragui M. 2021. Alzheimer's disease associated with Down syndrome: a genetic form of dementia. *Lancet Neurol* 20:930-42
88. Penke B, Paragi G, Gera J, Berkecz R, Kovacs Z, et al. 2018. The Role of Lipids and Membranes in the Pathogenesis of Alzheimer's Disease: A Comprehensive View. *Curr Alzheimer Res* 15:1191-212
89. Makin S. 2018. The amyloid hypothesis on trial. *Nature* 559:S4-S7
90. Loy CT, Schofield PR, Turner AM, Kwok JB. 2014. Genetics of dementia. *Lancet* 383:828-40
91. Michaelson DM. 2014. APOE epsilon4: the most prevalent yet understudied risk factor for Alzheimer's disease. *Alzheimers Dement* 10:861-8
92. Holtzman DM, Herz J, Bu G. 2012. Apolipoprotein E and apolipoprotein E receptors: normal biology and roles in Alzheimer disease. *Cold Spring Harb Perspect Med* 2:a006312
93. Guerreiro R, Wojtas A, Bras J, Carrasquillo M, Rogaevea E, et al. 2013. TREM2 variants in Alzheimer's disease. *N Engl J Med* 368:117-27
94. Jonsson T, Stefansson H, Steinberg S, Jonsdottir I, Jonsson PV, et al. 2013. Variant of TREM2 associated with the risk of Alzheimer's disease. *N Engl J Med* 368:107-16

95. Rajan KB, Weuve J, Barnes LL, McAninch EA, Wilson RS, Evans DA. 2021. Population estimate of people with clinical Alzheimer's disease and mild cognitive impairment in the United States (2020-2060). *Alzheimers Dement* 17:1966-75
96. Nelson PT, Head E, Schmitt FA, Davis PR, Neltner JH, et al. 2011. Alzheimer's disease is not "brain aging": neuropathological, genetic, and epidemiological human studies. *Acta Neuropathol* 121:571-87
97. 2021. 2021 Alzheimer's disease facts and figures. *Alzheimers Dement* 17:327-406
98. Snyder HM, Asthana S, Bain L, Brinton R, Craft S, et al. 2016. Sex biology contributions to vulnerability to Alzheimer's disease: A think tank convened by the Women's Alzheimer's Research Initiative. *Alzheimers Dement* 12:1186-96
99. Xu H, Wang R, Zhang YW, Zhang X. 2006. Estrogen, beta-amyloid metabolism/trafficking, and Alzheimer's disease. *Ann N Y Acad Sci* 1089:324-42
100. Greenfield JP, Leung LW, Cai D, Kaasik K, Gross RS, et al. 2002. Estrogen lowers Alzheimer beta-amyloid generation by stimulating trans-Golgi network vesicle biogenesis. *J Biol Chem* 277:12128-36
101. Sisodia SS. 1992. Beta-amyloid precursor protein cleavage by a membrane-bound protease. *Proc Natl Acad Sci U S A* 89:6075-9
102. Nordstedt C, Caporaso GL, Thyberg J, Gandy SE, Greengard P. 1993. Identification of the Alzheimer beta/A4 amyloid precursor protein in clathrin-coated vesicles purified from PC12 cells. *J Biol Chem* 268:608-12
103. Caporaso GL, Takei K, Gandy SE, Matteoli M, Mundigl O, et al. 1994. Morphologic and biochemical analysis of the intracellular trafficking of the Alzheimer beta/A4 amyloid precursor protein. *J Neurosci* 14:3122-38
104. Xu H, Gouras GK, Greenfield JP, Vincent B, Naslund J, et al. 1998. Estrogen reduces neuronal generation of Alzheimer beta-amyloid peptides. *Nat Med* 4:447-51
105. Pinto-Almazan R, Calzada-Mendoza CC, Campos-Lara MG, Guerra-Araiza C. 2012. Effect of chronic administration of estradiol, progesterone, and tibolone on the expression and phosphorylation of glycogen synthase kinase-3beta and the microtubule-associated protein tau in the hippocampus and cerebellum of female rat. *J Neurosci Res* 90:878-86
106. Brinton RD, Yao J, Yin F, Mack WJ, Cadenas E. 2015. Perimenopause as a neurological transition state. *Nat Rev Endocrinol* 11:393-405
107. McCarthy M, Raval AP. 2020. The peri-menopause in a woman's life: a systemic inflammatory phase that enables later neurodegenerative disease. *J Neuroinflammation* 17:317
108. Zhao L, Mao Z, Brinton RD. 2009. A select combination of clinically relevant phytoestrogens enhances estrogen receptor beta-binding selectivity and neuroprotective activities in vitro and in vivo. *Endocrinology* 150:770-83
109. Burger HG, Dudley EC, Robertson DM, Dennerstein L. 2002. Hormonal changes in the menopause transition. *Recent Prog Horm Res* 57:257-75
110. Horstman AM, Dillon EL, Urban RJ, Sheffield-Moore M. 2012. The role of androgens and estrogens on healthy aging and longevity. *J Gerontol A Biol Sci Med Sci* 67:1140-52
111. Baumgart M, Snyder HM, Carrillo MC, Fazio S, Kim H, Johns H. 2015. Summary of the evidence on modifiable risk factors for cognitive decline and dementia: A population-based perspective. *Alzheimers Dement* 11:718-26
112. Livingston G, Huntley J, Sommerlad A, Ames D, Ballard C, et al. 2020. Dementia prevention, intervention, and care: 2020 report of the Lancet Commission. *Lancet* 396:413-46
113. Nianogo RA, Rosenwohl-Mack A, Yaffe K, Carrasco A, Hoffmann CM, Barnes DE. 2022. Risk Factors Associated With Alzheimer Disease and Related Dementias by Sex and Race and Ethnicity in the US. *JAMA Neurol* 79:584-91

114. Ronnema E, Zethelius B, Lannfelt L, Kilander L. 2011. Vascular risk factors and dementia: 40-year follow-up of a population-based cohort. *Dement Geriatr Cogn Disord* 31:460-6
115. Kivimaki M, Luukkonen R, Batty GD, Ferrie JE, Pentti J, et al. 2018. Body mass index and risk of dementia: Analysis of individual-level data from 1.3 million individuals. *Alzheimers Dement* 14:601-9
116. Gottesman RF, Albert MS, Alonso A, Coker LH, Coresh J, et al. 2017. Associations Between Midlife Vascular Risk Factors and 25-Year Incident Dementia in the Atherosclerosis Risk in Communities (ARIC) Cohort. *JAMA Neurol* 74:1246-54
117. Gottesman RF, Schneider AL, Zhou Y, Coresh J, Green E, et al. 2017. Association Between Midlife Vascular Risk Factors and Estimated Brain Amyloid Deposition. *JAMA* 317:1443-50
118. Abell JG, Kivimaki M, Dugravot A, Tabak AG, Fayosse A, et al. 2018. Association between systolic blood pressure and dementia in the Whitehall II cohort study: role of age, duration, and threshold used to define hypertension. *Eur Heart J* 39:3119-25
119. Debette S, Seshadri S, Beiser A, Au R, Himali JJ, et al. 2011. Midlife vascular risk factor exposure accelerates structural brain aging and cognitive decline. *Neurology* 77:461-8
120. Anstey KJ, Ashby-Mitchell K, Peters R. 2017. Updating the Evidence on the Association between Serum Cholesterol and Risk of Late-Life Dementia: Review and Meta-Analysis. *J Alzheimers Dis* 56:215-28
121. LaPlume AA, McKetton L, Levine B, Troyer AK, Anderson ND. 2022. The adverse effect of modifiable dementia risk factors on cognition amplifies across the adult lifespan. *Alzheimers Dement (Amst)* 14:e12337
122. Fitzpatrick AL, Kuller LH, Lopez OL, Diehr P, O'Meara ES, et al. 2009. Midlife and late-life obesity and the risk of dementia: cardiovascular health study. *Arch Neurol* 66:336-42
123. Corrada MM, Hayden KM, Paganini-Hill A, Bullain SS, DeMoss J, et al. 2017. Age of onset of hypertension and risk of dementia in the oldest-old: The 90+ Study. *Alzheimers Dement* 13:103-10
124. Tin A, Bressler J, Simino J, Sullivan KJ, Mei H, et al. 2022. Genetic Risk, Midlife Life's Simple 7, and Incident Dementia in the Atherosclerosis Risk in Communities Study. *Neurology* 99:e154-63
125. Samieri C, Perier MC, Gaye B, Proust-Lima C, Helmer C, et al. 2018. Association of Cardiovascular Health Level in Older Age With Cognitive Decline and Incident Dementia. *JAMA* 320:657-64
126. Zhong G, Wang Y, Zhang Y, Guo JJ, Zhao Y. 2015. Smoking is associated with an increased risk of dementia: a meta-analysis of prospective cohort studies with investigation of potential effect modifiers. *PLoS One* 10:e0118333
127. Ogino E, Manly JJ, Schupf N, Mayeux R, Gu Y. 2019. Current and past leisure time physical activity in relation to risk of Alzheimer's disease in older adults. *Alzheimers Dement* 15:1603-11
128. Najjar J, Ostling S, Gudmundsson P, Sundh V, Johansson L, et al. 2019. Cognitive and physical activity and dementia: A 44-year longitudinal population study of women. *Neurology* 92:e1322-e30
129. Buchman AS, Yu L, Wilson RS, Lim A, Dawe RJ, et al. 2019. Physical activity, common brain pathologies, and cognition in community-dwelling older adults. *Neurology* 92:e811-e22
130. Tan ZS, Spartano NL, Beiser AS, DeCarli C, Auerbach SH, et al. 2017. Physical Activity, Brain Volume, and Dementia Risk: The Framingham Study. *J Gerontol A Biol Sci Med Sci* 72:789-95
131. Stephen R, Hongisto K, Solomon A, Lonroos E. 2017. Physical Activity and Alzheimer's Disease: A Systematic Review. *J Gerontol A Biol Sci Med Sci* 72:733-9

132. Blondell SJ, Hammersley-Mather R, Veerman JL. 2014. Does physical activity prevent cognitive decline and dementia?: A systematic review and meta-analysis of longitudinal studies. *BMC Public Health* 14:510
133. Guure CB, Ibrahim NA, Adam MB, Said SM. 2017. Impact of Physical Activity on Cognitive Decline, Dementia, and Its Subtypes: Meta-Analysis of Prospective Studies. *Biomed Res Int* 2017:9016924
134. Jensen CS, Simonsen AH, Siersma V, Beyer N, Frederiksen KS, et al. 2019. Patients with Alzheimer's disease who carry the APOE epsilon4 allele benefit more from physical exercise. *Alzheimers Dement (N Y)* 5:99-106
135. Felisatti F, Gonneaud J, Palix C, Garnier-Crussard A, Mezenge F, et al. 2022. Role of Cardiovascular Risk Factors on the Association Between Physical Activity and Brain Integrity Markers in Older Adults. *Neurology* 98:e2023-e35
136. Casaletto K, Ramos-Miguel A, VandeBunte A, Memel M, Buchman A, et al. 2022. Late-life physical activity relates to brain tissue synaptic integrity markers in older adults. *Alzheimers Dement* 18:2023-35
137. Ballarini T, Melo van Lent D, Brunner J, Schroder A, Wolfsgruber S, et al. 2021. Mediterranean Diet, Alzheimer Disease Biomarkers and Brain Atrophy in Old Age. *Neurology* 96:e2920-32
138. van den Brink AC, Brouwer-Brolsma EM, Berendsen AAM, van de Rest O. 2019. The Mediterranean, Dietary Approaches to Stop Hypertension (DASH), and Mediterranean-DASH Intervention for Neurodegenerative Delay (MIND) Diets Are Associated with Less Cognitive Decline and a Lower Risk of Alzheimer's Disease-A Review. *Adv Nutr* 10:1040-65
139. Morris MC, Tangney CC, Wang Y, Sacks FM, Bennett DA, Aggarwal NT. 2015. MIND diet associated with reduced incidence of Alzheimer's disease. *Alzheimers Dement* 11:1007-14
140. Morris MC, Tangney CC, Wang Y, Sacks FM, Barnes LL, et al. 2015. MIND diet slows cognitive decline with aging. *Alzheimers Dement* 11:1015-22
141. Lourida I, Soni M, Thompson-Coon J, Purandare N, Lang IA, et al. 2013. Mediterranean diet, cognitive function, and dementia: a systematic review. *Epidemiology* 24:479-89
142. Hardman RJ, Kennedy G, Macpherson H, Scholey AB, Pipingas A. 2016. Adherence to a Mediterranean-Style Diet and Effects on Cognition in Adults: A Qualitative Evaluation and Systematic Review of Longitudinal and Prospective Trials. *Front Nutr* 3:22
143. Health WCoSDo, Organization WH. 2008. *Closing the gap in a generation: health equity through action on the social determinants of health: Commission on Social Determinants of Health final report*. World Health Organization
144. Braveman P, Egerter S, Williams DR. 2011. The social determinants of health: coming of age. *Annu Rev Public Health* 32:381-98
145. Barbeau EM, Krieger N, Soobader MJ. 2004. Working class matters: socioeconomic disadvantage, race/ethnicity, gender, and smoking in NHIS 2000. *Am J Public Health* 94:269-78
146. Cutler DM, Lleras-Muney A. 2006. Education and health: evaluating theories and evidence. National bureau of economic research Cambridge, Mass., USA
147. Dewalt DA, Berkman ND, Sheridan S, Lohr KN, Pignone MP. 2004. Literacy and health outcomes: a systematic review of the literature. *J Gen Intern Med* 19:1228-39
148. Sanders LM, Federico S, Klass P, Abrams MA, Dreyer B. 2009. Literacy and child health: a systematic review. *Arch Pediatr Adolesc Med* 163:131-40
149. Bartley M, Plewis I. 2002. Accumulated labour market disadvantage and limiting long-term illness: data from the 1971-1991 Office for National Statistics' Longitudinal Study. *Int J Epidemiol* 31:336-41

150. Gabel J, Levitt L, Holve E, Pickreign J, Whitmore H, et al. 2002. Job-based health benefits in 2002: some important trends. *Health Aff (Millwood)* 21:143-51
151. Crissey SR. 2009. Educational attainment in the United States: 2007. *US department of Commerce*
152. O'Neil BA, Forsythe ME, Stanish WD. 2001. Chronic occupational repetitive strain injury. *Can Fam Physician* 47:311-6
153. Warburton DE, Nicol CW, Bredin SS. 2006. Health benefits of physical activity: the evidence. *CMAJ* 174:801-9
154. de Jonge J, Bosma H, Peter R, Siegrist J. 2000. Job strain, effort-reward imbalance and employee well-being: a large-scale cross-sectional study. *Soc Sci Med* 50:1317-27
155. Karasek R. 1990. Stress, productivity, and the reconstruction of working life. *Health work*
156. Egerter S, Dekker M, An J, Grossman-Kahn R, Braveman P. 2008. Work matters for health. *Robert Wood Johnson Foundation Commission to Build a Healthier America*
157. Collins SR, Davis K, Doty MM, Ho A. 2004. Wages, health benefits, and workers' health. *Issue Brief (Commonw Fund)*:1-16
158. Heymann J, Boynton-Jarrett R, Carter P, Bond JT, Galinsky E. 2002. Work-family issues and low-income families. *Retrieved June 1:2003*
159. Booth KM, Pinkston MM, Poston WS. 2005. Obesity and the built environment. *J Am Diet Assoc* 105:S110-7
160. Chuang YC, Cubbin C, Ahn D, Winkleby MA. 2005. Effects of neighbourhood socioeconomic status and convenience store concentration on individual level smoking. *J Epidemiol Community Health* 59:568-73
161. Gordon-Larsen P, Nelson MC, Page P, Popkin BM. 2006. Inequality in the built environment underlies key health disparities in physical activity and obesity. *Pediatrics* 117:417-24
162. Giles-Corti B, Donovan RJ. 2002. The relative influence of individual, social and physical environment determinants of physical activity. *Soc Sci Med* 54:1793-812
163. Heinrich KM, Lee RE, Suminski RR, Regan GR, Reese-Smith JY, et al. 2007. Associations between the built environment and physical activity in public housing residents. *Int J Behav Nutr Phys Act* 4:56
164. Morland K, Diez Roux AV, Wing S. 2006. Supermarkets, other food stores, and obesity: the atherosclerosis risk in communities study. *Am J Prev Med* 30:333-9
165. Sallis JF, Glanz K. 2006. The role of built environments in physical activity, eating, and obesity in childhood. *Future Child* 16:89-108
166. Fernandez RM, Su C. 2004. Space in the study of labor markets. *Annu. Rev. Sociol.* 30:545-69
167. Pastor M. 2001. Geography and opportunity. *America becoming: Racial trends and their consequences* 1:435-68
168. Williams DR, Collins C. 2001. Racial residential segregation: a fundamental cause of racial disparities in health. *Public health reports*
169. Diez Roux AV, Mair C. 2010. Neighborhoods and health. *Annals of the New York academy of sciences* 1186:125-45
170. Pickett KE, Collins JW, Jr., Masi CM, Wilkinson RG. 2005. The effects of racial density and income incongruity on pregnancy outcomes. *Soc Sci Med* 60:2229-38
171. Robert SA. 1999. Socioeconomic position and health: the independent contribution of community socioeconomic context. *Annual review of sociology* 25:489-516
172. Winkleby M, Cubbin C, Ahn D. 2006. Effect of cross-level interaction between individual and neighborhood socioeconomic status on adult mortality rates. *Am J Public Health* 96:2145-53

173. Williams DR, Mohammed SA, Leavell J, Collins C. 2010. Race, socioeconomic status, and health: complexities, ongoing challenges, and research opportunities. *Ann N Y Acad Sci* 1186:69-101
174. McEwen BS, Gianaros PJ. 2010. Central role of the brain in stress and adaptation: links to socioeconomic status, health, and disease. *Ann N Y Acad Sci* 1186:190-222
175. Steptoe A, Marmot M. 2002. The role of psychobiological pathways in socio-economic inequalities in cardiovascular disease risk. *Eur Heart J* 23:13-25
176. Braveman P, Marchi K, Egerter S, Kim S, Metzler M, et al. 2010. Poverty, near-poverty, and hardship around the time of pregnancy. *Matern Child Health J* 14:20-35
177. Evans GW, Kim P. 2007. Childhood poverty and health: cumulative risk exposure and stress dysregulation. *Psychol Sci* 18:953-7
178. Williams DR, Mohammed SA. 2009. Discrimination and racial disparities in health: evidence and needed research. *J Behav Med* 32:20-47
179. Seeman T, Epel E, Gruenewald T, Karlamangla A, McEwen BS. 2010. Socio-economic differentials in peripheral biology: cumulative allostatic load. *Ann N Y Acad Sci* 1186:223-39
180. McEwen BS. 2006. Protective and damaging effects of stress mediators: central role of the brain. *Dialogues Clin Neurosci* 8:367-81
181. Seeman TE, McEwen BS, Rowe JW, Singer BH. 2001. Allostatic load as a marker of cumulative biological risk: MacArthur studies of successful aging. *Proc Natl Acad Sci U S A* 98:4770-5
182. Seeman TE, Singer BH, Rowe JW, Horwitz RI, McEwen BS. 1997. Price of adaptation--allostatic load and its health consequences. MacArthur studies of successful aging. *Arch Intern Med* 157:2259-68
183. Charles CZ. 2003. The dynamics of racial residential segregation. *Annual review of sociology* 29:167-207
184. Rouse CE, Barrow L. 2006. U.S. elementary and secondary schools: equalizing opportunity or replicating the status quo? *Future Child* 16:99-123
185. Nuru-Jeter A, Dominguez TP, Hammond WP, Leu J, Skaff M, et al. 2009. "It's the skin you're in": African-American women talk about their experiences of racism. an exploratory study to develop measures of racism for birth outcome studies. *Matern Child Health J* 13:29-39
186. Holtzman DM, Morris JC, Goate AM. 2011. Alzheimer's disease: the challenge of the second century. *Sci Transl Med* 3:77sr1
187. Perrin RJ, Fagan AM, Holtzman DM. 2009. Multimodal techniques for diagnosis and prognosis of Alzheimer's disease. *Nature* 461:916-22
188. Craig-Schapiro R, Fagan AM, Holtzman DM. 2009. Biomarkers of Alzheimer's disease. *Neurobiol Dis* 35:128-40
189. Se Thoe E, Fauzi A, Tang YQ, Chamyuang S, Chia AYY. 2021. A review on advances of treatment modalities for Alzheimer's disease. *Life Sci* 276:119129
190. Teaktong T, Graham AJ, Court JA, Perry RH, Jaros E, et al. 2004. Nicotinic acetylcholine receptor immunohistochemistry in Alzheimer's disease and dementia with Lewy bodies: differential neuronal and astroglial pathology. *J Neurol Sci* 225:39-49
191. Mash DC, Flynn DD, Potter LT. 1985. Loss of M2 muscarine receptors in the cerebral cortex in Alzheimer's disease and experimental cholinergic denervation. *Science* 228:1115-7
192. Rinne JO, Brooks DJ, Rossor MN, Fox NC, Bullock R, et al. 2010. 11C-PiB PET assessment of change in fibrillar amyloid-beta load in patients with Alzheimer's disease treated with bapineuzumab: a phase 2, double-blind, placebo-controlled, ascending-dose study. *Lancet Neurol* 9:363-72

193. van Dyck CH, Swanson CJ, Aisen P, Bateman RJ, Chen C, et al. 2023. Lecanemab in Early Alzheimer's Disease. *N Engl J Med* 388:9-21
194. Sims JR, Zimmer JA, Evans CD, Lu M, Ardayfio P, et al. 2023. Donanemab in Early Symptomatic Alzheimer Disease: The TRAILBLAZER-ALZ 2 Randomized Clinical Trial. *JAMA*
195. Salloway S, Sperling R, Fox NC, Blennow K, Klunk W, et al. 2014. Two phase 3 trials of bapineuzumab in mild-to-moderate Alzheimer's disease. *N Engl J Med* 370:322-33
196. Liu E, Schmidt ME, Margolin R, Sperling R, Koeppe R, et al. 2015. Amyloid-beta 11C-PiB-PET imaging results from 2 randomized bapineuzumab phase 3 AD trials. *Neurology* 85:692-700
197. Morris JC, Selkoe DJ. 2011. Recommendations for the incorporation of biomarkers into Alzheimer clinical trials: an overview. *Neurobiol Aging* 32 Suppl 1:S1-3
198. Sperling RA, Jack CR, Jr., Aisen PS. 2011. Testing the right target and right drug at the right stage. *Sci Transl Med* 3:111cm33
199. Cushing H. 1914. Studies on the Cerebro-Spinal Fluid : I. Introduction. *J Med Res* 31:1-19
200. Henry MS, Passmore AP, Todd S, McGuinness B, Craig D, Johnston JA. 2013. The development of effective biomarkers for Alzheimer's disease: a review. *Int J Geriatr Psychiatry* 28:331-40
201. Hansson O, Zetterberg H, Buchhave P, Londos E, Blennow K, Minthon L. 2006. Association between CSF biomarkers and incipient Alzheimer's disease in patients with mild cognitive impairment: a follow-up study. *Lancet Neurol* 5:228-34
202. Mawuenyega KG, Sigurdson W, Ovod V, Munsell L, Kasten T, et al. 2010. Decreased clearance of CNS beta-amyloid in Alzheimer's disease. *Science* 330:1774
203. Brunello CA, Merezhko M, Uronen RL, Huttunen HJ. 2020. Mechanisms of secretion and spreading of pathological tau protein. *Cell Mol Life Sci* 77:1721-44
204. Pooler AM, Phillips EC, Lau DH, Noble W, Hanger DP. 2013. Physiological release of endogenous tau is stimulated by neuronal activity. *EMBO Rep* 14:389-94
205. Yamada K, Holth JK, Liao F, Stewart FR, Mahan TE, et al. 2014. Neuronal activity regulates extracellular tau in vivo. *J Exp Med* 211:387-93
206. Wang Y, Balaji V, Kaniyappan S, Kruger L, Irsen S, et al. 2017. The release and trans-synaptic transmission of Tau via exosomes. *Mol Neurodegener* 12:5
207. Katsinelos T, Zeitler M, Dimou E, Karakatsani A, Muller HM, et al. 2018. Unconventional Secretion Mediates the Trans-cellular Spreading of Tau. *Cell Rep* 23:2039-55
208. Merezhko M, Brunello CA, Yan X, Vihinen H, Jokitalo E, et al. 2018. Secretion of Tau via an Unconventional Non-vesicular Mechanism. *Cell Rep* 25:2027-35 e4
209. Arai H, Terajima M, Miura M, Higuchi S, Muramatsu T, et al. 1995. Tau in cerebrospinal fluid: a potential diagnostic marker in Alzheimer's disease. *Ann Neurol* 38:649-52
210. Ritchie C, Smailagic N, Noel-Storr AH, Ukoumunne O, Ladds EC, Martin S. 2017. CSF tau and the CSF tau/ABeta ratio for the diagnosis of Alzheimer's disease dementia and other dementias in people with mild cognitive impairment (MCI). *Cochrane Database Syst Rev* 3:CD010803
211. Rajan KB, Weuve J, Barnes LL, Wilson RS, Evans DA. 2019. Prevalence and incidence of clinically diagnosed Alzheimer's disease dementia from 1994 to 2012 in a population study. *Alzheimers Dement* 15:1-7
212. Potter GG, Plassman BL, Burke JR, Kabeto MU, Langa KM, et al. 2009. Cognitive performance and informant reports in the diagnosis of cognitive impairment and dementia in African Americans and whites. *Alzheimers Dement* 5:445-53
213. Gurland BJ, Wilder DE, Lantigua R, Stern Y, Chen J, et al. 1999. Rates of dementia in three ethnorracial groups. *Int J Geriatr Psychiatry* 14:481-93

214. Glymour MM, Manly JJ. 2008. Lifecourse social conditions and racial and ethnic patterns of cognitive aging. *Neuropsychol Rev* 18:223-54
215. Lines L, Sherif, N., & Wiener, J. . 2014. Racial and ethnic disparities among individuals with Alzheimer's disease in the United States: A literature review. *RTI Press*
216. Reitz C, Jun G, Naj A, Rajbhandary R, Vardarajan BN, et al. 2013. Variants in the ATP-binding cassette transporter (ABCA7), apolipoprotein E 4, and the risk of late-onset Alzheimer disease in African Americans. *JAMA* 309:1483-92
217. Logue MW, Schu M, Vardarajan BN, Buross J, Green RC, et al. 2011. A comprehensive genetic association study of Alzheimer disease in African Americans. *Arch Neurol* 68:1569-79
218. Rayaprolu S, Higginbotham L, Bagchi P, Watson CM, Zhang T, et al. 2021. Systems-based proteomics to resolve the biology of Alzheimer's disease beyond amyloid and tau. *Neuropsychopharmacology* 46:98-115
219. Yates JR, 3rd. 1998. Mass spectrometry and the age of the proteome. *J Mass Spectrom* 33:1-19
220. Wolters DA, Washburn MP, Yates JR, 3rd. 2001. An automated multidimensional protein identification technology for shotgun proteomics. *Anal Chem* 73:5683-90
221. Link AJ, Eng J, Schieltz DM, Carmack E, Mize GJ, et al. 1999. Direct analysis of protein complexes using mass spectrometry. *Nat Biotechnol* 17:676-82
222. Yates JR, 3rd. 2004. Mass spectral analysis in proteomics. *Annu Rev Biophys Biomol Struct* 33:297-316
223. Zhang Y, Fonslow BR, Shan B, Baek MC, Yates JR, 3rd. 2013. Protein analysis by shotgun/bottom-up proteomics. *Chem Rev* 113:2343-94
224. Aebersold R, Mann M. 2003. Mass spectrometry-based proteomics. *Nature* 422:198-207
225. Pappireddi N, Martin L, Wuhr M. 2019. A Review on Quantitative Multiplexed Proteomics. *Chembiochem* 20:1210-24
226. Gillet LC, Leitner A, Aebersold R. 2016. Mass Spectrometry Applied to Bottom-Up Proteomics: Entering the High-Throughput Era for Hypothesis Testing. *Annu Rev Anal Chem (Palo Alto Calif)* 9:449-72
227. Johnson ECB, Dammer EB, Duong DM, Yin L, Thambisetty M, et al. 2018. Deep proteomic network analysis of Alzheimer's disease brain reveals alterations in RNA binding proteins and RNA splicing associated with disease. *Mol Neurodegener* 13:52
228. Ping L, Duong DM, Yin L, Gearing M, Lah JJ, et al. 2018. Global quantitative analysis of the human brain proteome in Alzheimer's and Parkinson's Disease. *Sci Data* 5:180036
229. Rauniyar N, Yates JR, 3rd. 2014. Isobaric labeling-based relative quantification in shotgun proteomics. *J Proteome Res* 13:5293-309
230. Li J, Van Vranken JG, Pontano Vaites L, Schweppe DK, Huttlin EL, et al. 2020. TMTpro reagents: a set of isobaric labeling mass tags enables simultaneous proteome-wide measurements across 16 samples. *Nat Methods* 17:399-404
231. Bai B, Wang X, Li Y, Chen PC, Yu K, et al. 2020. Deep Multilayer Brain Proteomics Identifies Molecular Networks in Alzheimer's Disease Progression. *Neuron* 105:975-91 e7
232. Ping L, Kundinger SR, Duong DM, Yin L, Gearing M, et al. 2020. Global quantitative analysis of the human brain proteome and phosphoproteome in Alzheimer's disease. *Sci Data* 7:315
233. Brenes A, Hukelmann J, Bensaddek D, Lamond AI. 2019. Multibatch TMT Reveals False Positives, Batch Effects and Missing Values. *Mol Cell Proteomics* 18:1967-80
234. Meyer JG, Schilling B. 2017. Clinical applications of quantitative proteomics using targeted and untargeted data-independent acquisition techniques. *Expert Rev Proteomics* 14:419-29

235. Seyfried NT, Dammer EB, Swarup V, Nandakumar D, Duong DM, et al. 2017. A Multi-network Approach Identifies Protein-Specific Co-expression in Asymptomatic and Symptomatic Alzheimer's Disease. *Cell Syst* 4:60-72 e4
236. Johnson ECB, Carter EK, Dammer EB, Duong DM, Gerasimov ES, et al. 2022. Large-scale deep multi-layer analysis of Alzheimer's disease brain reveals strong proteomic disease-related changes not observed at the RNA level. *Nat Neurosci* 25:213-25
237. Johnson ECB, Dammer EB, Duong DM, Ping L, Zhou M, et al. 2020. Large-scale proteomic analysis of Alzheimer's disease brain and cerebrospinal fluid reveals early changes in energy metabolism associated with microglia and astrocyte activation. *Nat Med* 26:769-80
238. Parikshak NN, Gandal MJ, Geschwind DH. 2015. Systems biology and gene networks in neurodevelopmental and neurodegenerative disorders. *Nat Rev Genet* 16:441-58
239. Miller JA, Oldham MC, Geschwind DH. 2008. A systems level analysis of transcriptional changes in Alzheimer's disease and normal aging. *J Neurosci* 28:1410-20
240. Oldham MC, Konopka G, Iwamoto K, Langfelder P, Kato T, et al. 2008. Functional organization of the transcriptome in human brain. *Nat Neurosci* 11:1271-82
241. Prill RJ, Marbach D, Saez-Rodriguez J, Sorger PK, Alexopoulos LG, et al. 2010. Towards a rigorous assessment of systems biology models: the DREAM3 challenges. *PLoS One* 5:e9202
242. Zhang B, Horvath S. 2005. A general framework for weighted gene co-expression network analysis. *Stat Appl Genet Mol Biol* 4:Article17
243. Mostafavi S, Gaiteri C, Sullivan SE, White CC, Tasaki S, et al. 2018. A molecular network of the aging human brain provides insights into the pathology and cognitive decline of Alzheimer's disease. *Nat Neurosci* 21:811-9
244. Zambon AC, Gaj S, Ho I, Hanspers K, Vranizan K, et al. 2012. GO-Elite: a flexible solution for pathway and ontology over-representation. *Bioinformatics* 28:2209-10
245. Higginbotham L, Ping L, Dammer EB, Duong DM, Zhou M, et al. 2020. Integrated proteomics reveals brain-based cerebrospinal fluid biomarkers in asymptomatic and symptomatic Alzheimer's disease. *Sci Adv* 6
246. Swarup V, Chang TS, Duong DM, Dammer EB, Dai J, et al. 2020. Identification of Conserved Proteomic Networks in Neurodegenerative Dementia. *Cell Rep* 31:107807
247. McKhann GM, Knopman DS, Chertkow H, Hyman BT, Jack Jr CR, et al. 2011. The diagnosis of dementia due to Alzheimer's disease: Recommendations from the National Institute on Aging-Alzheimer's Association workgroups on diagnostic guidelines for Alzheimer's disease. *Alzheimer's and Dementia* 7:263-9
248. Albert MS, DeKosky ST, Dickson D, Dubois B, Feldman HH, et al. 2011. The diagnosis of mild cognitive impairment due to Alzheimer's disease: Recommendations from the National Institute on Aging-Alzheimer's Association workgroups on diagnostic guidelines for Alzheimer's disease. *Alzheimer's and Dementia* 7:270-9
249. Bittner T, Zetterberg H, Teunissen CE, Ostlund RE, Jr., Militello M, et al. 2016. Technical performance of a novel, fully automated electrochemiluminescence immunoassay for the quantitation of beta-amyloid (1-42) in human cerebrospinal fluid. *Alzheimers Dement* 12:517-26
250. Schindler SE, Gray JD, Gordon BA, Xiong C, Batrla-Utermann R, et al. 2018. Cerebrospinal fluid biomarkers measured by Elecsys assays compared to amyloid imaging. *Alzheimers Dement* 14:1460-9
251. Hansson O, Seibyl J, Stomrud E, Zetterberg H, Trojanowski JQ, et al. 2018. CSF biomarkers of Alzheimer's disease concord with amyloid-beta PET and predict clinical progression: A study of fully automated immunoassays in BioFINDER and ADNI cohorts. *Alzheimers Dement* 14:1470-81

252. Higginbotham L, Ping L, Dammer EB, Duong DM, Zhou M, et al. 2020. Integrated Proteomics Reveals Brain-Based Cerebrospinal Fluid Biomarkers in Asymptomatic and Symptomatic Alzheimer's Disease. *Science Advances* 6:eaaz9360
253. Dammer EB, Ping L, Duong DM, Modeste ES, Seyfried NT, et al. 2022. Multi-platform proteomic analysis of Alzheimer's disease cerebrospinal fluid and plasma reveals network biomarkers associated with proteostasis and the matrisome. *Alzheimers Res Ther* 14:174
254. Winiarska A, Zareba L, Krolczyk G, Czyzewicz G, Zabczyk M, Undas A. 2019. Decreased Levels of Histidine-Rich Glycoprotein in Advanced Lung Cancer: Association with Prothrombotic Alterations. *Dis Markers* 2019:8170759
255. Magistretti PJ, Allaman I. 2015. A cellular perspective on brain energy metabolism and functional imaging. *Neuron* 86:883-901
256. Maienschein-Cline M, Lei Z, Gardeux V, Abbasi T, Machado RF, et al. 2014. ARTS: automated randomization of multiple traits for study design. *Bioinformatics* 30:1637-9
257. Watson CM, Dammer EB, Ping L, Duong DM, Modeste E, et al. 2023. Quantitative Mass Spectrometry Analysis of Cerebrospinal Fluid Protein Biomarkers in Alzheimer's Disease. *Sci Data* 10:261
258. Dammer EB, Seyfried NT, Johnson ECB. 2023. Batch Correction and Harmonization of -Omics Datasets with a Tunable Median Polish of Ratio. *Front Syst Biol* 3
259. Chen X, Zhang B, Wang T, Bonni A, Zhao G. 2020. Robust principal component analysis for accurate outlier sample detection in RNA-Seq data. *BMC Bioinformatics* 21:269
260. Reimand J, Isserlin R, Voisin V, Kucera M, Tannus-Lopes C, et al. 2019. Pathway enrichment analysis and visualization of omics data using g:Profiler, GSEA, Cytoscape and EnrichmentMap. *Nature Protocols* 14:482-517
261. Morris JC, Schindler SE, McCue LM, Moulder KL, Benzinger TLS, et al. 2019. Assessment of Racial Disparities in Biomarkers for Alzheimer Disease. *JAMA Neurol*
262. Howell JC, Watts KD, Parker MW, Wu J, Kollhoff A, et al. 2017. Race modifies the relationship between cognition and Alzheimer's disease cerebrospinal fluid biomarkers. *Alzheimers Res Ther* 9:88
263. Bader JM, Geyer PE, Muller JB, Strauss MT, Koch M, et al. 2020. Proteome profiling in cerebrospinal fluid reveals novel biomarkers of Alzheimer's disease. *Mol Syst Biol* 16:e9356
264. Dayon L, Núñez Galindo A, Wojcik J, Cominetti O, Corthésy J, et al. 2018. Alzheimer disease pathology and the cerebrospinal fluid proteome. *Alzheimers Res Ther* 10:66
265. Tijms BM, Gobom J, Reus L, Jansen I, Hong S, et al. 2020. Pathophysiological subtypes of Alzheimer's disease based on cerebrospinal fluid proteomics. *Brain* 143:3776-92
266. Sharma K, Schmitt S, Bergner CG, Tyanova S, Kannaiyan N, et al. 2015. Cell type- and brain region-resolved mouse brain proteome. *Nat Neurosci* 18:1819-31
267. Zhang Y, Chen K, Sloan SA, Bennett ML, Scholze AR, et al. 2014. An RNA-sequencing transcriptome and splicing database of glia, neurons, and vascular cells of the cerebral cortex. *J Neurosci* 34:11929-47
268. Zhou M, Haque RU, Dammer EB, Duong DM, Ping L, et al. 2020. Targeted mass spectrometry to quantify brain-derived cerebrospinal fluid biomarkers in Alzheimer's disease. *Clin Proteomics* 17:19
269. Telano LN, Baker S. 2018. Physiology, cerebral spinal fluid.
270. Ujiie M, Dickstein DL, Carlow DA, Jefferies WA. 2003. Blood-brain barrier permeability precedes senile plaque formation in an Alzheimer disease model. *Microcirculation* 10:463-70

271. Dickstein DL, Biron KE, Ujiiie M, Pfeifer CG, Jeffries AR, Jefferies WA. 2006. Abeta peptide immunization restores blood-brain barrier integrity in Alzheimer disease. *FASEB J* 20:426-33
272. Zlokovic BV. 2011. Neurovascular pathways to neurodegeneration in Alzheimer's disease and other disorders. *Nat Rev Neurosci* 12:723-38
273. Desai BS, Schneider JA, Li JL, Carvey PM, Hendey B. 2009. Evidence of angiogenic vessels in Alzheimer's disease. *J Neural Transm (Vienna)* 116:587-97
274. Montagne A, Barnes SR, Sweeney MD, Halliday MR, Sagare AP, et al. 2015. Blood-brain barrier breakdown in the aging human hippocampus. *Neuron* 85:296-302
275. Nation DA, Sweeney MD, Montagne A, Sagare AP, D'Orazio LM, et al. 2019. Blood-brain barrier breakdown is an early biomarker of human cognitive dysfunction. *Nat Med* 25:270-6
276. Butts B, Huang H, Hu WT, Kehoe PG, Miners JS, et al. 2024. sPDGFRbeta and neuroinflammation are associated with AD biomarkers and differ by race: The ASCEND Study. *Alzheimers Dement* 20:1175-89
277. Jack CR, Jr., Bennett DA, Blennow K, Carrillo MC, Dunn B, et al. 2018. NIA-AA Research Framework: Toward a biological definition of Alzheimer's disease. *Alzheimers Dement* 14:535-62
278. Hanseeuw BJ, Betensky RA, Jacobs HIL, Schultz AP, Sepulcre J, et al. 2019. Association of Amyloid and Tau With Cognition in Preclinical Alzheimer Disease: A Longitudinal Study. *JAMA Neurology* 76:915-24
279. Visser PJ, Reus LM, Gobom J, Jansen I, Dicks E, et al. 2022. Cerebrospinal fluid tau levels are associated with abnormal neuronal plasticity markers in Alzheimer's disease. *Molecular Neurodegeneration* 17:27
280. Quinn JP, Kandigian SE, Trombetta BA, Arnold SE, Carlyle BC. 2021. VGF as a biomarker and therapeutic target in neurodegenerative and psychiatric diseases. *Brain Communications* 3
281. Wingo AP, Dammer EB, Breen MS, Logsdon BA, Duong DM, et al. 2019. Large-scale proteomic analysis of human brain identifies proteins associated with cognitive trajectory in advanced age. *Nat Commun* 10:1619
282. Libiger O, Shaw LM, Watson MH, Nairn AC, Umaña KL, et al. 2021. Longitudinal CSF proteomics identifies NPTX2 as a prognostic biomarker of Alzheimer's disease. *Alzheimers Dement* 17:1976-87
283. Llano DA, Devanarayan P, Devanarayan V. 2023. CSF peptides from VGF and other markers enhance prediction of MCI to AD progression using the ATN framework. *Neurobiology of Aging* 121:15-27
284. Xiao M-F, Xu D, Craig MT, Pelkey KA, Chien C-C, et al. 2017. NPTX2 and cognitive dysfunction in Alzheimer's Disease. *eLife* 6:e23798
285. Sjaarda J, Gerstein HC, Kutalik Z, Mohammadi-Shemirani P, Pigeyre M, et al. 2020. Influence of Genetic Ancestry on Human Serum Proteome. *Am J Hum Genet* 106:303-14
286. Ghosh S, Nehme R, Barrett LE. 2022. Greater genetic diversity is needed in human pluripotent stem cell models. *Nature Communications* 13:7301
287. Peterson RE, Kuchenbaecker K, Walters RK, Chen CY, Popejoy AB, et al. 2019. Genome-wide Association Studies in Ancestrally Diverse Populations: Opportunities, Methods, Pitfalls, and Recommendations. *Cell* 179:589-603
288. Zhang J, Dutta D, Köttgen A, Tin A, Schlosser P, et al. 2022. Plasma proteome analyses in individuals of European and African ancestry identify cis-pQTLs and models for proteome-wide association studies. *Nature Genetics* 54:593-602

289. Kachuri L, Mak ACY, Hu D, Eng C, Huntsman S, et al. 2023. Gene expression in African Americans, Puerto Ricans and Mexican Americans reveals ancestry-specific patterns of genetic architecture. *Nat Genet*
290. Robins C, Liu Y, Fan W, Duong DM, Meigs J, et al. 2021. Genetic control of the human brain proteome. *Am J Hum Genet* 108:400-10
291. Stepler KE, Mahoney ER, Kofler J, Hohman TJ, Lopez OL, Robinson RAS. 2020. Inclusion of African American/Black adults in a pilot brain proteomics study of Alzheimer's disease. *Neurobiology of Disease* 146:105129
292. Desaire H, Stepler KE, Robinson RAS. 2022. Exposing the Brain Proteomic Signatures of Alzheimer's Disease in Diverse Racial Groups: Leveraging Multiple Data Sets and Machine Learning. *Journal of Proteome Research* 21:1095-104
293. Hodes RJ, Buckholtz N. 2016. Accelerating Medicines Partnership: Alzheimer's Disease (AMP-AD) Knowledge Portal Aids Alzheimer's Drug Discovery through Open Data Sharing. *Expert Opin Ther Targets* 20:389-91
294. Reddy JS, Heath L, Vander Linden A, Allen M, de Paiva Lopes K, et al. 2024. Bridging the Gap: Multi-Omics Profiling of Brain Tissue in Alzheimer's Disease and Older Controls in Multi-Ethnic Populations. *bioRxiv*
295. Seifar F, Fox EJ, Shantaraman A, Liu Y, Dammer EB, et al. 2024. Large-scale Deep Proteomic Analysis in Alzheimer's Disease Brain Regions Across Race and Ethnicity. *bioRxiv*
296. Wesenhagen KEJ, Gobom J, Bos I, Vos SJB, Martinez-Lage P, et al. 2022. Effects of age, amyloid, sex, and APOE ϵ 4 on the CSF proteome in normal cognition. *Alzheimers Dement (Amst)* 14:e12286

CHAPTER 6: Appendix

Table 6.1: Cohort characteristics

Number Cases	GUID	TMT ID	SRM ID	Study	Diagnosis	Age	Sex	Race	Educ	MoCA	APOE	Aβ42	tTau	pTau	tTau/Aβ42	pTau/Aβ42	Cerebrovascular	Diabetes	Dyslipidemia	Hypertension	Outlier
1	37512	b1.131N	S011_P1002_37512	CRIN	AD	81.1	Female	Black or African American	18	19	e3/e4	498.5	277.1	31.12	0.5558676	0.0624273					
2	39138	b6.128C	S075_P1C10_39138	CRIN	AD	81	Female	Caucasian or White	16	23	e3/e4	644	680.5	76.64	1.056677	0.1190062					
3	42719	b12.130N	S147_P2D5_42719	CRIN	AD	73.9	Male	Black or African American	12	8	e4/e4	274.4	247.5	25.44	0.9019679	0.0927114					
4	44707	b15.129N	S192_P3D5_44707	CRIN	AD	68.9	Male	Caucasian or White	22	17	e3/e4	570.4	540.9	56.91	0.9482819	0.0997721					
5	44820	b15.132N	S187_P3G4_44820	CRIN	AD	50.9	Male	Black or African American	15	6	e3/e3	372.2	317.1	31.98	0.8519613	0.0859215					
6	45034	b1.129N	S005_P1E01_45034	CRIN	AD	76.6	Male	Caucasian or White	21	21	e3/e3	1066	464.8	44.54	0.4360225	0.0417824					YES
7	45101	b1.131C	S137_P2C8_45101	CRIN	AD	74.9	Male	Caucasian or White	22	22	e3/e3	759.6	435.2	51.52	0.5729331	0.0678252	YES				
8	45128	b13.128C	S160_P3D1_45128	CRIN	AD	74.8	Male	Black or African American	18	19	e4/e4	414.6	308.6	31.34	0.7483319	0.0755909					
9	45130	b2.128C	S021_P1E03_45130	CRIN	AD	50	Female	Caucasian or White	12	12	e3/e4	487.9	972.8	109.5	1.9938512	0.2244312					YES
10	45573	b3.128C	S037_P1E05_45573	CRIN	AD	72.6	Female	Caucasian or White	12	12	e3/e4	520.8	434.3	42.33	0.8339094	0.0812788					
11	45739	b13.131C	S161_P3E1_45739	CRIN	AD	75.5	Male	Caucasian or White	16	21	e3/e4	485.9	184.4	17.96	0.379502	0.0369623	YES		YES	YES	YES
12	45831	b12.132N	S149_P2G9_45831	CRIN	AD	75.8	Female	Caucasian or White	17	17		685.4	315.1	29.71	0.4655676	0.043347					
13	45918	b12.131C	S155_P2E10_45918	CRIN	AD	72.1	Female	Black or African American	18	18		475.2	195.3	18.51	0.4109848	0.038952					
14	46008	b11.132C	S140_P2F8_46008	CRIN	AD	68.7	Female	Caucasian or White	20	19	e3/e4	696.4	940.7	86.69	1.3508041	0.1244831					
15	46040	b3.131N	S038_P1F05_46040	CRIN	AD	84.1	Male	Caucasian or White	20	19	e3/e3	628.8	462.5	52.83	0.735528	0.0840172					
16	46076	b4.128C	S047_P1G06_46076	CRIN	AD	60.1	Female	Black or African American	12	20		677.4	199.5	22.21	0.2945084	0.0327871			YES		YES
17	46246	b13.130C	S168_P3D7_46246	CRIN	AD	75.2	Female	Black or African American	18	22	e3/e3	674.3	230.3	24.35	0.3415394	0.0361155					YES
18	46306	b14.130C	S173_P3A3_46306	CRIN	AD	61	Female	Caucasian or White	18	12	e3/e3	414	150.8	15.27	0.3642512	0.0368841					YES
19	46640	b6.127C	S076_P1D10_46640	CRIN	AD	76.1	Male	Black or African American	14	9		368.2	273.3	27.83	0.7422596	0.0755839					
20	46642	b1.132C	S012_P1D02_46642	CRIN	AD	68.3	Female	Caucasian or White	14	14	e4/e4	433.6	433.5	40.91	0.9997694	0.0943496		YES			
21	47135	b14.128N	S177_P3E3_47135	CRIN	AD	74.5	Male	Caucasian or White	16	21	e3/e4	965.3	543.5	65.97	0.5630374	0.0683414					
22	47232	b6.133N	S077_P1E10_47232	CRIN	AD	49.8	Female	Black or African American	12	15	e3/e3	405.8	403.9	40.19	0.9953179	0.0990389					
23	47248	b10.129N	S128_P2B7_47248	CRIN	AD	59.4	Female	Caucasian or White	14	20	e4/e4	280.7	333.5	30.38	1.1881012	0.1082294		YES		YES	
24	47251	b16.130C	S204_P3H4_47251	CRIN	AD	65.5	Female	Caucasian or White	17	17	e2/e3	294.7	256.2	27.05	0.8693587	0.0917883					
25	43738	b14.127N	S174_P3B3_43738	EHBS	Control	69.9	Female	Black or African American	14	27	e4/e4	1039	147.1	13.06	0.1415784	0.0125698	YES		YES		YES
26	44869	b5.128N	S053_P1E07_44869	EHBS	Control	66.1	Male	Black or African American	18	23	e3/e3	1124	136.3	11.51	0.1212633	0.0102402					
27	45707	b16.128N		EHBS	Control	72.7	Female	Black or African American	18	24	e2/e3	1709	254.8	23.86	0.1469824	0.0140353	YES				
28	46085	b1.128N	S009_P1A02_46085	EHBS	Control	51.3	Male	Black or African American	16	25	e2/e4	768.5	83.66	8	0.1088614	0.0104099		YES			YES
29	48153	b8.127N	S093_P2G2_48153	EHBS	Control	72.4	Female	Caucasian or White	16	30	e2/e3	1387	174.4	15.06	0.125739	0.010858					
30	48358	b14.129N	S176_P3D3_48358	EHBS	Control	66.1	Female	Caucasian or White	16	24	e3/e3	1700	197.4	17.56	0.1161176	0.0103294					
31	48617	b12.127C		EHBS	Control	57.7	Female	Black or African American	13	28	e3/e3	1285	153.2	13.09	0.1192218	0.0101868					
32	48769	b15.133N		EHBS	Control	75	Female	Caucasian or White	14	26	e3/e3	1700	227.9	19.72	0.1340588	0.0116			YES		YES
33	49324	b5.128C	S060_P1D08_49324	EHBS	Control	60.2	Female	Caucasian or White	20	27	e2/e3	1431	164.1	15	0.1146751	0.0104822					
34	49417	b2.128N	S016_P1H02_49417	EHBS	Control	71.6	Female	Caucasian or White	16	26	e3/e3	1411	177.8	15.41	0.1260099	0.0109213					
35	49537	b15.128N		EHBS	Control	51	Female	Black or African American	18	25	e2/e4	862.4	105.4	9.97	0.1222171	0.0115608					
36	49903	b10.131C	S126_P2H6_49903	EHBS	Control	64.9	Male	Caucasian or White	18	27	e3/e3	1084	180.2	15.51	0.1662362	0.0143081			YES		YES
37	49941	b6.132C	S074_P1B10_49941	EHBS	Control	69.7	Male	Caucasian or White	16	26	e3/e3	1165	156	13.65	0.1339056	0.0117167					
38	50259	b14.131N	S182_P3B4_50259	EHBS	Control	50.1	Female	Black or African American	20	28	e3/e4	447.4	80.22	8	0.1793026	0.0178811	YES				
39	50273	b8.133N	S094_P2H2_50273	EHBS	Control	69	Female	Caucasian or White	20	28	e3/e4	1700	220.9	19.62	0.1299412	0.0115412					
40	50409	b16.130N	S199_P3C6_50409	EHBS	Control	64.8	Female	Caucasian or White	18	23	e3/e4	823.1	166.1	14.15	0.2017981	0.0171911					
41	50452	b4.130N	S052_P1D07_50452	EHBS	Control	59.5	Female	Caucasian or White	18	29	e3/e4	920.5	123.8	10.98	0.1344921	0.0119283					YES
42	50502	b13.130C	S165_P3A2_50502	EHBS	Control	55.5	Female	Black or African American	13	28	e3/e3	892	105.2	9.58	0.1179372	0.0107999					
43	50534	b4.128N	S041_P1A06_50534	EHBS	Control	71.5	Female	Caucasian or White	14	25	e3/e4	1595	364.5	35.32	0.2285266	0.0221442					
44	50619	b5.127C	S056_P1H07_50619	EHBS	Control	64.7	Female	Caucasian or White	12	23	e3/e3	1700	191.3	17.42	0.1125294	0.0102471					
45	50650	b3.129C	S033_P1A05_50650	EHBS	Control	59.4	Female	Caucasian or White	18	28	e3/e3	1541	308.1	27.24	0.1999351	0.0176768					
46	51023	b9.129C	S107_P2E4_51023	EHBS	Control	68.4	Female	Black or African American	16	28	e3/e3	1239	236.4	21.54	0.190799	0.017385					
47	51123	b9.132C	S114_P2D5_51123	EHBS	Control	50	Female	Caucasian or White	14	26	e3/e3	1410	154	14.36	0.1092199	0.0101844					
48	51135	b6.129C	S067_P1C09_51135	EHBS	Control	61.9	Female	Caucasian or White	16	24	e3/e4	594.6	104.6	8.34	0.1759166	0.0140262					YES
49	51175	b12.128C	S153_P2C10_51175	EHBS	Control	65.5	Female	Caucasian or White	20	24	e3/e3	1442	233.3	21.18	0.1617892	0.0146879					
50	51224	b16.127C	S200_P3D6_51224	EHBS	Control	66.2	Male	Caucasian or White	18	28	e3/e3	1235	142.2	14.92	0.1151417	0.012081					
51	51264	b8.128N	S095_P2A3_51264	EHBS	Control	61.2	Female	Caucasian or White	12	31	e3/e3	1700	241.6	21.36	0.1421176	0.0125647					YES
52	51319	b8.132C	S096_P2B3_51319	EHBS	Control	68.7	Female	Black or African American	18	20	e3/e3	762.1	116.5	10.26	0.1528671	0.0134628					
53	51370	b1.130C	S010_P1B02_51370	EHBS	Control	70.4	Female	Caucasian or White	16	26	e2/e3	1353	136.8	13.55	0.1011086	0.0100148					
54	51431	b7.128C	S082_P2D1_51431	EHBS	Control	69.8	Female	Caucasian or White	14	29	e3/e4	1700	208.2	18.12	0.1224706	0.0106588					
55	51499	b4.132N	S042_P1B06_51499	EHBS	Control	74.5	Male	Caucasian or White	20	28	e2/e3	832.6	125.4	10.12	0.1506125	0.0121547					
56	51520	b9.133N		EHBS	Control	53.5	Female	Black or African American	15	23	e3/e3	699.8	113.7	9.14	0.162475	0.0130609	YES				
57	51551	b2.130N	S033_P1G03_51551	EHBS	Control	66.4	Female	Caucasian or White	13	24	e2/e3	1423	147.8	13.02	0.1038651	0.0091497					
58	51559	b4.132C	S045_P1E06_51559	EHBS	Control	64.5	Female	Caucasian or White	18	25	e3/e3	1176	122.4	11.5	0.1040816	0.0097789					
59	51760	b13.131N	S159_P3C1_51760	EHBS	Control	57.1	Male	Black or African American	13	26	e3/e3	856.5	128.3	11.73	0.1497957	0.0136953					
60	52055	b10.127C		EHBS	Control	66.8	Female	Black or African American	16	28	e2/e3	997	149.1	15.38	0.1495486	0.0154263		YES	YES		YES
61	52131	b3.130N	S034_P1B05_52131	EHBS	Control	75.7	Female	Caucasian or White	13	27	e2/e3	1242	170.1	14.81	0.1369565	0.0119243					
62	52154	b7.132N	S083_P2E1_52154	EHBS	Control	74.1	Female	Caucasian or White	18	28	e3/e3	1258	180.4	15.42	0.1434022	0.0122576					
63	52475	b12.128N	S145_P2C9_52475	EHBS	Control	69.5	Male	Caucasian or White	16	27	e3/e3	1700	234.6	19.29	0.138	0.0113471					YES
64	52524	b2.130C		EHBS	Control	62.1	Female	Caucasian or White	20	27	e3/e3	1171	139.8	11.55	0.1193851	0.0098634					

65	52538	b14.132N	S171_P362_52538	EHS	Control	58.7	Female	Caucasian or White	18	25	e2/e4	1700	194.6	17.49	0.1144706	0.0102882			
66	52626	09.131C	S108_P24_52626	EHS	Control	66.6	Female	Caucasian or White	18	26	e3/e6	1700	219.5	23.23	0.1291176	0.0136647			
67	52791	b11.129C	S132_P27_52791	EHS	Control	64.7	Female	Black or African American	13	28	e3/e6	1501	86.27	8	0.1719211	0.0159426			
68	53000	b15.127N	S100_P26_53000	EHS	Control	56.5	Female	Caucasian or White	18	29	e3/e6	1518	171.5	15.19	0.1128776	0.0106633			
69	53612	b1.132N	S002_P1801_53612	EHS	Control	62.7	Female	Black or African American	18	28	e3/e6	1240	174.9	16.67	0.1410484	0.0134435			
70	53618	b4.129N	S043_P1C06_53618	EHS	Control	70.5	Female	Black or African American	18	26	e3/e6	1004	124	11.5	0.123506	0.0114542			
71	53705	b12.129N	S146_P209_53705	EHS	Control	54.5	Female	Caucasian or White	16	23	e2/e3	1459	162.6	13.71	0.1114462	0.0093968			
72	53729	b5.130C	S054_P110_53729	EHS	Control	72.7	Female	Caucasian or White	18	28	e3/e6	986.2	144.7	14.81	0.1467248	0.0150172			
73	53731	b11.129N	S139_P25_53731	EHS	Control	70.9	Female	Black or African American	18	27	e3/e6	1479	136.5	12.51	0.0922931	0.0084584			
74	53741	b6.129N	S068_P1D09_53741	EHS	Control	53.6	Female	Caucasian or White	18	26	e3/e6	1532	213.8	18.31	0.1395561	0.0119517			
75	55244	b3.127N	S035_P1C05_55244	EHS	Control	64.6	Female	Black or African American	14	24	e3/e4	1158	161.4	14.97	0.1393782	0.0129275			
76	55286	b7.128N	S084_P2F1_55286	EHS	Control	56.6	Female	Black or African American	16	26	e3/e6	789.4	94.69	8.38	0.1199519	0.0106157			
77	55388	b13.132N	S166_P38_55388	EHS	Control	66.7	Female	Caucasian or White	16	23	e3/e4	1177	258.1	24.54	0.2192863	0.0258896			
78	56007	b11.127N	S133_P207_56007	EHS	Control	64.8	Male	Caucasian or White	16	25	e3/e6	1800	208.8	19.3	0.1228235	0.0113529			
79	56326	b10.127N	S121_P2C6_56326	EHS	Control	70.9	Female	Caucasian or White	16	25	e3/e6	1700	307.8	30.74	0.1810588	0.0180824			
80	56580	b12.127N	S154_P2D10_56580	EHS	Control	57.3	Male	Caucasian or White	16	26	e3/e6	835	100.9	9.51	0.1208833	0.0113892			
81	57907	b4.127C	S044_P1D06_57907	EHS	Control	64.4	Male	Caucasian or White	20	28	e3/e4	1005	133.1	10.98	0.1324378	0.0109254			YES
82	58595	b6.130N	S069_P1E09_58595	EHS	Control	64.9	Male	Black or African American	18	22	e2/e3	600.4	91.22	8	0.151932	0.0133245	YES	YES	YES
83	58615	b11.129C	S135_P246_58615	EHS	Control	51.6	Male	Black or African American	14	25	e3/e6	943.3	145.6	13.16	0.1543517	0.0139375			
84	59913	b2.129C	S017_P1A01_59913	EHS	Control	75.4	Male	Black or African American	12	22	e3/e6	1570	238.8	23.37	0.1521019	0.0148854			
85	62211	b2.131N	S018_P1B03_62211	EHS	Control	57.1	Male	Caucasian or White	16	30	e2/e3	1583	189.3	16.31	0.1195831	0.0103032			
86	62762	b11.127C	S119_P2A6_62762	EHS	Control	57.2	Male	Caucasian or White	18	29	e3/e4	1473	196.5	17.48	0.1334012	0.0118669			
87	63141	b10.131N	S119_P2A6_63141	EHS	Control	51.1	Male	Caucasian or White	16	25	e2/e3	1004	141	9.17	0.1105578	0.0091339			
88	63456	b1.127N	S003_P1C01_63456	EHS	Control	69.5	Male	Black or African American	18	27	e2/e3	835.3	128.7	11.11	0.1552636	0.0144248			
89	66352	b5.133N	S061_P1E08_66352	EHS	Control	77.8	Male	Black or African American	20	28	e3/e6	1498	176.6	15.66	0.1178905	0.0100059			
90	66827	b8.130C	S101_P2G3_66827	EHS	Control	72.5	Male	Caucasian or White	16	24	e2/e4	1125	147.8	12.48	0.1313778	0.0110933			
91	66984	b2.133N	S019_P1C03_66984	EHS	Control	51.7	Male	Black or African American	13	23	e3/e4	764.7	125.6	10.6	0.1642474	0.0138616			YES
92	68545	b9.130C	S110_P2H4_68545	EHS	Control	57.3	Male	Black or African American	18	27	e3/e4	1368	167.5	17.34	0.1224515	0.0126754	YES		
93	68620	b3.131C	S030_P1D04_68620	EHS	Control	51.5	Male	Black or African American	18	27	e3/e6	1205	10.99	10.89	0.1287806	0.0117452	YES		YES
94	70714	b14.129N	S172_P3H2_70714	EHS	Control	57.4	Male	Black or African American	12	21	e3/e4	1221	142	12.96	0.1162981	0.0106143			
95	72374	b6.131N	S070_P1F09_72374	EHS	Control	52.1	Male	Black or African American	13	23	e2/e3	686.6	101.8	10.21	0.1482668	0.0148704			
96	73786	b8.129C	S097_P2C3_73786	EHS	Control	61.6	Male	Caucasian or White	18	29	e2/e3	1700	244.2	20.31	0.1436471	0.0119471			YES
97	74622	b15.132C	S185_P3C4_74622	EHS	Control	64.5	Male	Black or African American	18	26	e3/e6	1180	143.7	12.27	0.1217797	0.0103983			
98	75951	b8.129C	S031_P1D01_75951	EHS	Control	72.1	Female	Caucasian or White	14	29	e2/e3	1700	185.7	17.01	0.1091762	0.0100059			
100	76348	b6.127N	S071_P1G09_76348	EHS	Control	52.1	Male	Caucasian or White	14	28	e3/e6	916.9	102	9.78	0.1112444	0.0106664			
101	76615	b15.130N	S186_P3F4_76615	EHS	Control	64.6	Male	Black or African American	16	23	e3/e6	876.8	154	13	0.1756387	0.0148266			
102	76950	b8.127C	S096_P2D3_76950	EHS	Control	69.4	Male	Caucasian or White	16	25	e2/e3	954.9	141.6	14.71	0.148333	0.0114048			
103	78096	b10.132N	S120_P2B6_78096	EHS	Control	69.5	Male	Black or African American	18	27	e2/e3	471.7	99.68	8.9	0.2113208	0.0188679			
104	86092	b13.129C	S167_P3C2_86092	EHS	Control	51.5	Male	Caucasian or White	16	24	e3/e4	1176	131.1	11.57	0.1114796	0.0098384			
105	41324	b1.127C	S001_P1A01_41324	Memory	AD	66.8	Female	Black or African American	13	26	e4/e6	666.9	358.2	33.78	0.537112	0.0056233			
106	41483	b7.127N	S081_P2C3_41483	Memory	AD	77.3	Female	Black or African American	18	28	e3/e6	1700	234.1	18.9	0.1377059	0.0111776	YES		
107	42541	b4.132N	S114_P1F02_42541	Memory	AD	58.2	Female	Black or African American	14	25	e3/e6	207.6	18.01	20.76	0.153218	0.0146085	YES		
108	42570	b8.130N	S103_P2A4_42570	Memory	AD	78.1	Female	Black or African American	18	22	e2/e3	1700	240.4	19.18	0.1441118	0.0112824	YES		
109	42947	b15.129C	S183_P3C4_42947	Memory	AD	82	Female	Black or African American	18	24	e3/e6	1700	341.5	25.9	0.2008824	0.0152353			
110	43820	b16.128C	S197_P3A8_43820	Memory	AD	60.7	Female	Caucasian or White	18	29	e3/e6	878.4	94.12	8	0.1071494	0.0091075			
111	44067	b1.130N	S013_P1E02_44067	Memory	AD	61.1	Female	Black or African American	18	26	e2/e3	983.5	128.3	10.76	0.1304525	0.0109405	YES		
112	44291	b1.132C	S105_P1D02_44291	Memory	AD	71.5	Female	Black or African American	14	29	e3/e6	1196	163.8	14.46	0.1386955	0.0120903			
113	44511	b9.132N	S105_P2C2_44511	Memory	AD	77	Female	Black or African American	20	26	e3/e6	739	213.9	21.26	0.2894552	0.0287696			
114	44893	b16.131N	S198_P3B6_44893	Memory	AD	60.7	Female	Black or African American	14	26	e2/e3	691.8	121.5	10.25	0.1756288	0.0148164			
115	45287	b14.132C	S175_P3C3_45287	Memory	AD	62.2	Female	Black or African American	16	21	e3/e6	1700	246.8	25.07	0.1451765	0.0147471			
116	45488	b14.131C	S175_P3C3_45488	Memory	AD	75.6	Female	Black or African American	16	21	e4/e6	327.9	478.9	42.26	1.4605003	0.1288808			
117	45861	b4.127N	S046_P1H05_45861	Memory	AD	66.4	Female	Black or African American	16	28	e2/e3	958.3	125.8	11.27	0.1440923	0.0125486			
118	46043	b13.127N	S157_P3A1_46043	Memory	AD	70.3	Female	Caucasian or White	16	23	e3/e6	1700	238.1	17.09	0.1400588	0.0111776			
119	46103	b12.131N	S144_P2B9_46103	Memory	AD	70.3	Female	Black or African American	13	28	e3/e6	1045	141.9	12.36	0.1357895	0.0118278			
120	46233	b13.129N	S158_P3H1_46233	Memory	AD	61.3	Female	Black or African American	16	28	e3/e6	1608	340.3	29.25	0.2116294	0.0181903			
121	46390	b4.129C	S051_P1C07_46390	Memory	AD	55.3	Female	Black or African American	18	28	e2/e4	1075	150.3	13.18	0.139814	0.0122605			
122	46931	b13.133N	S195_P1F01_46931	Memory	AD	64.6	Female	Black or African American	20	27	e3/e6	1239	157.3	15.01	0.1269792	0.0113095			
123	47147	b10.130N	S118_P2H5_47147	Memory	AD	60.2	Female	Caucasian or White	16	25	e3/e4	1185	188.1	15.74	0.1587342	0.0132827			
124	47480	b11.132N	S131_P2E7_47480	Memory	AD	72.1	Male	Black or African American	16	29	e3/e6	1547	226	19.56	0.1460892	0.0126438			
125	48786	b9.130N	S113_P2C5_48786	Memory	AD	72.4	Female	Black or African American	18	27	e3/e4	1700	231.6	19.17	0.1362353	0.0112765	YES		
126	48937	b12.129C	S152_P3D1_48937	Memory	AD	65.5	Female	Black or African American	18	25	e3/e6	1700	225.2	19.33	0.1324706	0.0113706			YES
127	50313	b8.132N	S106_P1E03_50313	Memory	AD	66.1	Female	Black or African American	16	24	e3/e6	1277	206.7	14.93	0.1618637	0.0140238			YES
128	56968	b5.131N	S055_P1G07_56968	Memory	AD	78.3	Male	Caucasian or White	18	27	e3/e6	1700	279	24.04	0.1641176	0.0141412			YES
129	57339	b2.129N	S020_P1D03_57339	Memory	AD	63.9	Female	Black or African American	20	27	e3/e6	816.1	125	10.81	0.1531675	0.0132459			
130	57450	b11.130C	S134_P3H7_57450	Memory	AD	69.4	Male	Black or African American	14	26	e2/e3	1034	146.2	12.62	0.1413927	0.012205			YES
131	57502	b1.131N	S045_P1E02_57502	Memory	AD	64.1	Female	Black or African American	12	24	e3/e6	917.7	150.6	12.35	0.1562917	0.0131311			
132	63982	b9.128C	S109_P2G4_63982	Memory	AD	75.2	Male	Caucasian or White	15	25	e3/e6	1566	234.8	19.28	0.1499361	0.0123116			
133	69030	b3.132N	S036_P1D05_69030	Memory	AD	69.7	Male	Black or African American	15	24	e3/e6	1700	285.2	21.76	0.1677647	0.01128			
134	46282	b8.131C	S102_P3H4_46282	NeuCog	AD	73.4	Female	Caucasian or White	16	22	e4/e6	490.6	383.2	40.13	0.7810844				

195	84355	b5.129N	S065_P1A09_84355	NeuCog	AD	76	Male	Black or African American	20	20		564.5	315.6	30.98	0.5590788	0.0548804						
196	84561	b5.132N	S059_P1C08_84561	NeuCog	AD	50.1	Female	Black or African American	14	7	e3/e4	308	215.2	20.51	0.6987013	0.0665909						
197	85026	b9.128N	S112_P285_85026	NeuCog	AD	63.1	Female	Black or African American	12	16	e4/e4	200	209	20.3	1.045	0.1015						
198	85961	b15.127C	S195_P2G5_85961	NeuCog	AD	67	Female	Caucasian or White	14	17	e3/e4	540.8	382.5	39.76	0.7072855	0.0792207	YES	YES	YES			
199	86582	b10.130C	S125_P2G6_86582	NeuCog	AD	58.2	Male	Caucasian or White	18	9	e3/e3	598.3	471.6	51.68	0.7882333	0.0863781						
200	86780	b15.128C	S188_P3H4_86780	NeuCog	AD	63.6	Male	Black or African American	16	20		515.3	356.3	40.27	0.6914419	0.0781487						YES
201	86840	b7.133N	S088_P2B2_86840	NeuCog	AD	52.1	Male	Caucasian or White	14	12	e3/e3	436.5	522.8	66.65	1.197709	0.1526919						
202	87070	b7.130N	S089_P2C2_87070	NeuCog	AD	77	Female	Caucasian or White	22	13	e3/e3	273.5	155.9	14.33	0.5700183	0.0523949						YES
203	87124	b15.130C	S189_P3A5_87124	NeuCog	AD	64	Female	Black or African American	20	7	e3/e4	383.6	294.7	33.76	0.7682482	0.0880083						YES
Empty Channel		b14.133N																				YES

Table 6.2: TMT Batch Arrangement.

	Batch 1	Batch 2	Batch 3	Batch 4	Batch 5	Batch 6	Batch 7	Batch 8	Batch 9	Batch 10	Batch 11	Batch 12	Batch 13	Batch 14	Batch 15	Batch 16
Plex	GIS	GIS	GIS	GIS	GIS	GIS	GIS									
126	63456	67976	55244	45861	73808	76348	41483	48153	47498	56326	56007	56580	46043	43738	53030	83314
127N	41324	64402	76023	57907	50619	46640	77792	76950	52945	52055	62762	48617	56582	83798	85961	51224
127C	46085	49417	47238	50534	44869	67579	55286	51264	85026	79243	53731	52475	49545	47135	49537	45707
128N	69732	45130	45573	46076	49324	39138	51431	66276	63982	73621	58815	51175	45128	47351	86780	43820
128C	45034	57339	54755	53618	84355	53741	70529	77355	53398	47248	82876	53705	46233	48358	44707	54601
129N	75351	59913	50650	46390	80265	51135	73518	73786	51023	74112	52791	48937	86092	70714	42947	49450
129C	44067	51551	52131	50452	59128	58595	87070	42570	48786	47147	47368	42719	73152	72191	76615	50409
130N	51370	52524	71200	68342	53729	66735	54179	66827	68545	86582	57450	84217	50502	46306	87124	47251
130C	37512	62211	46040	53819	56968	72374	57502	57056	57326	63141	57251	46103	51760	50259	77501	44893
131N	49419	74051	68620	83366	72848	83459	49087	46282	52626	49903	45101	45918	45739	45487	64149	GIS
131C	53612	42541	69030	51499	84561	50313	52154	48746	44511	78086	47480	45831	55838	52538	44820	GIS
132N	46642	44291	48024	51559	78317	49941	48615	51319	51123	51464	46008	46743	46246	45238	74682	GIS
132C	46442	66984	46931	58885	66352	47232	86840	50273	51520	80287	57498	48222	76896	48615	48769	GIS
133C	Low	Low	Low	Low	Low	Low	Low									
134N	High	High	High	High	High	High	High									

Table 6.3: TMT-MS ANOVA Table

Gene ID Uniprot ID	F-Value	Pr(>F)	ANOVA p-values with Tukey Adjustment									Difference (AD - CT)								
			AD-Cau vs AD-AA	CT-AA vs AD-AA	CT-AA vs AD-AA	CT-AA vs AD-AA	CT-AA vs AD-AA	CT-AA vs AD-AA	CT-AA vs AD-AA	CT-AA vs AD-AA	CT-AA vs AD-AA	CT-AA vs AD-AA	CT-AA vs AD-AA	CT-AA vs AD-AA	CT-AA vs AD-AA	CT-AA vs AD-AA	CT-AA vs AD-AA	CT-AA vs AD-AA		
ALB P02768	0.48887971	0.690420873	0.89793558	0.999594943	0.94632078	0.84908803	0.630942157	0.981868149	-0.063263322	0.00918691	0.041026296	0.072449512	0.104289618	0.031804106						
CLP P01024	1.59429782	0.12727241	0.634546933	0.904701626	0.99602058	0.915239454	0.430260021	-0.085730587	0.06284139	-0.093047686	0.148517726	0.046682901	-0.01894825							
FN1 P02751	0.89731014	0.443682271	0.841308959	0.997246177	0.86296618	0.917841838	0.317383771	0.75451727	0.030512959	0.00709267	-0.026847708	-0.023413692	-0.053786667							
CAB P00055	6.23935196	0.365843082	0.83589078	0.996880843	0.91026501	0.981018761	0.835972555	0.967275064	-0.06842031	-0.099073606	0.093265374	-0.065827333	-0.035174058							
CAA P00044	2.71074086	0.046428111	0.398912175	0.7844816	0.614746652	0.06039383	0.974151362	0.122031845	0.294618495	-0.171412736	0.178139145	-0.466031251	-0.076799551							
CAH P00863	3.29985656	0.021598496	0.192819355	0.112638003	0.014319858	0.997161397	0.790622714	0.879207825	0.061388536	0.067439797	0.088802174	0.006051271	0.021473648							
SPARG1 Q14515	9.9666779	4.00E-06	0.000138923	0.004024067	6.83E-06	0.25835705	0.966927351	0.094459222	0.22965254	0.137853957	0.2526274	-0.09178597	0.023614866							
PTP P02787	2.31737052	0.077033611	0.999830766	0.382995283	0.18541461	0.349592677	0.165862967	0.99933826	-0.003892071	0.077753477	0.095943693	0.081645548	0.099841434							
PCG6P Q9V6R7	21.20621033	7.49E-12	1.71E-09	0.43212066	1.54E-07	2.14E-06	0.67355382	0.000134496	-0.774670703	-0.170909112	-0.64273401	0.603789991	-0.471371689							
CP1 P00450	0.5905926	0.62179271	0.999164214	0.706542368	0.99545492	0.630880645	0.982755539	0.815866421	-0.011092584	0.082798993	0.18630138	0.098395177	0.029722722							
CHGB P05060	6.82329153	2.19E-05	0.82653642	0.011881298	5.45E-05	0.129020885	0.002189735	0.002472749	0.037083155	0.130430914	0.187419324	0.09347759	0.150386809							
HSPG2 P98160	0.64697481	0.585792512	0.898350192	0.748923842	0.534701269	0.992152884	0.9300495	0.987878692	-0.023741793	-0.03207564	-0.043626958	-0.00946577	-0.19885165							
REL1 P78509	0.00450591	0.987263171	0.99831838	0.85323634	0.993217131	0.997810216	0.99965546	0.999724569	0.00856181	0.01820354	0.01384117	0.006441724	0.005072307							
CP1 P00414	0.22293906	0.88036326	0.990848178	0.968499184	0.98987070	0.87576919	0.92766592	0.998510123	0.041307891	-0.061598734	-0.102060625	-0.01955795	0.02095894							
SERPINA1 P01009	0.06625047	0.91772511	0.999970634	0.994971873	0.997289507	0.99216892	0.99908691	0.97139134	0.004011129	-0.021828919	0.01616417	-0.025841108	0.011253027							
FAT2 Q9N7X3	1.9950873	0.166257838	0.098658	0.835618451	0.956326901	0.427520061	0.232093457	0.984749168	-0.147864412	-0.052199085	-0.031066134	0.09565327	0.116802798							
SPPI1 P01051	27.3800613	1.06E-14	0.284177182	1.64E-07	4.43E-13	0.000700377	2.19E-08	0.114750947	-0.068686076	-0.217467218	-0.29826735	-0.14878142	-0.229579699							
LRP1 Q09754	0.26395888	0.022628525	0.236068108	0.714158369	0.016037389	0.819605032	0.749008922	0.11250852	-0.040919615	-0.022380894	-0.06178115	0.018581522	-0.020862959							
GSN P05396	0.75733044	0.630598786	0.985725084	0.979304061	0.627485447	0.99813636	0.842146933	0.74010989	-0.011861787	-0.006560321	0.009128958	0.005098866	-0.074761772							
REL1 P78509	2.2370414	0.076122433	0.091867129	0.999206665	0.785528887	0.113248587	0.99965546	0.999724569	-0.142248695	-0.007688231	0.035932905	0.134558664	0.08816399							
CP1 P00414	0.0446045	0.000164569	0.006139845	0.000538149	0.000753636	0.936161513	0.97512335	0.979698928	0.28327252	0.332712677	0.317812476	0.049454206	-0.014900281							
ENPM2 Q13822	3.45917866	0.017540785	0.046203699	0.974222074	0.10847798	0.11529762	0.96304504	0.245071076	-0.153103854	-0.024111119	-0.126035811	0.128991736	0.027068043							
NRCAN Q92823	10.0375246	3.68E-06	0.001747814	0.000473932	2.67E-06	0.99474813	0.53211369	0.67152488	0.178931434	0.190148014	0.214371936	0.01175658	0.062980502							
CNTN1 Q12860	6.47487162	0.000343476	0.39853953	0.770267971	0.00208636	0.918263034	0.067404523	0.080057763	0.045803959	0.02727447	0.114723622	-0.018352912	0.069143263							
COL6A1 P12111	10.075929	4.67781397	0.983792323	0.876298973	0.42884734	0.982012524	0.6754397	0.817862799	-0.011975801	-0.024198968	-0.047804757	-0.012223167	-0.03288956							
SC1 P02774	2.01239092	0.11499116	0.468900491	0.763891357	0.999659885	0.07360838	0.40793922	0.767284694	-0.133615833	0.087209529	0.03097582	0.20925262	0.137603191							
CHL1 Q00533	8.12375984	4.13E-05	0.051163857	0.000952368	4.71E-05	0.99571756	0.72394298	0.91886612	0.180882771	0.01658453	0.23492006	0.020765682	0.025333525							
CP1 P00414	9.45982795	5.9E-06	0.00132803	0.067936818	4.99E-06	0.51919673	0.65918726	0.45559114	-0.219572722	-0.140661051	-0.28432992	0.078911671	-0.14367194							
NRXN1 Q9Y40C	8.10663877	4.04E-05	0.02192932	0.02337146	1.13E-05	0.999624804	0.252990293	0.186673708	0.135964156	0.13121747	0.21964309	-0.00462409	0.083679752							
MEF2L Q272M0	0.92144694	0.431582775	0.800418934	0.867854298	0.93274023	0.637552625	0.653451148	0.954731665	-0.039919656	0.005193424	0.01246828	0.07513081	0.052387936							
PLG P00747	0.713568	0.545101777	0.630234118	0.999771702	0.93461784	0.564422713	0.912933126	0.899844632	-0.119525284	0.008360151	-0.05632893	0.127912735	0.06323399							
TNFB P22105	10.075929	3.51E-06	0.000357284	0.99999324	0.00228235	0.002029133	0.895527298	0.009115854	-0.163278112	-0.166097729	0.162800256	0.026968856	-0.135818474							
CFB P00751	4.68486899	0.00352272	0.269195156	0.95383142	0.804901153	0.002588087	0.750773842	0.934842845	-0.028299575	0.087172831	-0.086163384	0.35362406	0.096746191							
NEIL2 Q9P495	11.0245791	0.00055666	0.00161206	0.00055666	4.71E-05	0.99571756	0.72394298	0.91886612	0.180882771	0.01658453	0.23492006	0.020765682	0.027532995							
CS1 P01031	0.0103905	0.93460444	0.999996951	0.999317014	0.66679609	0.99629001	0.964438735	0.02303974	0.013818511	-0.050073453	0.011484537	-0.052407426	-0.063891964							
NRXN1 Q9UL81	4.76724206	0.00311407	0.059704228	0.163327556	0.00158093	0.95708647	0.72319132	0.375510304	-0.112492008	0.090262534	0.157339525	-0.022227675	0.044845136							
LAMA2 P24043	1.04591634	0.165360266	0.964062062	0.356177688	0.87017464	0.153723476	0.959210783	0.866171241	-0.01385687	0.044903078	0.020396339	0.058288765	0.033782626							
IGHG1 P01875	11.8895927	9.31E-07	0.00029436	0.986017899	0.000148209	0.000254002	0.999204329	0.010063322	-0.484287002	-0.038714487	-0.46973903	0.445572515	0.014547999							
FS1 P2259	8.2290272	3.16E-05	0.000614342	0.928431764	0.000584009	0.004285637	0.935748939	0.01633292	-0.282982358	-0.042496555	-0.244488091	0.024085803	-0.199991537							
HFN1 P02750	0.2227478	0.880530808	0.906731516	0.959398385	0.965146076	0.973150013	0.999899391	0.974661998	0.067527466	0.021388181	0.059536254	-0.039141104	0.03683815							
SERPINA1 P01011	2.34591466	0.07302454	0.53364656	0.51182781	0.042778559	0.999991137	0.595100265	0.590521042	-0.095722608	-0.097787911	-0.18332567	-0.020055303	-0.087534159							
SERPINA1 P01008	0.84548819	0.02244997	0.502880161	0.999975997	0.967616309	0.514304178	0.947185917	0.00036278	-0.125964107	-0.003555971	-0.074859717	0.122303016	0.04748819							
FBN1 P23142	0.4262572	2.81E-08	2.59E-05	0.951570569	1.40E-05	0.000172942	0.999579044	0.00104985	-0.143622976	-0.05664277	-0.140543491	0.127958699	0.030794891							
NRXN2 Q9P252	3.72698217	0.01263972	0.616774643	0.254150328	0.006693593	0.934835279	0.200315979	0.499119077	0.04816252	0.017192181	0.123500203	0.023015929	0.075323985							
APP P05067	1.07318853	0.36173864	0.975058303	0.682707401	0.348600218	0.90377011	0.62605838	0.951724662	0.022688016	0.05848197	0.085246306	0.053793954	0.026764329							
FG8 P02675	1.4770661	0.22242208	0.86412122	0.94412679	0.186000126	0.995197479	0.639213498	0.484894298	-0.099914891	-0.06974466	-0.24586649	0.030170231	-0.16253598							
ITIH4 Q14624	0.38730788	0.762723426	0.801634356	0.908780026	0.769133778	0.993806096	0.999999335	0.991817867	0.100425724	0.072111072	0.101733802	-0.028314652	0.001308078							

Gene ID Uniprot ID	F-Value	Pr[F]	ANOVA p-values with Tukey Adjustment								Difference (AD - CT)							
			AD-Cau vs AD-AA	CT-AA vs AD-AA	AD-Cau vs AD-AA	CT-AA vs AD-AA	AD-Cau vs AD-AA	CT-AA vs AD-AA	AD-Cau vs AD-AA	CT-AA vs AD-AA	AD-Cau vs AD-AA	CT-AA vs AD-AA	AD-Cau vs AD-AA	CT-AA vs AD-AA				
VWF P04275	1.3751776	0.25178434	0.916302355	0.702061436	0.749992542	0.313617948	0.3480429	0.99954419	-0.0254996	0.0413887	0.03740041	0.066888169	0.062903901	-0.003984269				
COL6A1 P12109	1.5193755	0.21095964	0.329685867	0.69141933	0.99998452	0.920296749	0.270927074	0.629886919	-0.068285094	0.04048513	0.02079024	0.025236581	0.070293910	-0.045056437				
KLK6 Q92876	0.7735167	0.510163107	0.589296694	0.704674188	0.528980511	0.996385369	0.99991166	0.993927965	0.03947025	0.03782348	0.04034565	-0.006687902	0.000875395	0.007562327				
NFASC Q94856	1.4938332	3.39E-05	0.02947684	0.041370857	1.05E-05	0.997161965	0.200854791	0.114862111	0.10497517	0.09769088	0.17653025	-0.00746035	0.071556635	0.078961337				
EKM1 Q61610	5.98851432	0.001071829	0.438329846	0.000458421	0.11319556	0.026525096	0.910457037	0.226696629	0.058409566	0.152703118	0.028323902	0.094298151	0.024848936	-0.069449215				
MNZ2A2 P49641	1.31766584	0.270023556	0.99909929	0.454490266	0.619544289	0.504745333	0.543702388	0.999674232	0.002765641	0.06308651	0.050939480	0.060204301	0.056273807	-0.003969203				
COL1A1 P02452	1.39775873	0.244939355	0.86611329	0.971815904	0.620040787	0.192257191	0.870278392	0.997482392	-0.03553368	0.019327724	0.051675042	0.054880643	0.087238808	0.032477466				
PTPST1 P02725	2.20543017	0.08884731	0.117210337	0.991896564	0.438053698	0.195456941	0.835207488	0.607544709	-0.088716307	-0.0100245	-0.06664945	0.077713858	0.032071362	-0.045642966				
LROB1 Q8N251	18.2967197	1.94E-10	3.75E-05	0.99999367	4.37E-07	2.60E-05	0.89263995	0.89532999	-0.152719483	0.000385659	-0.175205046	0.151051442	-0.024855631	-0.175909259				
NID1 P14543	6.6861259	0.000261357	0.002908391	0.866219016	0.002779503	0.037664508	0.998291052	0.040628343	-0.110250732	-0.027256019	-0.105186028	0.082994713	0.005604704	-0.077930008				
APLP1 Q06481	0.5430244	0.652833056	0.82534297	0.984115189	0.999988369	0.609712851	0.791429988	0.986628227	-0.049427572	0.02007083	0.001738963	0.059498002	0.051166535	-0.018331867				
LAMB2 P55268	4.1194765	0.007399478	0.865837823	0.07772049	0.992617597	0.009480349	0.951162227	0.028698218	-0.017893361	0.054277324	-0.006064538	0.072170885	0.011828824	-0.060341861				
IGHG3 P01860	1.3019681	0.39E-06	0.000308442	0.872720092	0.05644552	9.76E-06	0.283504001	0.068483878	-0.622247424	0.111054025	-0.36380471	0.73301447	0.25849812	-0.474861635				
AGRN Q00468	1.0792407	2.35E-03	0.572806672	0.733314179	0.307935851	0.98403412	0.981427178	0.86820926	0.036602033	0.026527332	0.06890122	-0.010074701	0.010378089	0.020254729				
PKM1 P14618	2.1645069	0.37E-14	0.103546667	2.82E-06	4.68E-05	1.67E-11	4.27E-10	0.871315639	0.094973813	-0.210524424	-0.181018146	-0.305480803	-0.27599196	0.029060933				
PLXNB1 Q15031	2.5215705	0.005267974	0.071508784	0.09955437	0.387419336	0.99608165	0.763235198	0.89593492	-0.081737038	-0.074973599	-0.05039829	0.06079599	0.0313448	-0.02483533				
C9 P02748	0.2796217	0.84063947	0.9924705	0.956370495	0.99334826	0.86281599	0.99997421	0.852738721	-0.027673526	0.050601098	-0.025786651	0.078274624	0.001888875	-0.076837749				
FTL1 Q06272	2.60103299	0.047627048	0.819230175	0.249709083	0.040013284	0.777459599	0.306949742	0.895561048	0.052173786	0.108167664	0.152244004	0.055993878	0.100070217	0.04407634				
IGFBP3 P24592	1.6744892	0.174021184	0.524077565	0.984816345	0.51676055	0.309227477	0.999927547	0.828758877	-0.073185787	0.018966932	-0.027054337	0.003152719	0.01103105	-0.091042369				
CFI P05156	1.5715216	0.197825111	0.99990571	0.237109826	0.840510655	0.264011504	0.86393495	0.6707794	0.002517638	0.15573791	0.066088902	0.152320515	0.063581244	-0.08639809				
NCAN Q14594	1.28485107	0.280696511	0.693626264	0.542146525	0.220052065	0.96821516	0.869166168	0.9405175	0.067859482	0.008043939	0.11652492	0.012684457	0.0579301	-0.03108553				
NID2 Q14112	3.7751247	0.011609095	0.069367106	0.986661163	0.271126791	0.02596525	0.868283358	0.128402862	-0.105024023	0.014029135	-0.073451128	0.119035318	0.031572895	-0.087480263				
SERPINF1 P36955	0.2846757	9.56E-06	0.004329836	0.619850574	0.008720463	3.76E-05	0.682319959	0.001349979	-0.136992096	0.06551681	-0.093998799	0.183483777	0.042934017	-0.01495476				
B4GAT1 Q14305	5.7761292	0.000805959	0.2977124	0.11141434	0.00308358	0.98190806	0.110967216	0.017541009	0.054519793	0.06599274	0.12207026	0.01472947	0.067504313	0.05007466				
PTGDS P14222	1.6411766	0.181395942	0.164466998	0.98201514	0.82529546	0.30350434	0.554899949	0.96238683	0.092938954	0.010238632	0.023165059	0.04902023	0.036093895	-0.01298428				
FLNB P08095	1.10048893	0.350272694	0.490966695	0.995095611	0.51384052	0.622869092	0.99072158	0.070856292	-0.06508346	-0.00962208	-0.01232008	0.04746176	0.005257336	-0.042170801				
ATRN Q75882	4.8083407	0.000305536	0.066053799	0.684175222	0.65437406	0.002158085	0.478631478	0.094324641	-0.097344132	0.04233366	-0.043471679	0.196794999	0.05149654	-0.085480345				
LAMB1 P07942	2.94880034	0.004985958	0.457822126	0.446452666	0.925639955	0.017925576	0.29511429	0.858298264	-0.038704188	0.08140615	0.005947906	0.076844803	0.044652904	-0.03192709				
CNTNAP1 Q9C0A0	2.3826107	0.070883023	0.862627465	0.973388266	0.007015337	0.982698686	0.372942772	0.172758192	0.043294802	0.0231313	0.12934348	-0.20157627	0.08604862	0.106206354				
EN2A2 Q9A769	1.3118074	0.271948126	0.78174032	0.96260589	0.239078314	0.963500141	0.815408328	0.493090681	-0.040963984	-0.02044291	-0.07774617	0.020521074	0.076872163	-0.105932327				
FLN1 Q14767	12.2150738	2.50E-07	0.03294738	0.72075889	4.45E-07	0.291056864	0.042361694	4.38E-05	-0.13889498	-0.05097717	-0.267805796	0.087922381	-0.18951298	-0.216872679				
AZL3P1 P14311	3.67231297	0.0012406	0.47035637	0.97624707	0.953870907	0.717758735	0.754786176	0.99633189	-0.114021398	-0.03192097	-0.09311917	0.082710101	0.073269891	-0.007447713				
FLNA P12333	0.81042156	0.489564697	0.900285948	0.672634767	0.49825184	0.976240763	0.875360776	0.986324369	-0.04489456	-0.071427714	0.002135735	-0.02648259	-0.047146279	-0.02170802				
KRT10 P13645	1.0028781	0.392810793	0.99993949	0.570330853	0.606733772	0.616681028	0.65360381	0.99744369	0.011450799	0.25301919	0.326211529	0.21456852	0.22476023	0.016807796				
MMP21 P08253	0.82319209	0.482591465	0.94177838	0.621846317	0.970330668	0.467700671	0.894865439	0.81868318	-0.010316374	0.047682322	0.01716653	0.057946607	0.027482905	-0.03046172				
KRT19 P35527	0.38876404	0.754053858	0.85055885	0.99882056	0.996432025	0.926629252	0.718519771	0.972450014	-0.205518928	0.051068885	0.05219182	0.154453040	0.257710748	0.10325705				
SERPINF2 P06897	0.04664736	0.469980062	0.86113882	0.872145591	0.998032445	0.060426642	0.674455119	0.964975054	-0.069905602	0.065861417	0.026507621	0.135767019	0.096413223	-0.03953796				
GLI3 Q06830	2.17938887	0.091954999	0.381331987	0.988196601	0.02647843	0.561312451	0.961040177	0.026307179	-0.549628111	-0.108398335	-0.112206703	0.444249775	-0.162392562	-0.60823237				
DAC1 Q14118	3.67231297	0.0012406	0.47035637	0.97624707	0.953870907	0.717758735	0.754786176	0.99633189	-0.114021398	-0.03192097	-0.09311917	0.082710101	0.073269891	-0.007447713				
DAC1 Q14118	7.5784909	8.29E-05	0.10174643	0.119505809	0.00183371	0.514198747	0.15712102	0.00762311	0.048669423	0.016151177	0.06365101	-0.032554246	0.014945674	-0.04749924				
CTSD P07339	1.31758683	0.02109962	0.039504559	0.726614522	0.053867147	0.328062211	0.994151343	0.424247425	-0.165997973	-0.062578921	-0.102796977	0.103419052	0.15200995	-0.08281057				
COL12A1 Q9P9715	2.88952395	0.036826698	0.069596788	0.838914045	0.08491052	0.338999193	0.95676765	0.422006645	-0.097115002	-0.031969733	-0.088336095	0.065145269	0.008751097	-0.05639172				
PSAP P07602	0.63184847	0.595567693	0.681184428	0.908996068	0.704751241	0.839575892	0.9998826	0.86096947	0.04008888	0.010382391	0.03678677	-0.029706489	-0.00302102	0.026404387				
CNTNAP2 Q9UHQ6	2.17386581	0.00170083	0.169920386	0.529706822	0.07648622	0.874481884	0.994580616	0.919080879	0.119398618	0.06332425	-0.043057168	0.01389463	0.059951799	-0.01894263				
ITIH5 Q86UJ2	21.2820258	6.89E-12	3.98E-09	0.47398073	4.40E-07	1.54E-06	0.74591623	0.046999513	-0.064999513	-0.208733297	0.198174168	0.004640285	-0.161737894	0.004640285				
IGHA1 P01861	0.6348921	0.476271482	0.607847828	0.988994947	0.58647001	0.782424108	0.999091199	0.71510796	-0.06436505	-0.0542372	0.196211267	0.00635	-0.1908721	0.00635				
TGFBI Q15582	0.90135246	0.607006136	0.945972038	0.992566216	0.00958677	0.988041079	0.908285256	0.730170787	0.02097417	0.008787402	0.00483998	-0.012186769	0.02509828	-0.036695697				

Gene ID Uniprot ID	F-Value	Pr[F]	ANOVA p-values with Tukey Adjustment								Difference (AD - CT)							
			AD-Cau vs AD-AA	CT-AA vs AD-AA	AD-Cau vs AD-AA	CT-AA vs AD-AA	AD-Cau vs AD-AA	CT-AA vs AD-AA										

Gene ID Uniprot ID	F-Value	Pr(-F)	ANOVA p-values with Tukey Adjustment										Difference (AD - CT)																	
			AD-Cau vs AD-AA	CT-AA vs AD-AA	CT-AA vs AD-AA	CT-AA vs AD-AA	CT-AA vs AD-AA	CT-AA vs AD-AA	CT-AA vs AD-AA	CT-AA vs AD-AA	CT-AA vs AD-AA	CT-AA vs AD-AA	CT-AA vs AD-AA	CT-AA vs AD-AA	CT-AA vs AD-AA	CT-AA vs AD-AA	CT-AA vs AD-AA	CT-AA vs AD-AA	CT-AA vs AD-AA	CT-AA vs AD-AA	CT-AA vs AD-AA	CT-AA vs AD-AA								
F10 P00742	1.68252552	0.17258465	0.33328509	0.99156031	0.31038279	0.48351283	0.999971042	0.46357045	-0.097224804	-0.016207216	-0.09483178	0.080107588	0.002393024	-0.07862564	11.4585482	6.31E-07	3.20E-05	0.18376053	5.18E-06	0.03253393	0.99849951	0.013104089	-0.19612065	-0.02593692	-0.02644793	0.113548373	-0.00550278	-0.12051101		
LMA2 Q12907	3.96523161	0.009053683	0.016108063	0.621822563	0.04712162	0.25263466	0.98053708	0.40705454	0.069956265	0.027435819	-0.044252046	0.06387886	0.002378896	-0.03878986	CLE3C P05452	1.15128467	0.329752487	0.886011218	0.942539866	0.689539815	0.566426214	0.987421979	0.32782116	-0.01941274	0.014649707	-0.027921531	0.034062447	-0.00857809	-0.042571238	
SDA1 Q07473	21.6820795	4.44E-12	0.00642692	0.00023497	0.02738496	2.18E-11	1.87E-08	0.48285249	0.20890117	-0.2530505	-0.168864266	-0.462001198	-0.371814404	0.084185794	F11 P00748	5.87709942	0.000745926	0.29804125	0.986778693	0.004582668	0.151681807	0.483323208	0.001597684	0.228861888	0.015796856	0.408024192	-0.27199356	0.179162304	0.00576166	
CADM3 Q8N126	3.4121611	0.018650839	0.171198959	0.98438615	0.102672497	0.999257032	0.802763127	0.489752633	0.077920886	0.085293783	0.110878156	0.003766447	0.03295907	0.02554524	TAM31320 Q14C87	12.4166533	1.95E-07	0.000186797	0.00013892	0.0156707	0.99976756	0.550246649	0.085243344	0.271394949	0.2685806	0.352373623	-0.002814349	0.009878674	0.005979023	
PRNP P04156	6.31597272	0.000421969	0.002157468	0.036487812	0.000839533	0.753108643	0.999307926	0.436006514	0.129329511	0.094342483	0.13361407	-0.034987028	0.00248506	0.039271534	CACNA2D1 Q8ZS8	4.61106265	0.00389893	0.010198316	0.043219341	0.000879953	0.974131376	0.999857858	0.949714738	0.180523026	0.147684339	0.147642609	-0.032838687	0.004046817	0.012687817	
COMP P49747	0.18967443	0.90336606	0.886371667	0.949440447	0.96207497	0.996953035	0.989768857	0.999616681	-0.064983387	-0.046951297	-0.038411506	0.01803209	0.026571881	0.006539791	PLD1 Q02809	11.4585482	6.31E-07	3.20E-05	0.18376053	5.18E-06	0.03253393	0.99849951	0.013104089	-0.19612065	-0.02593692	-0.02644793	0.113548373	-0.00550278	-0.12051101	
SNED1 Q8TER0	1.9757026	0.769282805	0.961606432	0.979660948	0.968601514	0.815039521	0.774091604	0.999930619	-0.019976535	-0.015480178	0.017687395	0.035467113	0.002721217	0.005627217	GLD1 P80108	1.7782854	0.154072727	0.993881273	0.816414965	0.27359011	0.671144222	0.172510366	0.012878567	-0.020670226	0.068115004	0.136953697	0.08878523	0.157623923	0.06883693	
PRG4 Q02954	6.9865408	0.000177353	0.196395802	0.917203259	0.005320626	0.042368132	0.598673536	0.000383811	-0.234196634	0.073941933	-0.017455077	0.308138567	-0.14125844	-0.0449701	PCDH9 Q9CH56	4.0663459	0.007932077	0.051715201	0.31593972	0.009582024	0.794492838	0.932505076	0.389630152	0.10827422	0.070275235	0.13244385	-0.03802007	0.024166688	0.062168615	
RTNAR Q9BZ76	3.77412916	0.011624028	0.902174001	0.34114557	0.00988128	0.774683648	0.970097971	0.54578852	-0.03311435	0.078643828	-0.145182619	0.004572403	0.011201184	0.066538781	SUSD5 Q60279	1.222173	0.30300297	0.6348837	0.239831764	0.800945756	0.91436936	0.985361735	0.712898076	0.054459941	0.08392627	0.039056382	0.029466686	-0.013403559	-0.04847015	
LUM1 P51804	11.2559578	0.340013031	0.814192494	0.78650886	0.994860397	0.267729181	0.654007351	0.87446637	-0.055843674	0.057544908	0.014721121	0.113388572	0.070564795	-0.042823777	PEP1 P03086	13.7223946	0.04E-08	0.451805166	0.001033366	0.007107159	0.81520156	0.81520156	0.81520156	0.81520156	0.81520156	0.81520156	0.81520156	0.81520156	0.81520156	0.81520156
CFD P00746	3.21818316	0.02481881	0.999976947	0.958233363	0.11467838	0.96826036	0.11129185	0.072197084	0.002429994	0.029749415	-0.129791121	0.027319421	-0.132169106	-0.15488527	LDHA Q00338	59.6974558	4.86E-27	0.159858602	2.42E-12	1.24E-13	1.24E-13	1.12E-13	0.857451126	0.07938356	-0.289917152	-0.37049208	-0.368285508	-0.396417526	-0.005122055	
LAMP1 Q13449	6.31558216	0.000421969	0.027189347	0.014923619	0.000219329	0.999267312	0.600682605	0.661492115	0.102962524	0.107529767	0.146644437	0.004564543	0.043679213	0.03911467	SCN11 P07585	6.8213654	0.00021942	0.002558186	0.999646255	0.059872026	0.010480548	0.616568041	0.940928252	-0.129207043	0.005945946	-0.147234467	0.225152989	0.071972525	0.115380413	
CADH1 P04025	34.3796476	1.04E-17	0.279548183	4.34E-09	1.14E-07	3.06E-13	5.86E-12	0.859307816	0.075330271	-0.26587557	-0.234600999	-0.340978464	-0.399951215	0.039986611	RYR1 Q04695	11.2559578	0.340013031	0.814192494	0.78650886	0.994860397	0.267729181	0.654007351	0.87446637	-0.055843674	0.057544908	0.014721121	0.113388572	0.070564795	-0.042823777	
PCNA Q02954	3.13545887	0.02750409	0.50111116	0.673015295	0.553053857	0.057526159	0.032391558	0.998367514	-0.005958009	0.039953684	-0.055819999	0.009830674	0.00645314	0.00546314	CD14 P08571	0.38915971	0.76949208	0.788171657	0.977146712	0.99995874	0.948219373	0.780454157	0.978114247	0.035517985	0.015109483	0.000817041	-0.020480502	-0.034700944	0.014292442	
PEBP4 Q96596	10.9110282	1.24E-06	3.89E-05	0.990601263	0.989186946	6.59E-06	6.177E-05	0.921502951	-0.314593152	0.019787186	-0.02027802	0.334380338	0.294315132	-0.040605206	CABPA P04003	1.14243032	0.33328509	0.506774196	0.999632344	0.561508958	0.55939781	0.988616723	0.613856688	-0.237288253	-0.016730748	-0.251202156	0.220557050	0.025786097	-0.194774107	
FBN1 Q9UBX5	0.66414013	0.576761802	0.943181168	0.774805736	0.52892325	0.87473256	0.980869136	0.980869136	-0.016722524	-0.02767694	-0.03845547	-0.01094517	0.021622605	-0.010768827	LAMA1 Q16363	1.1890587	6.87E-10	6.08E-07	0.990332617	2.00E-05	1.70E-06	0.734476736	5.48E-05	-0.221941382	-0.011798219	-0.183199212	0.210143164	0.039544226	-0.170600903	
SAT1 P04045	1.42100622	0.33056498	0.79459837	0.99973858	0.00476549	0.76921504	0.867523182	0.99636656	-0.2284646	0.06521242	0.234857842	0.233656149	-0.233656149	-0.233656149	TCF12 P24821	1.0864952	0.256128156	0.99788788	0.96641522	0.65434284	0.500819834	0.558121982	0.999269229	0.008655324	-0.025924921	-0.067079777	0.016249643	0.005758333		
PENK P01210	10.1091266	3.36E-06	0.287626283	0.006192971	0.15136029	5.65E-06	0.000667813	0.107510619	-0.075637916	0.13692769	0.0856464	0.121256506	0.161302516	-0.05126309	PTPRG P23470	6.73120243	0.000425659	0.10185052	0.062087864	7.33E-05	0.98972543	0.175184893	0.280664691	0.088429333	0.093811299	0.016433041	0.005381566	0.07513307	-0.07331741	
COL1A1 Q02461	1.69891128	0.16984844	0.73115223	0.906059691	0.670975798	0.318410224	0.99997147	0.51173296	-0.06251993	0.014634379	-0.080033591	0.106923609	0.000741601	-0.10696791	COL3A1 Q02461	1.69891128	0.16984844	0.73115223	0.906059691	0.670975798	0.318410224	0.99997147	0.51173296	-0.06251993	0.014634379	-0.080033591	0.106923609	0.000741601	-0.10696791	
NR3C1 Q9D865	1.77709239	0.28403985	0.464031984	0.594631773	0.250072925	0.99572569	0.98516112	0.931819658	-0.102238002	-0.0683841	-0.125872111	0.016389072	-0.023648488	-0.040038111	RYR1 Q04695	11.2559578	0.340013031	0.814192494	0.78650886	0.994860397	0.267729181	0.654007351	0.87446637	-0.055843674	0.057544908	0.014721121	0.113388572	0.070564795	-0.042823777	
PCDH23 Q02954	3.77702328	0.011624028	0.59633084	0.99745247	0.17497905	0.46476705	0.905179789	0.52418331	-0.049597296	0.05240061	-0.01460585	0.002437357	0.004892054	0.004892054	ENDOD1 Q94919	0.37895705	0.530726981	0.924538601	0.472793742	0.752666076	0.856453427	0.987026172	0.964099023	0.015208318	0.034320945	0.0230724	0.011911212	0.007854082	0.011248545	
NRXN1 P58400	1.7582706	0.195041623	0.9393711	0.941416001	0.11734335	0.99995658	0.480787984	0.43978957	0.035484481	0.034096298	-0.001391827	0.008191267	0.008191267	0.008191267	OMG Q99983	7.4207347	0.000101445	0.001355223	0.027608453	0.000113489	0.73471179	0.97184133	0.20658141	0.13908494	0.0160496	-0.01749134	0.005130729			
CBD1 P07360	1.02924806	6.80E-05	0.00219038	0.592547425	0.000257333	0.07520806	0.981578463	0.813713727	-0.154985428	-0.052393941	-0.105823231	0.025914827	-0.015596895	-0.01188382	CBP P07360	1.02924806	6.80E-05	0.00219038	0.592547425	0.000257333	0.07520806	0.981578463	0.813713727	-0.154985428	-0.052393941	-0.105823231	0.025914827	-0.015596895	-0.01188382	
PP1A Q14773	1.26452448	0.288040657	0.361583176	0.9999618	0.857399969	0.32787497	0.796791778	0.827215209	-0.10002094	0.002807774	-0.046139867	0.103827868	0.053880227	-0.04894764	SCS1 P05408	7.4207347	0.000101445	0.001355223	0.027608453	0.000113489	0.73471179	0.97184133	0.20658141	0.13908494	0.0160496	-0.01749134	0.005130729			
SPOCK2 Q9Z563	1.9207257	0.12751514	0.291701275	0.30808957	0.11865857	0.99809077	0.98065195</																							

Gene ID Uniprot ID	F-Value	Pr(F)	ANOVA p-values with Tukey Adjustment										Difference (AD - CT)															
			AD-Cau vs AD-AA	CT-AA vs AD-AA	CT-AA vs AD-AA	CT-AA vs AD-AA	CT-AA vs AD-AA	CT-AA vs AD-AA	CT-AA vs AD-AA	CT-AA vs AD-AA	CT-AA vs AD-AA	CT-AA vs AD-AA	CT-AA vs AD-AA	CT-AA vs AD-AA	CT-AA vs AD-AA	CT-AA vs AD-AA	CT-AA vs AD-AA	CT-AA vs AD-AA	CT-AA vs AD-AA	CT-AA vs AD-AA	CT-AA vs AD-AA	CT-AA vs AD-AA						
PCDHGC Q5Y5F6	13.3685254	6.18E-08	0.022181954	5.59E-06	1.65E-07	0.16384207	0.034756896	0.925214531	0.15294962	0.26526811	0.29644571	0.10991849	0.141150799	0.03117895	0.14124342	1.77E-08	0.21353576	5.34E-06	2.00E-07	0.013855621	0.001756574	0.394019149	-0.071791603	-0.12886602	-0.20240521	-0.110899989	-0.13061098	-0.03191191
RGMB Q6NRW40	8.27957115	3.38E-05	0.07890804	0.014577098	9.94E-06	0.94620165	0.08377675	0.242234185	0.1059851	0.129851103	0.206941776	0.032866003	0.100956676	0.07709672	1.40869808	0.24187995	0.93914634	0.8919418	0.20074257	0.999391428	0.53031716	0.942478385	-0.01742933	0.02878596	0.036554885	0.030335664	0.039111953	0.022515688
FNCSA P14334	2.53674356	0.058128766	0.16266793	0.982047109	0.146367553	0.303578042	0.999935108	0.285937501	-0.652165712	-0.114101767	0.285937501	0.036554885	0.039111953	0.022515688	0.324711602	0.807487889	0.872701922	0.989909102	0.999103146	0.966122061	0.79257366	0.986751693	-0.041245177	-0.01244977	0.00701988	0.0250002	0.048264558	0.023264257
DRM2 P19652	1.160822	0.3068271	0.808529666	0.11596897	0.96731862	0.284552256	0.511452868	0.986652683	-0.095722669	0.092523303	0.064985081	0.188245972	0.14270751	0.04558221	1.7284427	7.88E-07	0.37505657	0.010387687	5.00E-07	0.457138699	0.000969531	0.079912905	0.032525489	0.066897849	0.116005982	0.03167236	0.080784039	0.049111733
DMH1 P55287	1.1172447	0.00012442	0.008406922	0.808849122	0.00201082	0.084812586	0.985559594	0.0114957189	0.115263846	0.031163164	0.132598205	-0.08410683	0.01734359	-0.01435041	6.93248107	0.000292442	0.0046922	0.008849122	0.00201082	0.084812586	0.985559594	0.0114957189	0.115263846	0.031163164	0.132598205	-0.08410683	0.01734359	-0.01435041
F13B P05160	1.12581436	0.340180157	0.857394723	0.764213107	0.965998165	0.291785816	0.527201605	0.949460962	-0.075906111	0.090699888	0.042549059	0.1666005	0.118449671	-0.048150829	1.69369363	0.000254833	0.04342677	0.711880199	0.58035052	0.01393995	0.998170823	0.53031716	0.942478385	-0.01742933	0.02878596	0.036554885	0.039111953	0.022515688
EMA3B Q13214	1.96839653	0.120256943	0.186140345	0.909351906	0.356491243	0.802252885	0.965587005	0.527534816	-0.100637599	-0.014702873	-0.07054895	0.085934726	0.02582703	-0.01054278	3.01320951	0.000292442	0.0046922	0.008849122	0.00201082	0.084812586	0.985559594	0.0114957189	0.115263846	0.031163164	0.132598205	-0.08410683	0.01734359	-0.01435041
HGFC Q04756	1.0192273	0.894963621	0.992792623	0.87056184	0.973432633	0.964151482	0.99026908	0.984166270	0.02966182	0.080475213	0.04240014	0.05081387	0.014542278	-0.036271109	3.01320951	0.000292442	0.0046922	0.008849122	0.00201082	0.084812586	0.985559594	0.0114957189	0.115263846	0.031163164	0.132598205	-0.08410683	0.01734359	-0.01435041
DLFML3 Q9NRN5	3.14152367	0.026540046	0.807251818	0.879629747	0.291184336	0.99807833	0.219038264	0.194611604	-0.030233857	-0.02440112	-0.0592829	0.00529745	-0.06274432	-0.028654177	3.01320951	0.000292442	0.0046922	0.008849122	0.00201082	0.084812586	0.985559594	0.0114957189	0.115263846	0.031163164	0.132598205	-0.08410683	0.01734359	-0.01435041
EMEGA Q2H26E	3.30379939	0.021482403	0.992807528	0.769531424	0.026655142	0.906270798	0.062224007	0.244860403	0.01059709	0.037575308	0.10749332	0.02681218	0.09653263	0.06991801	1.01320951	0.000292442	0.0046922	0.008849122	0.00201082	0.084812586	0.985559594	0.0114957189	0.115263846	0.031163164	0.132598205	-0.08410683	0.01734359	-0.01435041
F11 P039971	0.1751859	0.91309201	0.995495087	0.965435897	0.996336129	0.89607138	0.97702601	0.9986012	-0.02555525	0.05008094	0.01737869	0.075636465	0.02494224	-0.03702241	1.01320951	0.000292442	0.0046922	0.008849122	0.00201082	0.084812586	0.985559594	0.0114957189	0.115263846	0.031163164	0.132598205	-0.08410683	0.01734359	-0.01435041
DPF7 P08144	0.5477494	0.650264134	0.999982308	0.686633826	0.995654018	0.717093798	0.99818274	0.784643591	0.003433282	0.010660224	0.01900492	0.097426942	0.015571638	-0.08185304	1.01320951	0.000292442	0.0046922	0.008849122	0.00201082	0.084812586	0.985559594	0.0114957189	0.115263846	0.031163164	0.132598205	-0.08410683	0.01734359	-0.01435041
FNJ2 P20062	6.69369363	0.000258133	0.04342677	0.711880199	0.58035052	0.01393995	0.998170823	0.53031716	-0.12652598	0.02132656	0.11127253	0.14782556	0.03938645	-0.13345477	1.01320951	0.000292442	0.0046922	0.008849122	0.00201082	0.084812586	0.985559594	0.0114957189	0.115263846	0.031163164	0.132598205	-0.08410683	0.01734359	-0.01435041
PRP1 P04814	1.80362909	0.148042367	0.991351368	0.591613036	0.925539018	0.180714716	0.29886549	0.985860696	-0.010591098	-0.04429203	-0.01933859	0.02582703	-0.01054278	-0.02582703	1.01320951	0.000292442	0.0046922	0.008849122	0.00201082	0.084812586	0.985559594	0.0114957189	0.115263846	0.031163164	0.132598205	-0.08410683	0.01734359	-0.01435041
DKR1 Q08345	0.44948484	0.008157233	0.147937114	0.630607147	0.005562129	0.76079524	0.68039297	0.140562281	0.123978548	0.067742544	0.184903386	-0.05623603	0.060924839	-0.017160842	1.01320951	0.000292442	0.0046922	0.008849122	0.00201082	0.084812586	0.985559594	0.0114957189	0.115263846	0.031163164	0.132598205	-0.08410683	0.01734359	-0.01435041
PARK7 Q99497	56.032655	8.35E-26	0.777101688	3.01E-13	9.48E-11	1.24E-13	0.00803842	-0.02966933	-0.250360922	-0.31775504	-0.226091589	-0.28805571	-0.06793425	-0.16793425	1.01320951	0.000292442	0.0046922	0.008849122	0.00201082	0.084812586	0.985559594	0.0114957189	0.115263846	0.031163164	0.132598205	-0.08410683	0.01734359	-0.01435041
BCAM P09685	4.3576086	0.005418833	0.09693243	0.938427623	0.162716665	0.01983941	0.984592986	0.035614425	-0.058666465	0.014226621	-0.000026297	0.07289806	0.00864167	-0.064252918	1.01320951	0.000292442	0.0046922	0.008849122	0.00201082	0.084812586	0.985559594	0.0114957189	0.115263846	0.031163164	0.132598205	-0.08410683	0.01734359	-0.01435041
LTSH P08669	1.9876699	0.117326478	0.294117178	0.9511750	0.998076095	0.097890221	0.29471733	0.932486123	-0.135806622	0.039732828	0.01737869	0.075636465	0.02494224	-0.03702241	1.01320951	0.000292442	0.0046922	0.008849122	0.00201082	0.084812586	0.985559594	0.0114957189	0.115263846	0.031163164	0.132598205	-0.08410683	0.01734359	-0.01435041
CHIT1 Q13231	11.7232506	4.56E-07	0.98574652	0.000173904	7.51E-05	0.000832137	0.000401949	0.99959265	-0.06857788	-0.82504551	-0.84512177	-0.77246763	-0.76593889	-0.01917226	1.01320951	0.000292442	0.0046922	0.008849122	0.00201082	0.084812586	0.985559594	0.0114957189	0.115263846	0.031163164	0.132598205	-0.08410683	0.01734359	-0.01435041
FJ P00740	1.41328218	0.240174447	0.52303312	0.960821868	0.58047993	0.37059066	0.998170823	0.53031716	-0.12652598	0.02132656	0.11127253	0.14782556	0.03938645	-0.13345477	1.01320951	0.000292442	0.0046922	0.008849122	0.00201082	0.084812586	0.985559594	0.0114957189	0.115263846	0.031163164	0.132598205	-0.08410683	0.01734359	-0.01435041
FHMR1 Q08351	4.0412976	0.127374062	0.98033127	0.737543165	0.99056166	0.80258424	0.999620988	0.0229722	0.12906708	0.01706493	0.10605408	-0.02582703	-0.01054278	-0.02582703	1.01320951	0.000292442	0.0046922	0.008849122	0.00201082	0.084812586	0.985559594	0.0114957189	0.115263846	0.031163164	0.132598205	-0.08410683	0.01734359	-0.01435041
C1QC P02747	0.5574968	0.643745031	0.986026343	0.595590541	0.947000011	0.811668223	0.99770821	0.87879175	-0.013791091	-0.048854072	-0.020913649	-0.035062981	-0.007122558	-0.027940423	1.01320951	0.000292442	0.0046922	0.008849122	0.00201082	0.084812586	0.985559594	0.0114957189	0.115263846	0.031163164	0.132598205	-0.08410683	0.01734359	-0.01435041
HP90A1 P07900	27.576062	6.63E-25	0.929183768	3.29E-07	3.06E-11	1.56E-10	0.00821342	-0.21804536	-0.221329534	-0.193177456	-0.21450699	-0.239374871	-0.024867881	-0.024867881	1.01320951	0.000292442	0.0046922	0.008849122	0.00201082	0.084812586	0.985559594	0.0114957189	0.115263846	0.031163164	0.132598205	-0.08410683	0.01734359	-0.01435041
NDRG2 Q9UN36	4.0391234	0.008219626	0.9357276	0.353063645	0.343369471	0.119552398	0.72785578	0.040308703	0.017840097	-0.048758161	0.04814888	-0.066598259	0.030308791	0.096907049	1.01320951	0.000292442	0.0046922	0.008849122	0.00201082	0.084812586	0.985559594	0.0114957189	0.115263846	0.031163164	0.132598205	-0.08410683	0.01734359	-0.01435041
NUCB2 P80303	0.3903986	0.415262422	0.647667631	0.6160643	0.925590901	0.929006968	0.755018367	0.883691422	-0.080612426	-0.065730698	-0.014881728	0.05286219	0.05286219	-0.01941974	1.01320951	0.000292442	0.0046922	0.008849122	0.00201082	0.084812586	0.985559594	0.0114957189	0.115263846	0.031163164	0.132598205			

Gene ID Uniprot ID	F-Value	Pr[F]	ANOVA p-values with Tukey Adjustment										Difference (AD - CT)															
			AD-Cau vs AD-AA	CT-AA vs AD-AA	CT-AA vs AD-AA	CT-AA vs AD-AA	CT-AA vs AD-AA	CT-AA vs AD-AA	CT-AA vs AD-AA	CT-AA vs AD-AA	CT-AA vs AD-AA	CT-AA vs AD-AA	CT-AA vs AD-AA	CT-AA vs AD-AA	CT-AA vs AD-AA	CT-AA vs AD-AA	CT-AA vs AD-AA	CT-AA vs AD-AA	CT-AA vs AD-AA	CT-AA vs AD-AA	CT-AA vs AD-AA	CT-AA vs AD-AA						
COR1A1 P31146	5.39810778	0.0013167	0.821791327	0.67405576	0.00124965	0.955264203	0.026924077	0.042282662	-0.042692786	-0.05421169	-0.17642245	-0.011518905	-0.133729639	-0.122210735	1.44100995	0.232308426	0.20931948	0.649878117	0.39129515	0.83058735	0.962538467	0.978801862	-0.13490246	-0.076802873	-0.101914821	-0.056687372	0.031575424	-0.022113948
CH3L2 Q15782	3.7348953	0.01233743	0.083442704	0.858767587	0.020567727	0.357899441	0.977945678	0.143126015	-0.192837429	-0.062166934	-0.22413212	0.130674095	-0.031283893	-0.161943888	1.17471773	0.0262602	0.040798316	0.348797837	0.16243545	0.985219922	0.965789022	0.985219922	-0.099274198	-0.037654414	-0.082169256	0.0611619784	0.017104941	-0.045148483
ITPPI3 Q9NS15	3.1147773	0.0262602	0.034897037	0.712065358	0.08531242	0.31161854	0.961581147	0.558634318	-0.099274198	-0.037654414	-0.082169256	0.0611619784	0.017104941	-0.045148483	0.80545129	0.962476933	0.96749868	0.999999221	0.91494644	0.99848269	0.965789022	0.985219922	-0.038051091	-0.038051091	-0.038051091	-0.02416277	0.012863691	0.037028838
APF181 Q01547	2.9852459	0.0262602	0.034897037	0.712065358	0.08531242	0.31161854	0.961581147	0.558634318	-0.099274198	-0.037654414	-0.082169256	0.0611619784	0.017104941	-0.045148483	0.7928824	0.501361828	0.501361828	0.892202616	0.904398522	0.838603844	0.772314872	0.99805566	-0.171715236	-0.079165852	-0.070786051	0.092548385	0.100934622	0.008326327
PGYB1 P12116	4.7908288	0.00335977	0.04751865	0.13307021	0.00180252	0.800344076	0.95826266	0.800344076	0.95826266	0.800344076	0.95826266	0.800344076	0.95826266	0.800344076	0.9236974	0.04751865	0.04751865	0.13307021	0.00180252	0.00180252	0.00180252	0.00180252	0.193521788	0.157034396	0.258296679	-0.036487392	0.064774891	0.101622823
MG1 P20916	1.5801894	0.195675969	0.980653114	0.99993506	0.27522962	0.970067519	0.512434557	0.233093504	0.016451083	-0.002406569	0.073831913	-0.018857652	0.05693803	-0.077584822	3.84744306	0.010651545	0.12588972	0.951225617	0.01638734	0.92857827	0.90433055	0.90433055	0.137034946	-0.032172417	0.113948594	-0.169207378	0.022049107	0.175788271
LG1 Q09570	0.9999905	0.3941108	0.643997366	0.95557091	0.759147866	0.487140137	0.994580643	0.600606958	-0.05872888	0.01132735	-0.046789921	0.070100238	0.011982966	-0.058117272	1.33012709	0.269218743	0.489884116	0.304972723	0.335555117	0.921515982	0.999597968	0.999597968	0.064179884	0.0767499	0.07423264	0.012570017	0.008123238	-0.027598811
AGL1 P78504	6.8019062	0.00025052	0.478446832	0.09425576	0.00025052	0.87112575	0.044146792	0.781523216	0.052765515	0.113746042	0.146524044	0.069090526	0.093389809	-0.012863691	1.05637842	8.99E-08	0.320165016	1.26E-05	0.136E-06	0.11928875	0.002926945	0.982671487	0.12603377	0.350623223	0.37608732	0.24584887	0.250049495	0.025465674
EEF1A1 P68104	1.0354942	0.639207312	0.939596829	0.944863461	0.569690561	0.905211358	0.88290246	-0.04529498	-0.042767286	-0.07905511	0.002662012	-0.051625612	-0.052487620	0.52821291	0.89719457	2.46E-30	0.89719457	1.23E-13	1.25E-13	1.14E-13	1.21E-13	0.928412186	0.033448316	0.471222261	-0.449317829	-0.504666707	-0.477361645	0.027304341
PLBD2 Q8NHP8	2.1807308	0.019156707	0.166534382	0.922604452	0.17826946	0.450644783	0.999351026	0.478670205	-0.143327431	-0.042360163	-0.109837628	0.008117224	-0.029300044	-0.008117224	0.71023493	0.010651545	0.166534382	0.922604452	0.17826946	0.450644783	0.999351026	0.478670205	0.03448316	0.471222261	-0.449317829	-0.504666707	-0.477361645	0.027304341
NOMO2 Q5JPE7	1.5768785	0.196546373	0.246749321	0.999999904	0.862297955	0.22836605	0.649703136	0.849507318	-0.067293135	0.000477333	-0.026841493	0.067770467	0.040451642	-0.07318825	5.81533521	0.000080305	0.425839009	0.01123445	0.000919161	0.41895973	0.120904163	0.97432651	-0.067108653	-0.133689898	-0.151368689	-0.065680335	-0.094260216	-0.027598811
EN1 P16152	6.8019062	0.00025052	0.478446832	0.09425576	0.00025052	0.87112575	0.044146792	0.781523216	0.052765515	0.113746042	0.146524044	0.069090526	0.093389809	-0.012863691	1.05637842	8.99E-08	0.320165016	1.26E-05	0.136E-06	0.11928875	0.002926945	0.982671487	0.12603377	0.350623223	0.37608732	0.24584887	0.250049495	0.025465674
FRP43 Q06009	1.2278808	0.303737953	0.305869641	0.946963174	0.956576169	0.609496186	0.384348193	0.984910011	-0.10645305	-0.032557078	-0.01240486	0.073967977	0.094138196	0.020170129	0.96825752	0.0355977	0.00523739	0.182009486	0.006212404	0.50657225	0.834646979	0.998434863	0.156113978	0.092124296	-0.039896983	0.037831518	0.1018122	
SFRP4 Q6FH17	7.99825752	0.03E-05	0.001381524	0.91831439	0.04109662	0.000382513	0.591919215	0.015698954	-0.259868618	0.01938329	-0.175901231	0.279186947	-0.019219519	-0.019219519	1.96825752	0.0355977	0.00523739	0.182009486	0.006212404	0.50657225	0.834646979	0.998434863	0.156113978	0.092124296	-0.039896983	0.037831518	0.1018122	
ATP1B1 P05026	0.2190279	0.883108126	0.927957569	0.982268968	0.999947083	0.851185444	0.958842121	0.987053826	0.011904243	-0.010005466	-0.00138276	-0.002190709	-0.001382751	0.00862219	0.71023493	0.010651545	0.166534382	0.922604452	0.17826946	0.450644783	0.999351026	0.478670205	0.03448316	0.471222261	-0.449317829	-0.504666707	-0.477361645	0.027304341
CDH4 P55283	7.10227343	0.000152787	0.00523739	0.182009486	0.006212404	0.50657225	0.834646979	0.998434863	0.156113978	0.092124296	-0.039896983	0.037831518	0.1018122	0.96825752	0.0355977	0.00523739	0.182009486	0.006212404	0.50657225	0.834646979	0.998434863	0.156113978	0.092124296	-0.039896983	0.037831518	0.1018122		
LRN1 Q6JUX5	4.96288236	0.00245964	0.140187874	0.081661103	0.000988585	0.99797003	0.411298616	0.497229843	0.05743617	0.06212561	0.097152487	0.004689191	0.039716317	0.039716317	1.67811205	0.17236549	0.298897902	0.252885155	0.223503739	0.99969366	0.99969366	0.99969366	0.119528502	0.122737003	0.124329681	0.030280501	0.004801179	0.005021792
PCDH9 Q92306	6.18545008	0.000497983	0.10088792	0.905575994	0.07160074	0.319086995	0.852987868	-0.041709051	-0.041709051	-0.041709051	-0.041709051	-0.041709051	-0.041709051	-0.041709051	1.05637842	8.99E-08	0.320165016	1.26E-05	0.136E-06	0.11928875	0.002926945	0.982671487	0.12603377	0.350623223	0.37608732	0.24584887	0.250049495	0.025465674
CD59 P13987	4.87231994	0.003421884	0.692085042	0.006653472	0.196929749	0.146870994	0.297983191	0.97189431	0.032465447	0.099856003	0.087057263	0.065519456	0.052810176	-0.01278074	0.71023493	0.010651545	0.166534382	0.922604452	0.17826946	0.450644783	0.999351026	0.478670205	0.03448316	0.471222261	-0.449317829	-0.504666707	-0.477361645	0.027304341
TMEM321 Q6IEE7	0.76531294	0.464852715	0.945241101	0.934857898	0.721924219	0.161366577	0.447153741	0.98290246	-0.223611685	0.024467141	-0.07305002	0.048079006	0.06961687	0.012882591	0.21099711	0.010651545	0.166534382	0.922604452	0.17826946	0.450644783	0.999351026	0.478670205	0.03448316	0.471222261	-0.449317829	-0.504666707	-0.477361645	0.027304341
CD200 P41217	2.61099711	0.000483493	0.882982264	0.001898844	0.012110556	0.023931408	0.103450269	0.013137432	0.043629627	0.021682433	0.175980815	0.168713974	0.132017488	-0.036702248	0.71023493	0.010651545	0.166534382	0.922604452	0.17826946	0.450644783	0.999351026	0.478670205	0.03448316	0.471222261	-0.449317829	-0.504666707	-0.477361645	0.027304341
TXNDC3 Q8N859	0.07740383	0.972146799	0.999937707	0.998190546	0.981590555	0.958857233	0.97296132	0.996303084	0.001560263	-0.00466731	-0.01030583	-0.006276994	-0.001596093	-0.001596093	1.05637842	8.99E-08	0.320165016	1.26E-05	0.136E-06	0.11928875	0.002926945	0.982671487	0.12603377	0.350623223	0.37608732	0.24584887	0.250049495	0.025465674
CD226A1 Q2U109	4.04947234	0.068364738	0.697530369	0.99927352	0.989049258	0.733688619	0.845877289	0.959129048	-0.102888352	-0.007185117	-0.02832527	0.095403235	-0.067481825	-0.01214141	1.67811205	0.17236549	0.298897902	0.252885155	0.223503739	0.99969366	0.99969366	0.99969366	0.119528502	0.122737003	0.124329681	0.030280501	0.004801179	0.005021792
CDH6 Q9DHP0	1.62179116	0.000141263	0.045793286	0.000141263	0.000141263	0.000141263	0.000141263	0.000141263	-0.136450621	-0.02048271	-0.058926194	-0.02515682	-0.030337274	-0.075804794	1.05637842	8.99E-08	0.320165016	1.26E-05	0.136E-06	0.11928875	0.002926945	0.982671487	0.12603377	0.350623223	0.37608732	0.24584887	0.250049495	0.025465674
SAAI P25542	1.04100995	0.232308426	0.20931948	0.649878117	0.39129515	0.83058735	0.962538467	0.978801862	-0.13490246	-0.076802873	-0.101914821	-0.056687372	0.031575424	-0.022113948	1.05637842	8.99E-08	0.320165016	1.26E-05	0.136E-06	0.11928875	0.002926945	0.982671487	0.12603377	0.				

Gene ID Uniprot ID	F-Value	Pr(F)	ANOVA p-values with Tukey Adjustment										Difference (AD - CT)																
			AD-Cau vs AD-AA	CT-AA vs AD-AA	CT-AA vs AD-AA	CT-AA vs AD-AA	CT-AA vs AD-AA	CT-AA vs AD-AA	CT-AA vs AD-AA	CT-AA vs AD-AA	CT-AA vs AD-AA	CT-AA vs AD-AA	CT-AA vs AD-AA	CT-AA vs AD-AA	CT-AA vs AD-AA	CT-AA vs AD-AA	CT-AA vs AD-AA	CT-AA vs AD-AA	CT-AA vs AD-AA	CT-AA vs AD-AA	CT-AA vs AD-AA								
AKL1 P00568	1.5486607	0.204057025	0.606784367	0.484752464	0.144988786	0.987495338	0.848044487	0.050460585	-0.09133875	-0.102383507	-0.149318452	-0.011044756	-0.057979702	-0.046934946	0.67629194	0.000236673	0.000769368	0.988817514	0.100943035	0.327211557	0.191466887	-0.27709065	-0.12990065	-0.19190065	0.255019001	0.116129902	-0.138890609		
DKD20 Q9H816	2.3210295	0.076712601	0.52245062	0.87769076	0.05907906	0.915999604	0.704127969	0.280182235	0.051072772	0.027194065	0.089826129	-0.023878707	0.038753356	0.062632064	1.19460038	0.1252054	0.535051164	0.23072795	0.878117467	0.98081529	0.913960228	0.703610679	-0.076793242	-0.040846795	-0.015126078	0.035928447	0.051454525		
DYK1 P01178	1.67390898	0.17280186	0.60712221	0.76310701	0.996371908	0.122588294	0.442607518	0.856283115	-0.05986812	0.043143558	0.009975328	0.09911678	0.056343358	-0.03378832	0.67823093	0.000589257	0.015139815	0.020393548	0.000378602	0.988023635	0.803673684	0.680240344	0.179729419	0.169430117	0.231487833	-0.010389102	0.051158413	0.062147515	
EPK311 Q06083	0.50860132	0.000589257	0.015139815	0.020393548	0.000378602	0.988023635	0.803673684	0.680240344	0.179729419	0.169430117	0.231487833	-0.010389102	0.051158413	0.062147515	0.59192778	0.000695297	0.015139815	0.020393548	0.000378602	0.988023635	0.803673684	0.680240344	0.179729419	0.169430117	0.231487833	-0.010389102	0.051158413	0.062147515	
ENK51 Q09479	5.9719278	0.000695297	0.015139815	0.020393548	0.000378602	0.988023635	0.803673684	0.680240344	0.179729419	0.169430117	0.231487833	-0.010389102	0.051158413	0.062147515	11.8840738	3.748707	0.000352039	0.997559415	9.23E-05	0.000565091	0.999457383	0.000511977	-0.268857044	-0.012128088	-0.276991411	0.256748807	-0.002734367	-0.263981734	
ENK1 P03950	1.18440738	0.000695297	0.015139815	0.020393548	0.000378602	0.988023635	0.803673684	0.680240344	0.179729419	0.169430117	0.231487833	-0.010389102	0.051158413	0.062147515	1.32620309	0.26887517	0.302510172	0.147545622	0.000565091	0.999457383	0.000511977	-0.268857044	-0.012128088	-0.276991411	0.256748807	-0.002734367	-0.263981734		
PLNR Q03405	1.32620309	0.26887517	0.302510172	0.147545622	0.000565091	0.999457383	0.000511977	-0.268857044	-0.012128088	-0.276991411	0.256748807	-0.002734367	-0.263981734	0.06964003	0.003847204	0.0053150814													
PLAG13 Q8NCX5	0.1252054	0.535051164	0.23072795	0.878117467	0.98081529	0.913960228	0.703610679	-0.076793242	-0.040846795	-0.015126078	0.035928447	0.051454525	0.056343358	-0.03378832	0.1252054	0.535051164	0.23072795	0.878117467	0.98081529	0.913960228	0.703610679	-0.076793242	-0.040846795	-0.015126078	0.035928447	0.051454525	0.056343358	-0.03378832	
SALT15 Q8N371	1.9460038	0.1252054	0.535051164	0.23072795	0.878117467	0.98081529	0.913960228	0.703610679	-0.076793242	-0.040846795	-0.015126078	0.035928447	0.051454525	0.056343358	1.9460038	0.1252054	0.535051164	0.23072795	0.878117467	0.98081529	0.913960228	0.703610679	-0.076793242	-0.040846795	-0.015126078	0.035928447	0.051454525	0.056343358	-0.03378832
UBEL31 P68036	1.066761	0.805909185	3.61E-06	1.45E-08	0.000244852	2.31E-06	0.74941217								1.066761	0.805909185	3.61E-06	1.45E-08	0.000244852	2.31E-06	0.74941217								
NPOC1 Q9NQX5	5.75895972	0.000870219	0.09779683	0.175793937	0.000301275	0.988136441	0.329838053	0.161180546	0.11066593	0.095338082	0.188813898	-0.015326849	0.078147968	0.093474817	5.75895972	0.000870219	0.09779683	0.175793937	0.000301275	0.988136441	0.329838053	0.161180546	0.11066593	0.095338082	0.188813898	-0.015326849	0.078147968	0.093474817	
UCLH1 P09936	9.0433007	4.56E-36	0.708965133	8.82E-14	1.10E-13	1.07E-13	0.999436016								9.0433007	4.56E-36	0.708965133	8.82E-14	1.10E-13	1.07E-13	0.999436016								
MAMD2 Q72304	1.1512983	9.22E-07	0.000203163	0.113617676	1.45E-06	0.161980426	0.810911788	0.014117874	-0.207567626	-0.107151244	-0.24939761	0.100416382	-0.041829534	-0.142245916	1.1512983	9.22E-07	0.000203163	0.113617676	1.45E-06	0.161980426	0.810911788	0.014117874	-0.207567626	-0.107151244	-0.24939761	0.100416382	-0.041829534	-0.142245916	
UBEN2 P16088	37.669246	4.91E-19	0.9647717	2.90E-11	2.97E-12	7.32E-12	0.085699874								37.669246	4.91E-19	0.9647717	2.90E-11	2.97E-12	7.32E-12	0.085699874								
RAD23 P54725	5.6581447	0.000991754	0.999999992	0.02721919	0.11739702	0.024875902	0.019214526	0.999999955	0.000128806	-0.130597701	-0.131673764	-0.10776507	-0.118102571	-0.001706063	5.6581447	0.000991754	0.999999992	0.02721919	0.11739702	0.024875902	0.019214526	0.999999955	0.000128806	-0.130597701	-0.131673764	-0.10776507	-0.118102571	-0.001706063	
INCS1 Q07070	14.8000332	1.12E-08	0.15865201	0.04334298	0.00056467	2.47E-05	3.46E-08	0.567841356	-0.12939373	-0.159051697	-0.23371134	-0.28839143	-0.363050867	-0.074659347	14.8000332	1.12E-08	0.15865201	0.04334298	0.00056467	2.47E-05	3.46E-08	0.567841356	-0.12939373	-0.159051697	-0.23371134	-0.28839143	-0.363050867	-0.074659347	
INCS2 Q07070	14.8000332	1.12E-08	0.15865201	0.04334298	0.00056467	2.47E-05	3.46E-08	0.567841356	-0.12939373	-0.159051697	-0.23371134	-0.28839143	-0.363050867	-0.074659347	14.8000332	1.12E-08	0.15865201	0.04334298	0.00056467	2.47E-05	3.46E-08	0.567841356	-0.12939373	-0.159051697	-0.23371134	-0.28839143	-0.363050867	-0.074659347	
INCS3 Q07070	14.8000332	1.12E-08	0.15865201	0.04334298	0.00056467	2.47E-05	3.46E-08	0.567841356	-0.12939373	-0.159051697	-0.23371134	-0.28839143	-0.363050867	-0.074659347	14.8000332	1.12E-08	0.15865201	0.04334298	0.00056467	2.47E-05	3.46E-08	0.567841356	-0.12939373	-0.159051697	-0.23371134	-0.28839143	-0.363050867	-0.074659347	
INCS4 Q07070	14.8000332	1.12E-08	0.15865201	0.04334298	0.00056467	2.47E-05	3.46E-08	0.567841356	-0.12939373	-0.159051697	-0.23371134	-0.28839143	-0.363050867	-0.074659347	14.8000332	1.12E-08	0.15865201	0.04334298	0.00056467	2.47E-05	3.46E-08	0.567841356	-0.12939373	-0.159051697	-0.23371134	-0.28839143	-0.363050867	-0.074659347	
INCS5 Q07070	14.8000332	1.12E-08	0.15865201	0.04334298	0.00056467	2.47E-05	3.46E-08	0.567841356	-0.12939373	-0.159051697	-0.23371134	-0.28839143	-0.363050867	-0.074659347	14.8000332	1.12E-08	0.15865201	0.04334298	0.00056467	2.47E-05	3.46E-08	0.567841356	-0.12939373	-0.159051697	-0.23371134	-0.28839143	-0.363050867	-0.074659347	
INCS6 Q07070	14.8000332	1.12E-08	0.15865201	0.04334298	0.00056467	2.47E-05	3.46E-08	0.567841356	-0.12939373	-0.159051697	-0.23371134	-0.28839143	-0.363050867	-0.074659347	14.8000332	1.12E-08	0.15865201	0.04334298	0.00056467	2.47E-05	3.46E-08	0.567841356	-0.12939373	-0.159051697	-0.23371134	-0.28839143	-0.363050867	-0.074659347	
INCS7 Q07070	14.8000332	1.12E-08	0.15865201	0.04334298	0.00056467	2.47E-05	3.46E-08	0.567841356	-0.12939373	-0.159051697	-0.23371134	-0.28839143	-0.363050867	-0.074659347	14.8000332	1.12E-08	0.15865201	0.04334298	0.00056467	2.47E-05	3.46E-08	0.567841356	-0.12939373	-0.159051697	-0.23371134	-0.28839143	-0.363050867	-0.074659347	
INCS8 Q07070	14.8000332	1.12E-08	0.15865201	0.04334298	0.00056467	2.47E-05	3.46E-08	0.567841356	-0.12939373	-0.159051697	-0.23371134	-0.28839143	-0.363050867	-0.074659347	14.8000332	1.12E-08	0.15865201	0.04334298	0.00056467	2.47E-05	3.46E-08	0.567841356	-0.12939373	-0.159051697	-0.23371134	-0.28839143	-0.363050867	-0.074659347	
INCS9 Q07070	14.8000332	1.12E-08	0.15865201	0.04334298	0.00056467	2.47E-05	3.46E-08	0.567841356	-0.12939373	-0.159051697	-0.23371134	-0.28839143	-0.363050867	-0.074659347	14.8000332	1.12E-08	0.15865201	0.04334298	0.00056467	2.47E-05	3.46E-08	0.567841356	-0.12939373	-0.159051697	-0.23371134	-0.28839143	-0.363050867	-0.074659347	
INCS10 Q07070	14.8000332	1.12E-08	0.15865201	0.04334298	0.00056467	2.47E-05	3.46E-08	0.567841356	-0.12939373	-0.159051697	-0.23371134	-0.28839143	-0.363050867	-0.074659347	14.8000332	1.12E-08	0.15865201	0.04334298	0.00056467	2.47E-05	3.46E-08	0.567841356	-0.12939373	-0.159051697	-0.23371134	-0.28839143	-0.363050867	-0.074659347	
INCS11 Q07070	14.8000332	1.12E-08	0.15865201	0.04334298	0.00056467	2.47E-05	3.46E-08	0.567841356	-0.12939373	-0.159051697	-0.23371134	-0.28839143	-0.363050867	-0.074659347	14.8000332	1.12E-08	0.15865201	0.04334298	0.00056467	2.47E-05	3.46E-08	0.567841356	-0.12939373	-0.159051697	-0.23371134	-0.28839143	-0.363050867	-0.074659347	
INCS12 Q07070	14.8000332	1.12E-08	0.15865201	0.04334298	0.00056467	2.47E-05	3.46E-08	0.567841356	-0.12939373	-0.159051697	-0.23371134	-0.28839143	-0.363050867	-0.074659347	14.8000332	1.12E-08	0.15865201												

Gene ID Uniprot ID	F-Value	Pr(-F)	ANOVA p-values with Tukey Adjustment								Difference (AD - CT)							
			AD-Cau vs AD-AA	CT-AA vs AD-AA	CT-AA vs AD-AA	CT-AA vs AD-AA	CT-AA vs AD-AA	CT-AA vs AD-AA	CT-AA vs AD-AA	CT-AA vs AD-AA	AD-Cau vs AD-AA	CT-AA vs AD-AA	CT-AA vs AD-AA	CT-AA vs AD-AA	CT-AA vs AD-AA	CT-AA vs AD-AA	CT-AA vs AD-AA	
ERR41 Q85256	2.17224037	0.09278126	0.109738492	0.99697169	0.62593935	0.15694287	0.64472818	0.746726219	-0.084604131	-0.007421702	-0.042470948	0.077182429	0.042133183	-0.035049247				
FAM1 P16930	0.28791119	0.834080002	0.844868534	0.955295853	0.988260458	0.999891010	0.999891010	0.999891010	-0.062695077	-0.038343287	-0.05775542	0.024351791	0.004939688	-0.019412333				
S101 Q04760	27.1817132	1.30E-14	0.48729584	2.46E-06	8.29E-08	2.10E-09	3.85E-11	0.939598072	0.059043334	-0.212157618	-0.234445751	-0.271200953	-0.293489086	-0.022288133				
FNVS-51 Q0404D38	1.1552668	0.328209514	0.879494091	0.607851075	0.658318147	0.259140626	0.79181745	0.835819889	-0.095825076	0.136888047	0.034939464	0.230705902	0.13076454	-0.099469953				
DLR1 P01330	7.1415995	0.000112301	0.230720153	0.037586804	0.791203469	4.59E-05	0.021818181	0.244110414	-0.088219559	0.121886116	0.040804297	0.210105675	0.19033856	-0.081081819				
BILL Q09173	6.94304148	0.000187585	0.003846231	0.99978956	0.02748079	0.002403863	0.852131602	0.018615481	-0.158271234	0.003735254	-0.122756629	0.162004757	0.035514965	-0.126489793				
ENP4 Q9Y6X5	1.9542655	0.112247526	0.86170334	0.511248649	0.808386064	0.116622771	0.289077445	0.951126051	0.052713872	-0.082663854	-0.052135238	-0.135377726	-0.10448911	0.030528616				
CD44 P16070	5.15874169	0.00191372	0.098994262	0.715124095	0.23378852	0.004638004	0.950312804	0.014929615	0.080754332	-0.03597457	0.062735991	-0.116728901	0.01799794	0.098730961				
MPI P34949	0.7328036	0.533655353	0.961244252	0.77483047	0.999387842	0.474503147	0.604208247	0.783691701	0.023282587	-0.044208315	-0.029705988	-0.067490902	-0.025788535	0.047263791				
CR1M1 Q9NZV1	1.18636026	0.318274753	0.997709738	0.999610544	0.400641365	0.999752648	0.520799652	0.486636391	-0.021974127	-0.011818655	-0.173178847	0.010155472	-0.15120472	-0.161360192				
PC11 Q152979	1.82562179	0.144050233	0.956244972	0.977116683	0.954941863	0.954941863	0.956244972	0.956244972	-0.06674197	0.007392353	0.01984259	0.037666551	0.086117487	0.012450936				
WSP1 P01676	5.8112527	0.00071149	0.005230149	0.92652619	0.01337901	0.03051872	0.967104629	0.071914068	-0.136952605	-0.03637374	-0.17100919	0.160578871	0.02593415	-0.134635456				
HNRNP2A2 P22626	1.6299951	0.185432982	0.165037779	0.970577305	0.680018323	0.35397887	0.703463866	0.91318155	-0.244020542	-0.051548794	-0.12371936	0.192655737	0.102433155	-0.072226202				
TRIL Q170X0	0.45216864	0.71609034	0.736403426	0.975615805	0.99994177	0.923234869	0.744487655	0.98151699	-0.05650542	-0.022386645	-0.002860611	0.034118775	0.035644809	0.019526034				
SV2P1 Q4LDE5	0.38089514	0.766900249	0.955306141	0.76287326	0.998158475	0.967941602	0.984055874	0.8375501	-0.046994666	-0.08026941	-0.051329076	-0.041032210	0.031665589	0.072697864				
EMPI P50788	1.26150068	0.28898674	0.479091926	0.303780433	0.804311459	0.993386668	0.999951978	0.995793911	0.044314491	0.052415584	0.045832306	0.002101093	0.001518013	-0.00658308				
LSR Q08629	2.61287468	0.05268917	0.804000961	0.039611759	0.293764539	0.309169271	0.85133767	0.71363727	0.031238559	0.090389254	0.088114752	0.05910694	0.026878913	-0.032271782				
F35A6 Q9U274	0.52868743	0.42735644	0.369428089	0.689032652	0.999574479	0.995740623	0.98850151	0.728536077	-0.019580788	0.087142539	0.080135259	0.067561751	-0.011370943	-0.078921864				
EMASE1 Q15041	1.06236614	0.3659588	0.996080004	0.508079964	0.540502416	0.64364164	0.689162356	0.999602933	0.013596662	0.143490905	0.133239233	0.112748974	0.11157957	-0.017017017				
LAMP2 P13473	1.56557236	0.199246697	0.914860085	0.625501617	0.92072822	0.253028703	0.9999541	0.232122975	0.029696066	-0.05357377	0.074900034	-0.083042843	-0.020028672	0.080847412				
FAM69C Q0P602	1.8324854	1.32E-10	0.00011084	0.997372527	6.52E-07	0.000170777	0.53230365	1.03E-07	0.224519995	0.092922320	0.290956622	-0.152197692	0.066466627	-0.28173432				
WSD1C1 Q6S8N2	3.25275167	0.022974761	0.0306387	0.96437636	0.914934735	0.0482835	0.116051472	0.917822311	-0.13743054	-0.010116782	-0.028925688	0.12362673	0.103913486	-0.019721786				
HRNR Q08Y23	0.89591477	0.450991325	0.959328069	0.446279587	0.618079293	0.618079293	0.618079293	0.618079293	-0.114896293	-0.685341703	-0.973270733	-0.570843056	-0.278272006	0.292570977				
DYLL1 Q06F12	13.7779908	3.78E-08	0.055979165	0.013225982	0.034389135	4.19E-07	1.55E-06	0.974689104	0.081061318	-0.094877017	-0.086257652	-0.175938353	-0.16371897	0.012129365				
F35A6 Q9U274	0.52868743	0.42735644	0.369428089	0.689032652	0.999574479	0.995740623	0.98850151	0.728536077	-0.019580788	0.087142539	0.080135259	0.067561751	-0.011370943	-0.078921864				
FN3 Q170X0	1.7037608	0.05104824	0.386960385	0.573880708	0.05985822	0.178591527	0.941386264	0.220346649	-0.03993611	0.052391295	0.12752499	0.252172436	0.072411748	0.01756869				
KAP12 Q02952	2.16379069	0.095620111	0.999257722	0.908300759	0.37021586	0.855124278	0.401035668	0.071733534	-0.015571189	0.08120699	-0.196784236	0.096778179	-0.181213137	-0.27991316				
MOXD1 Q0U6V6	1.53812489	0.001911174	0.570568302	0.065678045	0.92511357	0.001519167	0.055520037	0.551451793	-0.065574394	0.122559894	0.082961327	0.188137528	0.125406717	-0.062730575				
FHR3 Q02985	0.38552404	0.763556414	0.852432444	0.739563437	0.940249497	0.997601379	0.993087778	0.996360364	0.11552843	0.142254030	0.078145923	0.026279373	0.037382507	-0.06414068				
S10A9 P06702	0.02802674	0.99592476	0.999766132	0.999766132	0.998703194	0.998703194	0.998703194	0.998703194	0.023809326	-0.023644502	-0.049453829	-0.047453829	-0.073262589	-0.02580876				
PI01825	1.80669789	0.150885396	0.113775172	0.71554627	0.41687264	0.579992049	0.795721049	0.971361607	-0.444749976	-0.193919351	-0.270953001	0.250806204	0.173769795	-0.0737365				
CD171 Q086Q3	8.32882975	3.18E-05	0.172611177	0.016426057	0.00088586	0.00088586	0.985767932	0.916715105	-0.366386999	0.017925626	0.017925626	0.064903352	0.054594962	-0.688925131				
OSY782	2.14630215	0.051925654	0.432889629	0.54748606	0.05985822	0.99415846	0.98947808	0.240775516	-0.03993611	0.052391295	0.12752499	0.252172436	0.072411748	0.01756869				
INAGL1 Q0GZM7	1.20354254	0.10108064	0.53113954	0.995924973	0.442415099	0.64554199	0.99882806	0.58013615	-0.080419873	0.011864601	-0.084678638	0.06555272	-0.004258765	-0.072814036				
B3GAT3 Q04766	1.58129185	0.163343396	0.160935796	0.542703	0.25410371	0.853244907	0.90686429	0.90686429	-0.065514915	-0.04072258	-0.05139429	0.024791615	0.010347466	-0.04146849				
THB53 P49746	0.97811196	0.404580704	0.715243207	0.976299516	0.39662858	0.912315473	0.960088965	0.64504674	-0.077728959	-0.030274654	-0.119925205	0.047454305	-0.034223426	-0.081675551				
CRNHP1 P24837	2.7329371	0.045306323	0.64920205	0.45249636	0.897271463	0.047632915	0.951776822	0.110673322	-0.088225774	0.108682790	-0.059905693	0.196904884	0.038320082	-0.01768802				
JAM3 Q08677	1.29134586	0.278699048	0.914482701	0.580383038	0.986220557	0.222627279	0.740388657	0.761388032	-0.026068173	0.049521262	0.012976167	0.075589435	0.03900434	-0.036450959				
FN3 Q170X0	1.7037608	0.05104824	0.386960385	0.573880708	0.05985822	0.178591527	0.941386264	0.220346649	-0.03993611	0.052391295	0.12752499	0.252172436	0.072411748	0.01756869				
FA2 P01037	1.0914927	0.09171304	0.61758209	0.99798117	0.002516211	0.002516211	0.002516211	0.002516211	-0.03993611	0.052391295	0.12752499	0.252172436	0.072411748	0.01756869				
ILP2 Q087M5	16.2425342	2.10E-09	3.84E-05	0.367807442	1.75E-08	0.011543956	0.539175715	3.61E-05	0.375070249	0.127657358	0.492174746	-0.47412892	0.104144696	0.351557388				
C1orf73 Q08Y13	1.45182188	0.004793836	0.230131547	0.10166344	0.002102515	0.98643698	0.380015621	0.569251806	-0.089459042	0.015019065	0.050240756	0.090506894	0.019051656	0.027817793				
ADAM17 P78536	4.07944627	0.007007298	0.021892799	0.992728886	0.129675191	0.04058381	0.83300099	0.214094488	-0.127528547	-0.01177677	0.091718657	-0.11570807	0.03580899	-0.07994997				
SNAI2 P04899	0.42932477	0.732368278	0.722259433	0.858363231	0.812610654	0.994102064	0.99704294	0.210094041	-0.081893495	-0.061885844	-0.066619456	0.020007651	0.015251549	-0.004756101				
SDCP1 Q05560	1.04866524	0.986591432	0.988636574	0.993651513	0.986036953	0.99899548	0.999999068	0.999993162	0.036124663	0.062707372	0.032243035	-0.006841731	-0.001378157	0.005465374				
NIP004 Q15848	0.17989496	0.518765725	0.664714937	0.990200809	0.860036033	0.464240492	0.999950219											

Gene ID Uniprot ID	F-Value	Pr[F]	ANOVA p-values with Tukey Adjustment										Difference (AD - CT)																	
			AD-Cau vs AD-AA	CT-AA vs AD-AA	CT-AA vs AD-AA	CT-AA vs AD-AA	CT-AA vs AD-AA	CT-AA vs AD-AA	CT-AA vs AD-AA	CT-AA vs AD-AA	CT-AA vs AD-AA	CT-AA vs AD-AA	CT-AA vs AD-AA	CT-AA vs AD-AA	CT-AA vs AD-AA	CT-AA vs AD-AA	CT-AA vs AD-AA	CT-AA vs AD-AA	CT-AA vs AD-AA	CT-AA vs AD-AA	CT-AA vs AD-AA	CT-AA vs AD-AA								
DSTN P60881	4.14214603	0.0077141	0.040725571	0.06126664	0.00777964	0.993599739	0.967236884	0.874736987	-0.279645614	-0.252803094	-0.32675527	0.0268452	-0.047103913	-0.073952433	0.70322942	0.551704536	0.712739289	0.984037178	0.596041993	0.881924548	0.999793688	0.806701573	-0.2580299	-0.079019766	-0.1738224	0.171783224	0.018923481	-0.193076704		
BPGM P07378	1.388251	0.24700144	0.453962991	0.991089686	0.53675712	0.622398476	0.999733407	0.512943489	-0.08347587	-0.01656573	-0.09038492	0.068781914	-0.00503605	-0.078814915	5.23947404	0.00171571	0.007588948	0.967671012	0.053538688	0.017607169	0.836688373	0.10942626	-0.29511662	-0.02913002	-0.2218773	0.266017359	0.07236481	-0.192753998		
PCD P52209	5.62434104	0.00106367	0.043989312	0.27034711	0.00052049	0.805727259	0.12879662	-0.17634577	-0.13158597	-0.12879662	-0.13158597	-0.12879662	-0.13158597	-0.12879662	REL1 Q96294	4.87389493	0.002891658	0.336285945	0.066889171	0.00143746	0.880839492	0.216005001	0.617520172	0.070739596	0.01385052	0.149175494	0.030645456	0.078435888	-0.047790402	
CARP Q12201	9.75524081	5.24E-06	0.593815809	0.916288525	0.000913376	0.002192129	4.48E-06	0.007563351	0.083193185	-0.041825695	-0.243056301	-0.125018881	-0.021294486	-0.201230605	INPEP Q9U106	1.4703547	0.224066673	0.916633875	0.758201585	0.175065242	0.988977425	0.533027217	0.176370009	-0.036120582	-0.05337791	-0.10864761	-0.017417209	-0.072526879	-0.055206091	
DLR2 Q95897	0.1941598	0.90052869	0.975915739	0.98424261	0.96142593	0.990917723	0.91522185	0.90042357	-0.016366642	-0.013990533	-0.008319075	0.00237609	-0.024685717	0.02309608	ADIR Q115847	2.69742405	0.048293698	0.876646458	0.245228986	0.095055626	0.655156682	0.234667036	0.887535178	-0.059798876	-0.149354538	-0.204641398	-0.08955662	-0.144842522	-0.05258686	
PCRN1 Q00264	9.93013368	1.34E-05	0.25018837	0.032718477	0.440154666	4.49E-05	0.966768887	0.000118132	0.085774961	-0.138077894	0.07274347	-0.233852855	-0.02031469	-0.21082365	PSP3 P53041	9.4304282	7.88E-06	0.994077321	0.900790157	0.004982706	0.000347152	0.002314392	0.02314392	0.010837708	-0.16075291	-0.135551271	-0.170112999	-0.146388979	-0.16388979	-0.12542402
SLC8A2 Q9UPR5	0.9707268	0.405074802	0.940758331	0.847788209	0.894922222	0.99637667	0.57858526	0.38225621	0.047837674	0.0657381	-0.05454334	0.017889607	-0.10327018	-0.121126625	HPP Q9H008	2.67982819	0.048322251	0.941038198	0.043139032	0.17736806	0.787150661	0.69058068	-0.223648126	-0.107037846	-0.06397381	-0.08339721	-0.03728665	-0.041010505	-0.02728665	
CDKN1 Q12765	1.0541802	1.01E-07	0.995786023	0.00127664	2.94E-05	0.000559819	1.02E-05	0.834799093	0.01381501	-0.21133388	-0.28354179	-0.226319838	-0.27153568	-0.045213041	SRN2 Q9H251	0.23149037	0.057203552	0.96296504	0.629651021	0.500240505	0.900041811	0.239178328	0.04105807	-0.036869343	-0.089936133	0.102094102	-0.0520679	-0.138963445	-0.051786327	
FAM19A5 Q7Z5A7	1.1042609	0.348714051	0.321502166	0.625675909	0.509092441	0.947088177	0.977226949	0.998583564	0.066373412	0.045441565	0.051182406	-0.020931848	-0.015191006	0.005740842	PCRN2 Q00264	5.92150295	0.431551898	0.886932287	0.897715442	0.899523322	0.48454762	0.477154646	0.999996382	-0.018575645	0.017398541	0.016883234	0.035914186	0.035457979	-0.000516207	
PXD Q92626	1.1822624	0.31806529	0.98794591	0.92305522	0.302473937	0.991134018	0.496591741	0.668334363	-0.014421962	-0.027163782	-0.071466505	-0.012721586	-0.059704209	-0.046982623	DLK2 Q6U117	6.41576617	0.000370792	0.077995714	0.052254542	0.000118484	0.999702646	0.270501712	0.291637004	0.123317003	0.128020042	0.212457922	0.004703039	0.08914199	0.084437881	
PMPL1 Q5SGD2	0.4759608	0.719336222	0.995364622	0.999639101	0.735718698	0.999039146	0.876633721	0.78840205	0.017746607	0.007407113	0.012737604	-0.010335993	0.05439088	0.064726027	PTG1 P21579	4.83197148	0.002961176	0.168031532	0.773004006	0.488621101	0.014022157	0.002734722	0.970134389	0.091446009	0.041279214	-0.059721396	-0.132725223	-0.151167405	-0.018442182	
SYB1 Q31641	4.0152973	0.00854178	0.939082146	0.11311484	0.014925895	0.336696039	0.071933192	0.880162423	0.036569532	0.141450121	0.18623647	0.104808589	-0.07166825	-0.04786327	HSD17B2 A0A0B4J1Y9	4.11111083	0.007480913	0.069497425	0.99995742	0.05666222	0.066628145	0.999599584	0.062253922	-0.32082871	-0.00288039	-0.307821165	0.317940332	0.130072026	-0.304931276	
THY3 Q95490	3.94477251	0.02027566	0.56152379	0.01513866	0.11494708	0.94031386	0.82221378	0.61503891	-0.07831173	0.178896908	0.12856717	0.10585195	0.05025464	-0.05025464	PNXN1 Q92626	1.9827625	0.11658653	0.94814044	0.999970671	0.440589019	0.4058904	0.16372656	-0.031027803	-0.00240774	-0.13353521	0.028621059	-0.082307519	-0.119292778		
DR1 P01721	10.752921	1.51E-06	0.002828934	0.772606439	0.00922875	5.87E-05	0.978468007	0.000117625	-0.443587067	-0.11698643	-0.39548479	-0.056573498	-0.048697323	-0.512475175	SPINK5 Q9NQ38	0.0659064	0.977887936	0.99882657	0.995792693	0.996167913	0.98215871	0.982667448	0.999769921	0.011713123	-0.017853587	-0.06097361	-0.028612931	-0.039997999	-0.039997999	
ANGPT4 Q9B7Y6	4.23105423	0.00657400	0.873545278	0.518281158	0.06866096	0.142484157	0.007180222	0.681183188	0.04781139	-0.084611286	-0.15043724	-0.13242676	-0.198248634	-0.06825957	PTG2 P01619	4.9774563	0.002537955	0.02978591	0.999825982	0.039271325	0.995254623	0.04249512	-0.417395554	-0.011442375	-0.381112	-0.05953179	0.042848354	-0.07166825		
EA P00778	9.9105777	0.437257959	0.98198828	0.99842383	0.556717815	0.949470827	0.80170633	0.439107296	-0.04543283	0.018485393	-0.15109853	0.064276677	-0.105667427	-0.169943924	NAIP Q95490	5.9011628	0.00043162	0.00517397	0.015320783	0.000721304	0.58396613	0.98174952	0.313710639	-0.156646163	0.098429234	0.12856717	0.10585195	0.05025464	-0.05025464	
ALNTL16 Q9A28	1.4589985	0.27137898	0.217383263	0.982258908	0.857317815	0.29207528	0.24378992	0.999897091	-0.047884373	0.01655648	-0.008103521	0.047594921	-0.028020719	-0.119292778	TSO1 P43234	1.092475	0.353624411	0.959774053	0.506263123	0.995234603	0.81993203	0.876111623	0.31136968	-0.0216092	-0.058918599	0.00949112	-0.073111679	0.031456032	0.068677711	
PTG2 P25713	1.8924491	0.13237617	0.980182107	0.123003588	0.88752467	0.728906146	0.988897865	0.39537177	0.023034377	0.128117259	0.040624621	-0.01052882	-0.017590244	-0.02786238	MSDC2 Q14696	0.34441703	0.79320472	0.911472711	0.98224553	0.993738076	0.75986038	0.97346555	0.934106308	-0.030775127	0.014229642	-0.01157093	0.040040769	0.019218034	-0.02578673	
INT7 Q9U185	6.27382603	0.000045663	0.02263318	0.54154593	0.998180764	0.000198507	0.026639798	0.40660600	-0.112955447	0.05066388	-0.00672614	0.0162901835	-0.05079005	-0.05079005	KVP1 P15151	12.8719445	1.13E-07	2.18E-06	0.10261205	3.26E-06	0.01247997	0.984471868	0.022926566	0.248691358	0.10576337	0.23236884	-0.17427821	-0.01614474	0.126773347	
AVR Q9H292	5.9011628	0.00043162	0.00517397	0.015320783	0.000721304	0.58396613	0.98174952	0.313710639	-0.156646163	0.098429234	0.12856717	0.10585195	0.05025464	-0.05025464	PVR P15151	12.8719445	1.13E-07	2.18E-06	0.10261205	3.26E-06	0.01247997	0.984471868	0.022926566	0.248691358	0.10576337	0.23236884	-0.17427821	-0.01614474	0.126773347	
AVR Q9H292	5.9011628	0.00043162	0.00517397	0.015320783	0.000721304	0.58396613	0.98174952	0.313710639	-0.156646163	0.098429234	0.12856717	0.10585195	0.05025464	-0.05025464	AVR Q9H292	5.9011628	0.00043162	0.00517397	0.015320783	0.000721304	0.58396613	0.98174952	0.313710639	-0.156646163	0.098429234	0.12856717	0.10585195	0.05025464	-0.05025464	-0.05025464
EDN3 P14138	6.778331	0.000232008	0.053699506	0.042271519	0.727E-05	0.99996797	0.29004177	0.274902182	0.134473009	0.135521493	0.23005558	0.01061985	0.08942575	0.088358365	RAB14 P61106	0.2379423	0.869809895	0.999523528	0.987496942	0.86253002	0.916699124	0.917525023	-0.003725402	-0.010948605	-0.024793572	-0.007223023	-0.010268169	-0.013844677		
SLRX P35754	0.0485821	0.007745089	0.99495172	0.127561343	0.045454484	0.105025007	0.037177356	0.983615151	0.004803603	-0.077950959	-0.09079575	-0.082034562	-0.094881114	-0.012846556	GFRL1 Q9B7X7	3.0011937	0.029124327	0.029420364	0.615079769	0.015911202	0.439079308	0.283516721	-0.099710001	-0.08383022	-0.015826979	-0.015826979	-0.015826979	-0.119717823		
GHV6 A0A0B4J1U7	2.4985469	0.061061946	0.320199886	0.942027087	0.069947643	0.640391603	0.91609739	0.262528996	-0.31082695	-0.09996738	-0.424253173	0.210855115	-0.113400479	-0.324285594	RTN3 Q16799	20.8441737	1.93E-11	0.29550361	7.30E-05	2.87E-05	2.88E-08	7.86E-09	0.999387807	0.115576542	-0.28832049	-0.29573706	-0.403895591	-0.41131248	-0.007417657	
BSPON1 Q9BVN8	2.79932255	0.041396585	0.051188919	0.341482841	0.07860525	0.765792843																								

Gene ID Uniprot ID	F-Value	Pr(-F)	ANOVA p-values with Tukey Adjustment										Difference (AD - CT)									
			AD-Cau vs AD-AA	CT-AA vs AD-AA	CT-AA vs AD-AA	CT-AA vs AD-AA	CT-AA vs AD-AA	CT-AA vs AD-AA	CT-AA vs AD-AA	CT-AA vs AD-AA	CT-AA vs AD-AA	CT-AA vs AD-AA	CT-AA vs AD-AA	CT-AA vs AD-AA	CT-AA vs AD-AA	CT-AA vs AD-AA	CT-AA vs AD-AA	CT-AA vs AD-AA	CT-AA vs AD-AA	CT-AA vs AD-AA	CT-AA vs AD-AA	
SPR85 Q9Y653	3.68472922	0.01306487	0.70046985	0.15896397	0.74178352	0.00961525	0.15153884	0.65530326	0.065625408	-0.123468461	-0.05781677	-0.18909388	-0.12347175	0.06561693								
LRP2 P98164	3.6742385	0.00747275	0.80271974	0.88501106	0.33143100	0.99730850	0.86800983	0.75001936	0.083566099	0.06597424	0.10759186	-0.07159186	0.06851147	0.08703346								
SELM Q8WVW9	1.50420833	0.21493889	0.87651317	0.89829180	0.16961921	0.99981397	0.59590213	0.15840579	0.03512556	0.03145366	0.0995005	-0.0036769	0.05829073	0.05949674								
ST51 P98147	2.341315	0.07469528	0.15234185	0.51088137	0.07234454	0.96305642	0.99633905	0.7226235	-0.15065918	-0.09565781	-0.15560363	0.054700136	-0.14913744	-0.0696798								
ILCSA1 Q92911	0.67694917	0.56718849	0.98328257	0.88105049	0.93665064	0.98402745	0.77401595	0.22318779	-0.036258863	-0.07140284	-0.05514059	-0.09514392	-0.001399372	0.12654353								
FAM1942 Q8NH30	7.86445953	5.75E-05	0.000207159	0.064092013	0.000264431	0.258495346	0.924464028	0.35254896	0.375413236	0.215005365	0.351698448	-0.160487872	-0.02371478	0.136693084								
HST17H1E P10412	0.15105903	0.92887171	0.93368673	0.94783273	0.97641937	0.9990979	0.999320082	0.99923562	0.10255879	0.094138271	0.08434043	-0.111117608	-0.02091544	-0.009797839								
LAMP5 Q9J0J1	6.60546301	0.000290081	0.51998805	0.97736261	0.00058249	0.75527425	0.06266006	0.00211252	-0.070058806	-0.02019471	-0.193302809	0.04968305	-0.12324183	-0.17305518								
FCGR3A P08637	4.0323413	0.008614705	0.19510803	0.15390441	0.003908209	0.999912174	0.54261312	0.05891931	-0.11843232	-0.12029172	-0.11947992	-0.00365988	-0.07636589	-0.02760201								
CIGAL1 Q9NS00	3.4364128	0.01806915	0.94042628	0.07239621	0.882114817	0.01627432	0.55003874	0.27840326	-0.026178487	0.108939853	0.032077042	0.13511894	0.05825529	-0.07688217								
NME2 P22392	32.406712	6.99E-17	0.99999999	0.442E-08	1.19E-12	6.30E-38	7.15E-12	0.41128758	0.000134561	-0.26590602	-0.33109978	-0.26604063	-0.3312435	-0.06519372								
FAM121A1 Q5UVU5	1.0140077	0.37659315	0.99923682	0.980693753	0.59609853	0.95660234	0.6896237	0.341865219	0.004936042	-0.01433484	-0.01269525	-0.01269525	-0.004936042	0.059007208								
PSMA4 P25789	12.182303	3.14E-07	0.99973818	0.000247578	0.000124242	0.000168459	0.000145506	0.99999232	0.002985734	-0.29937533	-0.29848907	-0.30236267	-0.30147554	0.00087726								
NRG3 P56975	1.3649751	0.255135186	0.720916287	0.289377813	0.00016808	0.889961486	0.907690671	0.999915931	0.08404986	0.140574582	0.13589214	0.056529596	0.051834227	-0.004993638								
DLFML2B Q88818	19.8968162	3.19E-11	5.00E-08	0.885765041	8.23E-07	1.13E-06	0.824301014	1.79E-05	-0.301113597	-0.035243564	-0.259735363	0.265789033	0.04137824	-0.224410799								
LRTM2B Q8N967	1.95317801	6.94E-06	0.02547965	0.000166012	9.30E-06	0.52820533	0.211053631	0.938309809	0.198577688	0.29194837	0.092113669	0.131173629	0.000787032									
PFM3 P06753	9.26780516	1.16E-05	0.04589671	0.000168327	2.22E-05	0.37118787	0.17290575	0.97562036	-0.17360253	-0.288301305	-0.31524513	-0.108914052	-0.13589426	-0.029592008								
RT3 P91304	11.4346943	7.06E-07	0.55742005	9.95E-05	1.87E-06	0.14866195	0.00247857	0.975051326	-0.06352574	-0.07200545	-0.2330884	-0.14367991	-0.16605827	-0.02387956								
FEMAA1 Q9H551	3.01760401	0.00197576	0.813091789	0.932601619	0.97902227	0.94488896	0.881428948	0.81865219	-0.07697655	-0.05215428	-0.04963462	0.024824227	0.062013191	0.037188964								
BGNT8 Q1277M8	4.4313656	0.00503729	0.24460877	0.907522807	0.04853398	0.053890844	0.97065194	0.01151937	-0.118815	0.041551234	-0.14341082	0.10366324	-0.024926802	-0.185292116								
PLAG7 Q13093	0.5162495	0.65807347	0.970957482	0.99991497	0.68683902	0.97564927	0.924074628	0.70453444	-0.029773455	-0.003990023	-0.03717295	0.025783416	-0.04054384	-0.066372526								
GLA3 P17931	3.5176703	0.01196719	0.297315201	0.580168062	0.603732304	0.41087743	0.930802942	0.056076898	-0.078061611	0.05059226	-0.0525885	0.13315837	0.025805756	-0.107348115								
PSMA5 P28066	1.3705646	0.02836842	0.99999634	0.434375207	0.057491584	0.456349320	0.063119448	0.738749439	-0.008232621	-0.157456149	-0.25601216	-0.15363289	-0.252228003	-0.098595115								
MB P02144	3.31096237	0.021282704	0.38989658	0.99689483	0.07644145	0.270386012	0.878992929	0.939863845	-0.301369392	0.03815363	-0.4378454	0.33952275	-0.16449484	-0.476007703								
HSP121 P02578	0.8298383	0.49312039	0.849090766	0.90228371	0.549090497	0.90361204	0.94849075	0.916618909	-0.03252788	0.169969152	0.132275907	0.17446071	0.00715807	-0.03671494								
HST17HD1 P16402	0.33578122	0.79948101	0.993148728	0.974301895	0.984401174	0.840480677	0.96523828	0.91665665	-0.041299813	0.08371484	-0.05365565	0.124931317	0.060416574	0.12909751								
MERTK Q12866	8.1331963	4.08E-05	0.000184967	0.282734215	0.00044333	0.053473787	0.968520775	0.117567603	0.171866913	0.07062149	0.154211767	-0.10180475	-0.17655147	0.08416816								
HSPD1 P18099	2.29109949	0.081836416	0.0724607	0.400590622	0.16642484	0.821665369	0.986766769	0.955641941	-0.373136677	-0.243747021	-0.23896732	0.129389666	0.050255945	-0.097193171								
GHV1-18 A0A0C4DH31	2.5072133	0.062707245	0.21164072	0.89465563	0.983562775	0.042608353	0.37090737	0.701930976	-0.15842699	0.054713571	-0.02834078	0.21314362	0.130065612	-0.08307765								
NLG3N1 Q9N294	1.66352697	0.1732244	0.199920118	0.98655181	0.962299275	0.134377141	0.26656136	0.99226367	-0.1070003	-0.01858367	-0.02113661	0.098866709	0.006721065									
NSG1 P42857	0.52211511	0.667590176	0.931286765	0.999519203	0.92617072	0.95873866	0.604679414	0.879243255	-0.024441543	-0.040353775	-0.0238528	0.020087767	0.0482943	0.028206576								
HP2 P11117	0.83891816	0.77510239	0.803909765	0.90228371	0.00132226	0.00132226	0.33517324	0.975746581	0.950939569	-0.02527898	0.06969532	0.000973673	0.021125807	0.164688104								
F10047 P11511	0.84448623	0.47126017	0.674142516	0.976801384	0.999915283	0.10533218	0.86523867	0.965688223	-0.23435211	-0.03825211	-0.012025381	0.131640552	0.16440222	0.094151368								
LN2 P80188	0.09709535	0.961542965	0.975607885	0.99709339	0.99965807	0.956580886	0.98645281	0.99432006	0.042001626	-0.009160937	0.09386467	-0.051162563	-0.0236316	0.015240303								
CD74 P04233	2.58723253	0.05469342	0.803126682	0.40018894	0.597159303	0.96952156	0.135186326	0.986351287	-0.03746855	0.062959699	0.04921651	0.100428249	0.08667906	-0.013478189								
ARHGDB2 P52566	1.93671451	0.125262057	0.909844338	0.999997885	1.87810767	0.89416681	0.551570822	0.160061973	-0.038830881	0.001007198	-0.112915212	0.03988079	-0.07408349	-0.119224248								
PIR124 P02577	1.0582843	7.99E-10	4.01E-07	0.515190779	0.1845107	0.001295058	0.992236367	0.000162223	-0.737862406	-0.175739855	-0.702399024	0.052122191	0.035463004	-0.566958187								
EPB41L3 Q04391	2.1137378	0.02674316	0.96548488	0.994861303	0.126226678	0.995700274	0.340875015	0.203296979	-0.043693662	-0.022295554	-0.193329892	0.021398108	-0.14963623	-0.171034383								
PC2 P10471	0.36891816	0.77510239	0.803909765	0.90228371	0.00132226	0.00132226	0.33517324	0.975746581	0.950939569	-0.02527898	0.06969532	0.000973673	0.021125807	0.164688104								
FAM3A1 Q9H713	1.07255732	0.29293171	0.91742516	0.9996161	0.95632081	0.10533218	0.86523867	0.965688223	-0.11882875	-0.00838245	-0.05849059	0.11402011	0.02997276	0.091004715								
LN2 P80188	0.09709535	0.961542965	0.975607885	0.99709339	0.99965807	0.956580886	0.98645281	0.99432006	0.042001626	-0.009160937	0.09386467	-0.051162563	-0.0236316	0.015240303								
CD74 P04233	2.58723253	0.05469342	0.803126682	0.40018894	0.597159303	0.96952156	0.135186326	0.986351287	-0.03746855	0.062959699	0.04921651	0.100428249	0.08667906	-0.013478189								
ARHGDB2 P52566	1.93671451	0.125262057	0.909844338	0.999997885	1.87810767	0.89416681	0.551570822	0.160061973	-0.038830881	0.001007198	-0.112915212	0.03988079	-0.07408349	-0.119224248								
PIR124 P02577	1.0582843	7.99E-10	4.01E-07	0.515190779	0.1845107	0.001295058	0.992236367	0.000162223	-0.737862406	-0.175739855	-0.702399024	0.052122191	0.035463004	-0.566958187								
EPB41L3 Q04391	2.1137378	0.02674316	0.96548488	0.994861303	0.126226678	0.995700274	0.340875015	0.203296979	-0.043693662	-0.022295554	-0.193329892	0.021398108	-0.14963623	-0.171034383								
PC2 P10471	0.36891816	0.77510239	0.803909765	0.90228371	0.00132226	0.00132226	0.33517324	0.975746581	0.950939569	-0.02527898	0.06969532	0.000973673	0.021125807	0.164688104								
FAM3A1 Q9H713	1.07255732	0.29293171	0.91742516	0.9996161	0.95632081	0.10533218	0.86523867	0.965688223	-0.11882875	-0.00838245	-0.05849059	0.11402011	0.02997276	0.091004715								
LN2 P80188	0.09709535	0.961542965	0.975607885	0.99709339	0.99965807	0.956580886	0.98645281	0.99432006	0.042001626	-0.009160937	0.09386467	-0.051162563	-0.0236316	0.015240303								

Gene ID Uniprot ID	F-Value	Pr(F)	ANOVA p-values with Tukey Adjustment										Difference (AD - CT)									
			AD-Cau vs AD-AA	CT-AA vs AD-AA	CT-AA vs AD-AA	CT-AA vs AD-AA	CT-AA vs AD-AA	CT-AA vs AD-AA	CT-AA vs AD-AA	CT-AA vs AD-AA	CT-AA vs AD-AA	CT-AA vs AD-AA	CT-AA vs AD-AA	CT-AA vs AD-AA	CT-AA vs AD-AA	CT-AA vs AD-AA	CT-AA vs AD-AA	CT-AA vs AD-AA	CT-AA vs AD-AA	CT-AA vs AD-AA	CT-AA vs AD-AA	
UNC5D Q6UXZ4	4.46261564	0.00472354	0.028640884	0.123668883	0.003735019	0.912735019	0.95731919	0.618463096	0.170882118	0.131365394	0.20061129	-0.039516724	0.029729172	0.06925896								
HDHD1 Q9H9R4	10.3784168	2.004626	0.261564282	0.012320287	0.061725986	1.166E-05	0.000114994	0.910632584	0.086405649	-0.141727441	-0.112490574	-0.23813309	-0.198866237	0.029236867								
HEBP2 Q9Y524	7.94595374	0.5142E-05	0.038959596	0.37234329	0.17289878	0.000142549	0.866913598	0.00127682	0.156558124	-0.091068103	0.113371314	-0.247626227	-0.0432099	0.20405238								
NTSE1 Q15189	1.65555834	0.18132974	0.22597982	0.99966996	0.99071175	0.25820105	0.28709391	0.97380661	-0.2061874	-0.010215048	-0.02931184	0.196303675	0.17727339	0.0202638								
L1C1A2 A0304	3.38765615	0.0205674	0.1006804	0.95702378	0.99287281	0.025476704	0.041425332	0.99544806	0.112678714	-0.02408711	-0.016799811	-0.136765824	-0.125378255	0.011387299								
S10A08 P05109	0.02690248	0.994025736	0.9754881	0.997917148	0.99250193	0.999998724	0.99983879	0.99693079	0.045577878	0.041984447	0.063115607	-0.0035943	0.017637229	0.0213116								
EM6AC Q9H372	4.23542082	0.006358094	0.8734727	0.99976048	0.01766638	0.87287331	0.14263675	0.011487821	0.038753818	-0.00437736	-0.043101554	0.105718053	0.14882005	0.01876558								
PLXND1 Q9Y4D7	1.20810116	0.30839401	0.67660231	0.888319132	0.97381863	0.252357905	0.880033556	0.67351084	-0.049167179	0.030719967	-0.017804908	0.079887147	0.033162271	-0.048524876								
AOC3 Q16853	0.0302065	0.992904478	0.9999603	0.980393934	0.999534851	0.980484444	0.999867453	0.993116551	0.003719592	-0.01879582	0.011385903	-0.022515772	0.007665925	0.010279296								
EP35 P18533	2.33231246	0.07588335	0.250777189	0.662671403	0.060179806	0.875635104	0.951267919	0.53263558	-0.13475401	-0.008489647	-0.17202312	0.054264963	-0.07258802	-0.091522665								
FBXA1 Q9Y9R7	1.42510566	0.23680825	0.91819388	0.997931884	0.531347181	0.838388199	0.190938975	0.673878942	-0.00705777	0.008653959	0.061561567	0.039313173	0.092317337	0.052995607								
TBCA1 Q75347	13.7200604	6.95E-08	0.792811038	2.43E-05	6.13E-06	0.001317176	0.000463095	0.907251004	-0.0398337	-0.17070666	-0.1697785	-0.18172706	-0.14294313	-0.00687017								
SNAP25 P06880	2.57461408	0.051821129	0.99903909	0.07597656	0.58659214	0.0914727	0.6685444	0.56091273	-0.010197496	-0.18530802	-0.90079444	-0.17511056	-0.08059698	0.094513598								
TMED4 Q727H5	2.15931997	0.09431123	0.328353962	0.89915475	0.94695024	0.078830468	0.209767638	0.59216886	0.063991037	-0.02548092	-0.06093934	-0.089471529	-0.07089491	0.018576558								
LOL2A P05997	1.8421879	0.14282319	0.595588508	0.716405073	0.049495344	0.996153404	0.73379486	0.476496654	0.07094627	0.058655073	0.126600086	-0.012291024	0.055653809	0.067945011								
CMC1 Q5UC4	7.07701403	7.03E-05	0.00703244	0.071836478	0.31465304	0.805453297	0.60584882	0.121434988	0.155093293	0.11301907	0.211474872	-0.04207423	0.05381579	0.09845802								
L1C1A23 Q9H29	7.027725	0.10563161	0.626064984	0.236314526	0.08782143	0.92420568	0.70472798	0.96797451	0.069672346	0.105070581	0.129571015	0.03539825	0.09898669	0.024500434								
PEAS15 Q15121	5.65510504	2.42E-25	0.75323773	1.32E-13	2.09E-13	1.23E-13	1.23E-13	0.923618454	0.039503994	-0.33971316	-0.161848539	-0.379217155	-0.359912533	0.022364622								
FRP1 Q8N474	5.12637608	0.0019188	0.82359598	0.046932495	0.007821166	0.124822414	0.02806479	0.94234788	-0.020784055	-0.142199104	-0.171627543	-0.12145049	-0.15088489	-0.02473439								
ADM1 P35318	1.73799346	0.16045263	0.360015043	0.464971068	0.12767093	0.99610193	0.9655785	0.88625209	0.06034797	0.052276039	0.07705409	-0.008071958	0.016662553	0.0274351								
BDNF P23560	1.51024297	1.61E-07	0.088937839	1.72E-05	5.51E-07	0.08571302	0.014155291	0.321345974	0.173488137	0.35440758	0.380013094	0.17195262	0.21544956	0.043492336								
HLA-DRA P1903	2.77643565	0.04264632	0.097540596	0.987250005	0.18093458	0.182271716	0.97755131	0.31729222	0.196028459	0.027382246	0.163108709	-0.16864213	-0.032919751	0.135726462								
GPC4 Q9625	0.6549998	0.520860119	0.632749565	0.999263687	0.999595779	0.594098653	0.636027352	0.99782815	-0.07176289	0.007431805	0.013219482	0.019293013	0.098491568	0.010279296								
PCSK5 Q9H29	0.6134384	0.607675997	0.99762328	0.904741302	0.750806444	0.830967598	0.51596851	0.990830911	-0.014387275	0.05030495	0.117512788	0.06490707	0.08603002	0.021405299								
PEAS15 Q15121	5.65510504	2.42E-25	0.75323773	1.32E-13	2.09E-13	1.23E-13	1.23E-13	0.923618454	0.039503994	-0.33971316	-0.161848539	-0.379217155	-0.359912533	0.022364622								
FRP1 Q8N474	5.12637608	0.0019188	0.82359598	0.046932495	0.007821166	0.124822414	0.02806479	0.94234788	-0.020784055	-0.142199104	-0.171627543	-0.12145049	-0.15088489	-0.02473439								
ADM1 P35318	1.73799346	0.16045263	0.360015043	0.464971068	0.12767093	0.99610193	0.9655785	0.88625209	0.06034797	0.052276039	0.07705409	-0.008071958	0.016662553	0.0274351								
BDNF P23560	1.51024297	1.61E-07	0.088937839	1.72E-05	5.51E-07	0.08571302	0.014155291	0.321345974	0.173488137	0.35440758	0.380013094	0.17195262	0.21544956	0.043492336								
HLA-DRA P1903	2.77643565	0.04264632	0.097540596	0.987250005	0.18093458	0.182271716	0.97755131	0.31729222	0.196028459	0.027382246	0.163108709	-0.16864213	-0.032919751	0.135726462								
GPC4 Q9625	0.6549998	0.520860119	0.632749565	0.999263687	0.999595779	0.594098653	0.636027352	0.99782815	-0.07176289	0.007431805	0.013219482	0.019293013	0.098491568	0.010279296								
PCSK5 Q9H29	0.6134384	0.607675997	0.99762328	0.904741302	0.750806444	0.830967598	0.51596851	0.990830911	-0.014387275	0.05030495	0.117512788	0.06490707	0.08603002	0.021405299								
PEAS15 Q15121	5.65510504	2.42E-25	0.75323773	1.32E-13	2.09E-13	1.23E-13	1.23E-13	0.923618454	0.039503994	-0.33971316	-0.161848539	-0.379217155	-0.359912533	0.022364622								
FRP1 Q8N474	5.12637608	0.0019188	0.82359598	0.046932495	0.007821166	0.124822414	0.02806479	0.94234788	-0.020784055	-0.142199104	-0.171627543	-0.12145049	-0.15088489	-0.02473439								
ADM1 P35318	1.73799346	0.16045263	0.360015043	0.464971068	0.12767093	0.99610193	0.9655785	0.88625209	0.06034797	0.052276039	0.07705409	-0.008071958	0.016662553	0.0274351								
BDNF P23560	1.51024297	1.61E-07	0.088937839	1.72E-05	5.51E-07	0.08571302	0.014155291	0.321345974	0.173488137	0.35440758	0.380013094	0.17195262	0.21544956	0.043492336								
HLA-DRA P1903	2.77643565	0.04264632	0.097540596	0.987250005	0.18093458	0.182271716	0.97755131	0.31729222	0.196028459	0.027382246	0.163108709	-0.16864213	-0.032919751	0.135726462								
GPC4 Q9625	0.6549998	0.520860119	0.632749565	0.999263687	0.999595779	0.594098653	0.636027352	0.99782815	-0.07176289	0.007431805	0.013219482	0.019293013	0.098491568	0.010279296								
PCSK5 Q9H29	0.6134384	0.607675997	0.99762328	0.904741302	0.750806444	0.830967598	0.51596851	0.990830911	-0.014387275	0.05030495	0.117512788	0.06490707	0.08603002	0.021405299								
PEAS15 Q15121	5.65510504	2.42E-25	0.75323773	1.32E-13	2.09E-13	1.23E-13	1.23E-13	0.923618454	0.039503994	-0.33971316	-0.161848539	-0.379217155	-0.359912533	0.022364622								
FRP1 Q8N474	5.12637608	0.0019188	0.82359598	0.046932495	0.007821166	0.124822414	0.02806479	0.94234788	-0.020784055	-0.142199104	-0.171627543	-0.12145049	-0.15088489	-0.02473439								
ADM1 P35318	1.73799346	0.16045263	0.360015043	0.464971068	0.12767093	0.99610193	0.9655785	0.88625209	0.06034797	0.052276039	0.07705409	-0.008071958	0.016662553	0.0274351								
BDNF P23560	1.51024297	1.61E-07	0.088937839	1.72E-05	5.51E-07	0.08571302	0.014155291	0.321345974	0.173488137	0.35440758	0.380013094	0.17195262	0.21544956	0.043492336								
HLA-DRA P1903	2.77643565	0.04264632	0.097540596	0.987250005	0.18093458	0.182271716	0.97755131	0.31729222	0.196028459	0.027382246	0.163108709	-0.16864213	-0.032919751	0.135726462								
GPC4 Q9625	0.6549998	0.520860119	0.632749565	0.999263687	0.999595779	0.594098653	0.636027352	0.99782815	-0.07176289	0.007431805	0.013219482	0.019293013	0.098491568	0.010279296								
PCSK5 Q9H29	0.6134384	0.607675997	0.99762328	0.904741302	0.750806444	0.830967598	0.51596851	0.990830911	-0.014387275	0.05030495	0.117512788	0.06490707	0.08603002	0.021405299								
PEAS15 Q15121	5.65510504	2.42E-25	0.75323773	1.32E-13	2.09E-13	1.23E-13	1.23E-13	0.923618454	0.039503994	-0.33971316	-0.161848539	-0.379217155	-0.359912533	0.022364622								
FRP1 Q8N474	5.12637608	0.0019188	0.82359598	0.046932495	0.007821166	0.124822414	0.02806479	0.94234788	-0.020784055	-0.142199104	-0.171627543	-0.12145049	-0.15088489	-0.02473439								
ADM1 P35318	1.73799346	0.16045263	0.360015043	0.464971068	0.12767093	0.99610193	0.9655785	0.88625209	0.06034797	0.052276039	0.07705409	-0.008071958	0.016662553	0.0274								

Gene ID Uniprot ID	F-Value	Pr[F]	ANOVA p-values with Tukey Adjustment										Difference (AD - CT)																	
			AD-Cau vs AD-AA	CT-AA vs AD-AA	CT-AA vs AD-AA	CT-AA vs AD-AA	CT-AA vs AD-AA	CT-AA vs AD-AA	CT-AA vs AD-AA	CT-AA vs AD-AA	CT-AA vs AD-AA	CT-AA vs AD-AA	CT-AA vs AD-AA	CT-AA vs AD-AA	CT-AA vs AD-AA	CT-AA vs AD-AA	CT-AA vs AD-AA	CT-AA vs AD-AA	CT-AA vs AD-AA	CT-AA vs AD-AA	CT-AA vs AD-AA									
MPST P25235	1.03211084	0.380811342	0.78277663	0.996785813	0.588024022	0.659102069	0.989371885	0.447519618	-0.089879174	0.020075098	-0.119107809	0.109954272	-0.029217915	-0.13982187	0.26087364	0.049969927	0.364739772	0.999913046	0.382866367	0.932047748	0.113770652	-0.105128913	-0.036986117	-0.142473566	0.101160797	-0.037344653	-0.13850545			
SQZTM1 Q13501	0.7835243	0.505102394	0.99790696	0.731566122	0.57424486	0.840144239	0.703435842	0.994600444	-0.011003238	-0.060630309	-0.07427482	-0.049600721	-0.063735582	-0.018673311	1.1262082	0.28964227	0.99914148	0.84296456	0.3716599	0.34381925	0.85522716	-0.008395759	0.07069414	0.16330781	0.075451173	0.141785339	0.06261367			
DNAB1 P25686	10.2370484	2.74E-06	0.3178927	0.04917087	0.01138716	0.11211848	1.46E-05	0.9668317	0.004324872	-0.13883153	-0.16220238	-0.23315605	-0.2569511	-0.023788705	MASP2 O00187	0.5988865	0.616624152	0.990017101	0.89047084	0.950521168	0.980055919	0.834249725	0.564596678	-0.04929482	-0.11041575	0.08063869	0.061120934	0.12997869	0.19109623	
IGK1V-54 A0A0758614	1.7544966	1.51E-06	0.000198553	0.94658007	0.00019441	0.001288139	0.996566178	0.001371225	-0.64794216	-0.083075074	-0.03724889	0.564411942	0.031269927	-0.53314921	GFV2 Q13361	1.52662666	0.20938106	0.564210816	0.998045326	0.448970393	0.440303438	0.999441626	0.32705058	-0.106551726	0.104085299	-0.114959787	0.11973705	-0.008944661	-0.128881086	
MLP18 A0A0758619	4.62272033	0.006302096	0.0045288	0.005800835	0.068303919	0.76325645	0.17116688	0.99809113	-0.694217527	-0.168508864	-0.163803825	0.129409903	0.208706661	-0.014602621	TIME059 Q9B544	0.60684215	0.578053224	0.991072905	0.744247885	0.611111178	0.900851909	0.813750022	0.998257925	0.014038484	0.046249568	0.053469112	0.032220884	0.039450628	0.007219745	
RANBP1 P43487	3.1832327	0.026315883	0.384865373	0.059828422	0.020093826	0.924532041	0.62261204	0.925198804	-0.18939986	-0.261656768	-0.32969774	-0.072406822	-0.140447438	-0.06840606	GLV4 A0A0758614	6.6246965	0.0001167	0.408673623	0.186238782	0.26570732	0.002085259	0.996243746	0.00563344	-0.385609524	0.49347536	-0.437476857	-0.80018406	-0.014837342	-0.932051393	
GAT4B Q9U053	1.76491841	0.155711008	0.946912532	0.878057301	0.137711511	0.997272915	0.37854237	0.469387437	0.032167345	0.042813662	0.12240757	0.010646018	0.9902432	0.07992415	FAM38 P58499	1.83355548	0.144916813	0.132918711	0.425179333	0.27779471	0.888514735	0.9532025	0.996564504	-0.33469032	-0.225193887	-0.143801794	0.109465146	0.076827455	-0.032637691	
PRND Q9U0Y0	1.52162356	0.210957386	0.99589278	0.433648626	0.981946025	0.372011833	0.993450994	0.201972373	0.010540152	-0.14954684	0.03958077	-0.159999692	0.025417926	0.185414918	IMMT1 Q9P052	0.53809291	0.001075726	0.304177074	0.338058886	0.199775956	0.999775956	0.990972074	0.998016639	-0.101989815	-0.09708067	0.004099145	-0.000499145	-0.016659617	-0.021568611	
CCDB3 Q76M96	1.0938265	0.354173008	0.72639412	0.39566748	0.385554499	0.962788743	0.96508725	0.99990281	-0.08118946	-0.11828563	-0.11713529	-0.037166617	-0.05010683	0.002150534	ANCY P23536	2.23273694	0.07721132	0.62849956	0.44917875	0.040256074	0.994528198	0.530306818	0.66997042	-0.120656956	-0.145446715	-0.32946072	-0.024789759	-0.12289116	-0.107499357	
GLV4 A0A0758614	6.6246965	0.0001167	0.408673623	0.186238782	0.26570732	0.002085259	0.996243746	0.00563344	-0.385609524	0.49347536	-0.437476857	-0.80018406	-0.014837342	-0.932051393	RN1P1 Q9H677	1.35838849	0.259755005	0.95938731	0.333353399	0.15772774	0.692361154	0.98162386	-0.012831498	-0.09035817	-0.071413029	-0.07474319	-0.018586821	0.018887498	0.018887498	0.018887498
CKX10L P02778	2.4727081	0.06624079	0.59516817	0.865746108	0.47975814	0.945622211	0.59731829	0.22040648	-0.1907162	-0.08571457	-0.3826004	0.08214563	-0.1918872	-0.024702583	PI017 H18	3.8158074	0.01002528	0.167730248	0.578250867	0.98438422	0.005154688	0.231826922	0.800710473	-0.345979458	0.28061196	-0.040034547	0.554040654	0.305935912	-0.248104743	-0.08252146
PDZ7 O75084	7.00525565	0.000193551	0.00025148	0.189361912	0.002968192	0.099575061	0.840521515	0.10112695	-0.248714567	-0.114689873	-0.20048019	0.134024664	0.047766548	-0.082652146	FRS2 Q07478	0.56309291	0.001075726	0.003237426	0.980168107	0.07270721	0.090189543	0.59329387	0.161010843	-0.249071406	-0.026648415	-0.163803825	0.224222991	0.004899145	-0.013791963	
PROX1 P30044	2.33579493	0.076435938	0.734783207	0.19000564	0.040200603	0.999959956	0.486635459	0.426819389	-0.093712395	-0.091674594	-0.119501835	0.002037801	-0.12578944	-0.178727241	PRDM5 P58584	1.48812871	0.219521015	0.828307066	0.418501495	0.193519172	0.91619769	0.699758401	0.971998081	0.037073009	0.064728079	0.08425287	0.027655071	0.045830078	0.017252008	0.017252008
EXM1 Q90565	3.33167828	0.259755005	0.02561509	0.552397494	0.064861704	0.800202913	0.96861953	0.308207205	0.123467341	0.300284023	-0.272153948	0.123467341	0.300284023	-0.170202864	TLN1 Q9BWA0	1.13512684	0.33668196	0.778209945	0.821875158	0.99644414	0.261386146	0.65801281	0.88118373	0.085271462	-0.07538139	-0.01395145	-0.160649601	-0.099221918	0.061426388	0.061426388
IGLV10-54 A0A0758614	0.3026096	0.823480278	0.841699082	0.853789385	0.969932429	0.99983925	0.975824399	0.98076783	-0.27882795	-0.266870089	-0.14380194	0.011957706	0.13502585	-0.12306815	CRSP1D1 Q9H336	0.90351222	0.44054701	0.775472748	0.99943519	0.630699785	0.696959086	0.997604268	0.54066111	0.040687608	-0.004826152	0.048436622	-0.04553176	0.007704014	0.053262774	0.053262774
IRMT1 Q16891	0.23584957	0.871202764	0.89561095	0.888196973	0.9253213	0.999999997	0.999130899	0.9990885209	-0.167992765	-0.167503829	-0.167503829	0.004088935	0.007704014	0.032018093	LPRT1 Q96911	1.68252964	0.14066775	0.10012678	0.463532823	0.403079336	0.814540546	0.842909995	0.999841485	0.248674988	0.15327301	0.163129973	-0.09347687	-0.085545015	0.007802673	0.007802673
FAM21 P14851	28.771707	9.82E-15	0.8394963	5.51E-08	9.68E-09	9.25E-09	5.09E-10	0.98014102	0.00428923	-0.032358	0.345311818	-0.37893214	-0.38558181	-0.02858243	PRP21 Q99946	1.6202412	0.188696887	0.94066374	0.27388008	0.223048421	0.17996853	0.41224594	-0.021870252	-0.00219687	-0.04466659	0.052009941	-0.112396717	0.012396717	0.012396717	
RARE51 P49788	4.79951482	0.00354139	0.01921732	0.94779466	0.700821407	0.003298789	0.246677924	0.360443727	-0.449622635	0.079560021	-0.162675328	0.52918266	0.286990097	-0.242325599	MTF3 Q9H2K0	0.53463737	0.65909449	0.95344657	0.99197692	0.80898431	0.97854825	0.611202273	0.833797704	0.024048422	0.00589364	-0.00576307	-0.018154782	-0.054624729	0.026469447	0.026469447
HST13A P68431	0.24369567	0.865744208	0.99873682	0.970223598	0.98167882	0.990670595	0.98107244	0.99670595	-0.01018968	0.062763413	-0.051777096	0.072953093	0.041587416	-0.114540509	ARL8B Q9NV12	1.1279138	0.30151024	0.708233679	0.276299902	0.433848716	0.910511843	0.98366421	0.987903621	0.068848472	0.13827556	0.052390688	0.028171893	-0.024218706	0.024218706	
MANF P55145	0.89740765	0.44443821	0.541798983	0.848018377	0.040200603	0.999959956	0.486635459	0.426819389	-0.093712395	-0.091674594	-0.119501835	0.002037801	-0.12578944	-0.178727241	SUNO1 P15907	0.48721274	0.420059105	0.786023388	0.841495485	0.193519172	0.91619769	0.699758401	0.971998081	0.037073009	0.064728079	0.08425287	0.027655071	0.045830078	0.017252008	0.017252008
CNPY1 Q9N129	0.95637923	0.41655004	0.58619432	0.906431622	0.406278404	0.953243989	0.997571511	0.81973041	-0.09720117	-0.092201752	-0.049620774	-0.110900519	0.047599344	-0.013680041	UBR4 Q51475	0.9299276	0.428823292	0.52421611	0.99927715	0.981563662	0.431684801	0.752121289	0.956189285	-0.304624104	0.027945007	-0.084311717	0.332581171	0.220330386	-0.112252755	-0.112252755
ARPP21 Q9UB10	0.00005402	4.83E-06	0.304194875	0.00765231	0.088902462	1.32E-05	0.000454997	0.004588519	0.11992723	-0.21448531	-0.15809519	-0.3341254	-0.275736749	0.058679791	MYK1 Q9H1E5	1.7667484	0.154310326	0.572907406	0.786358283	0.924791137	0.896388218	0.394490686	-0.133173156	0.093824612	-0.06190493	0.226997768	-0.018721072	-0.157260666	0.018721072	0.018721072
TMX4 Q15746	1.4650176	0.28543119	0.96163247	0.580997279	0.66447364	0.306739658	0.367826587	0.997896968	0.04657044	-0.109640401	-0.09509449	-0.153261064	-0.13721203	-0.014909299	DNAB1B Q9UB54	2.4204776	0.069237458	0.046135503	0.587378419	0.285970056	0.465105778	0.71987105	0.999169768	0.124661383	0.09519427	-0.082919456	-0.082919456	-0.057676108	0.025423448	0.025423448
VEGFA P15692	4.7671619	0.003409204	1.50551752	0.489954885	0.001811329	0.866450492	0.51531708	0.10591819	0.095213609	0.05164842	0.15380186	-0.0394867	0.05858977	0.05858977	CDR2 P27701	0.2526406	0.80071814	0.999791462	0.981266433	0.8629912739										

Gene ID Uniprot ID	F-Value	Pr[-F]	ANOVA p-values with Tukey Adjustment								Difference (AD - CT)							
			AD-Cau vs AD-AA	CT-AA vs AD-AA	CT-Cau vs AD-AA	CT-AA vs AD-Cau	CT-Cau vs AD-Cau	CT-Cau vs CT-AA	AD-Cau vs AD-AA	CT-AA vs AD-AA	CT-Cau vs AD-AA	CT-AA vs AD-Cau	CT-Cau vs AD-Cau	CT-Cau vs CT-AA				
MMP16 P54152	3.9782697	0.00984643	0.131672162	0.47996704	0.005211538	0.866187099	0.65325579	0.210067069	0.149363694	0.097451726	0.226235733	-0.051911968	0.078872039	0.128784008				
UST1 Q9Y2C2	0.33151745	0.802827631	0.999471719	0.91739823	0.826153332	0.957896417	0.894229161	0.997029618	0.010560341	0.057422192	0.075184813	0.046861852	0.064624472	0.1776262				
MEPE Q9NQC6	2.92133445	0.035729415	0.067198117	0.314038455	0.04201736	0.863811024	0.999796275	0.807333563	0.292649525	0.201196469	0.302098489	-0.09452856	0.009449324	0.10909218				
PIA1P Q8R978	8.0007878	4.83E-05	0.00360414	0.009045108	6.80E-05	0.99268072	0.83144105	0.973414502	0.250276286	0.26904821	0.30914476	0.019617535	0.05886809	0.030240555				
FZD3 Q9NPG1	1.4907748	0.333161262	0.546465447	0.845209914	0.991321448	0.951176991	0.347513761	0.663194607	0.11522357	0.06985492	-0.024234649	-0.045838078	-0.19958219	-0.094120141				
HS3T1 O14792	0.6589858	0.579115693	0.591058998	0.741275997	0.665928354	0.993374319	0.997765093	0.999716739	-0.0997741	-0.078883143	-0.085756183	0.02080957	0.014017917	-0.00687304				
ATP6B1 P36543	5.5842789	0.00131284	0.756772568	0.12164468	0.098187183	0.008032801	0.00532219	0.999990805	0.085639918	-0.191648312	-0.194054948	-0.27728823	-0.279694865	-0.00240636				
ATP1B3 P36549	1.2166344	0.306978126	0.915866089	0.36096338	0.041693383	0.75876937	0.801591174	0.99975736	-0.041948069	-0.103476162	-0.098183018	-0.061528602	-0.056232449	0.005296353				
COLEC1 Q9BWP8	3.5226902	0.01705811	0.187145486	0.656720594	0.998851481	0.008792388	0.208996361	0.127932144	-0.228863681	0.127932144	-0.016015044	0.386795825	0.212848637	-0.143947188				
SDC2 P34741	1.94775003	0.125771276	0.479943286	0.988258727	0.392737465	0.28842651	0.99962565	0.216786925	-0.08295456	0.018133502	-0.088060179	0.100696958	-0.005496723	-0.1019358				
CC18 P55774	5.2807578	4.83E-05	0.166602549	0.930406133	0.037775576	0.03752361	0.936633051	0.005304488	-0.327891922	0.095644059	-0.17718016	0.412615981	-0.089736094	-0.511363075				
TSLJ Q9BUA8	1.2430663	0.29749655	0.440335087	0.655339403	0.274623925	0.981150784	0.994253203	0.91369362	-0.163036315	-0.122386352	-0.189901982	0.040649963	-0.026827871	-0.067528234				
PLEKH2 Q96C57	6.19359178	0.000494533	0.005652829	0.186794814	0.000534762	0.502898958	0.962942029	0.203589437	0.187531624	0.110176182	0.213637379	-0.077355441	0.026105755	0.103461196				
TGFBR1 P36897	5.55670769	0.001304531	0.756324041	0.339792443	0.009142879	0.158711961	0.002311785	0.40897278	0.027255558	-0.108207987	-0.206831748	-0.135463544	-0.234087306	-0.098623761				
ACVR1 Q04771	1.33114797	0.266129889	0.281925983	0.988961707	0.627560073	0.444607729	0.89376528	0.7137879	-0.099227471	-0.016987158	-0.061719287	0.082240313	0.037508184	-0.044732129				
PDXP Q96GD0	25.2026342	3.25E-13	0.889422056	2.43E-06	4.48E-08	7.13E-08	9.29E-10	0.871751992	0.059684652	-0.428883259	-0.48766105	-0.48857911	-0.54746357	-0.05778545				
BGLAP Q92B18	7.8490911	6.39E-05	0.018601417	0.637280112	0.099449574	0.000271796	0.861929184	0.00193887	0.289645491	0.111059597	0.216103153	-0.400795088	-0.073542388	0.327162749				
NNL Q9V216	0.30759835	0.81987881	0.992166881	0.97178741	0.972102273	0.88859646	0.999103483	0.804959124	0.034282491	-0.051495043	0.050047063	-0.08575734	0.015754572	0.101542106				
CKK1 P06307	1.85360527	0.139294826	0.091907115	0.538475471	0.661142481	0.726213982	0.561127792	0.995248601	0.165804772	0.093116538	0.077284382	-0.089520389	-0.058321555	-0.015782844				
IGLV4-69 A0A075B6H9	9.9383911	4.17E-06	0.03822886	0.852177374	0.001073131	0.002472763	0.795797892	2.80E-05	-0.446388795	0.127559653	-0.990177003	0.573948448	-0.143788208	-0.17376656				
PSMA3 P25788	10.5799165	2.31E-06	0.96905648	0.000248814	0.002824319	0.000137858	0.001606712	0.88127546	0.01532637	-0.305619515	-0.247508999	-0.320752152	-0.262641635	0.058110516				
MAPRE1 Q15691	6.81997356	0.000316184	0.85288332	0.012773286	0.000992901	0.108520979	0.015788808	0.902091849	-0.074656022	-0.287652698	-0.346588948	-0.211196676	-0.270129926	-0.05893325				
ITGA7 Q13683	0.7265194	0.537671258	0.999498938	0.604219054	0.990852804	0.576243006	0.985311158	0.571481537	-0.004116431	0.095138402	0.099254823	0.099254823	0.023262555	-0.077923179				
MGAT5B Q3V5L5	2.41738557	0.070187176	0.136601699	0.99999494	0.419032879	0.134514759	0.868740363	0.411264173	0.20221011	0.00111949	0.139315774	-0.201209062	-0.068652527	0.132902825				
NNP19 Q9NS42	1.82028926	0.145452892	0.688901434	0.992270739	0.309536382	0.511600363	0.94496261	0.178975867	0.08605826	-0.021360296	0.17885252	-0.107416122	0.041829426	0.14034548				
CKK1 P06307	1.85360527	0.139294826	0.091907115	0.538475471	0.661142481	0.726213982	0.561127792	0.995248601	0.165804772	0.093116538	0.077284382	-0.089520389	-0.058321555	-0.015782844				
IGLV4-69 A0A075B6H9	9.9383911	4.17E-06	0.03822886	0.852177374	0.001073131	0.002472763	0.795797892	2.80E-05	-0.446388795	0.127559653	-0.990177003	0.573948448	-0.143788208	-0.17376656				
PSMA3 P25788	10.5799165	2.31E-06	0.96905648	0.000248814	0.002824319	0.000137858	0.001606712	0.88127546	0.01532637	-0.305619515	-0.247508999	-0.320752152	-0.262641635	0.058110516				
MAPRE1 Q15691	6.81997356	0.000316184	0.85288332	0.012773286	0.000992901	0.108520979	0.015788808	0.902091849	-0.074656022	-0.287652698	-0.346588948	-0.211196676	-0.270129926	-0.05893325				
ITGA7 Q13683	0.7265194	0.537671258	0.999498938	0.604219054	0.990852804	0.576243006	0.985311158	0.571481537	-0.004116431	0.095138402	0.099254823	0.099254823	0.023262555	-0.077923179				
MGAT5B Q3V5L5	2.41738557	0.070187176	0.136601699	0.99999494	0.419032879	0.134514759	0.868740363	0.411264173	0.20221011	0.00111949	0.139315774	-0.201209062	-0.068652527	0.132902825				
NNP19 Q9NS42	1.82028926	0.145452892	0.688901434	0.992270739	0.309536382	0.511600363	0.94496261	0.178975867	0.08605826	-0.021360296	0.17885252	-0.107416122	0.041829426	0.14034548				
CKK1 P06307	1.85360527	0.139294826	0.091907115	0.538475471	0.661142481	0.726213982	0.561127792	0.995248601	0.165804772	0.093116538	0.077284382	-0.089520389	-0.058321555	-0.015782844				
IGLV4-69 A0A075B6H9	9.9383911	4.17E-06	0.03822886	0.852177374	0.001073131	0.002472763	0.795797892	2.80E-05	-0.446388795	0.127559653	-0.990177003	0.573948448	-0.143788208	-0.17376656				
PSMA3 P25788	10.5799165	2.31E-06	0.96905648	0.000248814	0.002824319	0.000137858	0.001606712	0.88127546	0.01532637	-0.305619515	-0.247508999	-0.320752152	-0.262641635	0.058110516				
MAPRE1 Q15691	6.81997356	0.000316184	0.85288332	0.012773286	0.000992901	0.108520979	0.015788808	0.902091849	-0.074656022	-0.287652698	-0.346588948	-0.211196676	-0.270129926	-0.05893325				
ITGA7 Q13683	0.7265194	0.537671258	0.999498938	0.604219054	0.990852804	0.576243006	0.985311158	0.571481537	-0.004116431	0.095138402	0.099254823	0.099254823	0.023262555	-0.077923179				
MGAT5B Q3V5L5	2.41738557	0.070187176	0.136601699	0.99999494	0.419032879	0.134514759	0.868740363	0.411264173	0.20221011	0.00111949	0.139315774	-0.201209062	-0.068652527	0.132902825				
NNP19 Q9NS42	1.82028926	0.145452892	0.688901434	0.992270739	0.309536382	0.511600363	0.94496261	0.178975867	0.08605826	-0.021360296	0.17885252	-0.107416122	0.041829426	0.14034548				
CKK1 P06307	1.85360527	0.139294826	0.091907115	0.538475471	0.661142481	0.726213982	0.561127792	0.995248601	0.165804772	0.093116538	0.077284382	-0.089520389	-0.058321555	-0.015782844				
IGLV4-69 A0A075B6H9	9.9383911	4.17E-06	0.03822886	0.852177374	0.001073131	0.002472763	0.795797892	2.80E-05	-0.446388795	0.127559653	-0.990177003	0.573948448	-0.143788208	-0.17376656				
PSMA3 P25788	10.5799165	2.31E-06	0.96905648	0.000248814	0.002824319	0.000137858	0.001606712	0.88127546	0.01532637	-0.305619515	-0.247508999	-0.320752152	-0.262641635	0.058110516				
MAPRE1 Q15691	6.81997356	0.000316184	0.85288332	0.012773286	0.000992901	0.108520979	0.015788808	0.902091849	-0.074656022	-0.287652698	-0.346588948	-0.211196676	-0.270129926	-0.05893325				
ITGA7 Q13683	0.7265194	0.537671258	0.999498938	0.604219054	0.990852804	0.576243006	0.985311158	0.571481537	-0.004116431	0.095138402	0.099254823	0.099254823	0.023262555	-0.077923179				
MGAT5B Q3V5L5	2.41738557	0.070187176	0.136601699	0.99999494	0.419032879	0.134514759	0.868740363	0.411264173	0.20221011	0.00111949	0.139315774	-0.201209062	-0.068652527	0.132902825				
NNP19 Q9NS42	1.82028926	0.145452892	0.688901434	0.992270739	0.309536382	0.511600363	0.94496261	0.178975867	0.08605826	-0.021360296	0.17885252	-0.107416122	0.041829426	0.14034548				
CKK1 P06307	1.85360527	0.139294826	0.091907115	0.538475471	0.661142481	0.726213982	0.561127792	0.995248601	0.165804772	0.093116538	0.077284382	-0.089520389	-0.058321555	-0.015782844				
IGLV4-69 A0A075B6H9	9.9383911	4.17E-06																

Table 6.4: SRM Peptide Coefficients of Variation

Gene	Protein Accession	Peptide	ATneg CV Total Area Ratio	ATpos CV Total Area Ratio	CV Total Area Ratio
AHSG	P02765	EHAVEGDCDFQLLK	9.40%	6.70%	22%
ALB	P02768	LVNEVTEFAK	3.80%	1.90%	21.50%
ALB	P02768	LVTDLTK	3.60%	2.50%	21.20%
ALDOA	P04075	VLAAYYK	7.30%	5.60%	16.10%
APOA4	P06727	SLAPYAQDTQEK	5%	3%	21.30%
APOC1	P02654	QSELSAK	8.60%	12.70%	28.80%
APOC2	P02655	TAAQNLYEK	3.50%	4.40%	16.10%
APOE	P02649	ELQAAQAR	4.60%	1.90%	13.30%
C9	P02748	TSNFNAISLK	10.50%	8.50%	18.50%
C9	P02748	LSPYINLVVVK	9%	6.70%	17.40%
CALM2	PODP24	EAFSLFDK	9.80%	5.20%	18.30%
CD44	P16070	TEAADLCK	20.10%	14.60%	13.20%
CD44	P16070	ALSIGFETCR	26.80%	13.80%	13.40%
CHI3L1	P36222	IASNTQSR	6.60%	5.40%	20.10%
CHI3L1	P36222	GNQWVGYDDQESVK	8.90%	7.10%	21.20%
CHI3L1	P36222	QLLSAALSAGK	6.50%	14.80%	23.40%
CP	P00450	EVGPTNADPVCLAK	10.30%	9.60%	12.70%
CP	P00450	GEFYGSK	4.50%	2.90%	13.10%
CST3	P01034	ASNDMYHSR	15.40%	9.40%	15.70%
DCN	P07585	VDAASLK	7.40%	7.20%	8.70%
DDAH1	O94760	EFFVLSK	14.10%	9.40%	18%
DKK3	Q9UBP4	DQDGEILLPR	5.50%	2.70%	12.50%
ENO1	P06733	IEEELGSK	11.70%	8.80%	21.20%
ENO1	P06733	LNVTQEKE	9.20%	8.50%	18.20%
ENO2	P09104	IEEELGDEAR	10.80%	9.90%	16.60%
F2	P00734	YTACETAR	16.50%	16%	18%
F2	P00734	TATSEYQTFNPR	7.10%	6.60%	18.20%
GAPDH	P04406	AAFNSGK	16.90%	14.70%	27.60%
GAPDH	P04406	YDNSLK	11.60%	8.70%	20.40%
GDA	Q9Y2T3	DHLLGVSDSGK	13.70%	12.30%	23.20%
GOT1	P17174	VGNLTVVGK	7.90%	7.90%	18.40%
GOT1	P17174	IGADFLAR	6.80%	8.50%	16.40%
GSN	P06396	AGALNSNDAFVLK	4.70%	3.80%	12.60%
HBA1	P69905	FLASVSTVLSK	5.50%	2.90%	97.40%
HBA1	P69905	VGAHAGEYGAELER	11.70%	10.10%	93.90%
HBB	P68871	VNVDEVGGEALGR	4.40%	2.90%	97.20%
KNG1	P01042	EGDCPVQSGK	11.80%	10.80%	17.80%
KNG1	P01042	QVVAGLNFR	10.40%	5.50%	20.60%
KNG1	P01042	VQVVAGK	5%	2.20%	20.90%
L1CAM	P32004	GQLSFNLR	9.10%	16.10%	13.40%
LAMP1	P11279	VWVQAFK	11.80%	12.70%	16.90%
LAMP2	P13473	YLDVFAVK	13.10%	12.80%	15.10%
LDHB	P07195	FIIPIQVK	7.30%	5.90%	17.50%
LDHC	P07864	VIGSGCNLDSAR	7.30%	8.80%	23.60%
MDH1	P40925	GEFVTTVQQR	7.20%	5.50%	20%
NCAM1	P13591	GLGEISAASEFK	5.90%	7%	15.50%
NPTX2	P47972	VAELEDEK	10.50%	15.30%	19.60%
NPTXR	O95502	ELDLVLQGR	4.70%	3.10%	13.80%
NRXN1	P58400	LAIGFSTVQK	11.50%	9%	15.40%
OGN	P20774	LEGNPIVLGK	6.20%	3.10%	8.60%
OMG	P23515	LESPLAHLPR	8.50%	6.10%	14.90%
PARK7	Q99497	ALVILAK	7.70%	4.90%	18%
PEBP1	P30086	GNDISSGTVLSDYVSGPPK	7.40%	7.40%	17.70%
PEBP1	P30086	LYEQLSGK	11.70%	8.20%	17.70%
PEBP1	P30086	VLTPQVK	5.60%	3.10%	14.20%
PGLYRP2	Q96PD5	TFTLLDPK	5%	3.10%	20.30%
PKM	P14618	VVEVGSK	3.50%	5.90%	20%
PKM	P14618	GVNLPGAAVDLPVSEK	5.50%	5.90%	21.40%
PKM	P14618	GDLGIEIPAEK	6.20%	5.80%	17.70%
PKM	P14618	GDYPLEAVR	5.30%	4.40%	18.60%
PKMisoform		LFEELVR	5.30%	4.40%	20.60%
PON1	P27169	LLIGTVFHK	7.70%	10%	22.10%
PPIA	P62937	VSFELFADK	6.60%	9.80%	18.70%
PRDX2	P32119	QITVNDLPVGR	15.10%	14.20%	32.10%
PTPRZ1	P23471	AIDGVESVSR	6.50%	3.70%	13%
PTPRZ1	P23471	DIEEGAVNPNR	5%	4.20%	12%
SCG2	P13521	IESQTQEEVR	8.10%	7.40%	19%
SCG2	P13521	SGQLGIQEEDLR	7.10%	6.90%	21.30%
SMOC1	Q9H4F8	AQALEQAK	13.30%	9.20%	27.20%
SOD1	P00441	AVCVLK	13.60%	9.60%	23.30%
SOD1	P00441	GDGPVQGIINFEQK	11.40%	11.10%	18.50%
SOD1	P00441	HVGDIGNVTADK	11.10%	7%	19.90%
SPP1	P10451	GDSVVYGLR	24.30%	13.80%	14.70%
SPP1	P10451	YPDVAVTWLNPDPSQK	9.60%	8.30%	15.30%
SPP1	P10451	QETLPSK	6.70%	7.10%	18.80%
THY1	P04216	HVLFGTGVGPEHTYR	11.40%	10%	17.90%
TP1	P60174	IAVAANQCYK	20.90%	24.50%	18.60%
VGf	O15240	EPVAGDAVPPGK	3.90%	2%	24.20%
VGf	O15240	GLQEAAEER	5.10%	5.40%	24.50%
VTN	P04004	GQCYELDEK	10.50%	5.60%	20.50%
VTN	P04004	DVWGIEGPIDAAFTR	8.70%	7%	20.80%
YWHAB	P31946	NLLSVAYK	8.30%	9%	26.70%
YWHAB	P31946	VISSIEQK	11.80%	6.40%	18.60%
YWHAG	P61981	YLAEVATGEK	17.10%	9.30%	29.50%
YWHAZ	P63104	VVSSIEQK	15.10%	14.10%	35.40%

TABLE 1. UNITS AND DIMENSIONS OF THE VARIABLES

Table with 10 columns: Variable Name, Unit, Dimension, and Value. Rows include variables like WIND, WIND2, WIND3, etc., with their respective units and dimensions.

TABLE 2. UNITS AND DIMENSIONS OF THE VARIABLES

Table with 10 columns: Variable Name, Unit, Dimension, and Value. Rows include variables like WIND, WIND2, WIND3, etc., with their respective units and dimensions.

Appendix Table 6.6: Correlation Values Between SRM and TMT-MS

Gene ID Protein ID Peptide Sequence	bicor	p
AHS6 P02765 EHAVEGDG[+57]DFQLLK	0.7623983	1.14E-35
ALB P02768 LVNEVTEFAK	0.77247034	3.87E-37
ALB P02768 LVTDLTK	0.77556186	1.33E-37
ALDOA P04075 VLAAVYK	0.71463278	1.37E-29
APOA4 P06727 SLAPYAQDTQEK	0.78931886	9.04E-40
APOC1 P02654 QSLSAK	0.81232011	8.85E-44
APOC2 P02655 TAAQNLVEK	0.84048111	1.63E-49
APOE P02649 ELQAAQAR	0.6667207	1.25E-24
C9 P02748 TSNFNAAISLK	0.77327779	2.93E-37
C9 P02748 LSPYINLVVVK	0.77415659	2.16E-37
CD44 P16070 TEADLC[+57]K	0.33081839	5.40E-06
CD44 P16070 ALSIGFETC[+57]R	0.31900572	1.20E-05
CHI3L1 P36222 IASNTQSR	0.71941149	3.84E-30
CHI3L1 P36222 GNQWVGYDDQESVK	0.72160382	2.13E-30
CHI3L1 P36222 QLLLSAALSAGK	0.71404577	1.59E-29
CP P00450 EVGPTNADPVC[+57]LAK	0.69862608	7.98E-28
CP P00450 GEFYIGSK	0.70157352	3.85E-28
CST3 P01034 ASNDM[+16]YHSR	0.71430865	1.49E-29
DCN P07585 VDAASLK	0.34992095	1.37E-06
DDAH1 O94760 EFFVGLSK	0.48536443	4.36E-12
DKK3 Q9UBP4 DQDGEILLPR	0.64903925	5.04E-23
ENO1 P06733 IEELGSK	0.41121196	8.90E-09
ENO1 P06733 LNVTEQEK	0.39346754	4.26E-08
ENO2 P09104 IEELGDEAR	0.47383191	1.61E-11
F2 P00734 YTAC[+57]ETAR	0.66718198	1.13E-24
F2 P00734 TATSEYQTFNPR	0.7185046	4.90E-30
GAPDH P04406 AAFNSGK	0.82854423	5.90E-47
GAPDH P04406 YDNSLK	0.8186034	5.68E-45
GDA Q9Y2T3 DHLLGVSDSGK	0.78616363	2.93E-39
GOT1 P17174 VGNLTVVVGK	0.76070551	1.97E-35
GOT1 P17174 IGADFLAR	0.71338808	1.89E-29
GSN P06396 AGALNSNDAFVVK	0.32361528	8.84E-06
HBA1 P69905 FLASVSTVLTSK	0.83492507	2.68E-48
HBA1 P69905 VGAHAGEYGAEALER	0.76278902	1.00E-35
HBB P68871 VNVDEVGGEALGR	0.80742692	6.99E-43
KNG1 P01042 EGDG[+57]PVQSGK	0.75355351	1.93E-34
KNG1 P01042 QVVAGLNFR	0.8176424	8.71E-45
KNG1 P01042 QVVVAGK	0.79004004	6.89E-40
L1CAM P32004 GQLSFNLR	0.41209368	8.22E-09
LAMP1 P11279 VVVQAFK	0.38645987	7.72E-08
LAMP2 P13473 YLDFVFAVK	0.26890252	0.00025192
LDHB P07195 FIIPQIVK	0.58318093	7.04E-18
MDH1 P40925 GEFVTVVQQR	0.71399458	1.62E-29
NCAM1 P13591 GLGEISAASEFK	0.76507851	4.70E-36
NPTX2 P47972 VAELEDEK	0.82254472	9.61E-46
NPTXR O95502 ELDVLQGR	0.86521236	1.48E-55
NRXN1 P58400 LAIGFSTVQK	0.50862443	2.67E-13
OGN P20774 LEGNPVILGK	0.2992511	4.27E-05
OMG P23515 LESLPAHLPR	0.70425667	1.97E-28
PARK7 Q99497 ALVILAK	0.68806487	1.01E-26
PEBP1 P30086 GNDISSGTVLSDYVSGPPK	0.61326383	4.43E-20
PEBP1 P30086 LYEQLSGK	0.5461355	1.84E-15
PEBP1 P30086 VLTPTQVK	0.62020993	1.27E-20
PGLYRP2 Q96PD5 TFFLLDPK	0.75042625	5.11E-34
PKM P14618 VVEVGSK	0.79626334	6.31E-41
PKM P14618 GVNLPGAAVDLPVSEK	0.81283689	7.09E-44
PKM P14618 GDLEIPEAK	0.7631657	8.84E-36
PKM P14618 GDYPLEAVR	0.74440429	3.20E-33
PON1 P27169 LLIGTVFHK	0.85372793	1.30E-52
PPIA P62937 VSFELFADK	0.42243149	3.15E-09
PRDX2 P32119 QITVNDLPVGR	0.5266618	2.63E-14
PTPRZ1 P23471 AIIDGVESVSR	0.59743528	6.82E-19
PTPRZ1 P23471 DIEEGAINPGR	0.55556383	4.76E-16
SCG2 P13521 IESQTQEEVR	0.83392878	4.38E-48
SCG2 P13521 SGQLGIQEEDLR	0.69455479	2.15E-27
SMOC1 Q9H4F8 AQALEQAK	0.60304712	2.63E-19
SOD1 P00441 AVC[+57]VLK	0.64804803	6.15E-23
SOD1 P00441 GDGVPVQGIINFEQK	0.52708324	2.49E-14
SOD1 P00441 HVGDLGNVTADK	0.60438204	2.09E-19
SPP1 P10451 GDSVVYGLR	0.40604161	1.42E-08
SPP1 P10451 YPDVAVATWLNPDPSQK	0.57766062	1.69E-17
SPP1 P10451 QETLPSK	0.53791195	5.78E-15
THY1 P04216 HVLFGTVGVPEHTYR	0.55672045	4.02E-16
TPI1 P60174 IAVAAQNC[+57]YK	0.36815258	3.42E-07
VGf O15240 EPVAGDAVPGPK	0.91564949	9.22E-73
VGf O15240 GLQEAEEER	0.89844556	6.87E-66
VTN P04004 GQYC[+57]YELDEK	0.73038636	1.88E-31
VTN P04004 DVWVGIEGPIDAAFTR	0.79647096	5.82E-41
YWHAB P31946 NLLSVAYK	0.45898158	8.12E-11
YWHAB P31946 VISSIEQK	0.41491193	6.35E-09
YWHAG P61981 YLAEVATGEK	0.6193641	1.48E-20
YWHAZ P63104 VVSSIEQK	0.61819486	1.83E-20

Appendix Table 6.7: SRM Culled Protein List

Gene ID Protein ID Peptide Sequence	Short Name
AHSG P02765 EHAVEGDC[+57]DFQLLK	AHSG
ALB P02768 LVTDLTK	ALB
ALDOA P04075 VLAADVYK	ALDOA
APOA4 P06727 SLAPYAQDTQEK	APOA4
APOC1 P02654 QSLSAK	APOC1
APOC2 P02655 TAAQNLYEK	APOC2
APOE P02649 ELQAAQAR	APOE
C9 P02748 LSPIYNLVPVK	C9
CALM2 P0DP24 EAFSLFDK	CALM2
CD44 P16070 TEADLC[+57]K	CD44
CHI3L1 P36222 GNQWVGYDDQESVK	CHI3L1
CP P00450 GEFYIGSK	CP
CST3 P01034 ASNDM[+16]YHSR	CST3
DCN P07585 VDAASLK	DCN
DDAH1 O94760 EFFVGLSK	DDAH1
DKK3 Q9UBP4 DQDGEILLPR	DKK3
ENO1 P06733 IEEELGSK	ENO1
ENO2 P09104 IEEELGDEAR	ENO2
F2 P00734 TATSEYQTFNPR	F2
GAPDH P04406 AAFNSGK	GAPDH
GDA Q9Y2T3 DHLLGVSDSGK	GDA
GOT1 P17174 VGNLTVVGK	GOT1
GSN P06396 AGALNSNDAFVLK	GSN
HBA1 P69905 FLASVSTVLTSK	HBA1
HBB P68871 VNVDEVGGEALGR	HBB
KNG1 P01042 QVVAGLNFR	KNG1
L1CAM P32004 GQLSFNLR	L1CAM
LAMP1 P11279 VWVQAFK	LAMP1
LAMP2 P13473 YLDFVFAVK	LAMP2
LDHB P07195 FIIPQIVK	LDHB
LDHC P07864 VIGSGC[+57]NLDSAR	LDHC
MDH1 P40925 GEFVTTVQQR	MDH1
NCAM1 P13591 GLGEISAASEFK	NCAM1
NPTX2 P47972 VAELEDEK	NPTX2
NPTXR O95502 ELDVLQGR	NPTXR
NRXN1 P58400 LAIGFSTVQK	NRXN1
OGN P20774 LEGNPIVLGK	OGN
OMG P23515 LESLPAHLPR	OMG
PARK7 Q99497 ALVILAK	PARK7
PEBP1 P30086 VLTPTQVK	PEBP1
PGLYRP2 Q96PD5 TFTLLDPK	PGLYRP2
PKM P14618 GVNLPGAADVLPVSEK	PKM
PKMisoform NA LFEELVR	PKMisoform
PON1 P27169 LLIGTVFHK	PON1
PPIA P62937 VSFELFADK	PPIA
PRDX2 P32119 QITVNDLPVGR	PRDX2
PTPRZ1 P23471 AIIDGVESVSR	PTPRZ1
SCG2 P13521 IESQTQEEVR	SCG2
SMOC1 Q9H4F8 AQALEQAK	SMOC1
SOD1 P00441 AVC[+57]VLK	SOD1
SPP1 P10451 YPDAVATWLNPDPSQK	SPP1
THY1 P04216 HVLFGTVGVPEHTYR	THY1
TPI1 P60174 IAVAAQNC[+57]YK	TPI1
VEGF O15240 EPVAGDAVPGPK	VEGF
VTN P04004 DVWGIIEGPIIDAFTR	VTN
YWHAB P31946 NLLSVAYK	YWHAB
YWHAG P61981 YLAEVATGEK	YWHAG
YWHAZ P63104 VVSSIEQK	YWHAZ

Appendix Table 6.8: SRM ANOVA Table

Gene ID Protein ID Peptide Sequence	F-value	Pr(>F)	ANOVA p-values with Tukey Adjustment												Difference (AD - CT)			
			AD-Cau vs AD-AA	CT-AA vs AD-AA	CT-Cau vs AD-AA	CT-AA vs AD-Cau	CT-Cau vs CT-AA	AD-Cau vs AD-AA	CT-AA vs AD-AA	CT-Cau vs AD-AA	CT-AA vs AD-Cau	CT-Cau vs CT-AA	AD-Cau vs AD-AA	CT-AA vs AD-AA	CT-Cau vs AD-AA	CT-AA vs AD-Cau		
AHSG P02765 ELHAEVGDGQ(+57)DFRLQLK	1.3392616	0.2628129	0.47406776	0.567944286	0.231890054	0.998878903	0.974327169	0.940159403	0.160646479	0.144026653	0.208064664	0.016619826	0.047417985	0.064037811				
ALB P02768 LVTDLTK	1.4734736	0.2231127	0.560749882	0.998833888	0.386011551	0.52910704	0.998360008	0.361006177	0.151464229	0.008969364	0.181759163	0.003294359	0.030294934	0.190728526				
ALDOA P04075 VLAAYVK	10.174229	3.01E-06	0.017180245	0.05510928	0.891608238	1.06E-06	0.001827786	0.25670715	0.254410371	0.218243155	0.060023526	0.472655262	0.314438988	0.158219629				
ALPOA P06727 SLAPVAGDQTEK	7.068182	0.0015173	0.001073693	0.682409995	0.001938129	0.043786257	0.99626835	0.06896345	0.487403173	0.142354234	0.459208662	0.345048939	0.028194511	0.316854428				
APOC1 P02654 QSELSAK	4.7228839	0.0033382	0.023895768	0.604700618	0.005179218	0.383820233	0.971300003	0.169970479	0.32883891	0.141953217	0.379702922	0.186885693	0.050864012	0.237497505				
APOC2 P02655 TAAQNLYEK	4.0879524	0.0076726	0.055725971	0.220193185	0.005539559	0.92884694	0.888475114	0.530546559	0.355718941	0.268897924	0.458573753	0.086821017	0.102854812	0.189675828				
APOE P02649 ELQAAQAR	5.4560957	0.0012788	0.015879176	0.99920335	0.022145615	0.026818767	0.998585772	0.036804745	0.25881093	0.010664937	0.245112456	0.248145993	0.013697474	0.234485159				
C9 P02748 LSPYKLVK	0.3538492	0.7864062	0.797378492	0.991450105	0.999989941	0.928382144	0.815237848	0.993873772	0.110681286	0.035160214	0.003615085	0.075521072	0.107066201	0.031545129				
CALM2 P00294 AFSKFLDK	9.8850152	4.33E-06	0.008035563	0.13775141	0.923610412	2.09E-06	0.001202972	0.416682532	0.265238542	0.177851995	0.050690164	0.443090538	0.315928707	0.127161831				
CD44 P16070 TEADLC(+57)K	3.6944437	0.012848	0.044301701	0.955066897	0.896731038	0.012139633	0.215171448	0.627379969	0.172513572	0.033772955	0.045092249	0.206286527	0.127421323	0.078865204				
CH1BL1 P36222 GNQVWVYDQGEVSK	16.294013	1.80E-09	0.035954989	0.000155743	0.631102228	4.93E-10	0.000842457	0.011343903	0.27185023	0.430802889	0.117652276	0.702653119	0.389052066	0.313150612				
CP P00450 GFYFISK	0.5886242	0.6231266	0.553090124	0.943543602	0.878079104	0.880110799	0.938062504	0.998145304	0.135882844	0.057830795	0.075799988	0.087052409	0.060091856	0.017961933				
CST3 P01304 ASNQMI(+16)YHSR	6.2114283	0.0004776	0.001854471	0.999845797	0.108796562	0.003097524	0.490328835	0.141738964	0.320772007	0.006611731	0.031160275	0.314160275	0.124853833	0.189306892				
DCN P07585 VDAASLK	0.8397242	0.4736246	0.641646728	0.999388245	0.628956628	0.727773387	0.999999999	0.71754541	0.056956566	0.005778465	0.057018131	0.051178095	0.16E-05	0.051239666				
DDAH1 Q94760 EFFVGLSK	8.7911555	1.73E-05	0.030486889	0.076283343	0.98156867	4.93E-06	0.01070231	0.176587153	0.198120554	0.172840243	0.026491617	0.370960797	0.224612171	0.146348626				
DK3 Q9UB94 DQDGLLPR	4.1153167	0.0074023	0.018359658	0.949230362	0.065689771	0.080780776	0.9572743976	0.233183281	0.276084605	0.050420226	0.228441757	0.22566345	0.047642847	0.178021497				
ENO1 P06733 IEEELGSK	17.030119	7.64E-10	0.794881612	3.32E-06	0.007575116	6.49E-08	2.48E-05	0.543841784	0.069798944	0.393604211	0.291935805	0.463403154	0.361374479	0.101668405				
ENO2 R09104 IIEELGDEAR	5.7356845	0.00089	0.53270156	0.040546901	0.570576895	0.000652094	0.048143582	0.503654161	0.097334969	0.192713168	0.091566684	0.290048154	0.188901574	0.101146484				
F2 P00734 IATSEVYQTFNPR	0.1261625	0.9445471	0.94197397	0.999671166	0.99956457	0.967708979	0.967778778	0.999999851	0.064195398	0.011052583	0.011900774	0.053142815	0.052294624	0.000848131				
GAPDH P04406 IAGVNSGK	16.541109	1.34E-10	0.586856703	1.65E-05	9.17E-05	6.66E-08	4.39E-07	0.96662968	0.165600701	0.597993413	0.540178962	0.054149114	0.696679663	0.007814451				
GDA Q9Y273 DHLGVSDDGK	14.390617	1.72E-08	0.00285772	0.012872102	0.884685982	4.63E-09	0.000207764	0.092110587	0.33830207	0.294112343	0.068828728	0.632414413	0.407133048	0.225284064				
GOT1 P17174 VGLNLYVSK	8.5114058	2.46E-05	0.042023181	0.07647602	0.024504692	8.45E-06	0.007251447	0.276858489	0.245745412	0.223849661	0.056715579	0.469595973	0.302461002	0.167134071				
GSN P06396 IAGLNSNDVFLVK	3.6466483	0.0136775	0.066301657	0.884672384	0.923938722	0.010244588	0.243378466	0.54948903	0.181281559	0.053412143	0.043753808	0.234693703	0.137527751	0.097169591				
HBA1 P69905 FLASVTVLTK	1.8404758	0.1412143	0.688251008	0.99826558	0.237292623	0.597738457	0.876431725	0.185494127	0.600484676	0.092247722	0.1010991307	0.692731896	0.410506631	1.103238527				
HBB P68873 VNVDEVGGALGR	2.32807	0.0759095	0.471441228	0.999654801	0.154502976	0.43019762	0.924425675	0.137614742	0.974579116	0.066439448	1.396414228	1.041018564	0.421835112	1.462853676				
KN1 P10142 QVVAFLNFR	0.5385811	0.6564215	0.82025454	0.99799112	0.877461765	0.73356444	0.999148893	0.799653101	0.113986756	0.023313687	0.096423811	0.137300043	0.017562945	0.11937498				
L1CAM P32004 IAGLFLNLR	0.093145	0.9637523	0.99912402	0.985270534	0.989071967	0.92183337	0.95469588	0.954191413	0.003282144	0.018388678	0.009084311	0.015106534	0.012366455	0.027472989				
LAMP1 P11279 VVVQAFK	5.3514801	0.0014662	0.132341239	0.234292876	0.978930909	0.000534827	0.253359955	0.125649981	0.158505253	0.137629474	0.023387568	0.296134728	0.135117268	0.161017044				
LAMP2 P13473 YLDFVAVK	2.3748601	0.0719499	0.345176041	0.841812692	0.709686236	0.072737613	0.928418795	0.24511595	0.138832849	0.068927313	0.08720352	0.051212497	0.05547665	0.161077625				
LDHB P07193 FHPQVVK	10.870453	1.26E-06	0.102383459	0.024141047	0.088077021	5.98E-06	4.59E-05	0.950273544	0.189724271	0.236247714	0.191794518	0.425971985	0.381518788	0.04453197				
LDHC P07864 VIGSGCI(+57)NLD SAR	26.440708	2.38E-14	0.313834644	2.04E-05	8.99E-08	7.92E-09	1.31E-11	0.728779159	0.182827987	0.182827987	0.507006002	0.617322054	0.689833989	0.800150051				
MDH1 P40925 GFVPTVQGR	17.570267	4.09E-10	0.052687709	0.000269633	0.022401823	2.28E-09	1.25E-06	0.550298699	0.207863584	0.336973685	0.229624758	0.544836219	0.437486342	1.103238527				
NCAM1 P13591 GIGESASSEFK	9.6567936	5.77E-06	0.000205891	0.999998366	0.004881501	0.000306986	0.800774727	0.000644913	0.369089176	0.001441961	0.289621508	0.367464214	0.079465667	0.288180547				
NPTX2 P47972 VAELEDEK	14.320392	1.87E-08	0.002246385	3.24E-05	1.89E-07	0.118761312	0.052388836	0.4364647	0.318446168	0.14332353	0.546955533	0.094877361	0.22809364	0.133632003				
NPTXR Q95502 ELDVQGR	11.374712	6.74E-07	0.002975649	0.00208332	1.77E-07	0.986983258	0.138725346	0.062639117	0.289343027	0.261256179	0.467467578	0.028086848	0.178124551	0.206211399				
NRXN1 P58400 IAGVNSGK	4.3790295	0.0052388	0.012728391	0.873131688	0.08559094	0.180801632	0.973889004	0.239546117	0.293541207	0.072319195	0.252659369	0.212222011	0.040881838	0.180401474				
OGN P20774 LEGNPLVSK	1.3252112	0.2674555	0.971176757	0.82314577	0.511753895	0.57672992	0.27948397	0.96033897	0.029861405	0.05847352	0.092052756	0.08834935	0.121914711	0.033579236				
OMG J126892 LESLPAHLPR	7.1426892	0.0001428	0.011393561	0.999947435	0.003007118	0.016066064	0.985147457	0.004577326	0.278102215	0.00470359	0.309589204	0.017486899	0.30485614	0.04453197				
PARK7 Q99497 ALVILAK	15.799007	3.26E-09	0.443539456	0.000865847	0.000183232	2.36E-06	3.21E-07	0.987579629	0.121302854	0.314064558	0.340988963	0.435367412	0.462291818	0.026294406				
PEPPI P30086 VLPTIQVK	8.8334042	1.64E-05	0.031720403	0.08560362	0.88176623	6.56E-06	0.00347763	0.358867809	0.213046555	0.183073685	0.05599928	0.396120241	0.26945835	0.127047046				
PGLYN2 Q96905 TFFLLQPK	6.5011868	0.0003278	0.000324031	0.049125468	0.00481251	0.443481747	0.858830524	0.886566143	0.495458115	0.312335988	0.400024045	0.185122127	0.09543407	0.087688057				
PKM1 P14613 GVNPLGAADVAVSEK	16.384755	1.62E-09	0.008241931	0.002054457	0.27625835	1.29E-09	9.04E-06	0.254091924	0.293431272	0.331099883	0.1614606	0.624531255	0.455071872	0.169459383				
PKM1inform NA LFEELVR	12.429408	1.84E-07	0.083047304	0.04053063	0.146173467	3.09E-07	8.00E-05	0.584663751	0.202033174	0.2877427	0.177769226	0.489775874	0.379802399	0.195937475				
POM1 P27169 LLIGVTFHK	0.0470855	0.9864194	0.995868664	0.989097202	0.987404468	0.999762047	0.999651238	0.999999578	0.03217628	0.046251968	0.047803852	0.01304339	0.014586224	0.00151884				
PP1A P62937 VSEFLADK	13.936988	2.96E-08	0.79909781	0.000348451	0.000302146	1.05E-05	0.96	0.999991365	0.068196327	0.302190515	0.300057591	0.370386842	0.368253918	0.002132924				
PRDX2 P32119 QIVNLDVPR	0.2401885	0.8682331	0.984968071	0.998642824	0.965715815	0.997463739	0.849693359	0.927358961	0.05207842	0.023039908	0.068252002	0.029038511	0.120337621	0.09129911				
PTPRZ1 P23471 AIDGVESVSR	9.1786459	1.06E-05	0.001394099	0.797703029	0.05013076	5.40E-05												

Appendix Table 6.9: ROC-AUC Analysis Table

Gene ID Protein ID Peptide Sequence	AUC			P Value		AUC 95% Confidence Interval (CI)			Accuracy		Sensitivity		Specificity						
	Cau AdvsCT	AA AdvsCT	AdvsCT	Cau AdvsCT	AdvsCT	Cau AdvsCT	AA AdvsCT	AdvsCT	Cau AdvsCT	AA AdvsCT	AdvsCT	Cau AdvsCT	AA AdvsCT	AdvsCT					
AHSG P02765 EHAVEGDCI+57IDFQLLK	51.74%	58.41%	45.95%	0.617745687	0.076453495	0.164828231	0.4-6.6349	0.4686-6.9995	0.3782-0.5408	0.567	0.622	0.518	0.681	0.902	0.98	0.46	0.319	0.052	
ALB P02768 LVTDLTK	49.15%	49.90%	48.70%	0.444029899	0.494526325	0.376979717	0.3751-0.6079	0.3811-0.6168	0.4052-0.5687	0.526	0.582	0.533	0.574	0.804	0.949	0.48	0.34	0.113	
ALDOA P04075 VLAAVVK	71.11%	66.37%	66.79%	0.000173953	0.002655286	2.57E-05	0.6652-0.817	0.555-0.7725	0.5924-0.7434	0.711	0.663	0.631	0.532	0.804	0.439	0.88	0.489	0.825	
APOA4 P06727 SLAPYADQTEK	55.02%	56.70%	47.75%	0.198127405	0.127605796	0.23996845	0.4332-0.6672	0.4505-0.6834	0.3961-0.5589	0.608	0.602	0.508	0.638	0.647	0.408	0.58	0.553	0.608	
APOCI P02654 QSELSAK	51.49%	57.82%	54.33%	0.601122951	0.091794971	0.148168722	0.3974-0.6323	0.4638-0.6926	0.4619-0.6248	0.577	0.582	0.559	0.532	0.667	0.469	0.62	0.489	0.649	
APOC2 P02655 TAAQLYK	53.36%	59.91%	57.68%	0.2854767	0.04561561	0.032059364	0.4171-0.6501	0.4846-0.7136	0.4964-0.6572	0.577	0.602	0.585	0.383	0.569	0.5	0.76	0.638	0.67	
APOE P02649 ELQAAQR	49.79%	48.52%	50.19%	0.487043435	0.60124933	0.482287941	0.3816-0.6141	0.3693-0.6011	0.4203-0.5835	0.526	0.551	0.533	0.617	0.961	0.827	0.44	0.106	0.237	
C9 P02748 LSPINLVVVK	58%	51.98%	52.54%	0.087954609	0.36910549	0.270814996	0.4633-0.6967	0.4035-0.6362	0.4438-0.6069	0.639	0.571	0.554	0.362	0.843	0.337	0.9	0.277	0.773	
CALM2 P00724 EAFSLFDK	71.45%	64.96%	66.26%	0.000139267	0.005451587	4.39E-05	0.6096-0.8193	0.5373-0.7619	0.5866-0.7387	0.722	0.673	0.636	0.596	0.725	0.745	0.84	0.617	0.526	
CD44 P16070 TEAADI+57YK	65.74%	48.02%	56.15%	0.003241311	0.36910549	0.068988853	0.5464-0.7685	0.3396-0.6008	0.4806-0.6424	0.649	0.592	0.574	0.468	0.902	0.896	0.82	0.255	0.247	
CH1L1 P36222 GNQWVGDDQSEVK	71.40%	75.80%	72.39%	0.000143218	5.55E-06	3.35E-08	0.6121-0.816	0.66-0.8561	0.6526-0.7951	0.68	0.735	0.692	0.511	0.627	0.714	0.84	0.851	0.67	
CP P00450 GEFYGVK	54.17%	51.69%	50.47%	0.240771868	0.388034514	0.545964324	0.4257-0.6577	0.3974-0.6364	0.4225-0.587	0.557	0.612	0.559	0.638	0.863	0.857	0.48	0.34	0.258	
CS73 P01034 ANSDM+16IYHSR	57.06%	50.73%	51.75%	0.116111384	0.550925694	0.37728335	0.4549-0.6864	0.3883-0.6263	0.4359-0.599	0.588	0.582	0.544	0.553	0.725	0.704	0.62	0.426	0.381	
DCN P07585 VDAASLK	49.02%	52.19%	49.42%	0.567350796	0.646827408	0.556005755	0.3726-0.6078	0.4035-0.6403	0.4125-0.5759	0.577	0.612	0.528	0.255	0.745	0.551	0.88	0.468	0.505	
DDA1 Q94760 EFPVGLSK	69.70%	63.41%	65.72%	0.000421113	0.011247466	7.52E-05	0.5899-0.8041	0.5222-0.7461	0.5803-0.7341	0.68	0.633	0.636	0.681	0.784	0.663	0.68	0.468	0.608	
DNAI3 Q9UB9P DDDGELLPR	54.47%	48.69%	49.72%	0.225262955	0.412762212	0.5278196	0.4274-0.6619	0.3687-0.605	0.4155-0.5788	0.598	0.571	0.528	0.383	0.745	0.602	0.8	0.383	0.454	
EN1 P06733 IEEELSK	75.96%	78.06%	76.38%	5.42E-06	8.82E-07	9.85E-11	0.6631-0.8561	0.6893-0.8718	0.6977-0.8299	0.732	0.735	0.708	0.532	0.725	0.684	0.92	0.745	0.732	
ENO2 P09104 IEEELGDEAR	64.98%	67.29%	65.20%	0.005585823	0.001619945	0.000132333	0.5379-0.7617	0.5631-0.7827	0.5748-0.7292	0.66	0.673	0.631	0.596	0.745	0.62	0.72	0.596	0.742	
F2 P00734 TATSEYQTFNPR	55.23%	51.23%	51.42%	0.188278068	0.418308379	0.366424179	0.436-0.6687	0.3946-0.63	0.4326-0.5958	0.588	0.561	0.544	0.553	0.804	0.816	0.62	0.298	0.268	
GADPH P04466 AAFNSGK	79.91%	77.14%	78.25%	1.98E-07	1.90E-06	4.79E-12	0.712-0.8863	0.6768-0.866	0.7187-0.8462	0.732	0.724	0.718	0.596	0.745	0.735	0.86	0.702	0.701	
GDA Q9Y273 DHLLGVSDSGK	73.23%	72.38%	69.82%	4.11E-05	6.90E-05	8.76E-07	0.629-0.8357	0.6199-0.8277	0.6244-0.772	0.701	0.724	0.677	0.723	0.784	0.816	0.68	0.66	0.536	
GOT1 P17174 VGNLTVGSK	70.34%	65.71%	66.05%	0.000283626	0.00375	5.41E-05	0.595-0.8118	0.5451-0.769	0.5842-0.7368	0.711	0.673	0.641	0.489	0.765	0.765	0.92	0.574	0.515	
HSN1 P06396 IAGLMSDFAPLAK	62.13%	51.98%	55.82%	0.020049005	0.36910549	0.080034512	0.5083-0.7343	0.4023-0.6373	0.4773-0.6391	0.619	0.582	0.559	0.745	0.941	0.622	0.5	0.191	0.495	
HBA1 P09905 FLASVSTLTSK	54.72%	50.06%	52.71%	0.212540245	0.505673075	0.256719262	0.4305-0.664	0.3836-0.6176	0.4455-0.6088	0.588	0.571	0.549	0.404	0.647	0.561	0.48	0.76	0.106	0.619
HBB P06871 VNVDEGEALGR	53.62%	50.06%	52.35%	0.270944614	0.505673075	0.286149571	0.4185-0.6539	0.3837-0.6175	0.4417-0.6052	0.588	0.551	0.549	0.404	0.647	0.561	0.76	0.447	0.536	
KNG1 P01042 QVAGLVNFR	51.02%	51.73%	50.04%	0.570187641	0.385123843	0.5045592828	0.3927-0.6277	0.3997-0.6349	0.4185-0.5823	0.577	0.571	0.538	0.66	0.902	0.643	0.5	0.213	0.433	
LICAM P32004 GQLSFLNLR	52.09%	49.94%	51.30%	0.363133858	0.497163091	0.623983822	0.4036-0.6381	0.3825-0.6163	0.4313-0.5948	0.577	0.541	0.549	0.362	0.51	0.5	0.78	0.574	0.598	
LAMP1 P11129 VVVQVAFK	62.38%	60.03%	59.57%	0.017998834	0.043941449	0.010494997	0.5107-0.737	0.4857-0.715	0.5162-0.6752	0.629	0.612	0.585	0.532	0.667	0.592	0.72	0.553	0.577	
LAMP2 P13473 YLDVFAVK	54.98%	54.03%	46.29%	0.200187322	0.247409382	0.185843017	0.4333-0.6663	0.4228-0.6577	0.3816-0.5443	0.577	0.592	0.516	0.596	0.843	1	0.56	0.319	0.031	
LDH1 P07195 HIPIQVK	75.19%	67.05%	70.85%	9.79E-06	0.001816098	2.47E-07	0.6531-0.8507	0.5608-0.7809	0.636-0.781	0.722	0.684	0.687	0.638	0.745	0.765	0.8	0.617	0.608	
LHC1 P07864 WSGGCI+57INDSAR	86.72%	73.51%	80.63%	2.39E-10	3.12E-05	7.40E-14	0.7952-0.9393	0.6319-0.8383	0.7445-0.8682	0.814	0.724	0.754	0.851	0.882	0.735	0.78	0.553	0.773	
MDH1 P04925 GEFVTVQQR	77.28%	76.39%	75.37%	1.89E-06	3.49E-06	4.68E-10	0.6777-0.8679	0.6669-0.8608	0.6863-0.8211	0.763	0.714	0.692	0.66	0.686	0.612	0.86	0.745	0.773	
NCAM1 P13529 GLGEISAASEFK	56.34%	52.23%	51.85%	0.141873896	0.649511282	0.328018842	0.4471-0.6797	0.4045-0.6402	0.437-0.6	0.588	0.582	0.533	0.596	0.804	0.541	0.58	0.34	0.526	
NPTX2 P47972 VAELEDEK	63.32%	76.28%	69.73%	0.012042705	3.79E-06	9.69E-07	0.5216-0.7448	0.6657-0.8599	0.6235-0.7712	0.629	0.765	0.672	0.617	0.765	0.531	0.64	0.766	0.814	
NPTXR Q95502 ELDVLDGR	61.62%	68.21%	65.19%	0.024590991	0.000966116	0.000124461	0.5029-0.7295	0.5747-0.7895	0.575-0.7288	0.619	0.663	0.626	0.745	0.863	0.714	0.5	0.447	0.536	
NRXN1 P58400 LANGFSTVQK	53.70%	51.98%	50.55%	0.266183941	0.36910549	0.448008873	0.4197-0.6543	0.4028-0.6369	0.4237-0.5872	0.588	0.571	0.538	0.447	0.784	0.49	0.72	0.34	0.588	
OGN P20774 LKGNPVLGK	60.34%	53.40%	56.76%	0.039400019	0.282306899	0.051491516	0.491-0.7166	0.4178-0.6502	0.487-0.6483	0.588	0.561	0.574	0.511	0.451	0.449	0.66	0.681	0.701	
OMG P23515 LSLPAHVR	50.34%	51.81%	50.79%	0.478412474	0.622817883	0.425019432	0.3862-0.6206	0.4005-0.6358	0.4261-0.5897	0.577	0.582	0.549	0.191	0.647	0.684	0.94	0.511	0.412	
PARK7 Q94997 ALVILAK	82.09%	69.96%	76.40%	2.68E-08	0.00038011	9.53E-11	0.7359-0.9058	0.5939-0.8054	0.6971-0.831	0.784	0.704	0.708	0.745	0.863	0.847	0.82	0.532	0.567	
PEBP1 P30086 VLPFTQVK	69.15%	66.92%	66.03%	0.00087891	0.01988311	5.52E-05	0.5834-0.7996	0.5584-0.7799	0.5841-0.7366	0.711	0.673	0.631	0.553	0.706	0.735	0.86	0.638	0.526	
PLG1YR2 Q96P05 TITLDDPK	57.02%	62.08%	53.65%	0.117528197	0.019933784	0.189602939	0.4546-0.6858	0.5091-0.7325	0.455-0.618	0.608	0.602	0.564	0.66	0.373	0.224	0.56	0.851	0.907	
PKM P14618 QVNFQAVDLPVNSK	75.49%	73.34%	72.24%	7.79E-06	3.52E-05	4.08E-08	0.6547-0.8551	0.6319-0.835	0.6515-0.7933	0.753	0.714	0.667	0.532	0.843	0.694	0.96	0.574	0.639	
PKMisoform NA LFEELVR	74.21%	72.38%	71.94%	2.03E-05	6.90E-05	6.03E-08	0.6386-0.8456	0.6206-0.827	0.6477-0.7912	0.732	0.714	0.677	0.702	0.941	0.955	0.76	0.468	0.598	
PON1 P27169 LUGTVFK	51.66%	54.23%	51.48%	0.612227182	0.236309352	0.361183889	0.3997-0.6335	0.4251-0.6596	0.4331-0.5965	0.546	0.592	0.549	0.681	0.667	0.847	0.42	0.511	0.247	
PP1A P62937 VSELEADK	76.89%	72.92%	74.94%	2.58E-06	4.73E-05	8.94E-10	0.6707-0.8672	0.6275-0.831	0.6809-0.818	0.773	0.724	0.713	0.617	0.725	0.704	0.92	0.723	0.722	
PROX2 P31219 QITVNDPLVGR	59.70%	52.02%	55.14%	0.05027467	0.695675132	0.107537037	0.4813-0.7128	0.3528-0.5875	0.4701-0.6328										